UNIVERSITY OF CALIFORNIA, SAN DIEGO

The Natural Products Chemistry of Marine Ascidians: Structural Elucidation and Molecular Modeling Studies of Novel Secondary Metabolites

A dissertation submitted in partial satisfaction of the requirements for the degree

Doctor of Philosophy in Oceanography

by

Heonjoong Kang

Committee in charge:

Professor William H. Fenical, Chair

Professor D. John Faulkner

Professor Trevor C. McMorris

Professor Farooq Azam

Professor Jeffery L. Bada

1994

The dissertation of Heonjoong Kang is approved, and it is acceptable in quality and form for publication on microfilm:

Farooq Azam

D. John Faulkner

Jeffrey L. Bada

Trevor C McMorris

William Fenical
Chair

University of California, San Diego

1994

To my parents, parents-in-law, brothers, sister, and my wife, Sooyun,

for all of their love, support, and encouragement,

and my lovely daughter, Nah-Young.

TABLE OF CONTENTS

LIST OF FIGURES

LIST OF TABLES

Table Page

Chapter VII

ACKNOWLEDGEMENTS

I would like to express my gratitude to several people for their help in this work. First of all, I thank my advisor, Dr. Fenical, for his guidance and mentorship during Ph. D. research. He made me open my eyes as a scientist about how to approach problems and how to conduct research. Most importantly he taught me human relationship. I strongly feel that I am lucky to meet him. Dr. Faulkner, he gave invaluable advice and discussion about marine natural products. He also taught me how to conduct molecular modeling studies. I greatly appreciated his teaching. I thank all of my committee members for their reading my manuscript and advice.

Mr. Jensen collected all of my sample and conducted microbial isolation and fermentation. I really appreciate his help. Dr. Robert Jacobs at UC, Santa Barbara kindly performed antiinflammatory tests in his lab. Mr. Cummings conducted the rest of biotesting. I thank them so much. Without their help this research could not be possible. I am also extremely grateful to Dr. Monniot for her work on identification of many chemically interesting ascidians I investigated.

I also thank the mass spectrometry center at UC, Riverside, especially Dr. New. Without his help and suggestion, many projects could not be accomplished.

I am grateful to Drs. Wright, Trischman, Pathirana, and Mr. Brueggeman for NMR maintenance, good friendship, teaching me 2-D NMR and structure searching. Dr. Trischman helped me so much in many ways. At the time of my arrival, she kindly explained everything. Also she gave encouragement and wonderful friendship for several years at SIO. I thank everybody in Dr. Fenical and Dr. Faulkner's Lab. for their suggestion through the group meeting and joyable relationship.

I also thank all present and past members of Korean Scientific Seminar members in San Diego for their invaluable discussion and suggestion. I am also grateful to my exadvisor, Dr. Kim. His guidance and training of me at the previous graduate school made me everything easier during my Ph.D. study in all aspects. Dr. Park gave me encouragement, guidance, and support. His door was widely open anytime for me. I really thank him for everything. Special thanks go to Dr. Shin and Dr. Lee for their advice and encouragement. In the most difficult first two years, they helped me to adapt SIO as quickly as possible. Whenever I had difficult time, they encouraged me and

suggested some ways. I also thank Drs. D.-K. Lee, Y. Lee, Y.-H. Lee, H. Jeong, and Mr. D. Kim and D. Min for wonderful friendship.

Finally, I greatly thank my parents, parents-in-law, brothers, and sister for their endless love, support, and encouragement. Specially, I thank my wife Sooyun for her love and support. I would like to give all of joy from this research to my wife and daughter, Nah-Young.

Finally, I would like to acknowledge Korean Government and California Sea Grant for financial support.

VITA

May 7, 1963	Born, Jinju, Korea
1986	B.S., Honors, Oceanography Seoul National University, Seoul, Korea
1986-1988	M.S., Marine Chemistry (Chemical Instrumentation) Seoul National University, Seoul, Korea
1989-1992	Grantee of Korean Government Overseas Scholarship & Research Assistant Scripps Institution of Oceanography University of California, San Diego, La Jolla, CA
1992-1994	California Sea Grant Trainee Scripps Institution of Oceanography University of California, San Diego, La Jolla, CA
1994	Ph.D., Oceanography Marine Natural Products Chemistry Dr. William H. Fenical, advisor University of California, San Diego, La Jolla, CA

PUBLICATIONS

Heonjoong Kang and William Fenical. "Four Novel Condensed DOPA-Alkaloids from an unidentified Western Australian Ascidian *Didemnum* sp.," in preparation.

Heonjoong Kang and William Fenical. "Clavatamines, Dimmeric Disulfide Alkaloids from the Indian Ocean Ascidian *Polycarpa lavata,* " in preparation.

Heonjoong Kang and William Fenical. "Didemnocins, Novel Secondary Metabolites of Potential Microbial Origins," in preparation.

Heonjoong Kang and William Fenical. "Aplidiamines, Unique Zwitterion Structures from an Ascidian *Aplidium* sp." in preparation.

Heonjoong Kang and William Fenical. "Eudisins A-C, Unusual Dihydro β-Carbolines from a Western Australian Ascidian", in preparation.

Heonjoong Kang and William Fenical. "New Alkaloids of the Lamellarin Class from a Western Australian Ascidian *Didemnum* sp.", in preparation.

FIELDS OF STUDY

Major Field: Marine Bio-Organic Chemistry

Studies in Marine Natural Products Chemistry
Professors William H. Fenical and D. John Faulkner

Studies in Nuclear Magnetic Resonance Spectroscopy
Professors William H. Fenical, D. John Faulkner, Jay S. Siegel, and Dr. John M. Wright

Studies in Molecular Modeling
Professors William H. Fenical and D. John Faulkner

Studies in Organic Chemistry
Professors Daniel F. Harvey and Trevor C. McMorris

ABSTRACT OF DISSERTATION

The Natural Products Chemistry of Marine Ascidians:
Structural Elucidation and Molecular Modeling Studies of Novel Secondary Metabolites

by

Heonjoong Kang
Doctor of Philosophy in Oceanography
Scripps Institution of Oceanography
University of California, San Diego, 1994

Professor William H. Fenical, Chairman

Ascidians are well-known producers of amino acid-derived secondary metabolites. Recent chemical and biological investigations of taxonomically diverse ascidians have revealed a variety of pharmacologically potent natural products and the importance of these metabolites in the survival of physically vulnerable ascidians in predator-rich habitats. However, at issue are the real sources of novel secondary metabolites isolated from marine ascidians, which are related to symbiosis due to complex associations of the ascidians with microbial symbionts. Furthermore, rapidly developing resistance of infectious diseases and cancers toward traditional antibiotics and anti-cancer drug needs unprecedented novel natural products. Despite great advance in

separation science, marine natural products research in ascidians was relatively limited to nonpolar compounds. Furthermore, the aquatic environment implicates the significance of hydrophilic molecules in defensive adaptations and symbiosis. Therefore, the main objective of this research was to investigate biosynthetic diversity and limitation of ascidian secondary metabolism with emphasis of identification of hydrophilic bioactive molecules and unprecedented carbon skeletons. In this way, a broader understanding of ascidian secondary metabolism, and a chemical data base for studies of chemical ecology, could be established.

A variety of chromatographic methods, such as high performance liquid chromatography and high speed countercurrent chromatography, were used to isolate polar compounds. Extensive spectroscopic techniques, including a variety of two-dimensional NMR experiments and mass spectrometric methods as well as computer-molecular modeling, were utilized to elucidate their structures.

This research resulted in the structural elucidation of 25 new secondary metabolites in 10 different structural classes, including 8 new carbon skeletons from marine sources. A high diversity of chemical structures along with various bioactivities, such as cytotoxicity against colon cancer cells, antimicrobial activity, and anti inflammatory activity, were demonstrated. Several natural products showed cytotoxic activities directed against a drug-resistant human colon cell line, HCT 116. Some of these compounds are known to inhibit an enzyme which is frequently used as a chemotherapeutic target. In addition to them, some had antibacterial and antiinflammatory activities. However, not every compound was bioactive. Perhaps some of them may explain the chemical defense mechanism of marine ascidians against predators.

Chapter I

Introduction

A. General Aspects of Natural Products Chemistry

The introduction of powerful and automated physical methods, such as nuclear magnetic resonance spectroscopy (NMR), mass spectrometry, and X-ray analytical methods, has greatly reduced the time to identify the structures of natural products. However, it does not mean that the significance of structural identification of natural products has diminished. Secure molecular structures provide a basis for many inquiries in organic chemistry: synthetic chemistry, medicinal chemistry, conformation analysis, receptor-chemistry, biosynthetic chemistry, chemosystematics, and chemical ecology, all of which provide a deeper understanding of underlying factors that govern living processes and chemistry itself.

In the early days, marine natural products research was largely limited to simple, nonpolar compounds. Over the past decade, developments in organic spectroscopy and separation science, particularly the innovations in nuclear magnetic resonance and high performance liquid chromatography, have expanded the frontier of natural products chemistry. Molecules of greater size and complexity, and those of awkward solubilities, are now within reach of structural analysis.

B. Perspective of Marine Natural Products Chemistry

Isolation of unprecedented metabolites and access to novel biological sources of compounds are the characteristics of marine natural products chemistry. The discovery of unprecedented metabolites from marine organisms thus opens many promising fields of inquiry: the natural functions of bioactive metabolites, mechanisms of pharmacological action, biosynthesis, new molecular methods to engineer natural products, studies of microbial symbiosis with invertebrates, and studies of receptor binding phenomena.

C. Biology and Chemistry of Ascidians

The headless and unsegmented tunicates (Subphylum Urochordata or Tunicata) are grouped into four different classes: the Thaliacea, the Appendicularia, the Sorbercea, and the Ascidiacea (Monniot *et al.* 1990, Millar 1971, Goody 1974, Satoh 1994). The Ascidiacea (Figure 1-1) is subdivided into three orders depending upon the structure of the adult's branchial sac and the relative position of their gonads and gut-loop. The classification of ascidians into solitary and colonial ascidians, although not consistent with classical systematics, is rather convenient in the field of natural products chemistry. This notation along with the chemically investigated genera is presented in Table 1-1.

Studies of marine ascidians were stimulated by the high incidence of bioactivity and chemical uniqueness of their secondary metabolites. Even though over 300 compounds (including toxins and chelators) have been reported, little is known about the secondary metabolism of ascidians and the biological functions of the compounds.

There are several characteristics that make the animals unique among invertebrates in the marine environment: their immunology, iodine binding, and vanadium and iron accumulation. These subjects will be reviewed in the context of suggesting possible biological roles of the isolated metabolites from ascidians, in tunic formation, in metal accumulation, and in chemical adaptations for defense.

1. Biology of Ascidians

1.1. Ascidians in Relation to Immunology.

The potential importance of ascidian secondary metabolites in chemical defense, in tunic formation, and in the biochemistry of hemocytes make it necessary to review this subject briefly.

1.1.1. Hemocytes

The ability to differentiate between self and non-self, and to react to foreign materials seems to be widely spread among the invertebrates (Wright 1981). Definition of the types of ascidian blood cells are normally based on morphological evidence (at the electron microscope level) rather than possible and/ or presumed functional homologies. Various names have been adopted to designate the types. A unified scheme of classification has recently been proposed (De Leo 1992). Hemocytes were grouped under two main categories: stem cells and granulocytes, depending upon cellular differentiation

Figure 1. Generalized structure of a solitary ascidian adult.

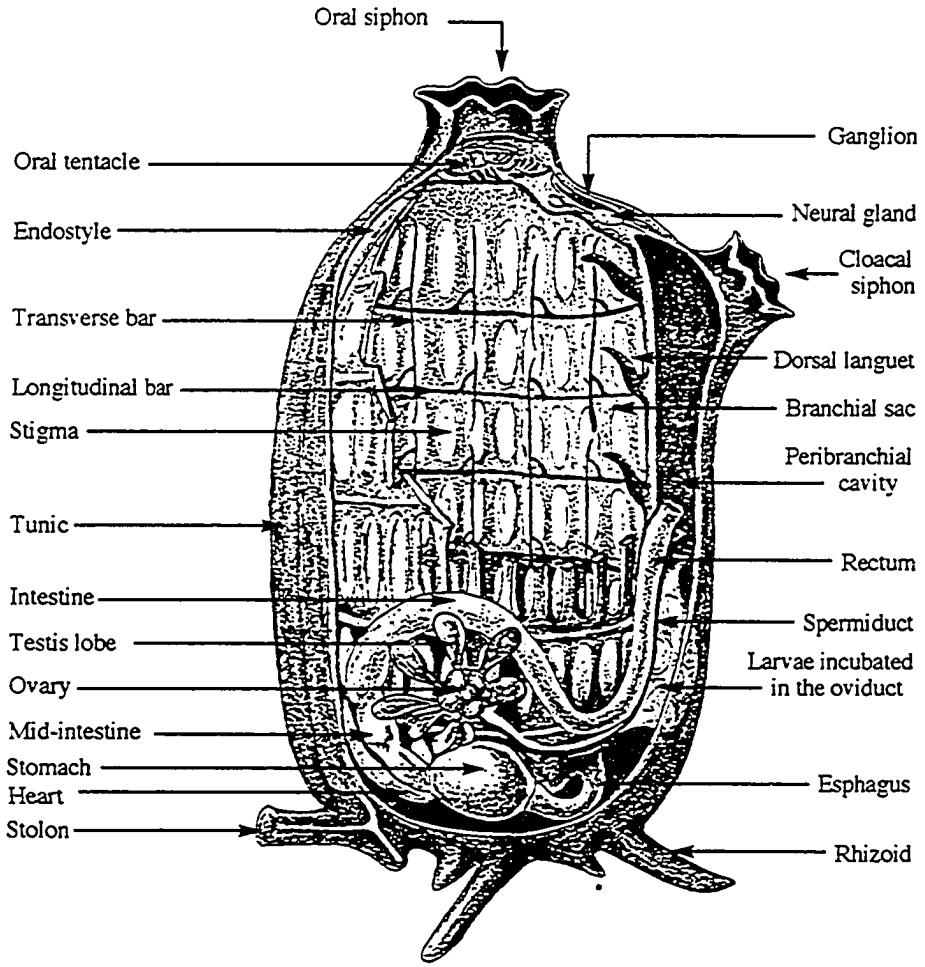

(a) Lateral view illustrating major internal organs.

Figure 1. (continued)

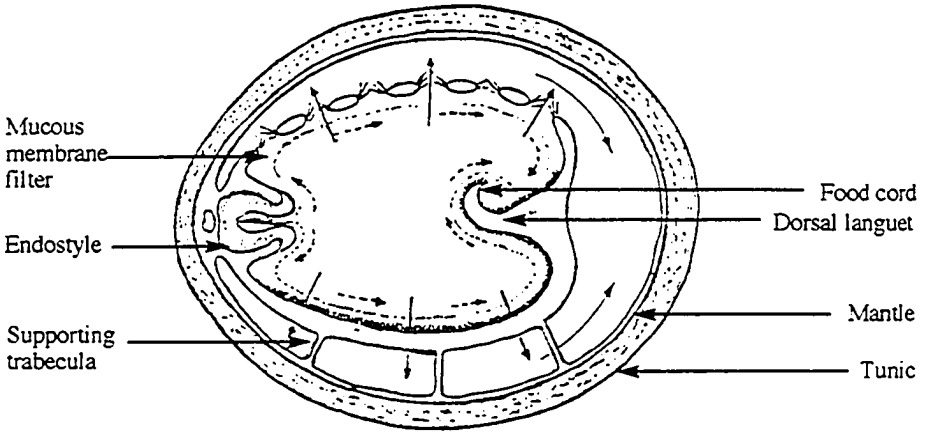

(b) Diagrammatic transverse section through the pharynx, passing on the left through the endostyle, and on the right through a dorsal languet. The small arrows indicate the direction of movement of the filtering sheets, and the large arrows the direction of the water currents.

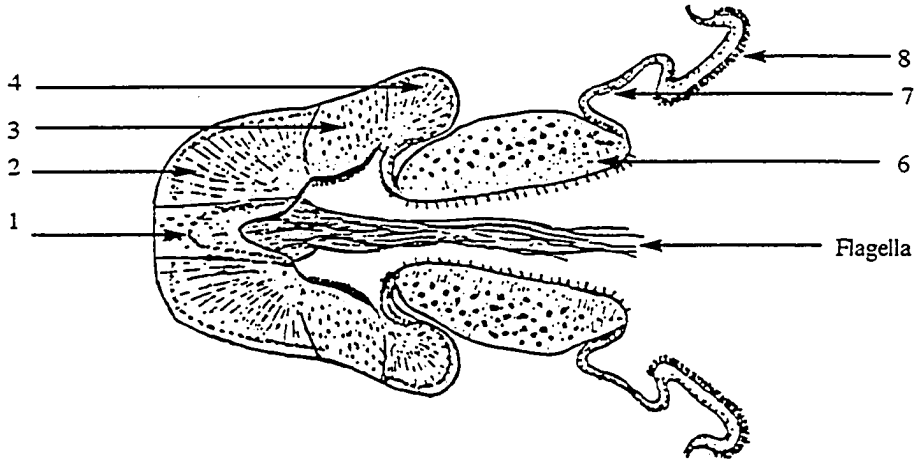

(c) Cross section of endostyle. 2, 4, and 6 show ventral, median, and dorsal ciliated tracts; 1, 3, 5, and 8 zones of predominant ciliated cells; 7 and 8 zones where iodine is located.

Table 1-1. Systematics of the class Ascidiacea and chemically investigated genera (underscored).

Subphylum **Urochordata**
Class Thaliacea (salps, doliolids, pyrosomes)
Class Appendicularia (or Larvacea)
Class Sorberacea
Class **Ascidiacea**

Order **Aplousobranchia (Enterogona)**

Family Polyclinidae (Synocidae)[a]
Aplidiopsis Lahille 1890
Aplidium Savigny, 1816
Atopogaster Herdman, 1886
Citorclinum Monniots & Millar 1990
Dumus Brewin 1952
Euhermania Ritter 1904
Homeodistoma Redikorzev, 1927
Monniotus Millar 1988
Pharyngodictyon Herdman, 1886
Placentella Redikorzev, 1927
Polyclinum Savigny, 1816
Protopolyclinum Millar, 1860
Pseudodistoma Michaelsen, 1924
Ritterella Harant, 1931
Sidneioides Kesteven 1909
Sidnyum
Synoicum Phipps, 1774

Family Polycitoridae (Clavelinidae)[a]
Archiascidia Julin, 1904
Archidistoma Garstang, 1891
Atapozoa Brewin, 1956
Citorclinum laboutei (only)
Monniot & Millar,1990
Clavelina Savigny, 1816
Cyathocormus Oka, 1912
Cystodytes Drasche, 1883
Distaplia Della Valle, 1891
Eudistoma Caullery, 1900
Hypodistoma Tokioka, 1967
Hypsistozoa Brewin, 1953
Millarus Monniot, 1989
Oxycorynia Drasche, 1882
Polycitor Renier, 1778
Polycitorella Michaeelson, 1924
Protoholozoa Kott, 1969
Stomozoa Kott, 1957
Sycozoa Lesson, 1830

Family Didemnidae[a]
Askonides Kott, 1962
Atriolum Kott, 1983
Coelocormus Herdman, 1886
Didemnum Savigny, 1816
Diplosoma Macdonald, 1859
Leptoclinides Bjerkan, 1905
Lissoclinum Verrill, 1871
Polysyncraton Nott, 1892
Trididemnum Della Valle, 1881

Order **Phlebobranchia (Enterogona)**

Family Cionidae[a,b]
Araneum Monniot & Monniot, 1973
Ciona Flemina, 1822[b]
Diazona Savigny, 1816
Dimeatus Monniot & monniot, 1982
Mysterascidia Monniot & Monniot, 1982
Pseudodiazona Millar, 1963
Pterygascidia Sluiter, 1904
Rhopalaea Philippi, 1843
Rhopalopsis Herdman, 1880
Syndiazona Pka, 1927[a]
Tantillulum Monniot &Monniot, 1982
Tylobranchion Herdman, 1886

Family Perophoridae[a]
Ecteinascidia Herdman, 1880
Perophora Wiegman, 1835

Family Ascidiidae[b]
Ascidiella Roule, 1883
Ascidia Linne, 1767
Phallusia Savigny, 1816
Psammascidia Monniot, 1963

Family Corellidae[b]
Abyssascidia Herdman, 1880
Chelyosoma Broderip & Sowerby, 1830
Clatripes Monniot & monniot, 1974
Corella Alder & Hancock, 1870
Corelloides Oka, 1926
Dextrogaster Monniot, 1962
Rhodosoma Ehrenberg, 1828
Xenobranhion Arnback, 1950

Family Agesiidae[a]
Adagnesia Kott, 1963
Agnesia Michaelson, 1898
Caenagnesia Arnback, 1938
Corynascidia Herdman, 1882
Proagnesia Monniot & Monniot, 1973

Family Plurellidae
Microgastra Kott, 1985

Table 1-1. (continued)

Plurella Kott, 1973

Family Octacnemidae[a,b]
Benthascidia Ritter, 1907
Cibacapsa Monniot & Monniot, 1985
Cryptia Monniot & Monniot, 1983
Dicopia Sluiter, 1905
Hypobythius Moseley, 1879
Octacnemus Moseley, 1879
Polyoctacnemus Ihle, 1935
Situla Vinogradova, 1967

Order **Stolidobranchia (Pleurogona)**

Family Molgulidae[b]
Anomopera Hartmeyer, 1923
Bostrichobranchus Traustedt, 1882
Eugyra Alder & Hancock, 1870
Eugyrioides Seeliger, 1906
Fungulus Herdman, 1881
Gamaster Pizon, 1896
Minipera Monniot C. & F., 1973
Molgula Forbes, 1848
Molguloides Huntsman, 1922
Paramolgula Traustedt, 1885
Pareugyrioides Hartmeyer, 1914
Protomolgula Monniot F., 1971
Rhizomolgula Ritter, 1901

Family Pyuridae[b]
Bathypera Michaelson, 1904
Bathypyura Monniot, 1971
Boltenia Savigny, 1816
Bolteniopsis Harant, 1927
Cratostigma Monniot C. & F., 1961
Ctenyura Van Name, 1918
Culeolus Herdman, 1881
Halocynthia Verrill, 1879
Hartmeyeria Ritter, 1913
Heterostigma Arnback, 1924
Microcosmus Heller, 1877
Pyura Molina, 1782

Family Styelidae[a,b]
Alloeocarpa Michaelson, 1900
Amphicarpa Michaelson, 1922
Arnbackia Brewin, 1950
Asterocarpa Brewin, 1946
Bathyoncus Herdman, 1882
Bathystyeloides Seeliger, 1904
Berrillia Brewin, 1952
Botryllus Savigny, 1816
Chorizocarpa Michaelson, 1904
Cnemidocarpa Hunstman, 1912
Dendrodoa Mac Leay, 1825
Dextrocarpa Millar, 1955
Dicarpa Millar, 1955
Distomus Gaertner, 1774
Gynadrocarpa Michaelson, 1900
Kukenthalia Hartmeyer, 1903
Metandrocarpa Michaelson, 1904
Monobotryllus Oka, 1915
Oculinaria Gray, 1868
Okamia Brewin, 1948
Oligocarpa Hartmeyer, 1911
Pelonaia Goodsir & Forbes, 1841
Polyandrocarpa Michaelson, 1904
Polycarpa Heller, 1887
Polyzoa Lesson, 1830
Protostyela Millar, 1954
Seriocarpa Diehl, 1969
Skaiostyela Sluiter, 1904
Stolonica Lacaze-Duthiers, 1892
Styela Fleming, 1822
Symplegma Herdman, 1886
Syndendrodoa Tokioka, 1951
Theodorella Michaelson, 1922
Tibitin Monniot, 1983

Family Hexacrobylidae[b]
Gasterascidia
Hexacrobylus

Note:
[a] Colonial.
[b] Solitary.
Source: Monniot *et al.* (1990), Berrill (1950), and Satoh (1994).
Genera underscored: chemically investigatigated genera.

and the presence of vesicles, vacuoles, and granules with a variable degree of electrodensity. The granulocytes are further categorized into clear granulocytes, clear vesicular granulocytes, microgranulocytes, and vacuolar granulocytes which are subdivided into unilocular granulocytes and globular granulocytes. The main hemocytes functions are summarized in Table 1-2.

Table 1-2. Main ascidian hemocyte functions

Types	alias names	fuctions
stem cell	hemocytoblast, hemoblast, lymphocyte, progenitor cell	hemopoiesis, immune responses
clear granulocyte	non vacuolar hyaline amoebocyte, hemostatic cell, microgranular amoebocyte, hyaline leucocyte	hemostasis, nutrition and nutrient transportation, phagocytosis, inflammation
clear vesicular granulocyte	vacuolar hyaline amoebocyte, phagocyte, vacuolar amoebocyte, clear granulocyte	genesis of vessel basal membrane, defense reactions, cell coagulation, phagocytosis, vanadium accumulation
microgranulocyte	granular amoebocyte, phagocyte, macrophage, granulocyte	defense reactions, antimicrobial properties, degranulation, tunic formation, phagocytosis, nutrition and metabolism, vanadium and iron accumulation
unilocular granulocyte	signet-ring cell	construction, regeneration, and repair of tunic cuticle, vanadium storage
globular granulocyte	compartment cell, morula cell, vacuolated cell, nutritive cell, nephrocyte, pigment cell	immune responses, encapsulation of foreign bodies, hemostasis, tunic repair, wound healing, storage of polysaccharides and proteins, vanadium and iron metabolism, nutrition, nitrogen excretion, pigmentation

The stem cell is referred to by several different names, such as the hemocytoblast (Mukai and Watanabe 1976), hemoblast (Srippa *et al.* 1987), lymphocyte (Fluke 1979, Srippa *et al.* 1987), or progenitor cell (Ratcliiffe *et al.* 1985). These cells participate in hemopoiesis (blood cell production) and immune responses.

The clear granulocytes, known as vacuolar hyaline amoebocytes (Rowley 1981),

hemostatic cell (Ratcliiffe *et al.* 1985), microgranular amoebocyte (Milanesi and Burighel 1978), hyaline leucocyte (Wright 1981), or clear granulocyte (De Leo *et al.* 1987), are involved in cell coagulation, nutrition and nutrient transportation, phagocytosis, and inflammation.

The clear vesicular granulocytes are involved in the genesis of vessel basal membrane, defense reactions, cell coagulation, phagocytosis, and vanadium accumulation. This cell is also designated as vacuolar hyaline amoebocyte, phagocyte, vacuolar amoebocyte, and clear granulocyte (Rowley 1981, Ratcliffe *et al.* 1985, Scrippa *et al.* 1987, De Leo *et al.* 1987).

The microgranulocyte, common by known as the granular amoebocyte, phagocyte, macrophage, or granulocyte, mediates defense reactions, provides antimicrobial properties, is involved in degranulation, tunic formation, phagocytosis, and nutrition and metabolism, and shows vanadium and iron accumulation (Rowley 1981, Ratcliffe *et al.* 1985, Wright 1981, Srippa *et al.* 1987, De Leo *et al.* 1987, Milanesi and Burighel 1978).

The unilocular granulocyte, among the vacuolar granulocytes, frequently known as signet-ring cells, intervenes in construction, regeneration, and the repair of tunic cuticle. This is also involved in vanadium storage (De Leo *et al.* 1981).

The globular granulocyte participates in immune responses, encapsulation of foreign bodies, hemostatsis (cellular aggregation), tunic repair and wound healing, storage of polysacchrides and proteins. It also takes part in vanadium and iron metabolism, nutrition, nitrogen excretion, and pigmentation. The cells are also designated under the names compartment cells, morula cells, vacuolated cells, nutritive cells, nephrocytes, and pigment cells (Milanesi and Burighel 1978, De Leo *et al.* 1981, Scrippa *et al.* 1987, Ratcliffe *et al.* 1985).

The classification scheme of ascidian blood cell types which is mostly frequently adopted, however, recognizes four main categories; stem cells, amoebocytes, vacuolated cells, and pigment cells. These cells are further subdivided into eight different cell types: lymphocytes, amoebocytes, macrophage, nephrocyte, pigment cells, three vacuolar cells, such as signet ring cells, compartment cells, and morula cells (Wever and Kustin 1990). The signet ring cell, colorless or grey, possesses one large vacuole. The morula cell containing roughly 11-14 uniformly sized spherical vacuoles appears mulberry in shape. The vacuolated cells are consistently associated with sequestered vanadium . In addition, they contains a high content of sulfur (Scippa *et al.* 1990). The topic of vanadium accumulation in ascidians will be discussed later in detail.

1.1.2. Defense mechanism

Defense mechanisms of ascidians are composed of two elements: humoral and cellular reactions. In addition to mechanical protection provided by the tunic barrier, defense in ascidians is a consequence of complex interaction between a cellular response and a humoral one, including the natural and or induced capacity of recognizing, destroying, and rejecting any foreign substance located either inside the tunic, or in contact with the inner tissues of the animals.

The humoral factors in defensive mechanisms are mainly attributed to the presence of antimicrobial substances against bacteria, fungi, and viruses. In ascidians, vacuolated cells are actively involved in phagocytosis. Halocyamines (Azumi *et al.* 1990a, b), antimicrobial compounds, and a lipopolysaccharide-binding hemagglutinin were localized in one type of the vacuolated cells of *Halocynthia roretzi* after separation of blood cells by discontinuous density gradient centrifugation in a solution of bovine serum albumin (Azumi *et al.* 1993). The hemagglutinin bound lipopolysaccharides can agglutinate both Gram-negative and -positive bacteria. In *Ciona intestinalis*, a possible antimicrobial function for vanadium has been claimed (Rowley 1983). Incubation of bacteria with the ascidian cells gave rise in the fusion of the vanadium-containing vacuoles with the bacteria-laid phagosomes during phagocytosis. Thus, these substances may function as humoral factors in the defense mechanism of ascidians.

Cellular reactions are involved in the ability to heal wounds, in cell coagulation, phagocytosis, encapsulation of foreign bodies, histocompatibility and cytotoxicity. As a consequence of tunic disruption caused by either environmental factors or by attacks of predators, the animal must defend against damage. Maintenance of internal structure and neutralizing foreign invaders would be crucial. There is a common process in wound-healing, cell aggregation, coagulation, inflammation, phagocytosis, and encapsulation. In wound repair, unilocular granulocytes (signet-ring cells) excrete their contents into the cuticular surface of the tunic. The morula cells also gather in the damaged region to provide collagen-like proteins, and as a result, contribute to the repair of the fibrous structure of the tunic (De Leo *et al.* 1981).

The inflammatory reaction of ascidians is a non-specific response. The phagocytic activity of clear vesicular- and micro-granulocytes (amoebocyte) is associated with the presence of large lysosomal bodies, and visualized by vacuoles containing bacteria or cell residues. In phagocytosis, in the process of enveloping foreign targets, the blood cells transform their outline by invaginating their membrane and/ or generating a variety of

pseudopodes, upon touching the invaders. An additional process which takes place in encapsulation of foreign substances is the degranulation of the unilocular and globular granulocytes, thus contributing to the production of the capsule matrix (Wright and Ermak 1982). The phenomenon is an extension of tunic formation and wound-healing (Wright 1981). The nature of the discharged materials, however, has not been characterized. Nevertheless, a metallo-protease was released from the small granular amoebocytes, lymphocytes, and compartment cells of the solitary ascidian *Halocynthia roretzi* in response to the lipopolysaccharide-binding hemagglutinin isolated from the vaculoated cells of the same species (Azumi *et al.* 1993). Cross-talk is therefore suggested among the hemocytes as a consequence of physiological stimuli. This proposal was also supported by the presence of an interleukin-I-like substance in ascidians (Beak *et al.* 1989).

Tissue transplantation studies have identified a sensitive histocompatibility system in the solitary tunicates. In the solitary ascidian *Molgula manhattensis*, signet ring cells and morula cells seem to infiltrate the transplanted tissues, forming vacuoles and discharging unknown materials. This process creates unrecognizable tissues and causes necrosis (Anderson 1971). However, grafts taken from the outer tunic layer of the solitary ascidian *Styela plicata* are actively rejected with concomitant alloimmune memory, exhibiting a high degree of immunological specificity (Raftos *et al.* 1987). The recognition of histocompatible antigens in *Styela plicata* is mediated by lymphocyte-like cells which specially infiltrate incompatible tissue prior to rejection through cytotoxic activity. Moreover, the second-set immunization elevates proliferation and migratory activity of the hemocytes. The immunological reactivity obeys the transplantation principle of mammalian-like histocompatibility systems, suggesting the existence of specific anti-allogeneic receptors (Raftos *et al.* 1988). In addition, the dependence of the cytotoxic activity upon temperature indicates the probable role of the plasma membrane components in the recognition of histocompatibility antigens (Parrinello and Arizza 1992). The signet ring cells, morula cells, and amoebocytes are evidently involved, but they take part in nonspecific inflammation and in wound healing (Raftos *et al.* 1987). The presence of a neurohormone peptide possessing hematogenic functions, a neuropeptide Y-alike, in the granular leukocytes and the lymphocytes of *S. plicata* suggests an involvement of this molecule in modulatory pathways of hematopoiesis in ascidians (Pestarino 1992).

On allelogeneic rejection in the colonial ascidian *Botrylloides simodensis*, the following reactions occurred: morula cells and tunic cells infiltrated into the tunic and migrated to the contact area after fusion of both tunics; the morula cells lysed in the tunic releasing humoral factors, and thus a new wall was established, separating the necrotic area

from each colony (Hirose *et al.* 1990).

It is thus obvious that the lymphocytes alone are sufficient for the specific response to allogeneic tissue in solitary ascidians, while various cells are needed in the colonial ascidians.

Judging by the extremely low incidence of malignant tumors, ascidians appear to posses a simple and rather effective defense mechanism against somatic mutations. It is proposed that special substances blocking the activity of oncogens may be present. Tumor markers, oncofetal antigens, are produced and released into circulation by neoplasms (Klavins 1986). Oncoprecipitin A, a substance that interacts specially with SP-1, an oncofetal antigen, in antigen-antibody manner has been identified (Moroz *et al.* 1993).

In relation to searching for precursors of vertebrate immune system, much attention has been given to putative hormones and neurotransmitters from ascidians. Since the first demonstration of serotonin (5-hydroxytryptamine, 5-HT) in an ascidian (Welsh and Loveland 1968), dopamine, noradrenaline, GABA, taurine, glycine, and aspartate have subsequently been isolated from various ascidians, including *Ciona intestinalis*, *Corella parallelogramma*, and *Ascidia metula.* Failure to detect 5-HT in the celebral ganglia questioned the putative hormonal roles of previously detected compounds. An alternative role, osmoregulation, has been proposed from a very high level of glycine and taurine in ascidians (Osborne *et al.* 1979). However, the absorption into cells and nuclei of *A. mentulosa* of adrenaline, serotonin, histamine, and a hormone precursor (5-hydroxy-tryptophane) from a culture medium suggests the roles of compounds as hormones and the involvement of amino acid receptors (Csaba 1987). The 5-HT containing cells are seated in the lateral portion of the endostyle between zone 7, a region known to have iodinating capacity, and zone 8 (Figure 1-1). Serotonin is stored in cytoplasmic granules which are located both in the apical and basal cytoplasm. The bipolarity and vicinity of the 5-HT containing cells indicate the homology of the cells to thyroid parafollicular C cells in mammals (Nilsson *et al.* 1988).

1.2. Iodine Binding in the Tunic and the Endostyle.

Ascidians have a remarkable capability for the uptake and utilization of environmental iodine. Broadly, two proposals for the iodination process have been made : tunic formation as an invertebrate characteristic and a protothyroidal function as a vertebrate element . Recent studies of iodine uptake and binding in tunicates have been strongly motivated by the view of the undoubted homology of the endostyle of protochordates with

the thyroidal gland of the vertebrate (Fredriksson *et al.* 1988, Dunn 1980). This analogy may contribute to an understanding of the origin of the thyroid gland and of thyroidal biosynthesis. The iodine binding process may equally contribute to the tunic formation (Thorndyke 1973, Barrington 1975).

1.2.1. The tunic formation

The chemical composition of the tunic

The tunic in a chemical sense is divided into three structural components: the hyaline substance (water and acid mucopolysaccharides), the fibers which penetrate the tunic, and the cuticle at the surface of the tunic (Krishnan 1975, Smith 1970a and b). The tunic is a complex tissue which is composed of protein, carbohydrate, and many wandering hemocyte cells. Some of these cells contribute to its production (see immunological reaction of hemocytes). A very high water content, ranging from 76 % in *Halocynthia papillosa* (Stievenart 1971) to over 90 % in *Phallusia mammillata* (Endean 1961), has been demonstrated. Originally, the carbohydrate was assumed to be present as cellulose, known as tunicin, and as a component of the acid mucopolysaccharides (Endean 1961, Smith 1970a). However, the carbohydrate is far more complex than cellulose. The cellulose-like polysaccharides of the tunic comprise a polysaccharide-protein complex together with the acid mucopolysaccharides (Krishnan 1975). The presence of serine and threonine in the hydrolysis mixture of the cellulosic component suggests their role as links between the cellulose-like substance and protein.

The cuticle contains a very high proportion of the total protein of the tunic, amounting to 85 % of its protein nitrogen in *Halocynthia* (Stievenart 1971). *Halocynthia* thus lacks acid mucopolysaccharides. A form of self-tanning, which involves the formation of dimers and trimers of tyrosine capable of cross-links, has been described (Krishnan and Ravindranath 1972). The phenomenon results from the nature of the protein substrate which is lacking of a lipid component indispensable for sclerotization. However, there is evidence of tanning involving quinone intermediates, in a process similar to typical tanning. Such evidence comes from the induction of artificial tanning by catechol, and subsequent loss of brown color (resulted from quinone tanning) upon applying sodium hypochlorite (Krishnan 1975).

Sulfated glycans are extremely abundant in ascidians (Toda *et al.* 1978, Albano and Mouroa 1986, Pavao *et al.* 1989a and b, Pavao *et al.* 1990, Albano *et al.* 1990, Santos *et al.* 1992). A linear novel sulfated gylcosaminoglycan like chitin sulfate was identified from

Halocynthia roretzi. The main structure is considered to be a (1-4)-2-acetoamide-2-deoxy-6-O-sulfo-β-D-glucopyranose homopolymer containing a little bit of galactosamine (Anno *et al.* 1974). The sulfated polysaccharides contain a high content of galactose and a small amount of D-glucose and hexosamine. Their major constituent is L-galactose, lacking totally the D-enantiomer of this sugar. Major fractions from *Halocynthia roretzi, Styela plicata, Clavelina oblonga, Ascidia nigra, Herdmania monus*, and *Ciona intestinalis* contain high amounts of α-L-galactopyranose residues, sulfated at position 3 and connected glycosidically through positions 1-4. *A. nigra and S. plicata* contain large amounts of α-L-galactopyranose units 1-3-linked and partially sulfated at position 4. Although the polysaccharides from *C. oblonga* are seldom branched, the major fraction from *S. plicata* and *A. nigra* are highly branched polymers, suggested by possessing high proportions of nonsulfated L-galactopyranose non-reducing end units (Pavao *et al.* 1989b). Approximately 20 % of the sugar residues from *C. oblonga* are 3-sulfated-4-linked α-L-fucopyranosyl units (Santos *et al.* 1992). Methylation studies show that 4-linked-3-sulfated-a-L-galactopyranose exists as a homopolymer with small amounts of galactose residues at the non-reducing ends. However, the polysaccharide from *C. intestinalis* is highly branched. Glucose occurs as a non-sulfated 3-linked unit and the branches are attached at position 6 of the central core (Santos *et al.* 1992). Interestingly, hydrolysis of the L-galactans from *H. roretzi* and *S. plicata* yield almost a 1 to 1 ratio of serine and threonine, suggesting the linkage between the galactans and protein is composed of O-glycosyl bonds to those amino acids (Toda *et al.* 1978). Small amounts of uronic acid-containing mucopolysaccharides have been isolated from *H. roretzi* (Anno *et al.* 1974). In *Halocynthia*, the total protein content of the tunic is about 50 % of the dry weight, but only 60 % of this protein can be hydrolyzed by pronase (Smith and Dehnel 1970).

Ascidian polysaccharides are characteristic in the following ways. They are different from other sulfated polysaccharides not only in the types of connectivity and position of sulfation (6-sulfated and 3-linked in other organisms: Roden 1981), but also in their extensive branching. They are the only group of compounds which have large amounts of L-galactose rather than the D-form. The abundance of sulfate in the polysaccharides may contribute to water binding capacity and the resilience of the tunic (Santos *et al.* 1992).

Mantle epithelial cells play an important role in the secretion of the tunic (Smith 1970 b). It seems that the mantle cells of *Ciona, Dendrodoa*, and *Styela*, and doubtless of other genera, are a likely source of both the carbohydrate and the protein moieties of the tunic, with polymerization and fiber formation taking place outside them. *Phallusia*,

however, is exceptional, for here the epidermal cells lining the tunic vessels produce mucopolysaccharide, while wandering vanadocytes are thought to produce the cellulose fibers which appear to arise directly from their surface (Endean 1961). This finding is indirectly supported by the fact that the vanadocytes show a high content of sulfur (Scippa *et al.* 1990) which may be a source of the sulfated glycans in the tunic.

There is another contribution made to the tunic by the hemocytes cells (Smith 1970b, Hirose *et al.* 1990). Mature morula cells are concentrated immediately above the mantle epithelium. These cells are perhaps responsible for the association of the fibers into the regular series of laminae which are a feature of this tunic, since the formation of the filaments appears after releasing eosinophilic and electron dense substances (Hirose *et al.* 1990). Dispersed vesicular cells concentrate at the periphery of the tunic, adjacent to the cuticle. The content of both types of cells reacts positively to a test for proteins, as also does the cuticle (Smith 1970b). The positional relationship of these cells indicates their functional importance in the production of the tunic, and this conclusion is further supported by the observation that the concentration of these cells in the tunic markedly increases after the tunic has been damaged (see immunology of ascidians).

Two types of granular cells, both of them large and conspicuous, traverse the mantle epithelium and concentrate in a dense compact layer immediately above the tips of the mantle cells, where they begin to show signs of degranulation (Wright and Ermak 1982). From there they pass through the tunic toward the cuticle, showing disruption and further loss of contents (Barrington and Thorpe 1968). One type of the cells contains granules. Strong argentaffin and chromaffin (histochemical tests for polyphenols, Pearse 1968) responses of the granules suggest that they are polyphenols. Because of this, these cells might be involved in the quinone tanning of protein (Krishnan,1975), a process which depends on the oxidation of DOPA-proteins by a polyphenol oxidase (Sugumaran *et al.* 1992). There is evidence of a polyphenol oxidase present in the tunic. The artificial tanning of a fragment of the tunic induced by catechol, and its reversibility by adding sodium hypochlorite, are used to demonstrate the presence of polyphenol oxidase (Barrington and Thorpe 1968). Furthermore, a catechol oxidase has been isolated from hemocytes of the ascidian *Pyura stolonfera*, which are the same cells possessing a DOPA-containing protein called ferrascidin (Dorsett *et al.* 1987). Stievenart (1971) also found some histochemical evidence of polyphenols in the tunics of *Ascidella* sp. and of *Halocynthia papillosa.*

Secretion of carbohydrates and proteins into the tunic by the mantle epithelium, and the involvement of the hemocytes in the tunic formation, are clearly important factors. The

production at the surface of a tough and proteinaceous cuticle, which is sometimes rich in tyrosine, is certainly equally crucial. These are the aspects that must be considered in explaining the presence and distribution of bound iodine in the tunic.

Iodine binding in the context of the tunic formation.

Bound radioiodine ^{125}I from a medium is mainly located in the cuticle of the tunic in a *Dendrodoa* sp., along with a sparse distribution of iodine in the rest of tunic (Barrington and Thorpe 1968). In *Styela*, the bound iodine is much more localized in the cuticle (Barrington 1975). The phenomenon is perfectly correlated with the distribution of tyrosine or tyrosine-containing polyphenols in the tunic of them. In *Dendrodoa*, the presence of tyrosine, and of presumptive polyphenol-containing cells, correlate very well with the autoradiographic evidence of bound iodine in the inner layers of the tunic. In *Styela*, dispersion of the iodine over the cuticle can be correlated with a higher tyrosine content of the cuticle (Krishnan 1975, Stievenart 1971). The location of bound iodine in the tunic of these ascidians is clearly determined by the pattern of the production and distribution of tyrosine-rich structural protein.

No trace of any bound iodine over mantle epitheial cells is found. Thus, no iodine is secreted into the tunic from the mantle epithelium cells (Barrington 1975). Radioiodine is, however, present in the blood (Kennedy 1966). X-ray dispersive elemental microanalysis of hemocytes in ascidians revealed that the vacuolated cells contains iodine (Scippa *et al.* 1990).

1.2.2. Endostyle

In vertebrates, the thyroid gland secretes two characteristic hormones, L-thyroxine (T4) and L-triiodothyronine (T3) (Lehninger 1982). Hormones T3 and T4 are synthesized in a series of enzymatic reactions beginning with the iodination of tyrosine residues in thyroglobulin, a glycoprotein, converting them into L-monoiodotyrosine residues. Before iodide can iodinate the tyrosine residues of thyroglobulin, it must be actively transferred from blood into the thyroid gland and oxidized to a different species, such as IO^- (Strum *et al.* 1971). There is a general agreement that oxidation is carried out by a thyroidal peroxidase in the presence of endogenous hydrogen peroxide (Lamas *et al.* 1972). Hormones T3 and T4 remain attached to thyroglobulin in the blood plasma until they are released into the blood in free form by the reaction of proteolytic enzymes. In this view, most of the thyroidal binding is seen to occur either at the cell/ colloid or within the

subapical vesicles. Thus, the site of oxidation of iodide is also apparently the site of iodination. A peroxidase enzyme is essential for the enzymatic conversions of the iodotyrosines to the thyroid hormones (Lame *et al.* 1972).

In ascidians, iodine-binding is associated with endostyle (Figure 1-1), extraendostylar pharynx, and gonads, as well as the tunic (Dunn 1975 and 1980a, Kennedy 1966, Suzuki and Kondo 1971). The endostyle produces a protein-rich secretion (Thorpe *et al.* 1972). There are eight clearly-defined zones of cells (Barrington 1957), each of which presumably plays a role in the production of their filtering membrane which is ultimately passed over the perforated walls of the pharynx. Iodine binding in the endostyle is mainly associated with the apical membrane, multivesicular bodies, and electron dense bodies in the zone 7 cells (Thorpe *et al.* 1972, Dunn 1974, Do Amaral *et al.* 1972, Fredriksson *et al.* 1988). Iodoproteins in the endostyle, in the pharynx, and in the tunic are present primarily in particulate or insoluble form (Dunn 1980a). The proteins are made of several subunits with different molecular weights of 22,000 in the tunic and of 14,000-15,000 in the endostyle in *Molgula, Ciona*, and *Styela* species. Hence the endostylar iodoproteins are distinct from those in the tunic (Dunn 1980a).

Only precursors of thyroid hormones, mono- and di-iodotyrosine (MIT & DIT), are detected in the extracts of these organs (Dunn 1975), suggesting that the iodine binding is an invertebrate character as a sclerotization (Barrington 1975). The process of scleroprotein formation in the mussel, *Mytilus galloprovincialis*, has the binding of iodine as its part (Roche *et al.* 1960), where the binding of iodine to scleroprotein results in the production of MIT and DIT, accompanied by only minimal amounts of iodothyronines (Roche *et al.* 1964). However, the presence of MIT, DIT, and T4 has been demonstrated both in the tunic and in the endostyle (Do Amaral *et al.* 1972), which supports the protothyroidal role of the endostyle. The conflicting issue has been solved by using a radioimmunoassay (Dunn 1980a). The results reveal that most of the T4 existing in the tunic is a protein-bound form, but traces T4 and T3 of the endostyle are in free forms. The blood is also recognized as a major iodine-binding system (Kennedy 1966, Dunn 1980a). Hormone T4 in the blood is noncovalently linked to serum proteins (Dunn 1980a), indicating that T4 normally circulates in the ascidian blood. Among the locations described, the highest content of T4 has been demonstrated in the tunic (Dunn 1980a). The enzyme responsible for iodination, a peroxidase, has been characterized from the endostyle as a membrane-bound protein in the form of molecular complex (M. W. ~ 340,000) (Dunn, 1980b). The enzyme catalyzes the iodination of tyrosine and protein, and is inhibited by high concentrations of iodide. It is also capable of catalyzing a coupling of iodotyrosyl

residues in thyroglobulin *in vitro*, forming T3 and T4. The results suggest that the lack of significant T3 and T4 formation in the endostyle *in vivo* is attributed to the absence of a suitable substrate rather than to an enzymatic deficiency.

Homogenates of the tunic incorporate ^{125}I into protein and free tyrosine *in vitro*. Furthermore, the activity depends upon a hydrogen-peroxide generating source and is inhibited by boiling of the homogenates or by addition of methimazole, an inhibitor of peroxidase, suggesting that a peroxidase-mediating iodination also occurs in the tunic (Dunn 1975). However, the pharynx and gonad are not able to bind iodine (Dunn 1975), although they demonstrate a pyrogallol peroxidase activity (Dunn 1980b).

1.2.3. Conclusion

In conclusion, two characteristic processes are observed in ascidian iodine metabolism. One of these is the binding of iodine to tunic protein. The other is intracellular binding which occurs within the cells of a specialized region (zone 7) of the endostyle. The second process may be related phylogenetically to the thyroid hormone biosynthesis of vertebrates. A significant amount of free T4 in the blood, the participation of several blood cells in tunic formation, and the highest content of T4 in the tunic, suggest that T3 and T4 produced in the endostyle are secreted in the blood stream to stimulate generation of the tunic. As a matter of fact, polyphenol oxidase activity, which catalyzes the tanning activity within the tunic, has been significantly increased by treatment of T3 (Thorndyke 1973). The products resulting from peroxidase-mediated iodination in the various regions of ascidians are determined by the nature and reactivity of the proteins present (Dunn 1980b). Various peroxidase enzymes are dependent upon vanadium, which could be inhibited at low pH and be activated by vanadate (Wever and Kustin 1990).

1.3. Vanadium accumulation

Vanadium exists in valence states of +2, +3, +4, and +5, the last two being the most stable. The chemistry of vanadium in natural waters is poorly understood, partly because of the complexity of these latter oxidation states.

Seawater contains dissolved vanadium ions at a concentration of 35 nM (Cole *et al.* 1983, Collier 1984). However, some ascidians accumulate vanadium in their blood cells to a maximum concentration of 1 M (Carlson 1975), which is more than 10 million times that of seawater.

Traditionally, morula cells were thought to be involved in the accumulation of vanadium ion (called vanadocytes), since the color of cells resembled that of vanadium complex, and dense granules were observed in the cells after fixation with osmium tetroxide (Robinson *et al.* 1984). Recently, X-ray microanalysis revealed that more vanadium ions were associated with the vacuole membranes of granular ameobocytes, signet ring cells, and compartment cells than the vacuoles of the morula cells of *Phallusia mammillata* and *Ciona intestinalis*. By using fluorescence-activated flow cytometry in conjugation with microanalysis, the morula cells contained nearly all of the free tunichrome detected and up to 30% of vanadium, whereas the signet ring cells yielded only a trace of free tunichrome but a majority of the vanadium (Oltz *et al.* 1989). A Japanese group tackled this problem using a combination of techniques of Ficoll density gradient centrifugation and neutron activation analysis (Michibata *et al.* 1989). It was apparent that the vanadocytes were the signet ring cells, not the morula cells.

The accumulation of vanadium has been noticed in several species of the Aplousobranchia and the Phlebobranchia, whereas species of the Stolidobranchia contain relatively smaller amounts of vanadium, but a high level of iron (Michibata 1989). Surprisingly, almost all of the vanadium is present in a reduced form in the blood cells, although the metal exists in a +5 oxidation state as monomeric vanadate (i.e. $H_2VO_4^-$ /HVO_4^{2-}; pK 8.3, seawater pH 8.3) in seawater. Analysis of the data obtained by a superconducting quantum interference susceptometery indicated that about 90 % and 10 % of vanadium in the ascidian blood cells were in the +3 and +4 oxidation states, respectively (Lee *et al.* 1988).

It has been known that a physiological concentration (0.75 μM) of pentavalent vanadium ions causes inhibition of Na^+-K^+-ATPase (Beaugé and Glynn 1977). Vanadium within ascidian tissues is much higher than the concentration needed to cause inhibition of phosphoenzyme activity (Macara 1980). The activity of myosin ATPase was inhibited by pentavalent vanadium but was not inhibited by tetra- or trivalent ion. The addition of 5 mM ascorbic acid, known to reduce pentavalent vanadium ion to its tetravalent state, to the reaction mixture of V^V and myosin ATPase reduced the inhibitory effect of V^V on ATPase (Michibata *et al.* 1989).

The complexation of vanadyl ion with oxalate is highly favored with the following equilibrium constants

$$VO^{2+} + 2C_2O_4^{2-} \text{ --- } VO(C_2O_4)^{2-} \qquad pK_{app} = 12$$

$$VO(OH)^+ + C_2O_4^{2-} \text{ ---- } VO(OH)C_2O_4^- \qquad pK_{app} = 6.5$$

at 0.1 M ionic strength.

Vanadium (V^{V}) complexes with oxalate were studied at pH values from 1 to 7 at 25°C in 0.6 M NaCl (mimicry of seawater) (Ehde *et al.* 1986). Using potentiometric and ^{51}V NMR data, the researchers determined apparent equilibrium constants for the complexes $H_4VO_4(C_2O_4)_2^{3-}$ and $H_4VO_4C_2O_4^-$, defined by the reactions:

$$2H^+ + H_2VO_4^- + 2C_2O_4^{2-} \text{ --- } H_4VO_4(C_2O_4)_2^{3-} \qquad pK_{app} = 17.11$$

$$2H^+ + H_2VO_4^- + C_2O_4^{2-} \text{ ---- } H_4VO_4C_2O_4^- \qquad pK_{app} = 13.07.$$

Ehde *et al.* also studied the equilibria between vanadate (V^{V}) and citrate at pH $\geq$ 3 and in 0.6 M NaCl. For the general formula of complexes $(H^+)_p(H_2VO_4^-)_q(C_6H_5O_7^{3-})_r$, they found apparent log $\beta_{p,q,r}$ values of $\log\beta_{1,2,1} = 12.84$, $\log\beta_{2,2,1} = 19.8$, $\log\beta_{3,2,1} = 24.12$. Based on the results, one of the reasons that ATPase within ascidians is intact, in spite of a high level of vanadium, may be that the pentavalent vanadium ion is readily reduced to the tetravalent and/or trivalent oxidation states by endogenous reducing substances in ascidian tissues. Still, due to the extreme-high affinity of metabolic products of TCA cycles for vanadium ions (V^{IV} and V^{V}), either the reducing materials must have much larger equilibrium constants than those of oxalate and citrate, or the accumulation of vanadium has to be confined to specialized tissues.

The accumulation mechanism of vanadium in ascidians will be reviewed from the viewpoint of three aspects: inorganic chemical species, organic ligands, and biochemical proteins.

1.3.1. Inorganic chemical species

To understand the solution chemistry of vanadium, each species of vanadium ions needs to be briefly described. When all of the possible species of each oxidation state are considered using reduction potentials and equilibrium constants, one can construct Eh-pH diagram of vanadium in an aqueous system (Pourbaix 1966, Figure 1-2). The hydrolysis of V^{III} has received considerable attention in the last several decades. Vanadium (V^{III}) is rapidly and completely hydrolyzed in aqueous solution, leading to precipitation of relatively insoluble vanadium (V^{III}) oxyhydroxides. Vanadium ions, V^{IV} and V^{V}, are the most likely forms in which vanadium is transported in natural waters. V^{IV} forms the oxocation VO_2^+, vanadyl, while V^{V} forms oxyanions such as $H_nVO_4^{n-3}$. V^{V} is also known to form polymeric species. However, vanadium exists in the +5 oxidation state in the ocean.

The intracellular pH of vanadocytes has been disputed. Following Henze's discovery of 1 N acidity in ascidian blood cells, Agudelo *et al.* (1983) recently claimed that the intracellular pH was neutral on the basis of measurements made by a new technique

Figure 1-2. Eh - pH diagram for vanadium aqueous species in the system V-O-H (adopted from Pourbaix 1966).

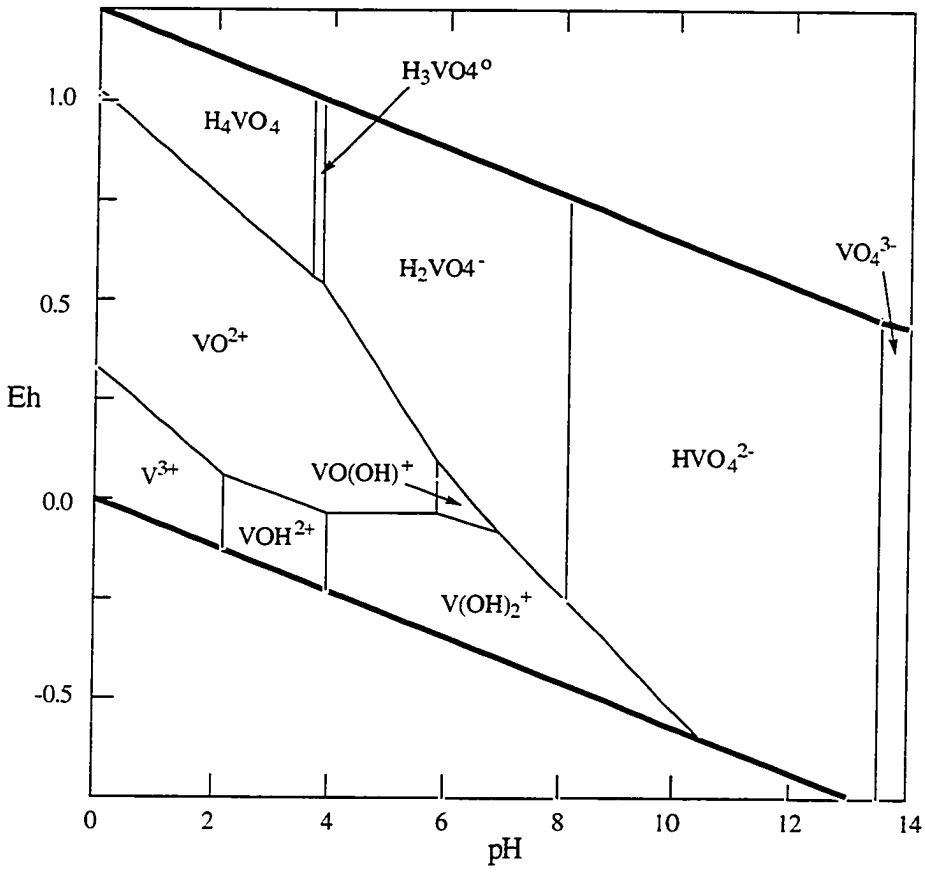

with improved trans-membrane equilibrium of ^{14}C-labeled methyl amine. Conversely, a blood cell of pH value 1.8 was reported, based on a new finding that the electron spin resonance (ESR or electron paramagnetic resonance, EPR) line width reflected accurately the intracellular pH (Frank *et al.* 1986, 1988). One of the reasons for the variation in the pH values reported for ascidian blood cells is probably the measurement of pH without cell fractionation. In other words, these determinations which indicate a neutral cytosol housing acidic vacuoles may resolve several disparities.

The low pH of 2.6 of the signet ring cells (Michibata 1989), and the higher content of sulfur in the blood cells, allowed the postulation that vanadium sulfate complex could be a strong candidate for the explanation of the vanadium accumulation mechanism. Several analyses using ^{1}H-NMR, EPR, and X-ray absorption spectroscopy of *Ascidia ceratodes* blood cells suggested that the vanadium was coordinated as $[V(III)SO_4(H_2O)_{4\text{-}5}]^+$ within vanadocytes (Tullius *et al* 1980, Frank *et al.* 1987), a complex which is stable below pH 3.

While membrane-bound alkyl sulfates are abundant in ascidian blood cells (Frank *et al.* 1987), they are very poor ligands for vanadium (V^{IV} or V^{V}), exhibiting K_{fs} approximately 10^2 (Wanty and Goldhaber 1992, Collier 1984). However, the complex will be discussed later in terms of storage of vanadium.

1.3.2. Organic ligands

Given the fact that the cytosolic pH of virtually all living cells is maintained near neutrality, if the final vanadium complex proves to be $[V(III)SO_4(H_2O)_{4-5}]^+$, vanadium must somehow reach an acidic vanadocyte. Therefore, it can be assumed that reducing agents for reduction of vanadate ion to the vanadyl form or the trivalent state exist in the blood cells.

At pH values above 4, the vicinal hydroxyl substituents of catechol and pyrogallol rings confer potent chelating properties toward vanadium and iron (Cantley *et al.* 1978, Ferguson and Kustin 1979, Jameson and Kiss 1986). Some formation constants of these ligands toward V^{IV}, V^{III}, Fe^{III}, and Fe^{II} are greater than 10^{10}, and several surpass 10^{28}.

Several years ago Kustin's group reported the successful isolation of a reducing ligand from the blood cells of *Ascidia nigra* and *Ciona intestinalis* under a reducing atmosphere (Macara *et al.* 1979). The substances were named tunichromes which were later identified as hydroquinoid peptides by Nakanishi's group only from *A. nigrra* (Oltz *et al.* 1988). The reducing property is due to the presence of catechol or pyrogallol subunits within the tunichromes (Figure 1-3).

Tunichrome has subsequently been found using UV and EPR measurements to reduce V^{V} to V^{IV} and V^{III}, V^{IV} to V^{III} (Michibata *et al.* 1990) and Fe^{III} to Fe^{II} *in vitro* (Ryan *et al.* 1992, Macara *et al.* 1979, Oltz *et al.* 1989). Aqueous solutions of vanadium sulfate $[V(III)_2(SO_4)_3]$ and vanadium oxosulfate $[V(IV)OSO_4]$ at low pH exhibit absorption maxima at 420 nm, 620 nm, and 760 nm with a shoulder around 625 nm, whereas an aqueous solution of sodium vanadate $[Na_3VO_4(V)]$ exhibits no absorption maximum in the visible range (only absorbs less than 500 nm). The oxovanadyl chemical species $[VO^{2+}(IV)]$ is the only species of vanadium that is detectable by EPR. Because the intensity of the EPR signal due to VO^{2+} (IV) depends on pH, the pH of samples was adjusted to achieve the maximum intensity of signals. Interestingly, the generation of V^{III} was more facile from V^{V} than from V^{IV} (Ryan *et al.* 1992). The intermediate V^{IV} could interact with its co-intermediate, a tunichrome (Mm-1) semiquinone, which is a powerful reductant. However, Mm-1 has been isolated only from *Molgula manhattensis* which is

Figure 1-3. The tunichromes. An designates *Ascidia nigra*, a vanadium accumulator, while Mm designates *Molgula manhattensis*, an iron accumulator.

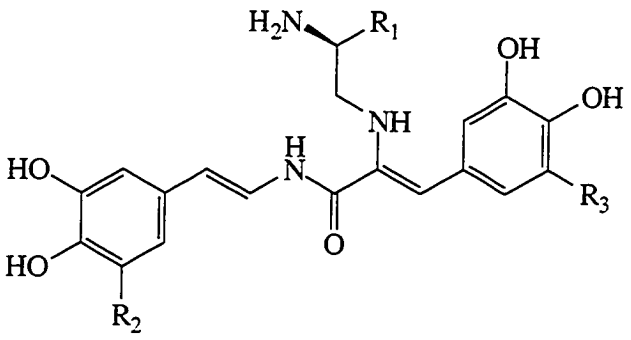

tunichrome	R_1	R_2	R_3
An-1	hydroxy-DOPA	OH	OH
An-2	DOPA	OH	OH
An-3	DOPA	H	OH
Mm-1	glycine	H	H
Mm-2	leucine	H	H

an iron sequestering Stolidobranch. Therefore, the results may not be applicable to the real system in ascidians which accumulate vanadium ions in the blood cells.

One of the concerns about this result was that this subpopulation of signet ring cells did not emit fluorescence, which contained high levels of vanadium. The intensity of fluorescence is indicative of the concentration of vanadium in blood cells because both tunichrome and vanadium have been presumed to be at approximately equimolar concentrations based on the stoichiometry of the reaction of vanadium with tunichrome purified from ascidians. However, failure to detect fluorescence or free tunichrome in the signet ring cells by peracetylation assay (acetylation of tunichromes and subsequent TLC analysis of tunichrome acetates) does not necessarily mean that tunichrome is absent. Specially, paramagnetic species such as vanadium or tunichrome semiquinone are likely to quench tunichrome's autonomous fluorescence and alter its acetylation pattern (Oltz *et al.* 1989).

Another explanation is that there may be almost no tunichrome in the signet ring cells. In the vanadium-containing blood cells (signet-ring cells) and the tunichrome-containing cells (the morula cells), semiquantitative comparison of the tunichrome content (determined by HPLC on polystrene phases) with the sulfate and vanadium content demonstrated roughly equivalent amounts of the vanadium compound (Bayer *et al.* 1992). Characteristic for tunichrome is the styrylamide structure, which may be formed

biogenetically by decarboxylation and dehydrogenation of a tripeptide with three trihydroxyphenylalanines (Figure 1-4).

In the strongly acidic milieu there, vanadate ($H_2VO_4^-$) may become VO_2^+ (See Figure 1-2 for clarity), which can attack the sulfur while itself being reduced to the trivalent sulfatovanadium aqua complex. At the same time the peptide is oxidized to quinone, which undergoes decarboxylation to form styrylamide **I**. While the positively charged sulfatovanadium complex can not pass through anionic channels, the tunichrome can leave the vanadium-containing blood cells and collect in the morula cells.

To clarify the subject, the location of tunichrome *in situ* has to be established. Traditionally, the formation of the 335 nm chromophore in the UV spectrum after lysis of cells, and a band at 515 nm on 436 nm excitation in the fluorescence spectrum, were utilized to locate tunichrome *in vivo* (Oltz *et al.* 1988). However, the most recent results showed that there was no evidence for tunichrome in intact blood cells of two Ascidiidae species, *Ascidia ceratodes* and *Phallusia julinea,* although the free tunichrome assay proved the existence of tunichrome in *A. ceratodes* (Parry *et al.* 1992). Spectrofluorometric emission peaks reported by previous workers as evidence of tunichrome *in vivo* seemed to be the same positions as water Raman bands. Microscopic observations of the process of blood cell lysis using HCl revealed that the signet ring and compartment cells lysed first, with the vacuoles of the morula cells being released later, leaving the outer membrane of the morula cells intact. The remnant of the morula cells closely resembled the signet ring cells. In the case of cell lysis in the presence of 1,10-phenanthroline, in which the 335 nm chromophore (attributed to tunichrome) did not form, the compartment and signet ring cells, but not the morula and pigment cells, lysed. Therefore, it was postulated that both the lysis of the morula and compartment-signet ring cells were necessary for the formation of tunichrome. So the morula cells may contain the precursor of tunichrome. However, should the previous mechanism of accumulation of vanadium be true, and fluorescence and UV be interfered with other cell materials, the results could be interpreted differently. Yellow fluorescence, which was believed to be associated with the morula cells due to tunichrome, can not be used to locate tunichrome *in situ* because the same florescence has been observed in the blood cells of species in which tunichrome has not been found, such as *Ciona intestinalis* and *Pyura stolonifera.*

1.3.3. Biochemical proteins

EPR studies confirmed the presence of vanadium (V^{IV}) in all vanadium-containing

Figure 1-4. Proposed scheme for vanadium accumulation in blood cells of *Phallusia mammilata* (Bayer *et al.* 1992).

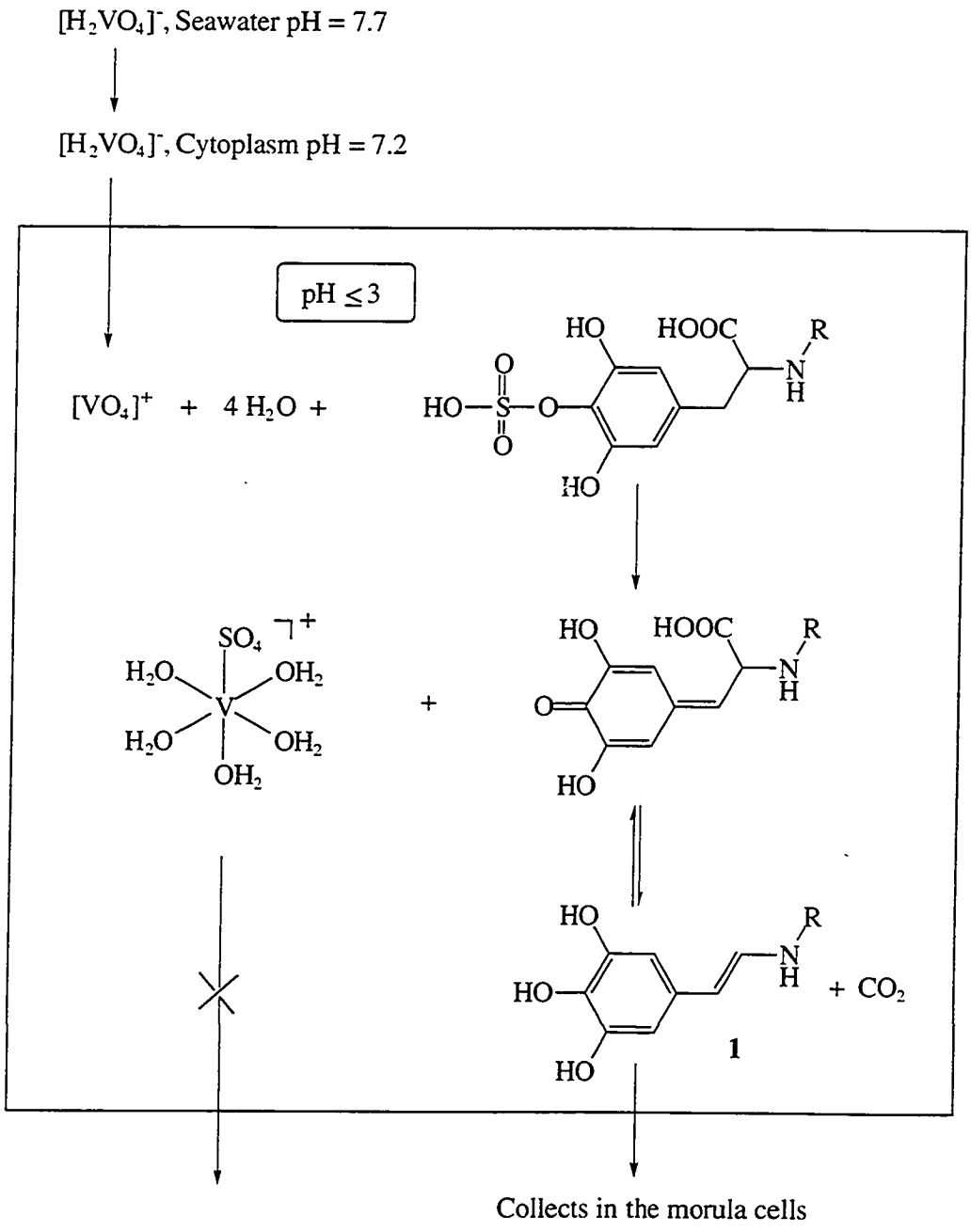

Aplousobranchia (Brand *et al.* 1989) in which no tunichrome has been detected so far. The results may be explained by the fact that there may be functionally analogous organic ligands, such as several cyclic peptides (Sesin *et al* 1986), or at least DOPA analogues

(Azumi *et al.* 1990, Lindquist *et al.* 1988). Another explanation may be possible through DOPA-containing proteins (Dorsett *et al* 1987). Recently, a vanadium-binding substance, called vanadobin, has been isolated from *Ascidia sydneiensis* by a combination of techniques including Sephadex G-15, neutron activation analysis, and EPR (Michibata *et al.* 1991, Michbata and Uyama 1990, Uyama *et al.* 1991). Vanadobin, a colorless protein, could reduce vanadate (V^{V}) to vanadyl (V^{IV}) even under aerobic condition and maintain it in the reduced form. The substance was associated with the signet ring cells. The substance recognized by monoclonal antibody was a single polypeptide of ca 45 kDa from *Ascidia sydneiensis*, *A. ahodon*, and *Ciona intestinalis*. The protein detected from *Halocynthia roretzi* gave a band that corresponded to a molecular weight of ca 43 kDa. Therefore, in the case of *C. intestinalis* vanadobin seems to be analogous to tunichrome for the accumulation of vanadium. A different molecular weight of vanadobin in *H. roretzi* may or may not reflect a different selectivity for iron instead of vanadium.

1.3.4. Conclusion

Three key considerations of vanadium-accumulation are the energy requirements, the ligands involved, and the attendant pH. The finding that vanadocytes (Dingley *et al.* 1981) translocate vanadate via specific anion transport systems utilized by phosphate ion suggests that some variant of Peter Mitchell's chemiosmotic model (Mitchell 1961) is engaged (Figure 1-5). Unblocking of vanadate uptake by inhibitors of glycolysis and of oxidative phosphorylation suggested that ascidians vanadium accumulation is not an active transport process (Dingley *et al.* 1981). The passive sequestration of vanadate against an apparent 10 million fold concentration gradient can be achieved in two ways: 1) vanadate in flux is coupled to the virtual efflux of ions with equivalent charge; 2) the internal vanadate concentration is effectively diminished, following influx. Vanadate undergoes a two-step reduction to vanadium (V^{III}), or are reduced to the trivalent sulfatovanadium aqua complex via VO_2^+ ion only if vanadate does not go through mitochondria membrane and not interfere intermediates of glycolysis in cytoplasm.

Several hypotheses for the biological roles of the vanadocytes have been proposed, although no conclusive evidence has been presented. Tunic formation (Robinson *et al.* 1986) analogous to sclerotization of insect cuticle via oxidation of catecholamine cross-linking agents (Sugumarau *et al.* 1992) has been proposed. Since the cellular milieu around vanadium (V^{III}) and tunichrome must be nonoxidative to a high degree, a new hypothesis (Smith 1989) correlated their redox activity to anaerobic metabolism. Similarly,

Figure 1-5. A model for the facilitated diffusion of vanadate into vanadocytes (Smith 1989)

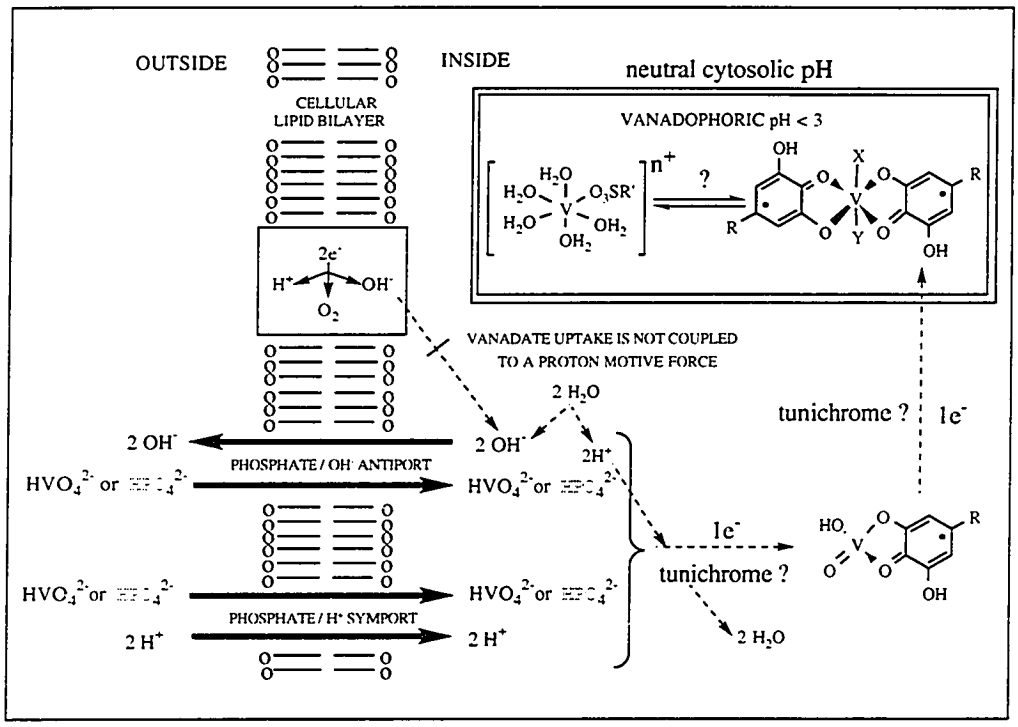

vanadium-accumulating cells may accommodate the metabolic end product problem by providing the animal with an alternative electron and proton sink (Hochachka and Mommsen 1983).

Lastly, the level of vanadium during embryogenesis increased dramatically 2 weeks (at metamorphosis) after fertilization (Uyama *et al.* 1993), and the amount of vanadium accumulated in juveniles reached 930 ng/individual, which was ca 420,000 times higher than the amount in unfertilized eggs. It was suggested that the accumulation of vanadium coincided with the differentiation of the vanadocytes during the development of ascidians. Various proposals for ecological functions of vanadium have been made, including a role in anti-fouling (Stoecker 1978), anti-predation (Stoecker 1980a, b), and anti-infection (Rowley 1983).

1.4. Chemical adaptation of ascidians

Marine natural products chemistry, mainly focused on unusual structural types which have never been encountered in the terrestrial environment, has changed the direction

of its research gradually toward defining the biological roles of novel secondary metabolites, especially their ecological functions. The higher metabolic cost of structurally-complex natural products, in conjugation with the absence of obvious physical protections in ascidians, often solicits marine natural products chemists to assume defensive functions of compounds from ascidians. Feeding-deterrence, anti-fouling, inhibition of overgrowth, and sun-screening are favorite subjects among the possible roles. Biological controls over unstability in marine invertebrate communities are grouped under predation, competition, and disease and parasitism (Nybakken 1982). In benthic marine communities, an intense competition for space among invertebrates has been inferred from the fact that most of benthos are sedentary filter-feeders. This is particularly important since most benthic invertebrates experience a larval stage during their life cycle, and thus the inhibition of larval settlement (anti-fouling) could be an important adaptation. Allelophathic effects are often a major adaptation among slower-growing species. Alternatively, no specific biological function of these novel secondary metabolites can also be considered. It has been proposed that metabolites are simply byproducts of biochemical process essential to the organisms, or remnants of adaptations in distant past (Pawlik 1993).

Either lack of pure-isolation of active constituents or providing the structural elucidation without experimental support to claim the ecological activity indicates a practical limitation of research, except for a few examples. In reality, both biologists and chemists have their own beneficial side of training to approach the ecological values of novel natural products: namely, ecological background and chemical discipline.

1.4.1. Feeding deterrence

Vanadium accumulated (over 100 ppm) in ascidians within the acidic bladder cells (pH less than 2) was proposed to deter predators (Stoecker 1980b). However, this proposal was criticized in terms of buffer capacity of seawater and rapid neutralization of acid by calcareous spicules in the tunic of some species, no universal vanadium accumulation in ascidians, and observation of predation on ascidians by mollusks and sea stars (Parry 1984). Nevertheless, the instantaneous effect of acid and less general importance of theses predators (mollusks and sea stars) in the role of constructing tropical benthic communities where ascidians are abundant are discussed (Lindquist *et al.* 1992).

Some ascidians which do not have the acidic bladder cells and do not accumulate vanadium showed unpalatability to fish (Stoecker 1980b). The result may be attributed to chemical defense of ascidians (Young and Bingham 1987). One of the most important

factors to limit the dispersal of ascidian larvae is predation. In the case of *Lissoclinum patella*, the majority of larvae (87 %) were consumed by fish before settlement (Olson and McPherson 1987). Among the survivors only two-thirds of the larvae could settle after being killed by corals and zoanthids. The larvae of *Ecteinascidia turbinata* , which were rejected by juvenile pinfish, contained deterrent chemicals that were nonproteinic nature and molecular weight of less than 14,000. The responsible compounds, thus, may be the ecteinasidins (Wright *et al.* 1990, Rinehart *et al.* 1990a, b, c, and 1991, Sakai *et al.* 1992, Guan *et al.* 1993), a novel class of cytotoxic alkaloids isolated from the species. However, there is no conclusive evidence to support this hypothesis.

There are a limited number of studies of chemical defense from ascidian secondary metabolites. A recent study revealed that both adults and larvae were unpalatable to a variety of predators (Lindquist *et al.* 1992). Didemnin B and nordidemnin B from *Tridemnum solidum* (Rinehart *et al.* 1981a, b, 1988, Hossain *et al.* 1988, McKee *et al.* 1989), and polycarpidines A - D (Carte and Faulkner 1982) from *Polyandrocarpa* sp. deterred predation of reef fishes, a hermit crab, and snails, respectively. However, a prenyl hydroquinone (Howard *et al.* 1979), didemnenones A and B (Lindquist *et al.* 1988), patellamide C (Sesin *et al.* 1986) did not deter feeding. In contrast to previous study (Paul *et al.* 1990), tambjamine E was also active in deterring reef fishes. In addition, eudistomins G and H, ascidian metabolites reported as antiviral agents (Kobayashi *et al.* 1984), were not effective as fish deterrents (Davis 1991). The results clearly showed that not all pharmacologically-active compounds function as feeding deterrents in marine environment (Schulte and Bakus, 1992).

Both an ascidian *Atapozoa* species and its predator *Nembrotha* species contained tambjamines C, E, F, and a related aldehyde (Lindquist and Fenical 1991). They were the major component of mucus secreted by nudibranchs upon irritation (Carté and Faulkner 1983). In addition, the nudibranchs possessed a novel tetrapyrrole (Kazlauskas *et al.* 1982), but the ascidian had a trace amount of that compound. Tambjamines C and F, and the tetrapyrrole were significant feeding deterrents toward a variety of carnivorous fish at natural or below the natural concentrations (Paul *et al.* 1990). Among them, the tetrapyrrole was the most potent. However, tambjamines E and the aldehyde were not deterrents at or above natural concentrations. The relative abundance of tetrapyrrole in the nudibranchs compared with its paucity in the ascidian suggested that the nudibranchs sequestered the defensive metabolites from the ascidian. There are cases where this has been observed. Lamellarin alkaloids have been isolated from two different sources, a mollusc of *Lamellaria* species (Anderson *et al.* 1985) and the ascidian *Didemnum*

chartaceum (Lindquist *et al.* 1988). Similar results have been obtained on both an ascidian (maybe a *Cystodytes* sp.) and its predator mollusc *Chelynotus semperi* which contained the pentacyclic alkaloids kuanoniamines A-D (Carroll and Scheuer 1990). No experimental evidence was given to support a defensive evolution even though it seemed that they followed the same tracts of molluscs (Karuso 1987).

The presence of L-galactose as a major constituent in the tunic (Pavao *et al.* 1989) may make the tunic of ascidians resistant to degradation by D-galactosidase by microorganisms and common mollusk predators which have the capability of boring.

1.4.2. Anti-fouling

Fouling is normally established in the following sequence composed of four phases: biochemical conditioning, bacterial colonization, unicellular and multicellular colonization (Wahl 1989). However, not always the microbial film may be required. The attachment of the larval barnacle, *Balanus amphitrite*, showed no preference to settle on surfaces with a microbial film generated by bacteria (Maki *et al.* 1988). There are three kinds of phenomena resulted from the fouling: tolerance, avoidance, and defense. Avoidance characterized by accelerated growth does not seem to be the choice of ascidians. Tolerance is often observed in the ascidians which have a very thick tunic, such as *Polycarpa* species (Monniot *et al.* 1990). Most of ascidians would appear to have a variety of adaptive mechanisms. These mechanisms are composed of mechanical and chemical defenses. Periodical shedding of the cuticle as a mechanical defense has been reported in the ascidian *Polysyncraton lacazei* (Wahl and Banaigs 1991).

The conspicuous growth form and apparent lack of mechanical defenses has resulted in speculation of chemical defenses in numerous ascidians. Highly diverse and abundant ascidians in the marine environment are well known to sequester vanadium at extremely high concentrations and to possess an acidic tunic. Those factors were proposed to explain the deficiency of epibionts of ascidians (Stoecker 1980a, b). However, epizoic recruitment did not appear to be affected by vanadium accumulation. Furthermore, there was no correlation between acidity and antifouling in *Botrylloides* species since they lack acidic bladder cells and do not accumulate vanadium but are free of epibionts (Parry 1984). Even acidity has been positively correlated to fouling (Davis and Wright 1989). The ascidian *Eudistoma capsulatum* was colonized by 17 species of epibionts, although the animal was highly acidic (pH = 1-2). In addition, measuring pH on the surface of the tunic utilizing pH paper can be problematic. Obviously the pH is dependent upon the amount of

water present and the precise methods used (Wahl and Banaigs 1991).

The proposition that secondary metabolites may function as antifoulants has been made frequently over the last decade. However, there are limited numbers of studies on that subject. The ascidian *Eudistoma olivaceum* possessed a relatively clean surface compared to *E. capsulatum*. The bioactivities of their extracts, such as cytotoxicity, antimicrobial and antiviral activities, were negatively related to the extent of colonization on the ascidians (Davis and Wright 1989). Eudistomins G and H were identified as the antifoulants for invertebrate larvae (Davis 1991, Davis and Wright 1990). One additional nontoxic substance was also isolated as an inhibitor of settlement, but it was not characterized (Davis and Wright 1990). The ascidian *Polysyncraton lacazei* contained several antibiotic and mutagenic compounds in a butanol fraction of its extract. These compounds combined efficiently inhibited development and survival of settling larvae (Wahl & Banaigs 1991). However, the exact nature of the compounds was not identified. Extracts of the ascidian *Cystodytes lobatus* from La Jolla significantly inhibited bacterial colonization (Richards-Gross 1993). Possible ecological roles of pharmacological activities in Mediterranean benthic communities were investigated (Uriz *et al.* 1991). Antibacterial and antifungal activities appeared to correlate to general observations of antifouling, but cytotoxic and antimitotic activities seemed to be less effective.

Various ascidians excrete riboflavin, isoxanthopterin and 2-amino-4-hydroxyptheridine into ambient water. Because these compounds serve as vitamins for marine animals, they thus may play an inducible role in the settlement of other species (Gaill and Momzikoff 1975, Momzikoff and Gaill 1973).

1.4.3. Microbial origins of natural products

The isolation of compounds from ascidians which are identical or similar to microbial metabolites and the highly specific microbial associations of some ascidians evoke the question of the possible microbial biosyntheses of the compounds. The same situation happens when phylogenetically distant invertebrates, without an obvious relationship of prey-predator with ascidians, contain secondary metabolites which are similar or identical to ascidian compounds.

Ascidians are associated with a variety of organisms. In didemnid ascidians, symbiotic (referring to living together) algae are localized in the cloacal systems (Eldrige 1966). The association is considered to be species specific (Knott 1977). Unicellular algae are also abundant in the tunic tissue of *Trididemnum solidum* (Sybesma *et al.* 1981). The

algae, prokaryotic procyanophyte bounded by a typical gram-negative wall (Cox *et al* 1985), were spherical and reddish in color. The algae contained chlorophyll a, but not chlorophylls b or c. Such absence of chlorophylls b and c, and the presence of phycobilisomes are characteristic of the blue-green algae, thus this organism was named *Synechocystis trididemni* (Lafargue and Duclaux 1979). Another ascidian, *T. clinides*, seemed to have a non-specific association with the unicellular cyanophyte (Cox *et al.* 1985). *T. tegulum* was associated with the same cyanophyte and with a diatom (Cox *et al.* 1985). The cyanophytes contained phycoerythrins possessing both phycourobilin and phycoerythrobilin chromophores (Parry 1984, Cox *et al.* 1985, Larkum *et al.* 1987). The absorbance maxium at 500 nm coincides with the maxium wavelength of transmitted light in tropical water (Jerlov 1976). The main role of these pigments is to enhance the light harvesting capability of the phycobilisomes in the region between 460 nm and 500 nm. No significant difference of pigments except for phycourobilin was observed with the ascidians from different depths (Symbesma *et al.* 1981). However, oxygen production of deep water colonies was significantly higher than that of shallow water colonies, although oxygen consumption remained the same magnitude. The variation in chromophore content was viewed as a result of chromatic adaptation (Parry 1988a, b), a phenomenon known in macroalgal systems. The pigments thus extended the habit range of ascidians (*Didemnum* spp. and *Trididemnum* spp.). Two unidentified filamentous cyanophytes, *Oscillatoria* species, were found in *T. miniatum* along with numerous *Prochloron* (prochlorophyte) cells (Larkum *et al.* 1987).

Lewin (1977) reported associations between a didemnid ascidian and prokaryotic algae (*Prochloron* spp.) which contained chlorophyll a and b but no phycobilins. Symbionts of colonial ascidians are mainly of this group, the Prochlorophyta (Kott *et al.* 1984). DNA-DNA reassociation results revealed that all *Prochloron* spp. from different didemnids (*Lissoclinum patella, Diplosoma similis*, and unknown) are closely related but slightly related with the *Synchocystis* sp. (Stam *et al.* 1985), which indicated conspecific association of the *Prochloron* and the didemnids.

The association of light-mediated nitrogenase activity with intact colonies of *Lissoclinum patella* but not of isolated *Prochloron* cells or symbiont-free *L. patella* indicated that a strong dependence of N_2 fixation upon the intact symbiosis in oligotrophic tropical water (Pearl 1984). No ascidians such as *Didemnum molle*, *L. voeltskowii*, and *Diplosoma virens*, showed N_2 fixation activity. However, the light-dependent assimilation of ^{15}N labelled ammonium sulfate into glutamine monitored by NMR seemed to suggest N_2 fixation (Parry 1985). Transfer of photosynthate from *Prochloron* to the ascidians was

reported (Pardy and Lewin 1981, Griffiths and Thinh 1983). Often phagocytosis of *Prochloron* cells by amoebocytes occurred in the ascidian *Lissoclinum voeltzkowi* (Cox 1983). However, transfer of metabolites in the opposite direction remains to be demonstrated.

Several cyclic peptides have been isolated from the ascidians *Lissoclinum patella* and *L. bistratum* (Degnan *et al.* 1989a and b, Sesin *et al.* 1986). Patellamide D, and lissoclinamides 4 and 5 were suggested to be present in the obligate symbiotic alga *Prochloron* and in the host ascidian in almost equal amounts (Degnan *et al.* 1989a). The ascidian *L. bistratum* contained bistratamides A and B (Foster *et al.* 1992a), and bistramides A and B. After separation of the symbionts from the host, the former compounds were located in the algal symbionts but two macrocyclic ethers (bistramides) were confined to the host cells (Degnan *et al.* 1989b). Hence, it was suggested that the peptides were synthesized by the algal symbionts and the macrocyclic ethers by the ascidian. These results were indirectly supported by the fact that the cycloxazoline isolated from *L. bistratum* was found to be identical to westiellamide, a compound produced by the free-living blue-green alga *Westiellopsis prolifica* in culture (Hambley *et al.* 1992, Prinsep *et al.* 1992). A very unusual chlorinated terpenoid dichlorolissoclimide identified from the ascidian *L. voeltzkowi* had a close resemblance to common algal metabolites (Malochet-Grivois *et al.* 1991). The isolation of dehydrodidemnin B from the ascidians *Aplidium albicans* and *Tridemnum solidium*, and the association between *T. solidium* and the symbiotic cyanophyte *Synechocystis trididemni* indicated a potential microbial origin of the compound (Rinehart *et al.* 1981a,b, and 1988, Hossain *et al.* 1988, McKee *et al.* 1989, Lafargue and Duclaux 1979). However, no data have been presented to confirm these proposals.

There is also circumstantial evidence of the bacterial origin of some ascidian compounds. The ascidian *L. patella* also contained a non-nitrogenous compound lissclinolide (Davidson and Ireland 1990) which had the same general structure as a bacterial metabolite tetrenolin (Pagani *et al.* 1973, Gallo *et al.* 1969). An unidentified ascidian *Eudistoma* sp. contained 11-hydroxystaurosporine (Kinnel and Scheuer 1992). Compounds containing the same basic structure have been isolated from numerous soil bacteria of the genus *Streptomyces* (Omura *et al.* 1977, Furusaki *et al.* 1978, Tsubotani *et al.* 1991). Tambjamines were isolated from *Atapozoa* sp., *Sigillina cyanea* (= *Atapozoa*), and the bryozoan *Bugula dentata* (Lindquist and Fenical 1991, Kang unpubl., Paul *et al.* 1990). Bacteria produce many related compounds. A blue pigment, a tetrapyrrole, was characterized from an undescribed ascidian, *Atapozoa* sp., the bryozoan *B. dentata*, and a

mutant bacterium *Serratia marcescens* (Kazlauskas *et al.* 1982; Mastunaga *et al.* 1986). Isoquinoline compounds are very common in diverse groups of organisms. An unidentified sponge *Reniera* sp. contained renieramycin E (He and Faulkner 1989). Complex alkaloids ecteinascidins have been purified from *Ecteinascidia turbinata* (Wright *et al.* 1990, Rinehart *et al.* 1990a,b,c, and 1991, Sakai *et al.* 1992, Guan *et al.* 1993). The ascidian was shown to have a variety of symbiotic organisms, including blue-green algae, bacteria, and possibly small algae (Fenical, unpublished result). Furthermore a related alkaloid saframycin B was isolated from the soil bacterium *Streptomyces lavendulae* (Arai *et al.* 1979). It is therefore supposed that ecteinascidins may be produced by microorganisms, possibly by bacteria. However, direct evidence supporting this claim has not been provided.

Remotely related organisms sometimes yielded identical or similar compounds. Dercitamide (from a sponge *Dercitus* sp.) and kuanoniamine D (from an ascidian *Cystodytes* sp.) were proven to be identical (Carroll and Scheuer 1990, Gunawardana *et al.* 1992). An unidentified sponge *Biemna* sp. contained pentacyclic alkaloid dihydro-11-hydroxyascididemnin, the main skeleton of which was originally isolated from an ascidian *Leptoclinides* sp. and later from the ascidian *Didemnum* sp. (Zeng *et al.* 1993, de Guzman and Schmitz 1989, Schmitz *et al.* 1991). All of the compounds implicate possible microbial sources. However, there is an alternative explanation for the phenomenon. Convergent evolution of biosyntheses can be proposed if no sizable common or similar microorganisms are not detectable at both of organisms and the compounds come from common precursors (Faulkner *et al.* 1993). Another explanation is given in terms of a common dietary source which produces the compounds, or an accumulation of exuded products produced by others.

To prove the microbial origins of the compounds two important factors have to be considered: biomass and/ or common existence of symbionts (Faulkner *et al.* 1993). Even when symbionts are present, direct evidence is needed to prove the proposal. The best approach is to culture symbionts. However, this method has some problems. First of all, most of the symbionts are obligate (Lewin 1984). The culture medium often changes the characteristic of the symbionts, since the environment they experience has shifted from a oligotrophic surroundings to a eutrophic one. If the symbionts are obligate, they may require unknown host specific factors. The last is a translocation of the final or an intermediate between the symbionts and the host. If that holds truth, the following approaches would be also problematic. With the assumption of no exchange of metabolites between the host and the symbionts, sufficient complexity of the compounds, and

confinement of the biosynthesis of the substances in only one type of cells, the localization of the compounds at either type of the cells is to be enough to demonstrate the true source of the compounds. The separation of the symbionts from the host cells using flow cytometry, and an immunological technique such as fluorescent antibody or radioimmunoassay have been used (Faulkner *et.al.* 1993, Levine *et al.* 1988). Once the biosynthetic pathway is known, a group-specific hybridization probe complementary to those RNA or DNA can be utilized (Cary *et al.* 1993). Many questions in symbiosis still remain to be answered in the future.

2. Chemistry of ascidians

2.1. Review of secondary metabolites of ascidians.

All known secondary metabolites isolated from ascidians were surveyed under the scheme of ascidian systematics (Figures 1-6 - 1-14). The synthetic and pharmacological studies were also included as references. However, the specific bioactivities of compounds were deliberately not mentioned. When the species or genus was not known, the structural types of compounds from each genera were used as criteria. Some correction of structures was made if the original structures were revised based on synthesis or spectral studies. The compounds in this study are included in the following figures. This review is intended to give a quick reference for all described natural products from ascidians to date. The comprehensive reviews of ascidian secondary metabolites in chemical aspects were given in many literatures (Faulkner 1984, 1986, 1987, 1988, 1990, 1991, 1992, 1993, Lindquist 1989, Richards-Gross 1993, Davidson 1993).

2.2. Collection

About 150 collections of ascidians were made by SCUBA from Western Australia in the Indian Ocean in December of 1990 and 50 collections by Hookah diving from northwest of Australia in the Indian Ocean in December of 1992. The ascidians were immediately frozen after collection and preserved in the freezer until use.

2.3. Voucher

The general procedure of making vouchers is the following: place a living animal in

a container filled with seawater; anaesthetize the animal by adding a few crystals of menthol to prevent contraction for about 2 hrs; place the animal in a jar containing 10 % formalin seawater at least for 48 hrs. In colonial ascidians, only a part of colony is needed, but whole animal is required for identification of solitary ascidians.

2.4. Preliminary chemical analysis

For preliminary analysis, small portions of the animals were lyophilized and triturated with 70% MeOH/$CHCl_2$ for 30 seconds. The powered tissue was extracted three times with 70% MeOH/$CHCl_2$. The combined extract was percolated through a filter paper and the solvent was evaporated under vacuum. The extract was partitioned between hexane and methanol, and the methanol soluble material was further partitioned between ethyl acetate and water. The water-solubles were finally partitioned between n-butanol and water.

Ascidians were chosen for chemical analysis using a combination of TLC (with EtOAc, 5% MeOH/CH_2Cl_2 - 20% MeOH/CH_2Cl_2) and proton NMR analysis (with $CDCl_3$ and MeOH-d_4) searching for some unusual TLC spots and characteristic proton signals. Every fraction was tested for antimicrobial and cytotoxic activities. Interesting secondary metabolites from the ascidians were purified using size exclusion chromatography on Sephadex LH-20 and TSK HW-40, silica flash chromatography, preparative TLC, reversed-phase flash chromatography, reversed-phase, cyano-, and amino-HPLC's, and other methods such as high speed countcurrent chromatography.

2.5. Structure elucidation

A number of different spectroscopic techniques were used. To establish the molecular formula, high resolution mass spectrometry (FAB, DCI, and DEI), with a variety of matrices, were used in conjugation with ^1H and ^{13}C NMR spectroscopy. IR spectroscopy was adopted for identifying functional groups such as OH (or NH), carbonyl, thiocarbonyl, and guanidine groups, etc. UV-visible spectroscopy was utilized for recognizing chromophores and comparing them to those of known compounds. Two dimensional NMR spectroscopy, involving hetero and homocorrelation methods, was used to elucidate novel secondary metabolites. COSY and DQFCOSY spectra and TOCSY spectra were used to recognize vicinal protons and spin systems, respectively. HMQC and XHCORR experiments allowed the assignment of proton directly attached to specific

carbons. When polyaromatic compounds were concerned, HMBC and COLOC experiments made it possible to assign all signals unambiguously using $^{2}J_{CH}$, $^{3}J_{CH}$, and sometimes $^{4}J_{CH}$ couplings (depending on the coupling constant adopted in the experiment). Finally, NOEDS or NOESY experiments were used to define the stereochemistry and the conformation of each molecule. Chemical reactions were also used to identify functional groups of natural products. Acetylation with acetic anhydride/pyridine, and methylation with diazomethane or methyl iodide were commonly used. Various other reactions were also utilized on a case by case basis to prove the structure.

Figure 1-6. Natural products from the family Polyclinidae (O. Aplousobranchia)

Aplidiopsis sp.

1. aplidiamine A R = Br
2. aplidiamine B R = H

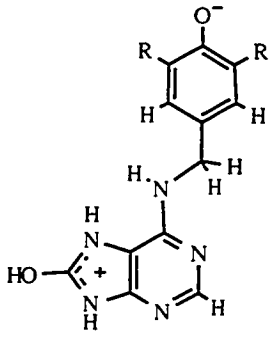

Aplidium albicans

dehydrodidemnin B (see Figure 1-8 *Tridemnum f. solidium*)

Aplidium antillense (Benslimane, A. F. *et al.* 1988)

geranylhydroquinone (see *Aplidium* sp.)

cordiachromene A (see A. *constellatum*)

Aplidium calfornicum (isolation and synthesis: Howard *et al.* 1979
bioactivity: Cotelle *et al.* 1991)

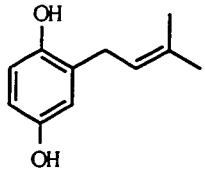

3. prenylhydroquinone

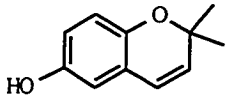

4. dimethylchromenol

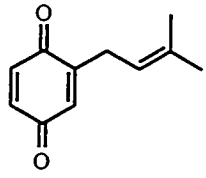

5. prenylquinone

Aplidium constellatum (Targett and Keeran 1984)

6. cordiachromene A

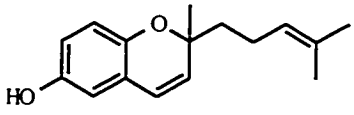

Aplidium fuscum (Dematte *et al.* 1986)

7. thymidine-5'-carboxylic acid R = H
8. 2'-deoxyuridine-5'-carboxylic acid R = CH_3

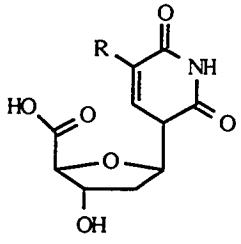

Aplidium multiplicatum (Sato *et al.* 1989)

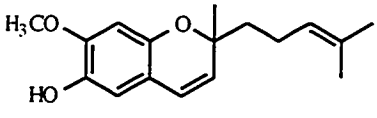

9. a chromene

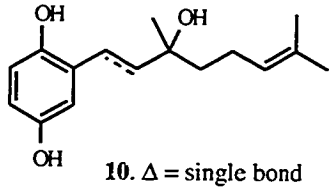

10. Δ = single bond
11. Δ = double bond

also isolated geranylhydroquinone and cordiachromene A

Figure 1-6. (continued)

Aplidium multiplicatum (Kobayashi *et al.* 1994)

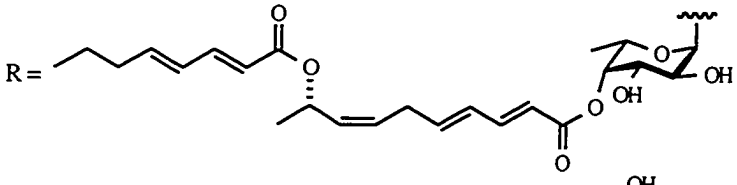

12. shimofuridin A

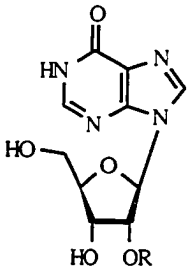

Aplidium pantherinum (Kim *et al.* 1993)

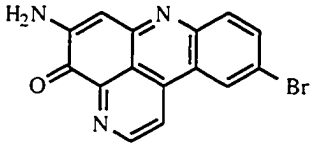

13. pantherinine

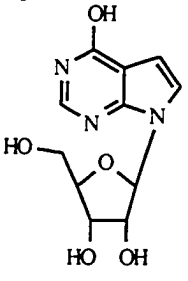

14. 7-deazainosine

Aplidium pliciferum (Arabshahi and Schmitz 1988)

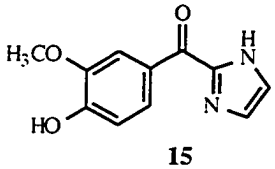

15

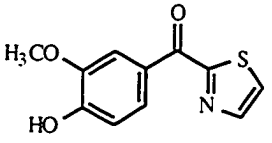

16

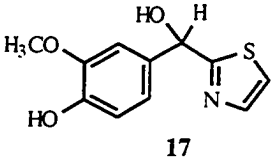

17

Aplidium pliciferum (Matsuno *et al.* 1985)

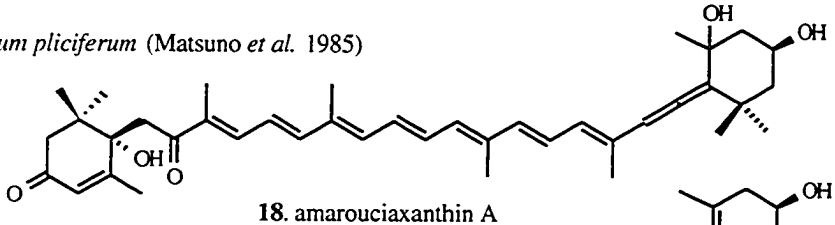

18. amarouciaxanthin A

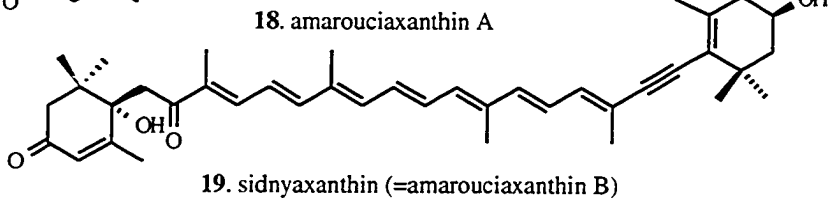

19. sidnyaxanthin (=amarouciaxanthin B)

Aplidium pliciferum (Copp *et al.* 1989)

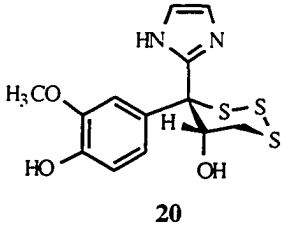

20

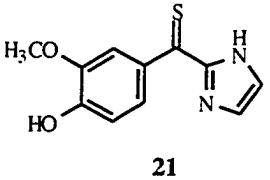

21

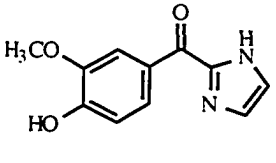

22

Aplidium sp. (Fenical 1974)

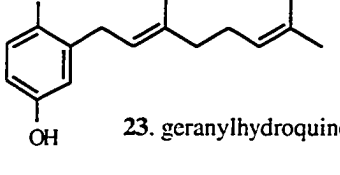

23. geranylhydroquinone

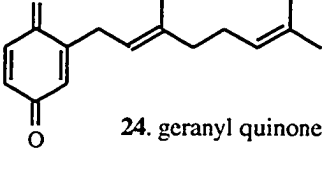

24. geranyl quinone

Figure 1-6. (continued)

Aplidium sp. (Guella *et al.* 1987)

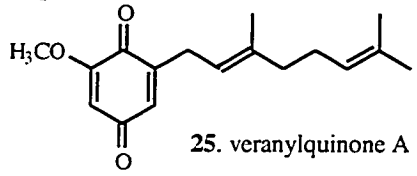

25. veranylquinone A

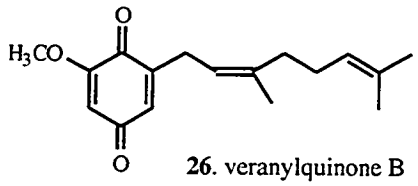

26. veranylquinone B

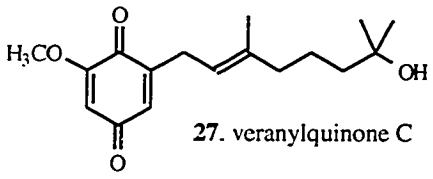

27. veranylquinone C

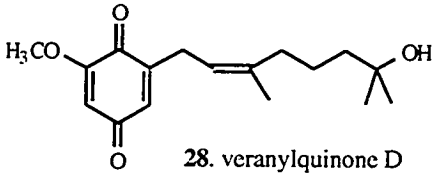

28. veranylquinone D

Aplidium sp. (isolation: Carter and Rinehart 1978; synthesis: Mori and Umemura 1981a, b and 1982)

29. aplidiasphingosine

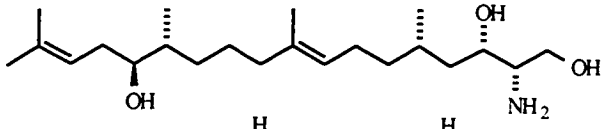

Aplidium sp. (Carroll *et al.* 1993)

30. $R_1 = H, R_2 = Me$
31. $R_1 = I, R_2 = Me$
32. $R_1 = R_2 = H$

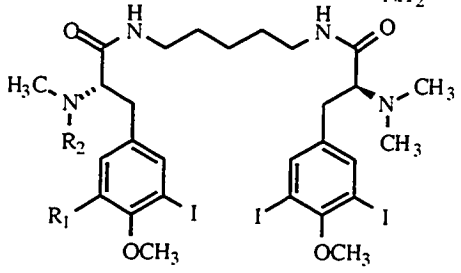

Polyclinum planum (Lindquist *et al.* 1991)

33. polyclinal

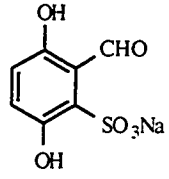

Pseudodistoma arborescens (Chabani *et al.* 1993)

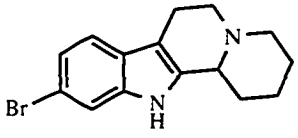

34. arborescidine A

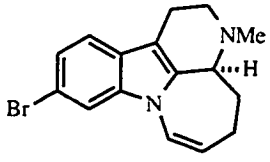

35. arborescidine B

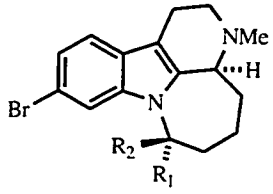

36. C $R_1 = OH, R_2 = H$
37. D $R_1 = H, R_2 = OH$

Pseudodistoma crucigaster (Jares-Errijman *et al.* 1993)

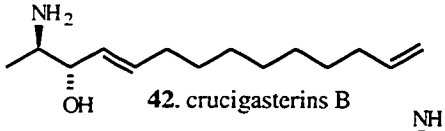

42. crucigasterins B

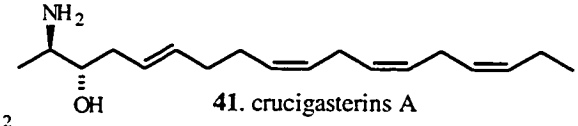

41. crucigasterins A

43. crucigasterins C

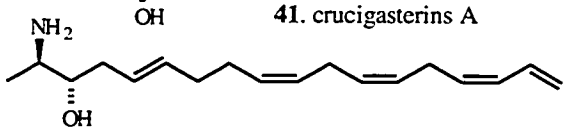

Figure 1-6. (continued)

Pseudodistoma kanoko (Ishibashi *et al.* 1987)

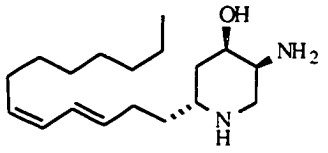

44. pseudodistomin A

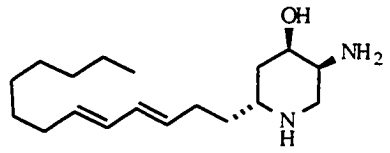

45. pseudodistomin B

Pseudodistoma novaezelandiae (isolation: Perry *et al.* 1991; synthesis: Enders and Finkam 1993)

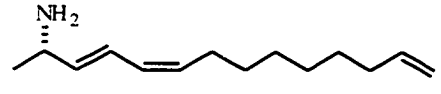

46

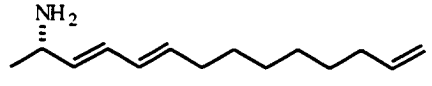

47

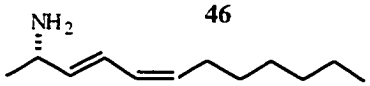

48

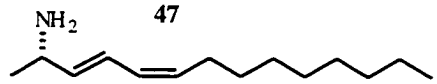

50

Ritterella rubra (Miao and Anderson 1991)

rubrolides A - H

51. A R = Z = H, X = Y= Br
52. B R = H, X = Y = Br, Z = Cl
53. C R = Y = Z = H, X = Br
54. D R = X = Z = H, Y = Br
55. E R = X = Y = Z = H
56. F R = Me, X = Y = Z = H

57. G Z = H
58. H Z = Cl

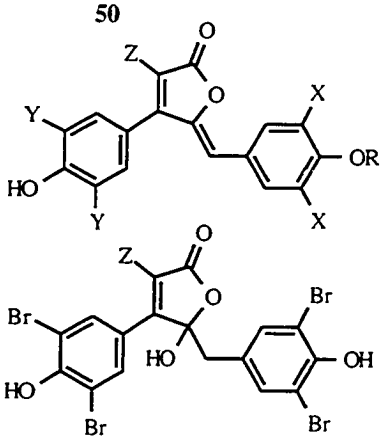

Ritterella sigillinoides (stereochemistry: Blunt *et al.* 1987 and Lake *et al.* 1988a; eudistomin K sulfoxide: Lake *et al.* 1988b; debromoeudistomin K: Lake *et al.* 1989)

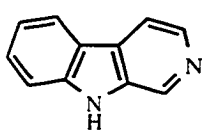

59. β-carboline

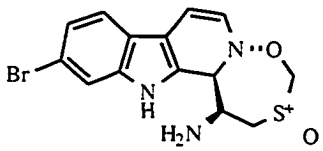

60. eudistomin K sulfoxide

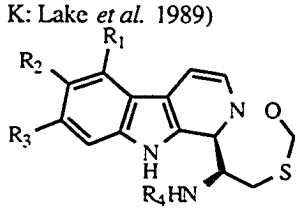

61. C $R_1 = R_4 = H$, $R_2 = OH$, $R_3 = Br$
62. K $R_1 = R_2 = R_4 = H$, $R_3 = Br$
63. debromo K $R_1 = R_2 = R_3 = R_4 = H$

Sidnyum argus (Belaud and Guyot 1984)

sidnyaxanthin (= amarouciaxanthin B, see *Aplidium pliciferum*)

Synoicum castellatum (Carroll *et al.* 1993)

64. a tetrahydrocannabiol derivative

additional compds: **6**, **23**, and **24**

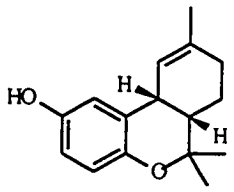

Figure 1-7. Natural products from the family Polycitoridae (O. Aplousobranchia)

Atapozoa sp. (isolation: Lindquist and Fenical 1991; chem. ecol.: Paul *et al.* 1990; related compounds: Carté and Faulkner 1983)

tambjamines

65. E R = CH_2CH_3
66. F R = CH_2CH_2Ph
67. C R = $CH_2CH(CH_3)_2$

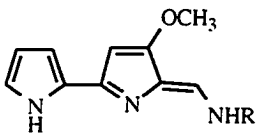

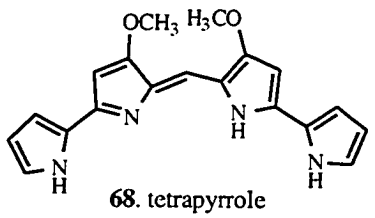

68. tetrapyrrole

An identified species (Kazlauskas *et al.* 1982)

tetrapyrrole (68)

Clavelina cylindrica (Blackman *et al.* 1993)

69. cylindricine A

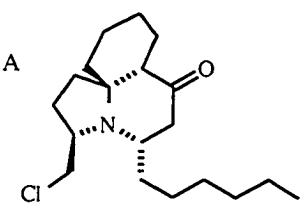

70. cylindricine B

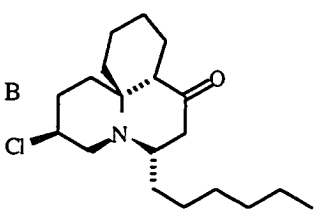

Clavelina lepadiformis (Steffan 1991)

71. lepadin A

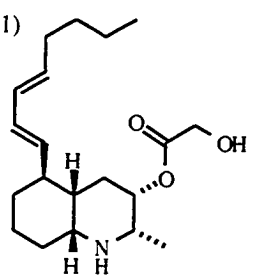

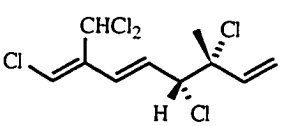

72. pentachlorooctatriene

Clavelina lepadiformis (Biard *et al.* 1994)

72. lepadiformine

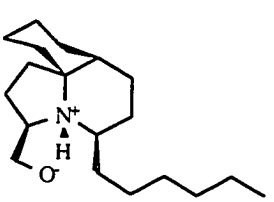

Clavelina picta (Raub *et al.* 1991; Kong and Faulkner 1991)

clavepictines

73. A $R_1 =$  , $R_2 = C_3H_7$

74. B $R_1 = H$, $R_2 = C_3H_7$

pictamine

75. $R_1 =$, $R_2 = Me$

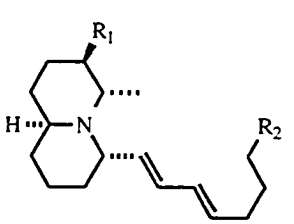

Clavelina picta (Raub *et al.* 1992)

piclavines

76. A_1 $R_1 = X$, $R_2 = H$
77. A_2 $R_1 = Y$, $R_2 = H$
78. A_3 $R_1 = H$, $R_2 = X$
80. A_4 $R_1 = H$, $R_2 = Y$

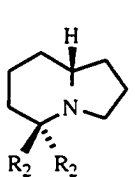

X = 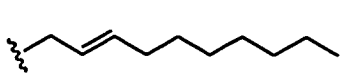

Y = 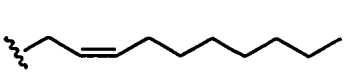

Figure 1-7. (continued)

Clavelina picta (Raub *et al.* 1992)

81. piclavine B 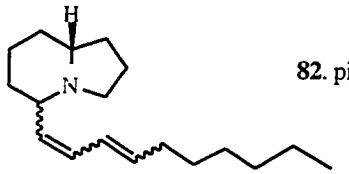

82. piclavine C 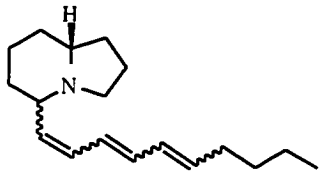

Clavelina sp. (Copp *et al.* 1991)

83. wakayin 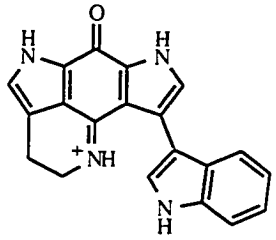

Cystodytes delle chiajei (Kobayashi *et al.* 1988 and 1991)

cystodytins **84.** A $R_1 = X$, $R_2 = H$
85. B $R_1 = Y$, $R_2 = H$
86. C $R_1 = Z$, $R_2 = H$
87. C $R_1 = X$, $R_2 = OH$
88. D $R_1 = Y$, $R_2 = OH$
89. E $R_1 = X$, $R_2 = OMe$
90. F $R_1 = Y$, $R_2 = OMe$
91. G $R_1 = X$; $R_2 = OCO(CH_2)_7CH=CH(CH_2)_7CH_3$
92. H $R_1 = Y$, $R_2 = OCO(CH_2)_7CH=CH(CH_2)_7CH_3$

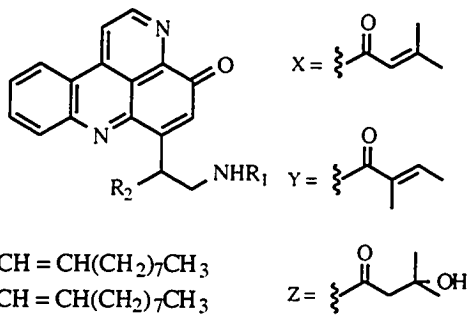

Cystodytes delle chiajei (Aracil *et al.* 1991)

three cyclotetrapeptides **92.** cyclo (L-Pro-L-Leu)$_2$
93. cyclo (L-pro-L-Val)$_2$
94. cyclo (L-Pro-L-Phe)$_2$

Cystodytes delle chiajei (Steffan *et al.* 1993: biosynthesis of shermilamine B)

kuanoniamine D and shermilamine B (see *Eudistoma* sp. Rudi and Kashman 1989; *Tridemnum* sp. Carroll *et al.* 1989)

Cystodytes species (Carroll and Scheuer 1990; synthesis: Bishop and Ciufolini 1992; related compds: Gunawardana *et al.* 1992;)

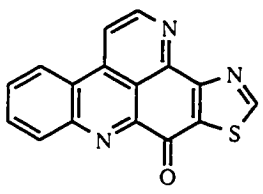

95. kuanoniamine A

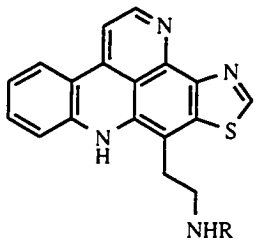

96. kuanoniamine B R = 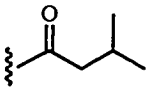

97. kuanoniamine C R = 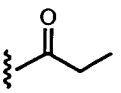

98. kuanoniamine D R = 

Figure 1-7. (continued)

Eudistoma album (Adesanya *et al*. 1992)

99. eudistalbin A $R_1 = H$, $R_2 = NH_2$
100. eudistalbin B $R_1 = R_2 = O$

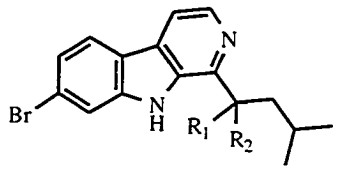

Eudistoma fragum (Debitus *et al.* 1988)

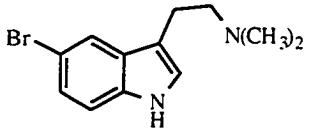

101. 5-bromo-N,N-dimethyltrytamine

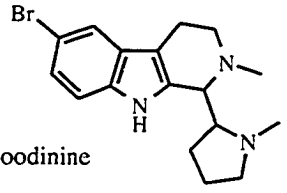

102. woodinine

Eudistoma glaucus (Kabayashi *et al.* 1986 and 1990; Murata *et al.* 1991)

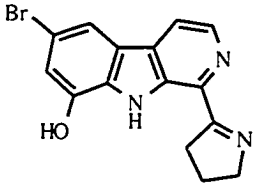

103. eudistomidin A

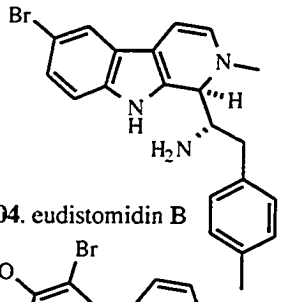

104. eudistomidin B

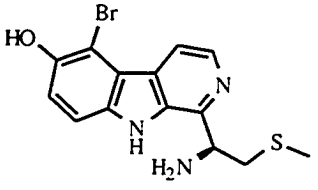

105. eudistomidin C

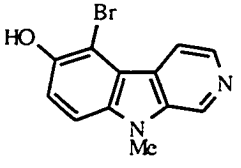

106. eudistomidin D

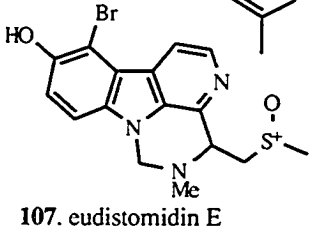

107. eudistomidin E

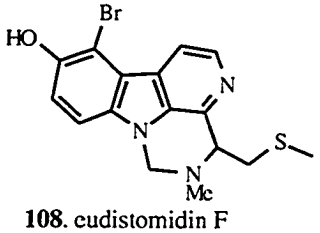

108. eudistomidin F

Eudistoma olivaceum (Rinehart *et al*. 1984 and 1987; Kobayashi *et al.* 1984; Nakamura *et al*. 1986; synthesis: Nakagawa *et al.* 1986; Plate *et al.* 1987; Liu *et al.* 1991; Molina *et al.* 1992; bioactivity: Hudson *et al*. 1988; Hudson and Towers 1988; Kobayashi *et al.* 1989; Seino *et al*. 1990)

eudistomins A - Q

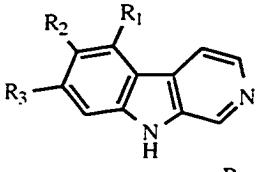

110. D R_1 = Br, R_2 = OH, R_3 = H
116. J R_1 = H, R_2 = OH, R_3 = Br
119. N $R_1 = R_3$ = H, R_2 = Br
120. O $R_1 = R_2$ = H, R_3 = Br
123. bromo D $R_1 = R_3$ = Br, R_2 = H

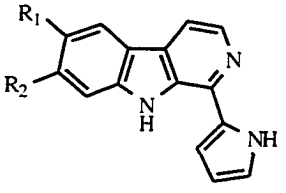

109. A R_1 = OH, R_2 = Br
118. M R_1 = OH, R_2 = H

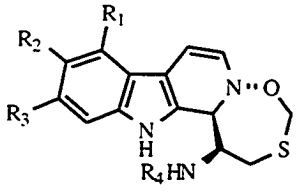

61. C $R_1 = R_4$ = H, R_2 = OH, R_3 = Br
111. E R_1 = Br, R_2 = OH, $R_3 = R_4$ = H
112. F R_1 = H, $R_2 = R_3$ = OH, $R_4 = C_2H_2O_2$
62. K $R_1 = R_2 = R_4$ = H, R_3 = Br
117. L $R_1 = R_3 = R_4$ = H, R_2 = Br
63. debromo K $R_1 = R_2 = R_3 = R_4$ = H

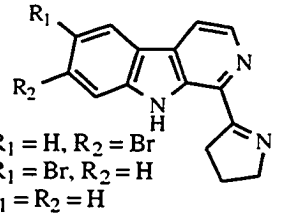

113. G R_1 = H, R_2 = Br
114. H R_1 = Br, R_2 = H
115. I $R_1 = R_2$ = H
121. P R_1 = OH, R_2 = Br
122. Q R_1 = OH, R_2 = H

Figure 1-7. (continued)

Eudistoma olivaceum (Kinzer and Cadellina 1987; synthesis: Still and McNulty 1989)

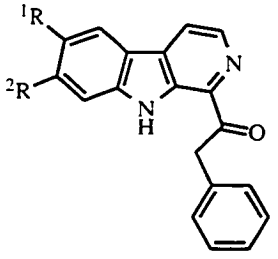

eudistomins R - T

124. R R_1 = H, R_2 =Br
125. S R_1 = Br; R_2 = H
126. R_1 = R_2 = H

Eudistoma cf. rigida (Kabayashi *et al.* 1988; Kikuchi *et al.* 1991)

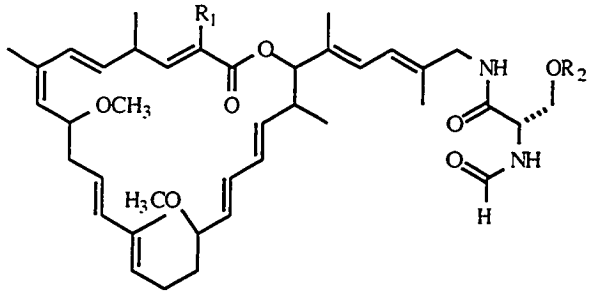

iejimalides A - D

127. A R_1 = R_2 = H
128. B R_1 = Me, R_2 = H
129. C R_1 = H, R_2 = SO_3Na
130. D R_1 = Me, R_2 = SO_3Na

Eudistoma cf. rigida (Kabayashi *et al.* 1990; synthesis: Sakamoto *et al.* 1994)

131. rigidin

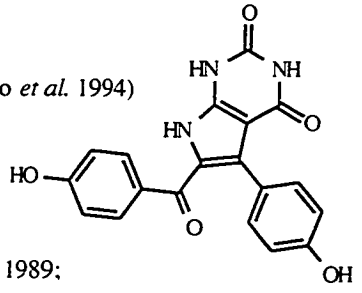

Eudistoma sp. (Rudi *et al.* 1988a and 1988b; Rudi and Kashman 1989; bioactivity: Shochet *et al.* 1993)

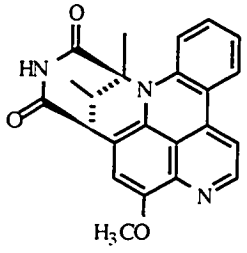

132. segoline A

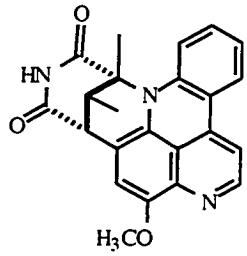

133. segoline B

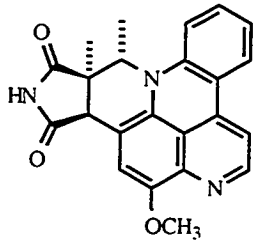

134. isosegoline

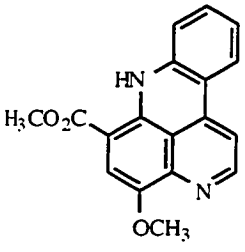

135. norsegoline

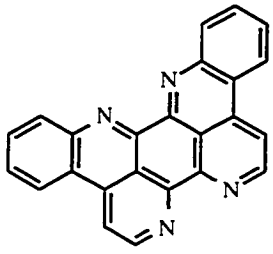

136. eilatin

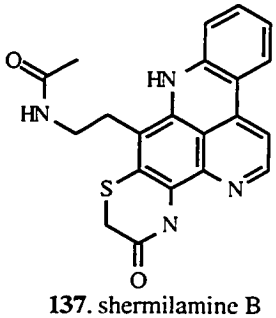

137. shermilamine B

Figure 1-7. (continued)

Eudistoma sp. (He and Faulkner 1991)

138. eudistone A

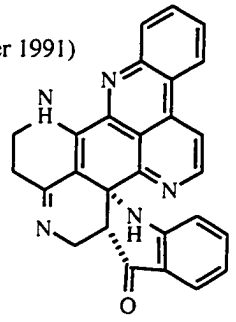

139. eudistone B

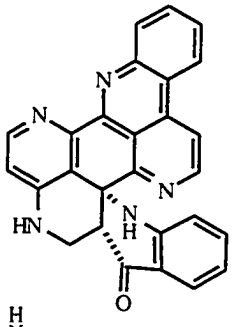

ascididemnin also isolated (see *Didemnum* sp. Kobayashi *et al.* 1988)

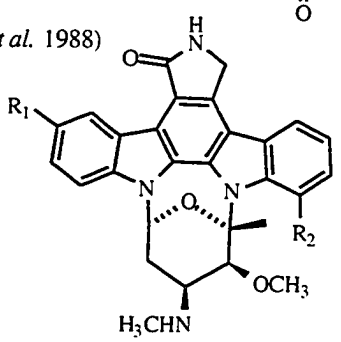

Eudistoma sp. (Kinnel and Scheuer 1992)

139. 11-hydroxystaurosporine
$R_1 = H, R_2 = OH$
140. dihydroxystaurosporine
$R_1 = R_2 = OH$ (not fully charaterized)

Eudistoma sp. (in this dissertation)

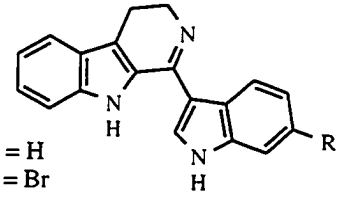

141. eudisin A R = H
142. eudisin B R = Br

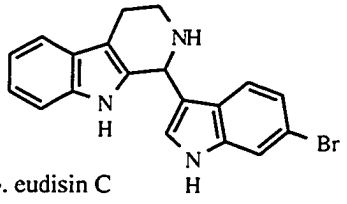

143. eudisin C

Polycitor sp. (Rudi *et al.* 1994)

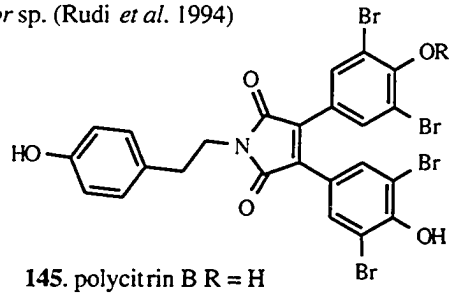

145. polycitrin B R = H
146. polycitrin C R = Me

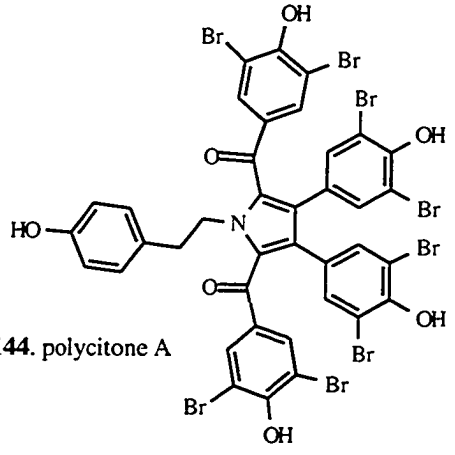

144. polycitone A

Polycitorella mariae (isolation: Roll and Ireland 1985-incorrect; synthesis Moriarity *et al.* 1987)

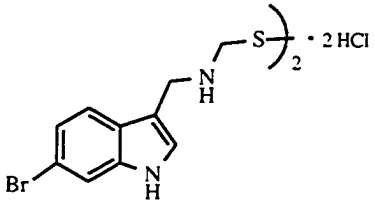

147. citorellamine

Figure 1-8. Natural products from the family of Didemnidae (O. Aplousobranchia)

Didemnum candidum (Lindquist and Fenical 1989; synthesis and structure revision: Congreve *et al.* 1993)

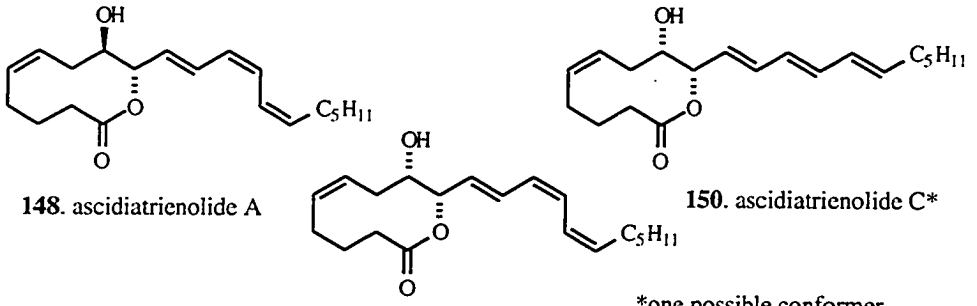

148. ascidiatrienolide A

149. ascidiatrienolide B*

150. ascidiatrienolide C*

*one possible conformer

Didemnum candidum (Fahy *et al.* 1991)

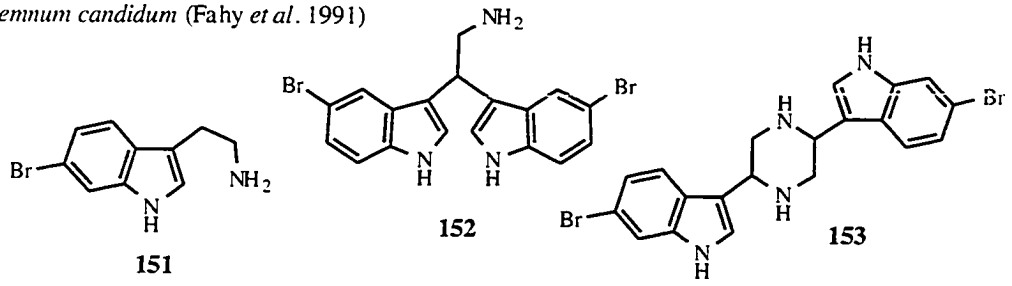

151

152

153

Didemnum chartaceum (Lindquist *et al.* 1988), *Didemnum* sp. (Carroll *et al.* 1993), and related: *Lamellaria* sp. (Mollusc)Anderson *et al.* 1985

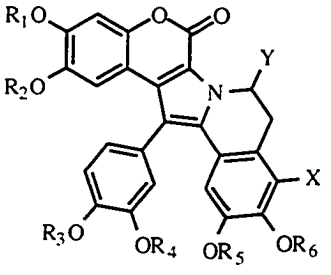

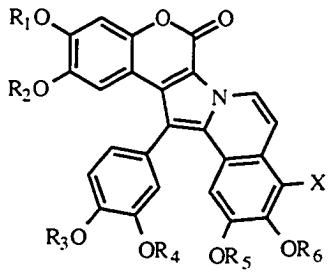

lamellarin	R_1	R_2	R_3	R_4	R_5	R_6	X	Y
154. A	H	Me	H	Me	Me	Me	OMe	OH
156. C	H	Me	H	Me	Me	Me	OMe	H
158. E	H	Me	Me	H	Me	Me	OH	H
159. F	H	Me	Me	Me	Me	Me	OH	H
160. G	Me	H	Me	H	Me	H	H	H
162. I	H	Me	Me	Me	Me	Me	OMe	H
163. J	H	Me	Me	Me	Me	H	H	H
164. K	H	Me	H	Me	Me	Me	OH	H
165. L	H	Me	Me	H	Me	H	H	H

	R_1	R_2	R_3	R_4	R_5	R_6	X
155. B	H	Me	H	Me	Me	Me	OMe
157. D	H	Me	H	Me	Me	H	H
161. H	H	H	H	H	H	H	H
166. M	H	Me	H	Me	Me	Me	OH
167. N	H	Me	Me	H	Me	H	H

* A - D: Anderson *et al.* 1985
E - H: Lindquist *et al.* 1988
A - N: Carroll *et al.* 1993

Figure 1-8. (continued)

Didemnum sp. (this study)

lamellarins

168. O $R_1 = R_2 = R_3 = R_4 = R_5 = R_6 = OH$
169. P $R_1 = R_2 = R_4 = R_5 = R_6 = OH$, $R_3 = OCH_3$
170. Q $R_1 = OCH_3$, $R_2 = R_3 = R_4 = R_5 = R_6 = OH$
171. R $R_1 = R_2 = R_4 = R_6 = OH$, $R_3 = R_5 = OCH_3$
172. S $R_1 = R_3 = OCH_3$, $R_2 = R_4 = R_5 = R_6 = OH$
173. T $R_1 = R_5 = OCH_3$, $R_2 = R_3 = R_4 = R_6 = OH$

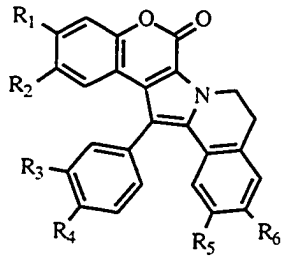

An unidentified species (Yoshida *et al.* 1992)

174. lukianol A X = H
175. lukianol B X = I

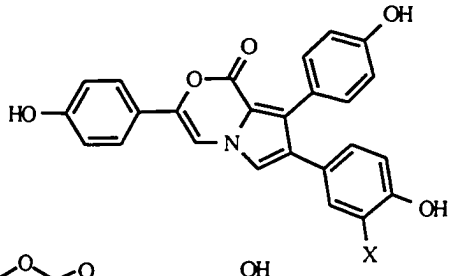

Didemnum sp. (this study)

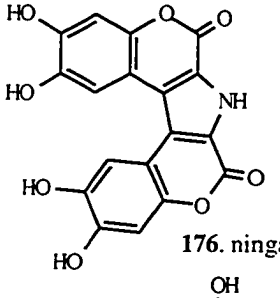

176. ningalactone

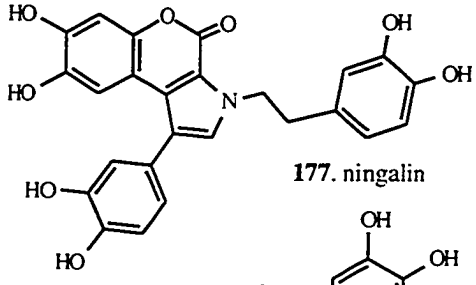

177. ningalin

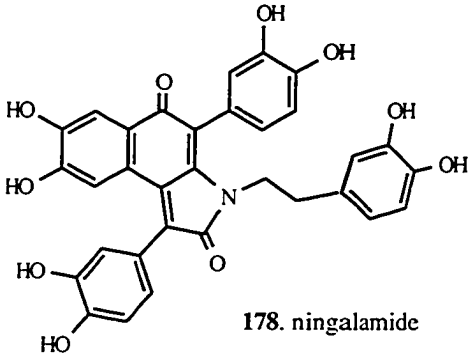

178. ningalamide

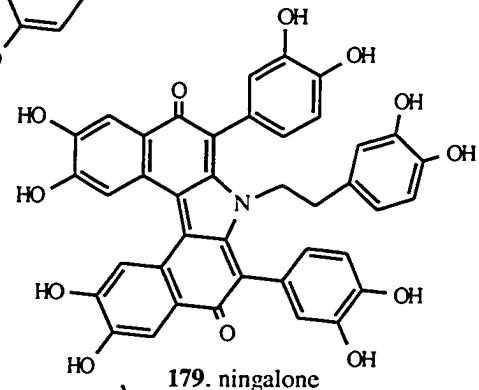

179. ningalone

Didemnum molle (Carroll *et al.* 1994)

180. mollamide

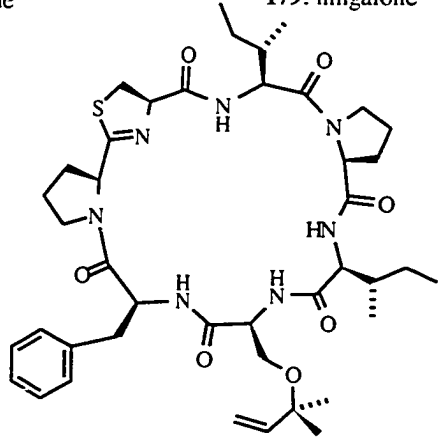

Figure 1-8. (continued)

Didemnum moseleyi (Niwa *et al.* 1991)

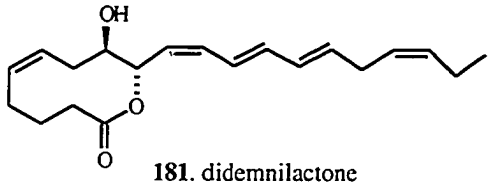

181. didemnilactone

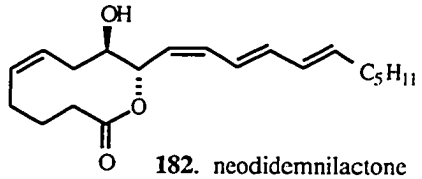

182. neodidemnilactone

Ddidemnum sp. (Searle and Molinski 1993)

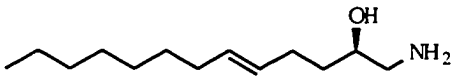

183

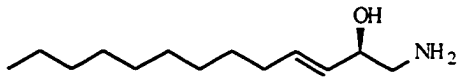

184

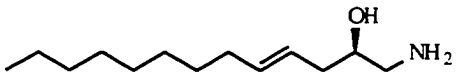

185

Didemnum sp. (Kobayashi *et al.* 1988; synthesis: Moody *et al.* 1992; Kitahara *et al.* 1993))

186. ascididemnin

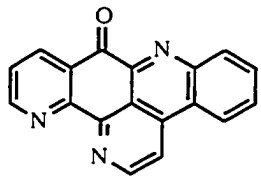

Didemnum sp. (Sesin and Ireland 1984)

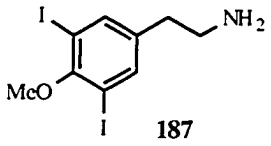

187

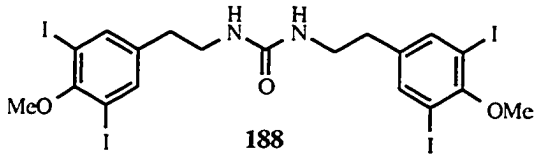

188

Didemnum ternatanum (Ireland *et al.* 1981)

189. N,N'-diphenethylurea

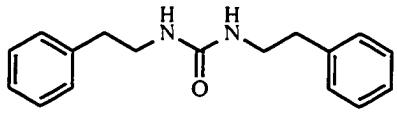

Didemnum voeltzkowi (Lindquist *et al.* 1988; synthesis: Forsyth and Clardy 1990; Sugahara *et al.* 1990)

190. didemnenone C

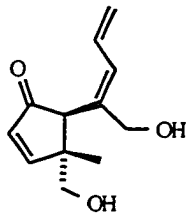

191. didemnenone D

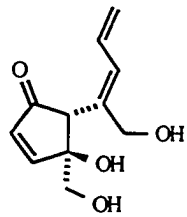

Figure 1-8. (continued)

Didemnum sp. (in this study)

192. deoxyenterocin R = H
193. enterocin R = OH
194. didemnocin A

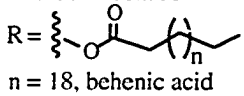

n = 18, behenic acid
195. didemnocin B

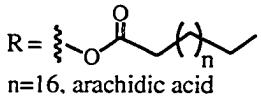

n=16, arachidic acid

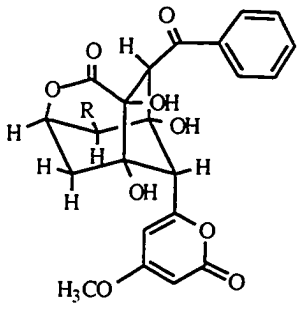

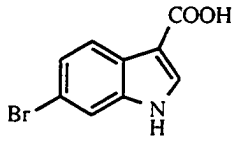

348. 6-bromoindole-3-carboxylic acid

Didemnum sp. (Potts *et al.* 1991)

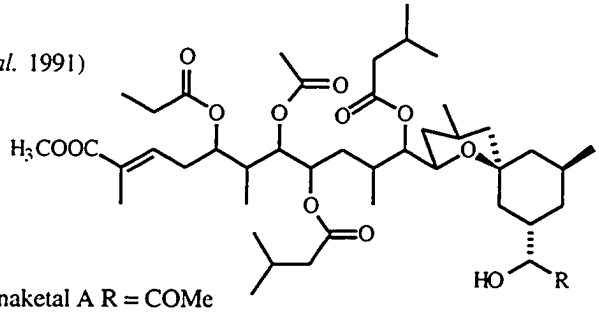

196. didemnaketal A R = COMe

197. didemnaketal B R =

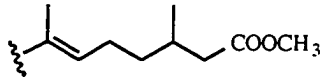

Didemnum sp. (Richards-Gross 1993)

didemneimides A - D
343. A $R_1 = R_2 = H$
344. B $R_1 = H$, $R_2 = Me$
345. C $R_1 = Br$, $R_2 = Me$
346. D $R_1 = Br$, $R_2 = H$

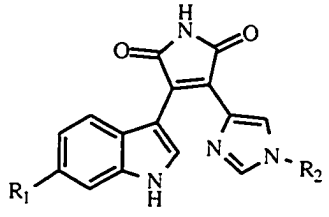

Diplosoma sp. (Charyulu *et al.* 1989)

198. diplamine

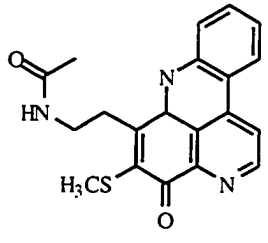

Leptoclinides sp. (Bloor and Schmitz 1987; de Guzman and Schmitz 1989; Schmitz *et al.* 1991; synthesis: Kitahara *et al.* 1993; bioactivity: Goulle *et al.* 1991)

199. 2-bromoleptoclinidione R_1=Br, R_2=H
200. 11-hydroxyascididemnin R_1=H, R_2=OH

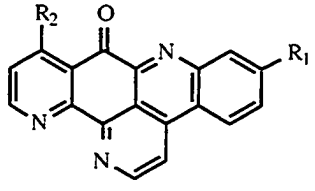

Figure 1-8. (continued)

Lissoclinum bistratum (Gouiffes *et al.* 1988; Degnan *et al.* 1989a; Foster *et al.* 1992a; bioactivity: Gouiffes *et al.* 1988; Watters *et al.* 1990 and 1992; Stanwell *et al.* 1993)

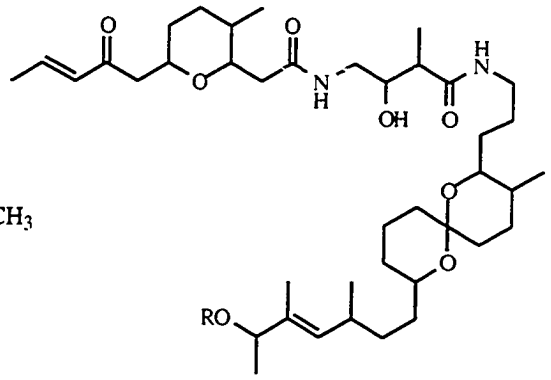

201. bistramide* A R = H
202. bistramide B R = $COCH_3$

*also called bistratene

Lissoclinum bistratum (Degnan *et al.* 1989a; Foster *et al.* 1992b; synthesis: Aguilar and Meyers 1994a and b; chemistry related: Meyers and Trvares 1994)

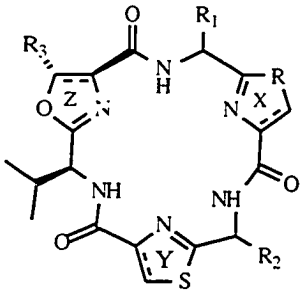

203 - 206. bistratamides A-D

A X = Y = thiazoline, Z = oxazoline, R_1 = Ala, R_2 = Phe, R_3 = Me
B X = thiazoline, Y = thiazole, Z = oxazoline, R_1 = Ala, R_2 = Phe, R_3 = Me
C X = Y = thiazole, Z = oxazole, R_1 = L-Ala, R_2 = L-Val, R_3 = H
D X = oxazole, Y = thiazole, Z = oxazoline, R_1 = L-Val, R_2 = L-Val, R_3 = Me

Lissoclinum bistratum (Hambley *et al.* 1992; different source: Prinsep *et al.* 1992)

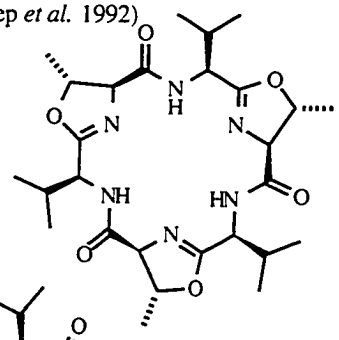

207. cycloxazoline*

* also called westiellamide from a blue-green alga

Lissoclinum bistratum (Foster and Ireland 1993)

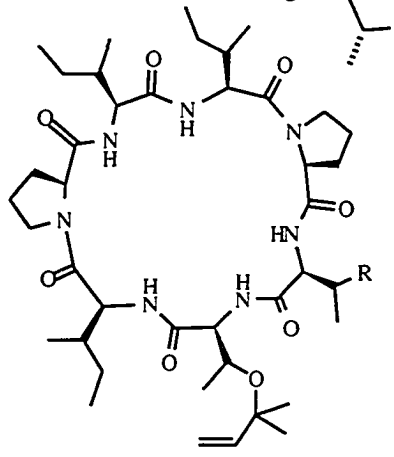

208. nairaiamide A R = Me
209. nairaiamide B R = CH_2CH_3

Figure 1-8. (continued)

Lissoclinum patella (A: Ireland and Scheuer 1980; B: Williams *et al.* 1989; synthesis: Kato *et al.* 1985; Schmidt and Weller 1986; Kato *et al.* 1986a and b; conformation: Ishida *et al.* 1989; stereochemistry: Biskupiak and Ireland 1983)

ulithiacyclamide **210**. A R = D-Leu
211. B R = D-Phe

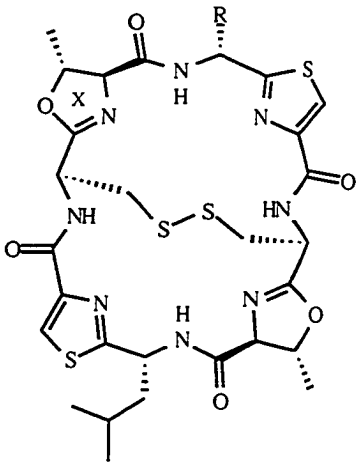

An unidentified species (ascidiacyclamide: Hamamoto *et al.* 1983; Ishida *et al.* 1987a and b, 1988, and 1992; synthesis: Kato *et al.* 1985; Hamada *et al.* 1985a)

Lissoclinum patella (patellamides and pre-: Ireland *et al.* 1982; Sesin *et al.* 1986; Schmitz *et al.* 1989; McDonald and Ireland 1992; synthesis: Hamada *et al.* 1985b, c, and d; Schmidt *et al.* 1985; Schmidt and Griesser 1986; bioactivity: Williams and Jacobs 1993)

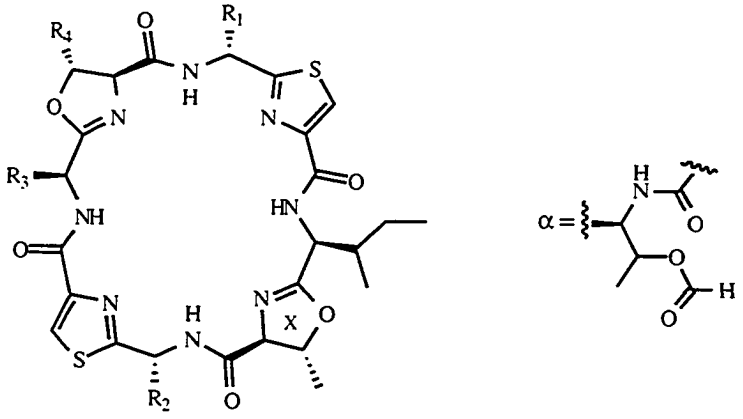

212. ascidiacyclamide $R_1 = R_2 =$ D-Val, $R_3 =$ L-Ile, $R_4 =$ Me
213. patellamide A $R_1 = R_2 =$ D-Val, $R_3 =$ L-Ile, $R_4 =$ H
214. patellamide B $R_1 =$ D-Ala, $R_2 =$ D-Phe, $R_3 =$ L-Leu, $R_4 =$ Me
215. patellamide C $R_1 =$ D-Ala, $R_2 =$ D-Phe, $R_3 =$ L-Val, $R_4 =$ Me
216. patellamide D 16 $R_1 =$ D-Ala, $R_2 =$ D-Phe, $R_3 =$ L-Ile, $R_4 =$ Me
217. patellamide E 17 $R_1 = R_3 =$ L-Val, $R_2 =$ D-Phe, $R_4 =$ Me
218. perpatellamide-B-formate $R_1 =$ Ala, $R_2 =$ D-Phe, R3 = Leu, X = α

Figure 1-8. (continued)

Lissoclinum patella (lissoclinamides and pre-: Wasylyk *et al.* 1983, Degnan *et al.* 1989b, Schmitz *et al.* 1989, Hawkins *et al.* 1990, Sesin *et al.* 1986)

Lissoclinum patella (ulicyclamide and pre-: Ireland and Scheuer 1980, Wasylyk *et al.* 1983, Sesin *et al.* 1986; synthesis: Kato *et al.* 1986b, Sugiura *et al.* 1987)

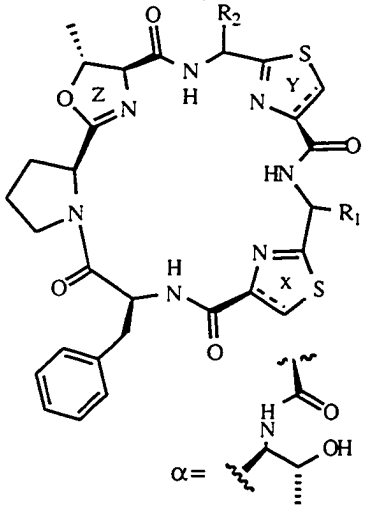

219 - 226. lissoclinamides 1 - 8

1 X = Y = thiazole, R1 = D-Ile, R2 = L-Val
2 X = thiazole, Y = thiazoline, R1 = D-Ala, R2 = D-Ile
3 X = thiazole, Y = thiazoline, R1 = L-Ala, R2 = D-Ile
4 X = thiazole, Y = thiazoline, R1 = L-Phe, R2 = D-Val
5 X = Y = thiazole, R1 = L-Phe, R2 = D-Val
6 X = thiazole, Y = thiazoline, R1 = D-Phe, R2 = D-Val
7 X = Y = thiazoline, R1 = D-Phe, R2 = Val
8 X = thiazole, Y = thiazoline, R1 = D-Phe, R2 = L-Val

227. prelissoclinamide 2 X = thiazole, Y = thiazoline, R1 = D-Ala, R2 = D-Ile, Z = α

228. ulicyclamide X = Y = thiazole, R1 = D-Ala, R2 = L-Ile

229. preulicyclamide X = Y = thiazole, R1 = D-Ala, R2 = D-Ile, Z = α

Lissoclinum patella (McDonald *et al*. 1992)

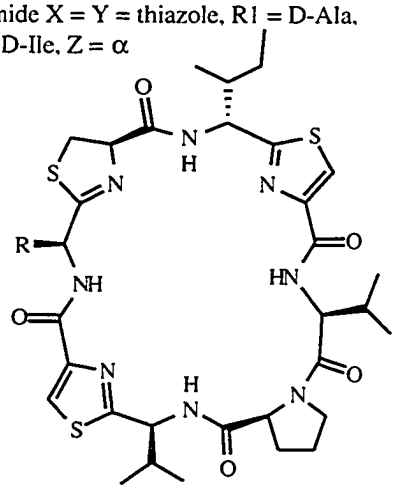

230 - 231. tawicyclamides A, B
A X = thiazoline, R = L-Phe
B X = thiazoline, R = L-Leu

Lissoclinum patella (Zabriskie *et al.* 1988, Corley and Moore)

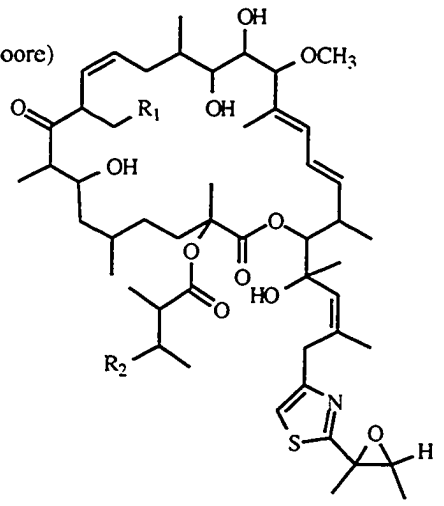

232. patellazole A $R_1 = R_2 = H$
233. patellazole B $R_1 = H$, $R_2 = OH$
234. patellazole C $R_1 = R_2 = OH$

Figure 1-8. (continued)

Lissoclinum patella (Zabriskie *et al.* 1990, Zabriskie 1989)

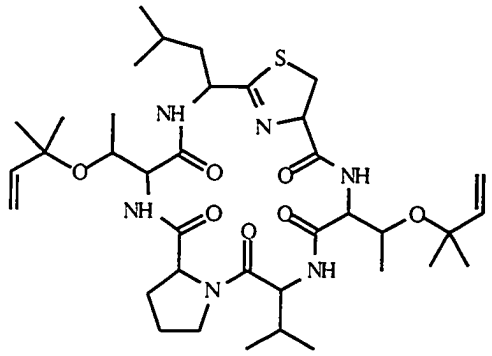

235. patellin 1

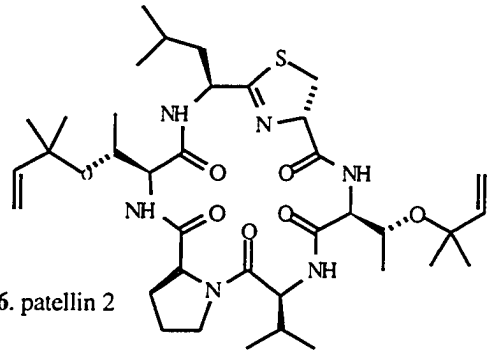

236. patellin 2

237 - 239. patellin 3-5
3 $R_1 = R_2$ = Leu
4 R_1 = Leu, R_2 = Val
5 R_1 = Val, R_2 = Phe

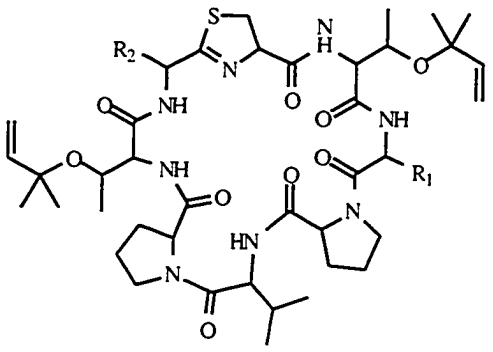

Lissoclinum patella (Davidson and Ireland 1990)

240. lissoclinolide

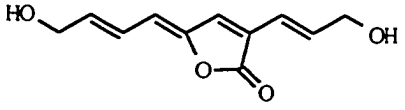

Lissoclinum perforatum (Litaudon and Guyot 1991)

241. lissoclinotoxin

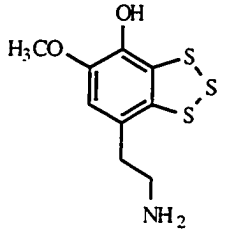

Lissoclinum vareau (Davidson *et al*. 1991, Ford and Davidson 1993; Molinski and Ireland 1989)

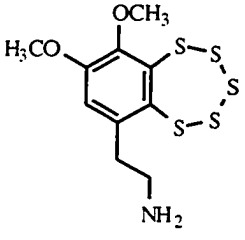

242. varacin

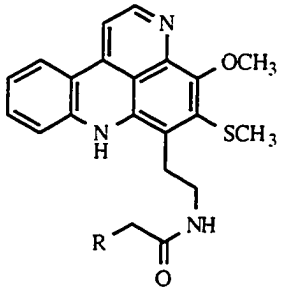

243. varamine A R = CH_3
244. varamine B R = H

Figure 1-8. (continued)

Lissoclinum voeltzkowi (Malochet-Grivois *et al.* 1991)

245. dichlorolissoclimide

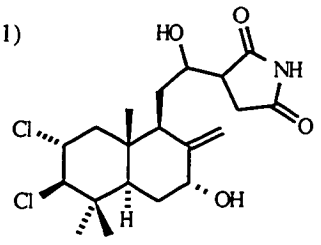

Lissoclinum sp. (Barrow and Capon 1992)

246. sulfone

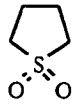

Tridemnum cereum (Demette *et al.* 1985)

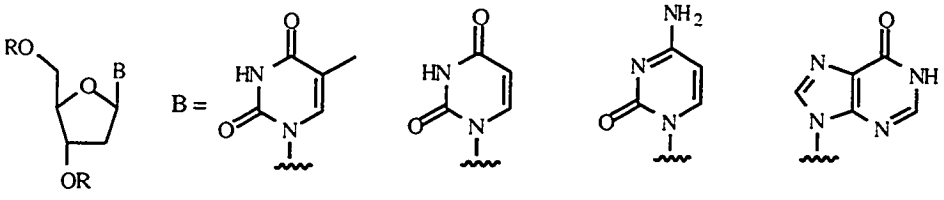

247. R = H **248.** R = H **249.** R = H **250.** R = H

Tridemnum cyanophorum (Lindquist *et al.* 1988)

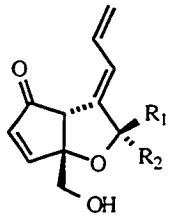

251. didemnenone A R_1 = H, R_2 = OH
252. didemnenone B R_1 = OH, R_2 = H

also didemnin B (= isodidemnin B)

Trididemnum solidum (Bible *et al.* 1988; Pettit *et al.* 1993)

253. tunichlorin

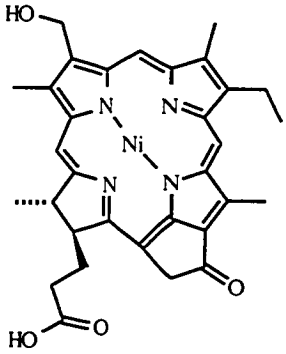

Figure 1-8. (continued)

Trididemnum solidum (Rinehart *et al.* 1981a and b, and 1988, Hossain *et al.* 1988, McKee *et al.* 1989; conformation: Banaiga *et al.* 1989, Kessler *et al.* 1989 and 1990; synthesis: Hamada *et al.* 1987, Rinehart *et al.* 1987, Harris *et al.* 1987, Schmidt *et al.* 1988a, 1988b, Jouin *et al.* 1989, Hamada *et al.* 1989, Li *et al.* 1990; bioactivity: Jiang *et al.* 1983, Stevens *et al.* 1989, Yuh *et al.* 1989)

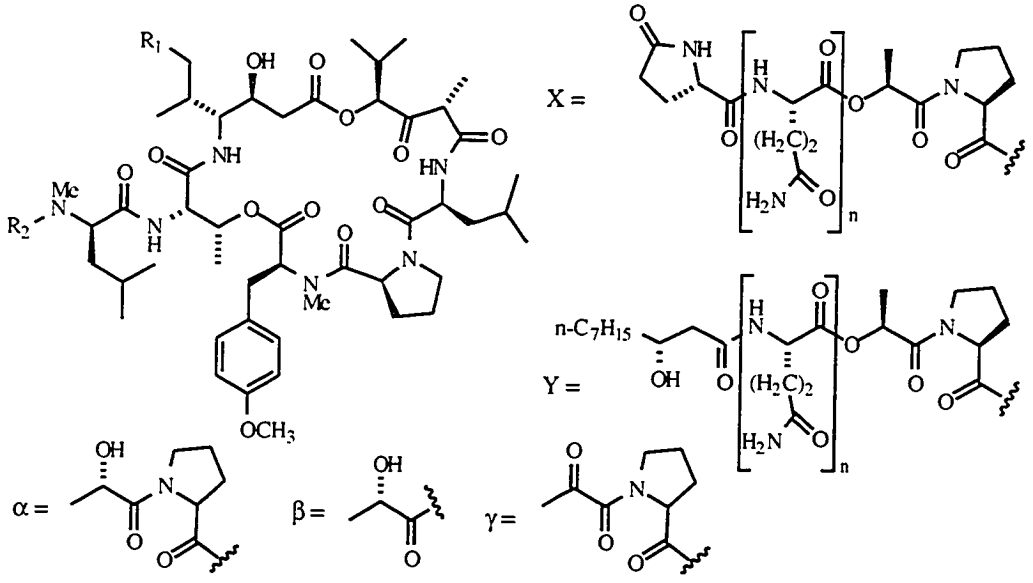

254 - 262. didemnins A - Y

A $R_1 = H$, $R_2 = H$
B $R_1 = H$, $R_2 = \alpha$
C $R_1 = H$, $R_2 = \beta$

nor-B $R_1 = Me$, $R_2 = \alpha$
dehydro-B $R_1 = Me$, $R2 = \gamma$
D $R_1 = Me$, $R_2 = X$ (n = 2)
E $R_1 = Me$, $R_2 = X$ (n = 3)
X $R_1 = Me$, $R_2 = Y$ (n = 3)
Y $R_1 = Me$, $R_2 = Y$ (n = 4)

Trididemnum sp. (de Silva *et al.* 1992)

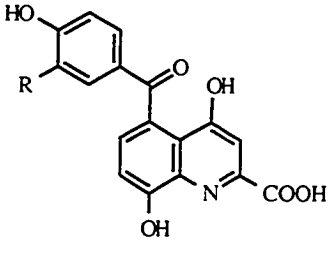

263. trididemnic acid A R = H
264. trididemnic acid B R = OH

Trididemnum sp. (Cooray *et al.* 1988, Carroll *et al.* 1989)

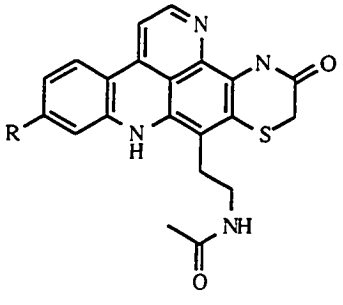

265. shermilamine A R = Br
137. shermilamine B R = H

Figure 1-9. Natural products from the family of Cionidae (O. Phlebobranchia)

Ciona intestinalis (Guyot and Durgeat 1981)

266. sterol peroxide

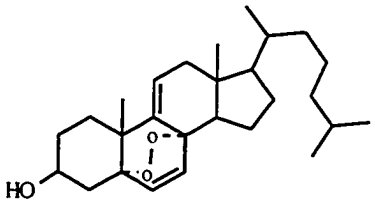

Ciona intestinalis (Guyot *et al.* 1982)

267. 24-hydroperoxy-24-vinyl-cholesterol

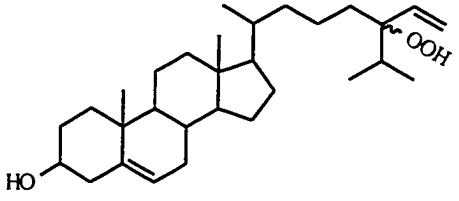

Ciona intestinalis (Gupta *et al.* 1979, Morris 1983)

sterol composition of the species (C26 - C29 sterols, see the references)

Ciona savignyi (Tsukamoto *et al.* 1993)

268. urochordamine A R1 = X, R2 = Y
269. urochordamine B R1 = Y, R2 = X

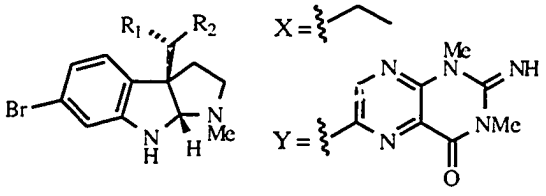

Diazona chinensis (Lindquist *et al.* 1991, Lindquist 1989)

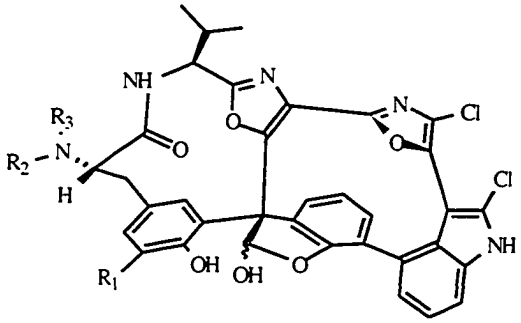

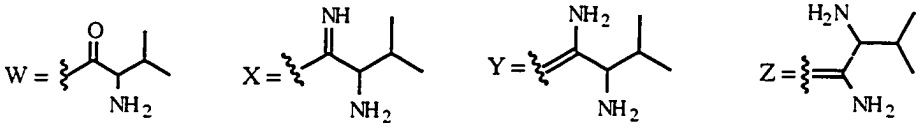

270. diazonamide A $R_1 = R_3 = H$, $R_2 = W$
271. diazonamide B $R_1 = Br$, $R_2 = R_3 = H$
272. diazonamide C $R_1 = R_3 = H$, $R_2 = X$
273. diazonamide Da $R_1 = H$, $R_2 = R_3 = Y$
274. diazonamide Db $R_1 = H$, $R_2 = R_3 = Z$

Figure 1-10. Natural products from the family of Perophoridae

Ecteinascidia turbinata (Wright *et al.* 1990, Rinehart *et al.* 1990a,b,c and 1991, Sakai *et al.* 1992 (crystal structure), Guan *et al.* 1993; related compds: Ikedao *et al.* 1983, Arai 1989; Cooper and Unger 1985, He and Faulkner 1989)

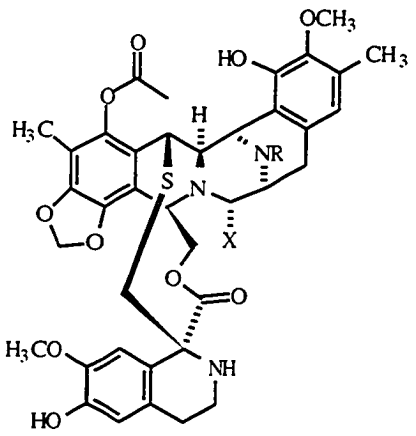

275. ecteinascidin 1 R = H, X = OH
276. ecteinascidin 2 R = Me, X = OH
277. ecteinascidin 3 R = CHO, X = OH
278. ecteinascidin 4 R = methyl N-oxide, X = OH
*ecteinascidin (745) R = Me, X = H
*ecteinascidin (770) R = Me, X = CN

* ecteinascidins 745 and 770 may not be correct structures because the mass units (M + H), 746.2775 and 771.2704, can not explain the proposed structures.

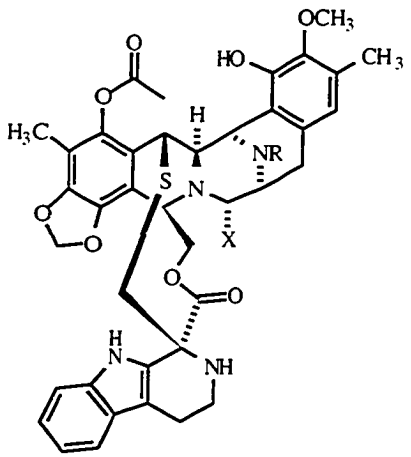

279. ecteinascidin 6 R = H, X = OH
280. ecteinascidin 7 R = Me, X = OH

Perophora viridis (Oltz *et al.* 1988) tunichrome An-1 (see *Ascidia nigra*)

Figure 1-11. Natural products from the family of Ascidiidae (O. Phlebobranchia)

Ascidia ahodori (Nakamura *et al.* 1991, 1992, Anthoni *et al.* 1991-revised)

281. ascidian peroxide

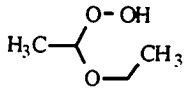

Ascidia ceratodes, A. nigra (Bruening *et al.* 1985 and 1986, Oltz *et al.* 1988, Kim *et al.* 1991; biosynthesis: He *et al.* 1992; synthesis: Horenstein and Nakanishi 1989)

282. tunichrome An-1(B-1) $R_1 = R_2 = OH$
283. tunichrome An-2 $R_1 = H, R_2 = OH$
284. tunichrome An-3 $R_1 = R_2 = H$

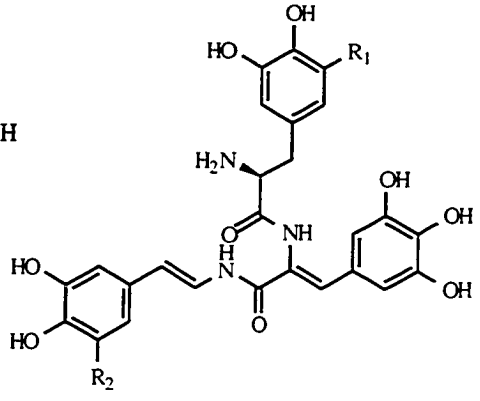

Ascidia nigra (Zielinski *et al.* 1983, Tam Ha *et al.* 1982)

isolation of new sterols and syntheses of some of them (see the references for detail)

Ascidi elia asperrsa (Jimenez *et al.* 1986)

285. epidioxy sterol

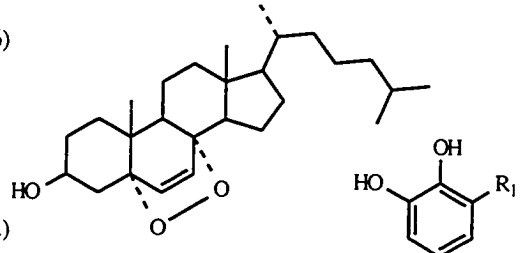

Phallusia mammillata (Bayer *et al.* 1992)

286. tunichrome Pm-1 $R_1 = R_2 = OH$
287. tunichrome Pm-2 $R_1 = H, R_2 = OH$
288. tunichrome Pm-3 $R_1 = OH, R_2 = H$

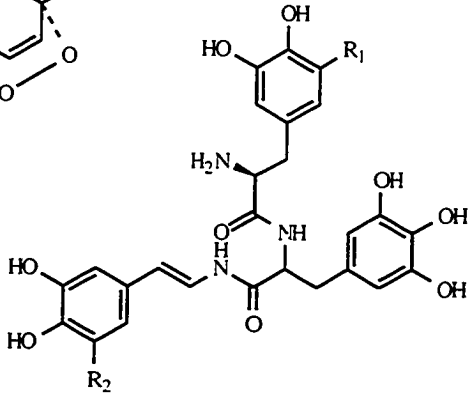

Phallusia mammillata (Guyot and Durgeat 1981, Guyot *et al.* 1982)

266. sterol peroxide 1 R = H
289. sterol peroxide 2 R = ξ=CH_2
290. sterol peroxide 3 R = CH_3 Δ^{22}
291. sterol peroxide 4 R = CH_2-CH_3

*also compd **267** has been isolated (see *Ciona intestinalis*).

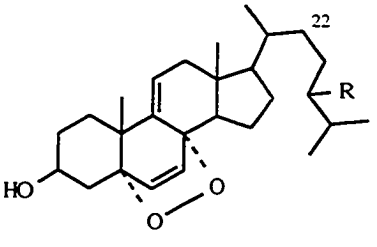

Phallusia mammillata (Nakamura *et al.* 1991 and 1992)

281. ascidian peroxide (see *Ascidia ahodori*)

Figure 1-12. Natural products from the family of Molgulidae (O. Stolidobranchia)

Mogula manhattensis (Gaill and Lafont 1978)

292. homarine

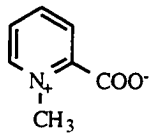

293. uric acid (a purine degradation product)

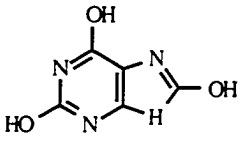

Molgula manhattensis (Oltz *et al.* 1988, Ryan *et al.* 1992, synthesis: Kim *et al.* 1990, Tayor *et al.* 1991)

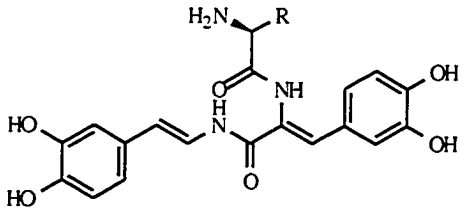

294. tunichrome Mm-1 R = H
295. tunichrome Mm-2 R = i-Bu

Figure 1-13. Natural products from the family of Pyuridae (O. Stolidobranchia)

Halocynthia roretzi (Nakamura *et al.* 1991)

281. ascidian peroxide (see *Ascidia ahodori*)

Halocynthia roretzi (Zollo *et al.* 1986, Kljaijic *et al.* 1983)

sterols (see detail in the references)

Halocynthia roretzi (Mastuno and Ookubo 1981 and 1982)

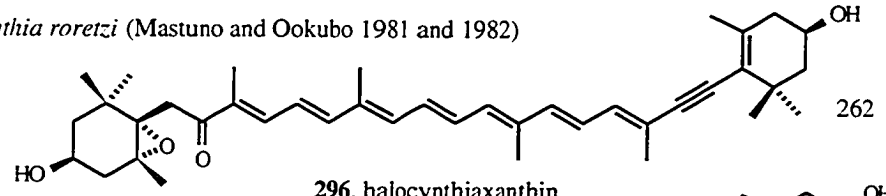

296. halocynthiaxanthin

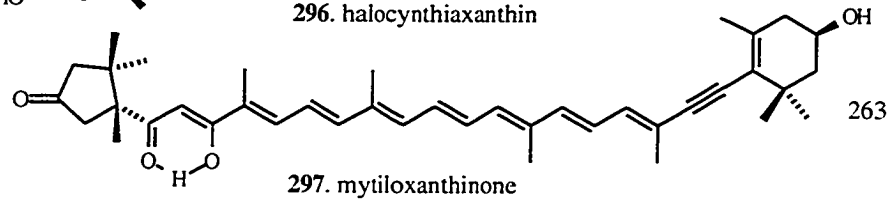

297. mytiloxanthinone

*mytiloxanthin, fucoxanthin, and focuxanthinol isolated (see detail the references)

Halocynthia roretzi (Kobayashi *et al.* 1981, related compds Hirata *et al.* 1979)

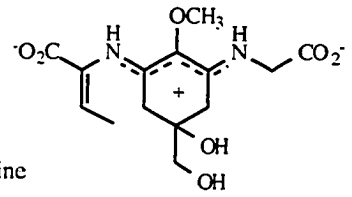

298. mycosporine

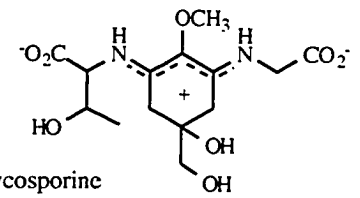

299. mycosporine

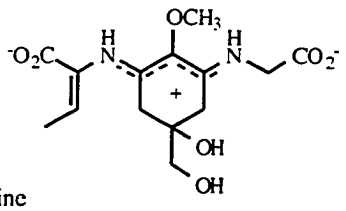

300. mycosporine

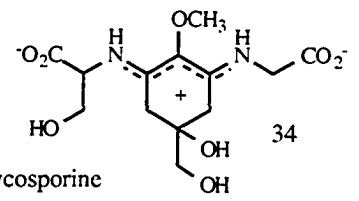

301. mycosporine

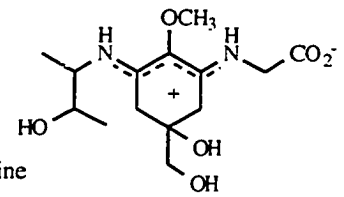

302. mycosporine

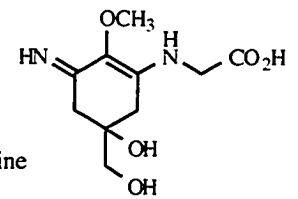

303. mycosporine

Figure 1-13. (continued)

Halocynthia roretzi (Watanabe *et al.* 1984)

304. halocyanine

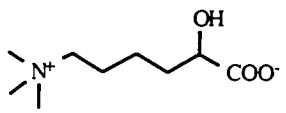

Halocynthia roretzi (Azumi *et al*. 1990a)

305. halocyamine A

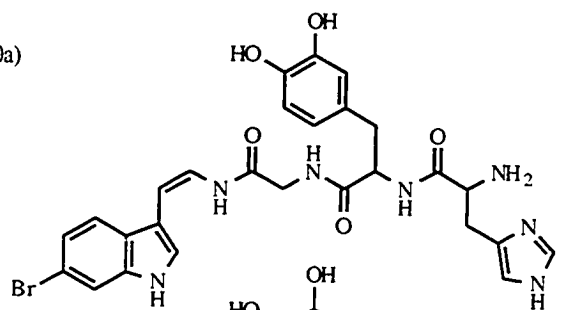

306. halocyamine B

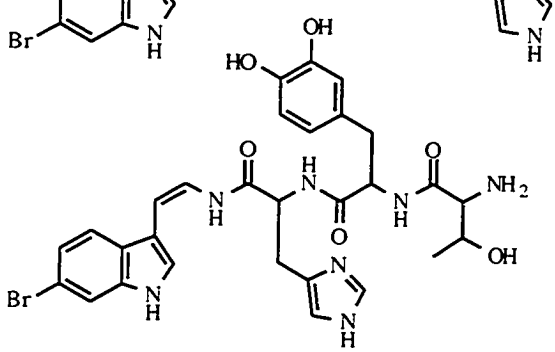

Halocynthia roretzi (Tsukamoto *et al.* 1993)

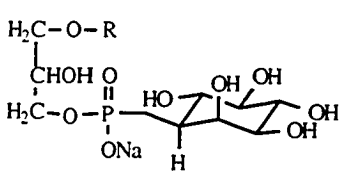

new lysophosphadtidylinositol **307**. A R_1 =

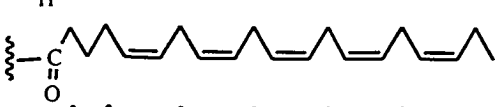

new lysophosphadtidylinositol **308**. B R_2 =

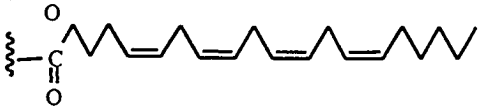

Microcosmus savignyi and M. sulcatus (Kljajic *et al*. 1983, Zollo *et al*. 1986)

sterols (see detail in the references)

Pyura sacciformis (Niwa *et al.* 1988)

309. brominated quinazolinedione

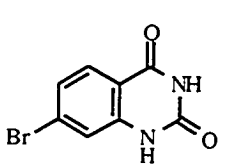

Figure 1-14. Natural products from the family of Styelidae (O. Stolidobranchia)

Amphicarpa meridiana (Schmitz *et al.* 1991)

310. meridine

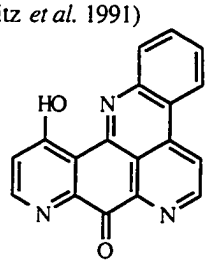

311. isomeridine

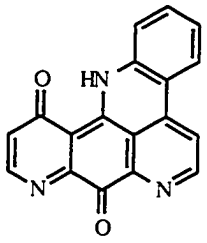

Dendrodoa grossularia (Jimenez *et al.* 1986) * compd **266** also isolated.

312 - **317**. epidioxy sterols

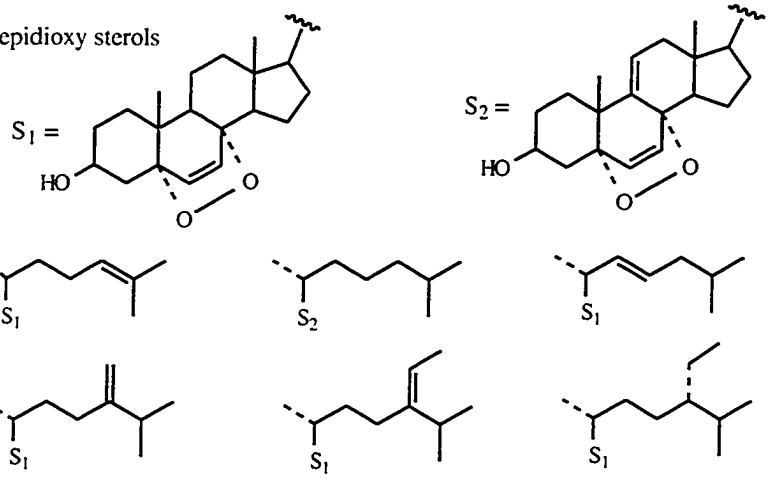

Dendrodoa grossularia (Heitz *et al.* 1980, Guyot and Meyer 1896, Moquin and Guyot 1984 and 1989; synthesis: Hogan and Sainsbury 1984; bioactivity: Helbecque *et al.* 1987)

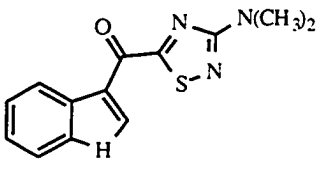

318. dendrodoine

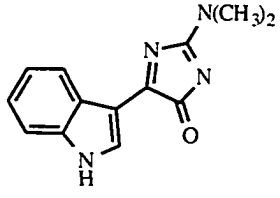

319. 3-indoyl-imidazol-4-one

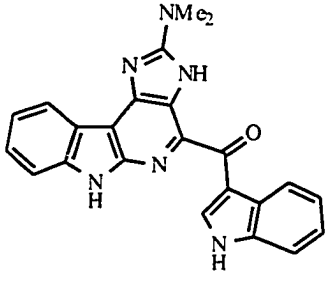

320. grossularine-1

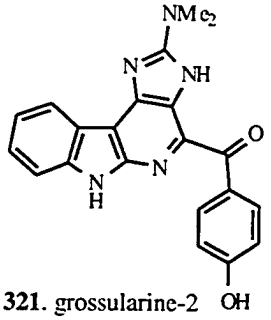

321. grossularine-2

Figure 1-14. (continued)

Polyandrocarpa sp. (Cheng and Rinehart 1978, Carte and Faulkner 1982; synthesis: Rinehart *et al.* 1983)

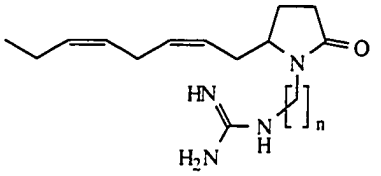

322. polyandrocarpidine A n = 5
324. polyandrocarpidine C n = 4

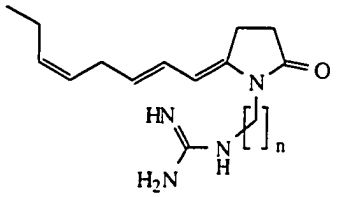

323. polyandrocarpidine B n = 5
325. polyandrocarpidine D n = 4

Polyandrocarpa sp. (Lindquist and Fenical 1990)

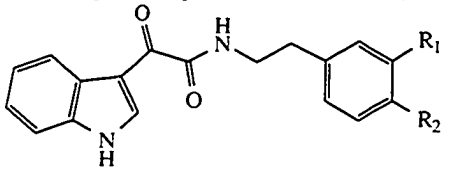

326. polyandrocarpamide A R_1 = Br, R_2 = OH
327. polyandrocarpamide B R_1 = I, R_2 = OH
328. polyandrocarpamide C R_1 = H, R_2 = OH

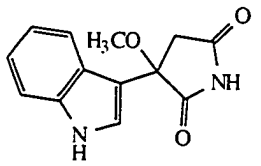

329. polyandrocarpamide D

Polycarpa auzata (Lindquist and Fenical 1990)

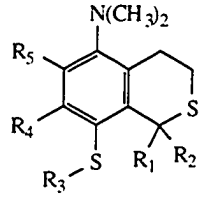

polcarpamines A - E

330. A R_1 = H, R_2 = R_4 = R_5 = OCH_3, R_3 = SCH_3
331. B R_1 = R_2 = O, R_3 = SCH_3, R_4 = R_5 = OCH_3
332. C R_1 = R_2 = S, R_3 = SCH_3, R_4 = R_5 = OCH_3
333. D R_1 = R4 = R_5 = OCH_3, R_2 = Ac, R_3 = SCH_3
334. E R_1 = H, R_2 = R_3 = OCH_3, R_4 = H, R_5 = OH

Polycarpa clavata (this study)

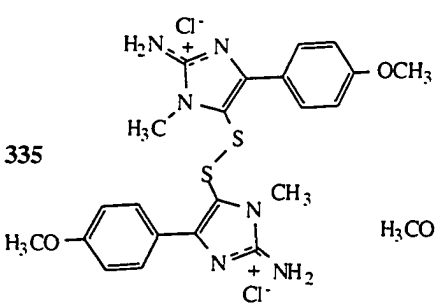

335

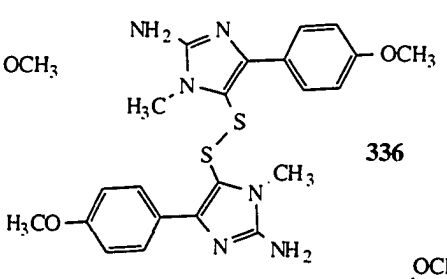

336

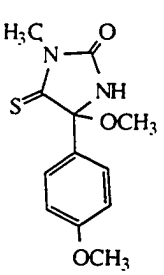

337

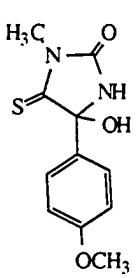

338

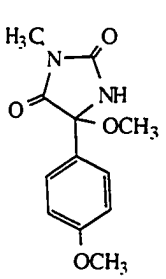

339

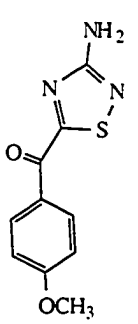

340

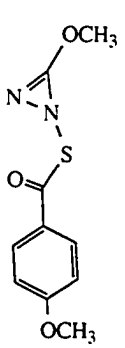

341

Figure 1-14. (continued)

Styela plicata (Nakamura *et al.* 1991)

281. ascidian peroxide (see *Ascidia ahodori*)

Styela plicata (Wasylak and Alam 1989)

342. styelolide

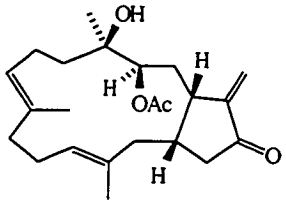

An unidentified species (no information about taxonomy - certainly not *Styela* sp.: Hirsch *et al.* 1989)

347. etzionin

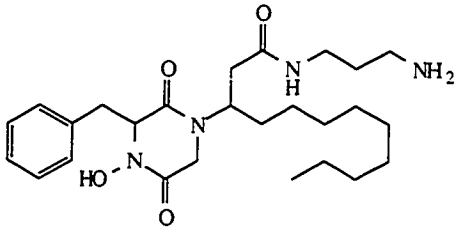

* Note: compds **343-346, 348** (see *Didemnum* sp., Figure 1-8)

**Note: Salps (*Ihlea racovitzai and Salpa thompsoni*) had been investigated for sterols.

Ihlea racovitzai (Schor and Seldes 1989)
Salpa thompsoni (Mimura *et al.* 1986)

An unidentified species

348a

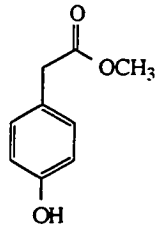

Chapter II

The Natural Products Chemistry of a Purple *Didemnum* sp. (WA9019 and WA9058)

A. Introduction to Chapter II

The genus *Didemnum* is the most diversified among the family Didemnidae. The genus is distinctively different from the related genus *Trididemnum* since it has four rows of branchial stigmata rather than three (Monniot *et al.* 1990). All species of the genus *Didemnum* are colonial with tiny zooids which have common cloacal channels. *Didemnum* colonies are usually thin and flat encrusting forms. The consistency of the tunic within *Didemnum* species varies from thin and very delicate in *D. perlucidem* to rough surfaced and leathery in *D. maculosum* (Berrill 1950).

Several structurally and pharmacologically novel natural products have been reported to date from species of the genus *Didemnum.* One of the characteristic features of ascidian chemistry is the prevalence of amino acid-derived compounds (Davidson 1993). In the chemistry of the genus *Didemnum*, tyrosine and tryptophan are the major amino acid components. Lamellarins (**154-167**), isolated originally from prosobranch mollusc *Lamellaria* sp. (Anderson *et al.* 1985) and later from the ascidian *D. chartaceum* (Lindquist *et al.* 1988) and an unidentified *Didemnum* sp. (Carroll *et al.* 1993), are presumably condensation products of 3-(3,4-dihydroxyphenyl) alanines (or 3-hydroxytyrosines, *viz* DOPA's) which are derived from tyrosines. Two iodinated derivatives (**187-188**) have been isolated from an unidentified *Didemnum* species (Sesin and Ireland 1984). Due to the relationship between iodine metabolism and tunic formation (see the discussion of iodine metabolism in Chapter I), and the recognition of DOPA as a cross-link in the quinone tanning of insect cuticles (Nevelle 1975, Anderson 1985), DOPA-originated alkaloids and the iodo-compounds may have importance in the tunic formation of ascidians. Presumptive DOPA-alkaloids, lukianols (**174-175**), have been identified from an unclassified ascidian (Yoshida *et al.* 1992). The structural similarity of the compounds to the lamellarins suggests that the ascidian may be a species of the genus *Didemnum.* The ascidian *D. ternatanum* contained a symmetric urea derivative, N,N-diphenyl urea (**189**, Ireland *et al.* 1981).

Three bromotryptamine derivatives (**151-153**) were isolated from *D. candidum* (Fahy *et al.* 1991). Interestingly, the dimeric piperazine compound (**153**) was the demethyl derivative of dragmacidin which was identified from a sponge *Dragmacidon* sp. (Kohmoto *et al.* 1988). Didemneimides (**342-345**) are other examples of putative conjugates of a tryptophan and a histidine (Richards-Gross 1993).

The abundance of fatty acid-derived secondary metabolites from the genus *Didemnum* is another characteristic of its chemistry. *D. candidum* and *D. moseleyi* contained ascidiatrienolides (**148-150**, Lindquist and Fenical 1989) and didemnilactone and neodidemnilactone (**181-182**, Niwa *et al.* 1991). The original structures, 9-membered lactones, were recently revised to 10-membered rings by total synthesis of ascidiatrienolide A (**148**, Congreve *et al.* 1993). Sphingosine-type amino alcohols (**183-185**, Searle and Molinski 1993), didemnenones (**190-191**, Lindquist *et al.* 1988) are fatty acid-derived secondary metabolites of the genus *Didemnum.* Didemnaketals (**196-197**, Potts *et al.* 1991) are the first examples of terpenoids from the genus *Didemnum.*

A recent study (Carroll *et al.* 1994) revealed the first example of cyclic peptide from this genus, mollamide (**180**), from *D. molle.* Ascididemnin (**186**), the first pentacyclic compound from an ascidian source, is a unique example of novel *Didemnum* chemistry (Kobayashi *et al.* 1988).

In terms of pharmacological activity, these compounds displayed a variety of bioactivites. Lamellarins I, K, and L (**162**, **164-165**) showed cytotoxicity against murine leukemia P388 and human lung carcinoma A549 cell lines (IC_{50} = 0.25 μg/ml). Moderate immunomodulatory activity for lamellarins K and L was also reported (Carroll *et al.* 1993). Lukianol A (**174**) exhibited KB cell line cytotoxicity at 1 μg/ml (Yoshida *et al.* 1992). Mollamide (**180**) possessed a broad spectrum of cytotoxicity against P388 (1 μg/ml), A549 (2.5 μg/ml), human colon carcinoma HT29 (2.5 μg/ml), and monkey kidney fibroblast cells CV1 (2.5 μg/ml) and inhibitory activity of RNA synthesis at 1μg/ml (Carroll *et al.* 1994). Antineoplastic activity was also recognized for ascidemnin (**186**) at the level of 0.39 μg/ml against the murine leukemia cell line L1210. The compound also possessed Ca^{2+} release actvitity seven times more potent than caffeine (Kobayashi *et al.* 1988). The following bioactivities were reported in the fatty acid-derived compounds: binding activity to leukotriene B4 receptors (didemnilactone and nor derivative), antifugal activity (sphingosine-type amino alcohols). Didemniketals, terpenoids, showed HIV-1 protease inhibitory activity (Potts *et al.* 1991).

For this investigation, a purple unidentified *Didemnum* sp. (other than *D. chartaceum*) was collected by hand using SCUBA (-10 m) from western Australia in the

Indian Ocean in December 1990. Specimens of the ascidians were immediately frozen after collection and preserved for 5 months at -40 °C. The sample was lyophilized and extracted twice each with 70 % methanolic chloroform and methanol. The combined extract was concentrated under vacuum and fractionated between hexane and methanol. The methanol-soluble material was further partitioned between ethyl acetate and water. The final solvent partition was accomplished between n-butanol and water. Gel filtration of the ethyl acetate-soluble material through Sephadex LH-20 and Spectra Gel HW-40S, followed by chromatography on reversed-phase HPLC (ODS - silica), gave ningalactone (**176**), ningalin (**177**), ningalamide (**178**), ningalone (**179**), and lamellarins O-T (**168-173**) along with the known compounds lamellarins G, H, and L (Figures 2-1 and 2-11). The novelty of the first four alkaloids was easily recognized by the combination of ^{1}H NMR and TLC of fractions from the preliminary gel-filtration.

This chapter describes the structure elucidation of these compounds using spectroscopic methods including the extensive use of 2-dimensional NMR correlation experiments. Molecular modeling studies of the alkaloids were also conducted. The issue of chirality, the shielding effect of phenyl rings, and possible biosynthetic pathways are discussed in detail. In relation to unusual ascidian biology such as metal sequestration and tunic formation, the implication of the compounds in their potential biological roles is also considered. Spectral data for the secondary metabolites are summarized in tables and in the experimental section at the end of the chapter.

Figure 2-1. Ningalactone, ningalin, ningalamide, ningalone, and their acetylated derivatives **349-352**.

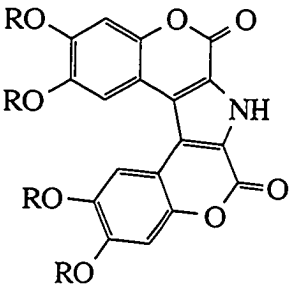

176. ningalactone R = H
349. R = Ac

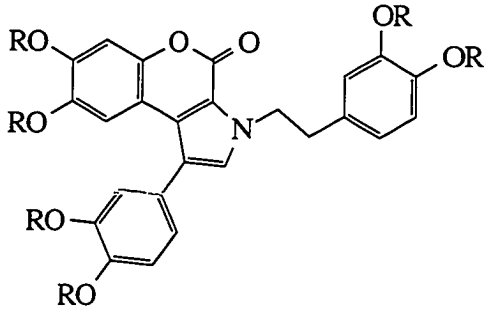

177. ningalin R = H
350. R = Ac

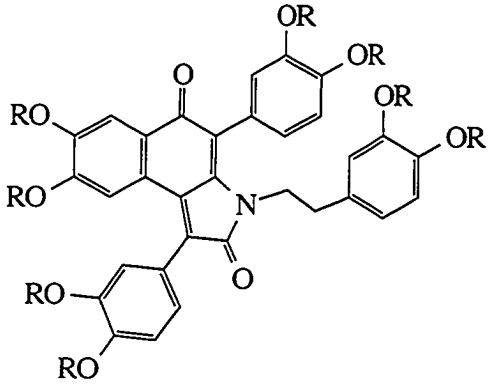

178. ningalamide R = H
351. R = Ac

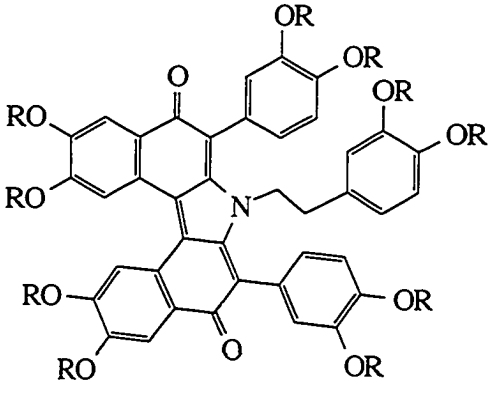

179. ningalone R = H
352. R = Ac

B. Structure Elucidation of Ningalactone (176), Ningalin (177), Ningalamide (178), and Ningalone (179).

Ningalactone (**176**) was obtained as an amorphous solid. The molecular formula, $C_{18}H_9NO_8$, established by HRFABMS [$(M + H)^+$ obsd. *m/z* 368.0420, dev. 3.7 ppm], showed 15 degrees of unsaturation. Since only five proton resonances in the ^1H NMR spectrum of **176** were observed, there was a two-fold axis of symmetry in the molecule, where the nitrogen atom and one hydrogen lay. Therefore, $C_9H_4O_4$ had to be explained for each side of the symmetric plane. The extended conjugation of **176** was suggested by its UV spectrum [(10 % DMSO/MeOH) λ_{max}: 370 (ε 2160), 325 (sh), 303 (8450), 262 (8650), and 235 (10000) nm]. Strong IR absorptions at 3377, 3186, and 1702 cm^{-1}, in conjugation with carbon signals at δ 142.7, 144.4, 146.3, and 154.8, suggested that there were an NH, OH's, and a conjugated ester. A bathochromic shift upon addition of base (NaOH), and no change in the UV spectrum on addition of acid (HCl) supported the phenolic nature of the compound and the non-basicity of the nitrogen.

The proton NMR spectrum of compound **176** showed only five signals, three of which were exchangeable (1 drop D_2O in DMSO-d_6 solution of compound **176**). Each of the four signals, except for the proton resonance at 14.0 ppm, represented two protons by integration. Since there was no coupling between the two proton signals at δ 6.89 (s, 2H) and 7.79 (s, 2H), these protons were para-positioned. The HMBC (Kogler *et al.* 1983) experiment established a 3,4-disubstituted catechol moiety (Table 2-1). The assignment of two hydroxyl groups at the two most deshielded carbons, C7 (δ 146.3) and C8 (δ 142.7), was also supported by the upfield-shift of two adjacent carbon signals at δ 104.2 [C-6 (C-6')] and 110.3 [C-9 (C-9')]. Analysis of the HMBC experiment showed that $^2J_{CH}$ couplings were often weaker than $^3J_{CH}$ couplings. That resulted in the assignment of the two carbon signals at δ 146.3 and 142.7 to C-7 (C-7') and C-8 (C-8'), respectively.

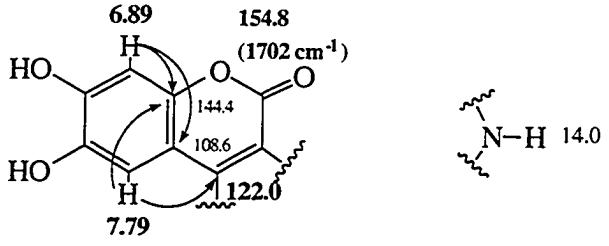

The carbon resonance at δ 122.0 was assigned to C-3 since $^4J_{CH}$ coupling was not likely. The same reasoning was applied to assign the carbon signal at δ 108.6 to C-4. Since only

Table 2-1. Physical and spectral properties of ningalactone (**176**)

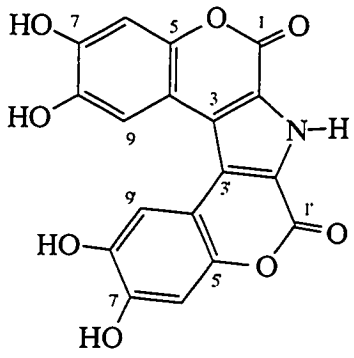

176. ningalactone

Source: *Didemnum* sp.
Exmouth, Western Australia
Amorphous solid
Molecular formula: $C_{18}H_9NO_8$
LRFABMS: obsd. *m/z* 368 $(M + H)^+$
UV (10 % DMSO/MeOH) λ_{max}: 370 (ε 2160), 325 (sh), 303 (8450), 262 (8650), 235 (10000) nm
IR (NaCl) ν_{max}: 3377, 3186, 1702, 1617, 1494, 1375, 1256, 1153 cm^{-1}
$[\alpha]_D = 0°$

NMR data

No.	^{13}C[a]	^{1}H[b]	HMBC (8 Hz)[b,c]
1, 1'	154.8		
2, 2'	110.3		
3, 3'	122.0		
4, 4'	108.6		
5, 5'	144.4[d]		
6, 6'	104.2	6.89 (s, 2H)	C4, C4', C5, C5', C7, C7', C8, C8'
7, 7'	146.3[d]		
8, 8'	142.7[d]		
9, 9'	110.3	7.79 (s, 2H)	C3, C3', C5, C5', C7, C7', C8, C8'
OH		9.41 (bs, 2H)	
OH		9.88 (bs, 2H)	
NH		14.0 (bs, 1H)	

All spectra was recorded in DMSO-d_6. Assignments were aided by DEPT sequence experiments and HMQC experiments. Chemical shifts are reported in δ units (downfield of TMS). [a] ^{13}C NMR spectrum was recorded at 50MHz. [b] Spectra were recorded at 500 MHz. [c] HMBC experiment was optimized for observing 8 Hz couplings to see $^{2\text{-}3}J_{CH}$ correlations. [d] Assignments may be interchanged.

four oxygens were available from the partial formula for each side of the symmetry plane, an oxygen in the lactone moiety and one in the catechol moiety had to be the same. That explained only half of the molecule.

There were two plausible ways to put these two moieties together with retention of C_2 symmetry (Scheme I). However, structure **II** was eliminated based on the following reasoning: i) Since C2 (C2') and C3 (C3') were α and β to the conjugated ester C1 (C1') respectively, C3 (C3') had to be more deshielded than C2 (C2'). In case of structure **II**, the carbon resonance at C3 (C3') had to be downfield of at least δ 150 due to the presence of the nitrogen next to that carbon. The carbon C3 (C3'), however, appeared at only δ 122.0. Therefore, the assignment of the carbon resonance at δ 122.0 to C3 (C3') was more reasonable in structure **I** than in structure **II**. ii) The proton H9 (H9') at δ 7.79 (s, 2H) was much more deshielded than the proton H6 (H6') at δ 6.89 (s, 2H). The phenomenon could be explained by the anisotropic effect of catechol rings in structure **I**, but not in structure **II**, because structure **I** could not be planar due to a high steric interaction. Therefore, one of the catechol rings had to be below or above the plane of the pyrrole ring. Consequently, each benzene ring would give a deshielding effect to H-9 or H-9'. In structure (**II**), the effect could not be explained. Thus, the structure of ningalactone (**176**) was assigned as **I**. Methylation of compound **176** with diazomethane in methanol resulted in an unseparable mixture. However, acetylation of compound **176** yielded the expected tetraacetate **349** which analyzed for $C_{26}H_{18}NO_{12}$.

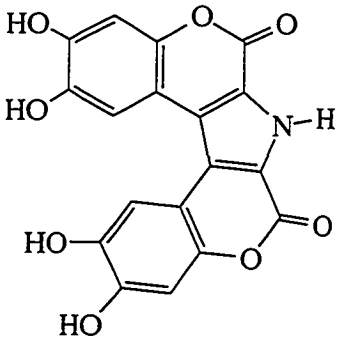

I (176)

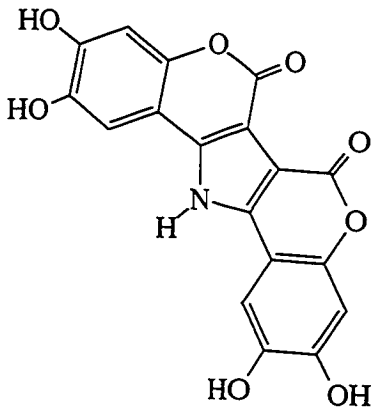

II

Scheme I

A molecular modeling study of compound **176** using a computer-assisted molecular modeling program, pcmodel (released from Serena Software), yielded the expected results (Figure 2-2). The two lactone rings were twisted to avoid steric crowding and, as a result, the catechol rings were 30 degrees out of plane in one of the energy-minimized conformers. The distance between H9 and H9' was 2.25 Å, a position located in the deshielding zone of the benzene rings. The shortest distance between H9 (H9') and the catechol ring C4'-C9' (C4-C9) was 2.7 Å. The magnitude of the deshielding effect of the catechol ring on the proton H9, with that distance (2.7 Å), obtained from Johnson and Bovey's work (1958) was 0.9 ppm. Thus, the estimated chemical shift of the protons would be around δ 8.0. The observed resonance at δ 7.79 was in a good agreement with the predicted value. Therefore, the molecular modeling results also supported the assigned structure **I**.

Ningalin (**177**) was obtained as an amorphous solid (Table 2-2). The molecular formula, $C_{25}H_{19}NO_8$, was determined from interpretation of the $(M + H)^+$ ion (*m/z* 462.1189, dev. -0.11 ppm) in the high resolution FAB mass spectrum, and in combination with ^1H and ^{13}C NMR data. All protons and carbons were observed as distinct bands, indicating that there was no symmetry. The high degree of unsaturation (17 degrees), indicated by the molecular formula, was supported by the UV spectrum of **177** [(MeOH) λ_{max} : 332 nm (ε 8700), 289 (10000), 236 (sh), and 204 (46000)]. A bathochromic shift (1N NaOH) in the UV spectrum of **177** and ^{13}C NMR data (8 resonances downfield of δ 140) suggested that the compound contained phenolic moieties. A strong IR absorption at 1698 cm^{-1}, which correlated with a carbon resonance at δ 156.0 (s), indicated that a conjugated ester was present.

The proton NMR spectrum of compound **177** revealed the existence of two mutually coupled methylenes [δ 2.94 (t, 2H, *J* = 7.3 Hz) and 4.55 (t, 2H, *J* = 7.3 Hz)], two 1,2,4-trisubstituted benzene rings [δ 6.47 (dd, 1H, *J* = 8, 1.5 Hz), 6.60 (d, 1H, *J* = 1.5 Hz), 6.67 (d, 1H, J = 8), 6.70 (dd, 1H, J = 8, 1.5 Hz), 6.84 (d, 1H, J = 1.5 Hz), and 6.86 (d, 1H, *J* = 8 Hz)] and three singlet aromatic protons [δ 6.80 (s, 1H), 7.06 (s, 1H), and 7.13 (s, 1H)].

A 1,2,4-trisubstituted benzene ring (C12-C17) was constructed from analysis of coupling constants [δ 6.47 (dd, 1H, *J* = 8, 1.5 Hz), 6.60 (d, 1H, *J* = 1.5 Hz), and 6.67 (d, 1H, *J* = 8 Hz)], COSY (Bax and Freeman 1981) coupling analyses and HMBC spectral features (Table 4). The proton signals at δ 6.60 (d, 1H, *J* = 1.5 Hz) and 6.67 (d, 1H, *J* = 8 Hz) were coupled to carbon signals at both δ 144.4 and 145.9. However, the proton

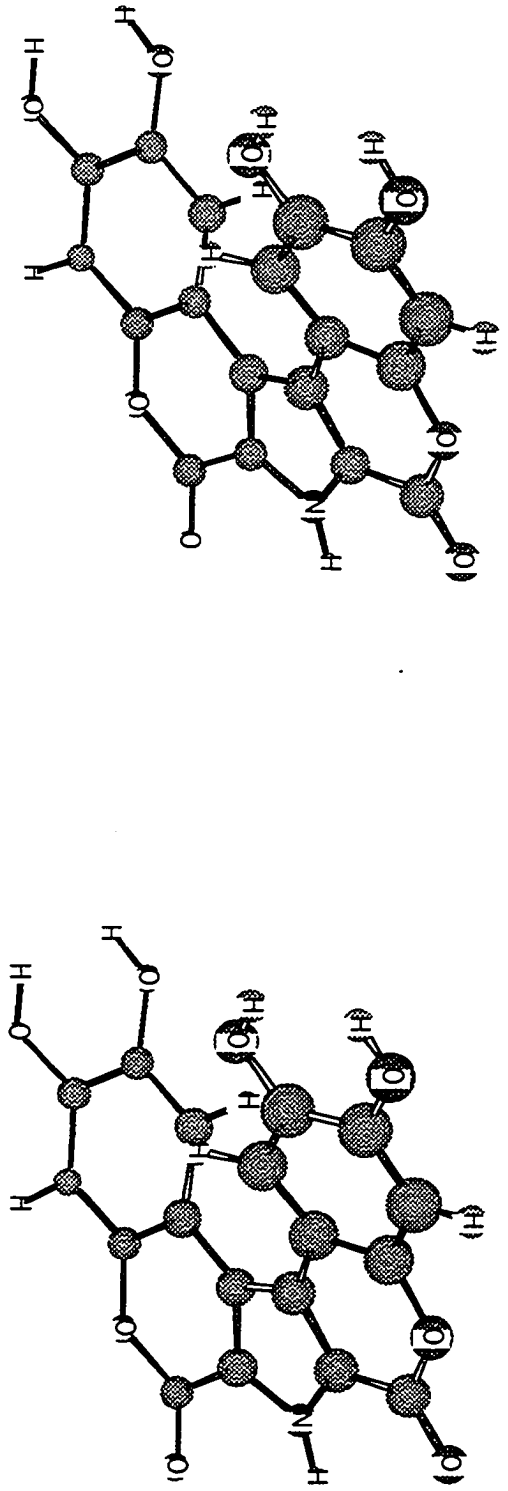

Figure 2-2. An energy-minimized conformer of ningalactone (**176**) in a stereo view. Two lactone rings were twisted to avoid steric hindrance and, in consequence, the catechol rings were 30 degrees out of the plane in an energy-minimized conformer. Energy minimization of **176** was performed using a Serena software, pcmodel, which adopts a MMX force field. The actual presentation of **176** was obtained using a combination of a Chem3D program and a ChemDraw software released from the Cambridge Scientific Computing, Inc.

Table 2-2. Physical and spectral properties of ningalin (**177**).

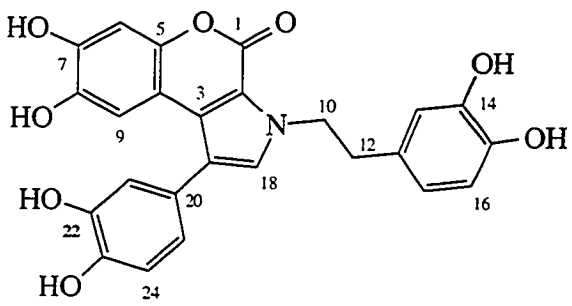

177. ningalin

Source: *Didemnum* sp.
Exmouth, western Australia
Amorphous solid
Molecular formula: $C_{25}H_{19}NO_8$
LRFABMS: obsd. *m/z* 462 $(M+H)^+$
UV (MeOH) λ_{max}: 332 (ε 8700), 289 (10000), 236 (sh), 204 (46000) nm
IR (NaCl) ν_{max}: 3700-3000, 1698, 1602, 1561, 1527, 1414, 1281, 1158, 1023, 984 cm^{-1}
$[\alpha]_D = 0°$

NMR data

No	^{13}C	^{1}H	HMBC (8 Hz)	NOESY
1	156.0			
2	114.8			
3	127.6			
4	110.6			
5	146.0			
6	104.0	6.80 (s, 1H)	C4, C5, C7, C8	
7	142.9			
8	146.8			
9	109.3	7.13 (s,1H)	C3, C5, C7, C8	H21, H25
10	50.9	4.55 (t, 2H, *J* = 7.3)	C2, C11, C12, C18	H11, H13, H17, H18
11	37.9	2.94 (t, 2H, *J* = 7.3)	C10, C12, C13, C17	H10, H13, H17, H18
12	130.2			
13	116.9	6.60 (d, 1H, *J* = 1.5)	C14, C15, C17	H10, H11
14	145.9			
15	144.4			
16	116.1	6.67 (d, 1H, *J* = 8)	C12, C14, C15	H17
17	120.6	6.47 (dd, 1H, *J* = 8, 1.5)	C13, C15	H10, H11, H16
18	133.5	7.06 (s, 1H)	C2, C3, C19, C20	H10, H11, H25
19	120.0			
20	126.4			
21	117.7	6.84 (d, 1H, *J* = 1.5)	C19, C23, C25	H9
22	145.8			
23	145.5			
24	116.4	6.86 (d, 1H, *J* = 8)	C20, C22	H25
25	112.7	6.70 (dd, 1H, *J* = 8, 1.5)	C19, C21, C23, C24	H9, H18

Spectra were acquired in a DMSO-d_6/CD_3OD mixture (5:1) with internal TMS. All 1-bond-couplings are based on the results of XHCORR experiments on a Brucker WP-200. All experiments except for XHCORR were done on a 500 MHz NMR spectrometer.

proton signal at δ 6.47 (dd, 1H, J = 8, 1.5 Hz) correlated only to the carbon signal at δ 144.4. Since $^{4}J_{CH}$ couplings are rarely observed in HMBC (8 Hz) spectra, the carbon signal at δ 144.4 had to be within three bonds. Therefore, the carbon signal at δ 144.4 was assigned to C15. Two hydroxyl groups were placed on the carbons C14 and C15, which resonated at δ 144.4 and 145.9, respectively. The assignment was supported by the upfield-shift of two adjacent carbons C13 (δ 116.9) and C16 (δ 116.1).

The mutually coupled proton signals at δ 2.94 (t, 2H, J = 7.3 Hz) and 4.55 (t, 2H, J = 7.3 Hz) directly correlated to carbon signals at δ 37.9 and 50.9, respectively. The downfield shift of C10 (δ 50.9) suggested that C10 had to be connected to a heteroatom (N or O). In the HMBC spectrum, the proton signal at δ 4.55 (t, 2H, J = 7.3 Hz) was coupled to two carbon signals at δ 133.5 and 114.8. Since two correlations of $^{2\text{-}3}J_{CH}$ through an oxygen atom were not reasonable, a nitrogen atom was connected to C10 (δ 50.9). The proton signal at δ 2.94 (t, 2H, J = 7.3 Hz) was also coupled to carbon signals at δ 130.2, 120.6, and 116.9. These results gave a N,N-disubstituted dopamine (**A**).

A

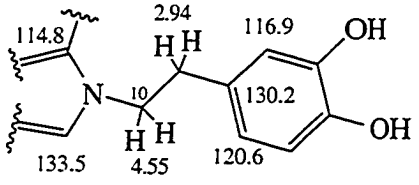

The presence of another 1,2,4-trisubstituted benzene ring (**B**, C20-C25) was confirmed by cross peaks of H25 (δ 6.70) to H21 (δ 6.84) and H24 (δ 6.86) in the COSY spectrum. Once again, the presence of two hydroxyl groups at C22 (δ 145.8) and C23 (δ 145.5) was supported by the up-field shift of two adjacent carbon resonances at δ 117.7 (C21) and 116.4 (C24). The assignment of C23 (δ 145.5) was based on the correlation of H25 (δ 6.70) to C23 in the HMBC spectrum. A carbon signal at δ 126.4 was assigned to C20 by a cross peak of H24 to C20. The proton signals at δ 6.70 (H25) and 6.84 (H21) were observed to be coupled to a carbon signal at δ 120.0 (C19).

B

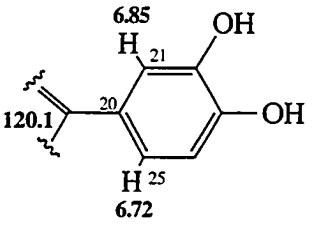

The carbon signal at δ 120.0 (C19) was further coupled to the proton signal at

δ 7.06 (H18). The proton H10 (δ 4.55) correlated with the carbon C18 at δ 133.5. Through these observations, the connectivities of C19-C18 and C18-N-C10 were established (**C**).

C

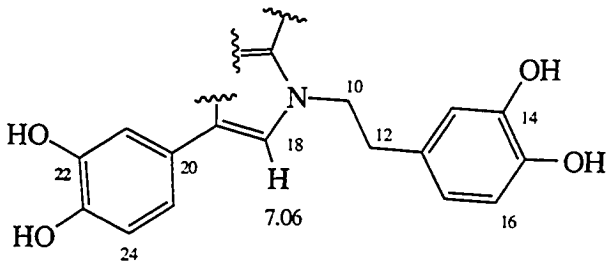

The two remaining proton signals [δ 6.80 (s, 1H) and 7.13 (s, 1H)] were singlets, thus they were para-positioned, or each signal came from a different spin system. In the HMBC spectrum, the proton signal at δ 6.80 (H6) was coupled to four carbon signals at δ 110.6 (C4), 142.9 (C7), 146.0 (C5), and 146.8 (C8). Among them, two signals at δ 142.9 and 146.8 were also coupled to the proton signal at δ 7.13 (H9). These protons were thus para-positioned (**D**). Analysis of these HMBC experiments showed that $^{2}J_{CH}$ couplings were often weaker than $^{3}J_{CH}$ couplings (for example, the 1,3,4-trisubstituted benzene ring of the dopamine moiety). That resulted in the assigning of two carbon signals at δ 142.9 and 146.8 to C7 and C8, respectively. Since the carbon signal at δ 146.0 was coupled to both protons H6 and H9, the carbon could be either C4 or C5. However, the carbon signal at δ 146.0 was assigned to C5 because C6 (δ 104.0) was more shielded than C9 (δ 109.3), indicating that C6 was influenced by both of oxygens which were attached to C5 and C7 respectively.

D

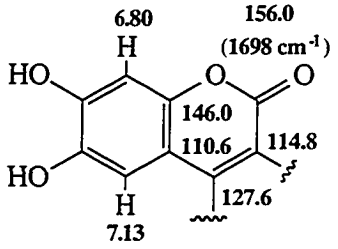

The connectivity of C3 and C4 was confirmed by a correlation of H19 (δ 7.13) to C3 (δ 127.6). The carbon signal at δ 127.6 was also coupled to the proton signal at δ 7.06 (H18) which also coupled to carbon signals at δ 120.0 (C19), 126.4 (C20), and 114.8 (C2). These couplings made it possible to assign connectivities between C3 and C19, and between C18 and C19. To meet the molecular formula, C2 (δ 114.8) had to be α and C3 (δ 127.6) β to the conjugated ester C1 (δ 156.0).

In the HMBC spectrum, five $^{1}J_{CH}$ coupling constants could be measured at positions : C13, C16, C17, C22, and C25. The $^{1}J_{CH}$ coupling constant at position C17 was 185 Hz. The rest of them were 160.2 Hz's. These observed heteronuclear coupling constants were consistent with the assigned structure (Breitmaier and Voelter 1987). Acetylation of compound **177** (excess acetic anhydride in pyridine) yielded the expected hexaacetate **350** [HRFABMS obsd. $(M + H)^+$ *m/z* 714. 1811, $C_{37}H_{32}NO_{14}$, dev. -1.7 ppm].

Ningalin was a very interesting molecule, because from the results of a molecular modeling (Figure 2-3), the proximity of the two benzene rings (C4-C9 and C20-C25) might seriously hinder free rotation of the catechol ring at C19. The catechol ring was 58 degrees out of the plane of the pyrrole ring. The coumarin moiety and the pyrrole ring were also twisted approximately 7 degrees. In one atropoisomer of the energy-minimized structures, only one of the two protons (H21 and H25) was close enough to provide nOe enhancement of proton H9 or proton H18. The rotational barrier of the bond between C19 and C20 was estimated at 300 Kcal/mol. However, in the NOESY spectrum of compound **177** (MeOH-d_4) two cross peaks of H9 and H21, and H9 and H25 were observed (Figure 2-4).

Ningalin (**177**) possessed a structure which is formerly the seco-analogue of the lamellarin skeleton, a novel alkaloid isolated by Anderson and coworkers (1985) from a marine mollusc, *Lamellaria* species.

Ningalamide (**178**) was obtained as a dark-red amorphous solid. The molecular formula, $C_{32}H_{23}NO_{10}$, possessing 22 degrees of unsaturation, was determined by HRFABMS. Extended conjugation was very obvious from the long wavelength absorption observed in the UV spectrum of the compound [(MeOH) λ_{max}: 450 nm (sh), 355 (ε 5800), 301 (sh), 289 (9400), and 204 (34000)]. A bathochromic shift was observed upon addition of a base (1N NaOH), while addition of acid (HCl) caused no change, suggesting the non-basicity of the nitrogen atom in **178**. The data, along with 11 carbon resonances downfield of δ 140, were indicative of a phenolic compound which was also supported by a strong IR absorption at 3700-3000 cm^{-1}. Intense absorption bands at 1699 and 1623 cm^{-1} in the IR spectrum of **178**, in conjugation with carbon resonances at δ 182.8 (s) and 170.4 (s), indicated the presence of a conjugated ketone and an amide group. The spectral data of ningalamide (**178**) are summarized in Table 2-3.

The interpretation of ^{1}H NMR, ^{13}C NMR, HMQC (Bax *et al.* 1983) spectra and HMBC spectra for ningalamide (**178**), in conjugation with HRFABMS data, led to the

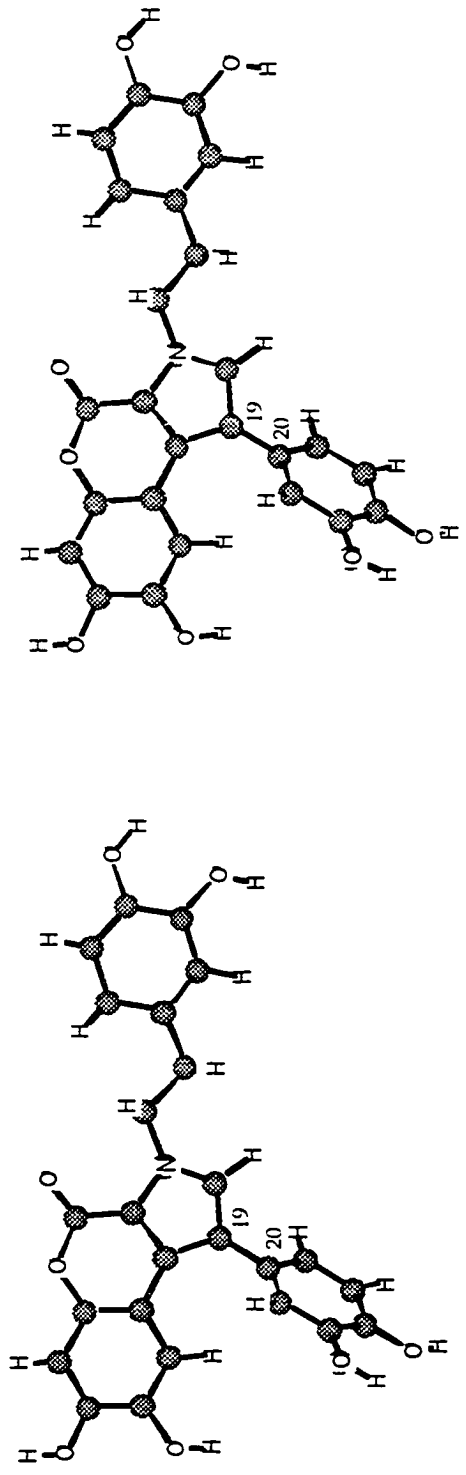

Figure 2-3. An Energy-minimized Structure of Ningalin (**177**) in a stereo view. The proximity of a coumarin moiety and the catechol ring at C19 seriously hindered free rotation of the catechol ring at C19. The rotational barrier of the bond between C19 and C20 was estimated at 300 kcal/mole. The catechol ring was 58 degrees out of the plane of the pyrrole ring. The coumarin moiety and the pyrrole ring were also twisted approximately 7 degrees. Energy minimization of **177** was performed using a Serena software, pcmodel, which adopts a MMX force field. The actual presentation of **177** was obtained using a combination of a Chem3D program and a ChemDraw software released from the Cambridge Scientific Computing, Inc.

Figure 2-4. NOESY correlations of ningalin (**177**)[a]

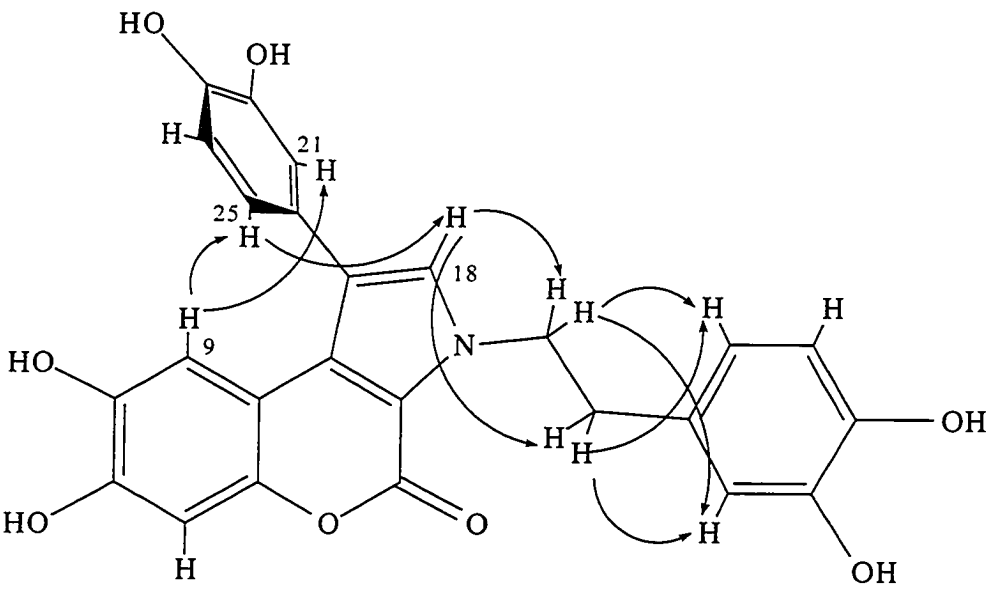

a) One possible atropoisomer is presented. The presence of cross peak between H18 and H21 was not determined due to the proximity of two proton resonances in the proton spectrum of **177**. Two cross peaks of H9 and H21 , and H9 and H25 in the NOESY spectrum of compound **177** suggested the catechol ring (C20-C25) is almost orthogonal to the plane of the pyrrole ring.

assignment of several subunits (Scheme II). The 1-dimensional ^{1}H NMR and COSY spectra of compound **178** revealed that there were four different spin systems, three 1,2,4-trisubstituted benzene rings, and a N,N,2-trisubstituted ethyl amine. Analyses of HMQC and HMBC (8 Hz) spectra showed that the N,N,2-trisubstituted ethyl amine moiety (C17 and C18) was connected to one of the 1,2,4-trisubstituted benzenes (C19-C24). Further analysis showed that the proton at C17 were coupled to an amide carbonyl (C25) at δ 170.4 and a quaternary carbon (C9) at δ 146.4 through the nitrogen (**A**). A quaternary carbon (C26) at δ 129.5 was connected to another 4-monosubstituted catechol moiety (C27-C32) (**B**). Similar connectivity was established between C2 (δ 118.7) and C3 (δ 123.4) by ^{1}H -^{13}C correlation methods (**C**). In each 4-monosubstituted catechol moiety, two hydroxyl groups were placed at the two most deshielded positions, which was supported by the up-field shift of two adjacent carbons. The last subunit, a 3,4- disubstituted catechol moiety (C1-C16), was also assigned by HMQC and HMBC correlations (**D**). In addition to correlating to the carbon C11 (δ 122.3), the isolated proton H13 (δ 7.33) coupled to the conjugated ketone C1 (δ 182.8). The proton signal at δ 7.12 (H16) coupled to two quaternary carbons at δ 133.1 (C12) and 122.9 (C10). The assignment of four carbons, C11 (δ 122.3), C12 (δ 133.1), C14 (δ 147.8), and C15 (δ 149.6), were based on the fact that $^{3}J_{CH}$ couplings are often stronger than $^{2}J_{CH}$ couplings in phenolic systems. Thus, four

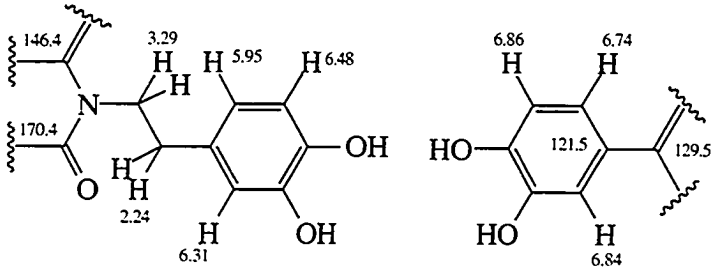

Scheme II

Table 2-3. Physical and spectral properties of ningalamide (**178**).

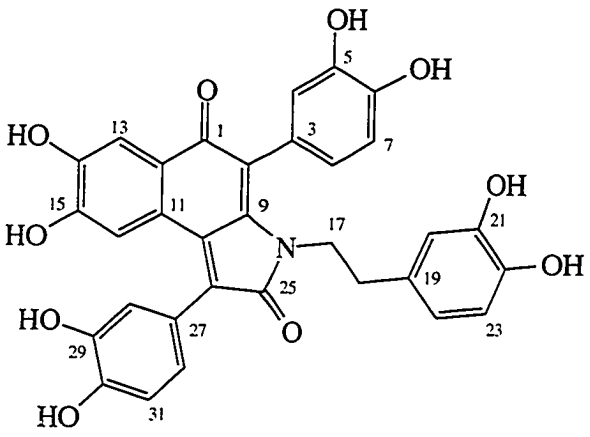

178. ningalamide

Source: *Didemnum* sp.

Exmouth, Western Australia

Amorphous solid

Molecular formula: $C_{32}H_{23}NO_{10}$

LRFABMS (NBA matrix): molecular ion not observed

(SGly Matrix): obsd. *m/z* 582 $(M + H)^+$, *m/z* 603 $(M + Na)^+$, *m/z* 625 $(M + 2Na)^+$, *m/z* 279, 237, 221, 159

UV (MeOH) λ_{max}: 450 (sh), 355 (ε 5800), 301 (sh), 289 (9400), 204 (43000) nm

IR (NaCl) ν_{max}: 3700-3000, 1699, 1623, 1593, 1515, 1431, 1393, 1360, 1292, 1200, 1117, 1022, 983 cm^{-1}

$[\alpha]_D = 0^o$

NMR data

No	^{13}C	^1H	HMBC (8 Hz)	HMBC (2.5 Hz)	NOESY
1	182.8				
2	118.7				
3	123.4				
4	118.4	6.72 (d, 1H, *J* = 1.5 Hz)	C2, C5, C6, C8	C1, C2, C3, C5, C6, C7, C8, C9	H17, H18
5	144.6				
6	145.4				
7	115.0	6.79 (d, 1H, *J* = 7.8)	C3, C5, C6	C2, C3, C5, C6	H8
8	122.1	6.58 (dd, 1H, *J* = 7.8, 1.5)	C4, C6	C1, C2, C5, C6, C7, C9	H7, H17, H18

Table 2-3 (continued).

No	^{13}C	^{1}H	HMBC (8 Hz)	HMBC (2.5 Hz)	NOESY
9	146.4				
10	122.9				
11	122.3				
12	133.1				
13	113.4	7.33 (s, 1H)	C1, C11, C14, C15	C1, C2, C11, C12, C14, C15, C16	
14	147.8				
15	149.6				
16	112.3	7.12 (s, 1H)	C10, C12, C14, C15	C1, C2, C10, C12, C13, C14, C15, C26	H28, H32
17	42.6	3.30 (dt, 1H, J = 14.7, 7.8) 3.23 (dt, 1H, J = 14.7, 7.8)	C9, C18, C19, C25		H4, H8, H18, H20, H24
18	33.9	2.24 (t, 2H, J = 7.8)	C17, C19, C20, C24		H4, H8, H17, H20, H24
19	128.7				
20	116.0	6.31 (d, 1H, J = 1.5)	C18, C21, C22, C24	C21, C22, C23, C24	H17, H18
21	144.9				
22	143.6				
23	115.3	6.48 (d, 1H, J = 7.8)	C19, C21, C22	C19, C20, C21, C22	H24
24	119.1	5.95 (dd, 1H, J = 7.8, 1.5)	C18, C20, C22	C20, C21, C22, C23	H17, H18, H23
25	170.4				
26	129.5				
27	121.5				
28	116.8	6.84 (d,1H, J = 1.5)	C26, C29, C30, C32	C26, C29, C30, C32	H16
29	145.6				
30	146.6				
31	115.9	6.86 (d, 1H, J = 7.8)	C27, C29, C30	C26, C27, C28, C29, C30	H32
32	121.2	6.74 (dd, 1H, J = 7.8, 1.5)	C26, C28, C30	C26, C28, C29	H16, H31
OH		8.68 (s, 1H)[a]			
OH		9.14 (s, 1H)[a]			
OH		9.82 (s, 1H)[a]			
OH		9.99 (s, 1H)[a]			
OH		9.09 (s, 1H)[a]			
OH		8.64 (s, 1H)[a]			
OH		9.24 (s, 1H)[a]			
OH		9.42 (s, 1H)[a]			

^{1}H NMR spectra were recorded in DMSO-D_6 at 500 MHz. J values are reported in Hz's and the chemical shifts are given in δ units (ppm downfield of TMS). ^{13}C NMR spectrum was recorded at 125 MHz in DMSO-d_6. Multiplicities were obtained by analysis of DEPT experiments at 50 MHz in MeOH-d_4. All $^{1}J_{CH}$ couplings are based on the results of HMQC experiments. All 2-D NMR experiments were performed with a 500 MHz NMR spectrometer.

[a]All values were obtained in DMSO-d_6 with trace amount of TFA with reference to internal TMS at 0.00 ppm.

partial structures were established.

The UV spectrum of compound **178** contained an absorption band at 450 nm. It suggested that the compound had an extended quinone chromophore. Normally the carbon signal at the α-position of an α,β-unsaturated ketone is shielded, and that at the β-position is deshielded. Consequently, a quinone methide moiety (**E**) was constructed by six carbons: C1 (δ 182.8), C2 (δ 118.7), C9 (δ 146.4), C10 (δ 122.9), C11 (δ 122.3), and C12 (δ 133.1). To meet the molecular formula, connectivities between C10 and C26, and between C25 and C26 were established.

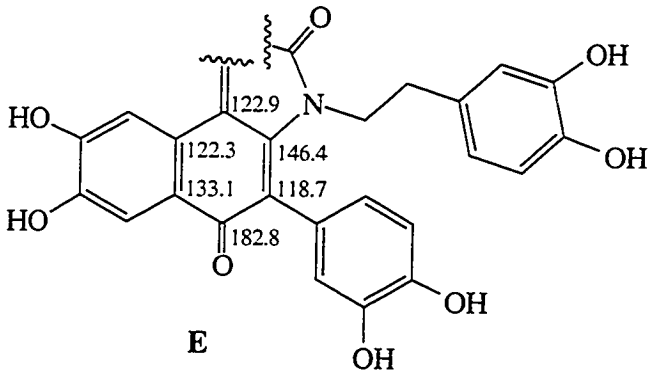

E

A very-long-range correlation experiment (2.5 Hz-HMBC) was performed to confirm the proposed structure since $^{4}J_{CH}$ couplings were not likely in normal HMBC experiments which specify coupling constants of 6 to 10 Hz. The experiment fully supported the previous assignment by showing critical 4-bond couplings. The proton H8 (δ 6.58) coupled to two carbons, C1 (δ 182.8) and C9 (δ 146.4). The proton H13 (δ 7.33) also coupled to C2 (δ 118.7). Furthermore, C26 (δ 129.5) was observed to be coupled to H-16 (δ 7.12).

The molecular modeling study of **178** showed that once again the catechol ring at C26 was twisted at 58 degrees from the plane of the pyrrolidone. The catechol ring at C2 was completely orthogonal to the quinone methide plane (Figure 2-5). The rotation of the catechol rings appeared to be highly restricted because of their proximity to the ethylene moiety and the 3,4-disubstituted catechol ring (C11-C16). When the rotational barrier was estimated using a MMX calculation, the maximum barrier to rotation about the C2-C3 bond was in excess of 800 Kcal/mole. The energy barrier of the rotation was very sensitive to the exact placement of the aromatic hydrogens. The initial geometry obtained from the energy-minimized structure of **178** was arbitrarily given as 0 degree of the rotation. The energy barrier rapidly increased for rotations beyond approximately 30 degrees in either

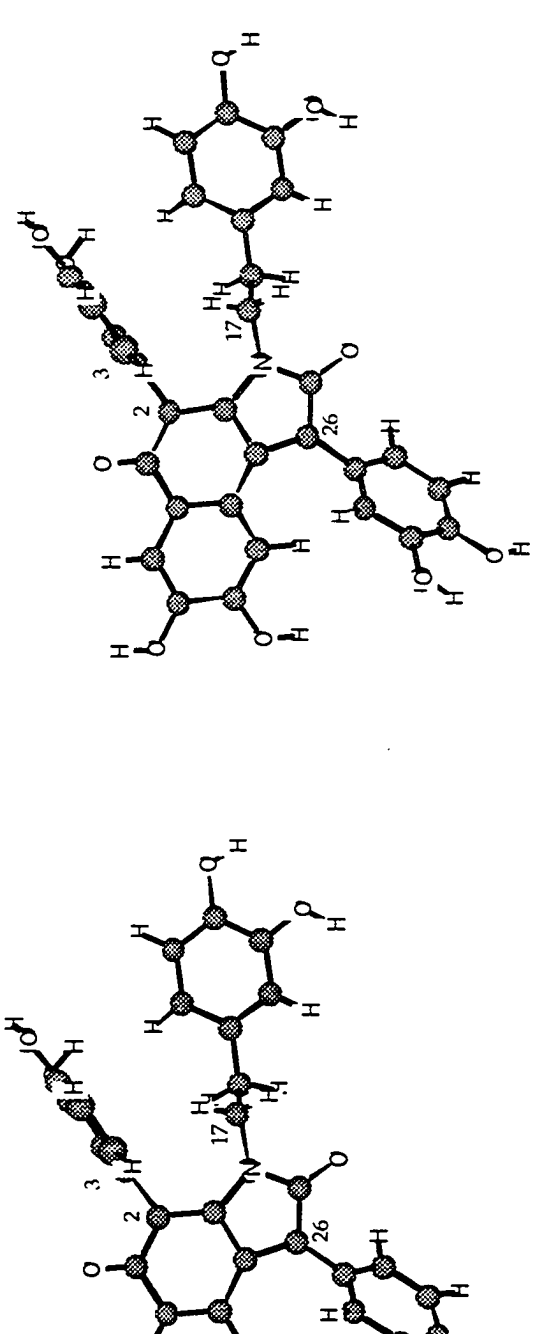

Figure 2-5. An Energy-minimized Structure of Ningalamide (**178**) in a Stereo View. One of four possible atropoisomers is presented. The catechol ring at C26 was twisted at 58 degrees from the plane of the pyrrolidone. The catechol ring at C2 was completely orthogonal to the quinone methide plane. The rotation of the catechol rings appeared to be highly restricted because of their proximity to the ethylene moiety and the 3,4-disubstituted catechol ring (C11 - C16). The maxium barrier to rotation about the C2-C3 bond was estimated to be in excess of 800 Kcal/mole. Two protons H17's were predicted to be diastereostopic since each proton was directed toward two different functional groups such as an amide carbonyl and the catechol ring at C2, respectively. Energy minimization of **178** was performed using a Serena software, pcmodel, which adopts a MMX force field. The actual presentation of **178** was obtained using a combination of a Chem3D program and a ChemDraw software released from the Cambridge Scientific Computing, Inc.

direction. When the bond started to rotate more than 30 degrees in either directions, the aromatic protons at C4 and C8 approached one of the methylene protons at C17 within their van der Waals radii and thus they became very repulsive each other. However, the energy barrier to rotation about the bond C26-C27 was not symmetrical as was that of the C2-C3 bond. Because the catechol ring at C26 was not orthogonal to the main skeleton, the energy increased very rapidly for rotations beyond either about 20 degrees in one direction or 60 degrees in the other. Although the absolute value of the barrier was much less than the previous one, it was still comparable to the van der Waals term. Two protons H17's were diastereotopic since each proton was directed toward two different functional groups such as an amide carbonyl and the catechol ring at C2 respectively, and free rotations of C17-C18 and C17-N bonds were not permitted under the circumstances. Indeed, the proton spectrum of **178** showed two distinctive resonances for these protons. The distance between the amide carbonyl group and the methylene unit (H17) in ningalamide was 2.7 Å which is the same distance between the ester carbonyl group and the identical methylene unit in ningalin (**177**). The up-field shift of two methylene units in the dopamine moiety in the proton and the carbon spectra of **178**, compared to those values in **177,** provided further proof that the catechol ring C2 was coplanar to the dopamine side chain.

NOESY (Levitt *et al.* 1984) experiments, performed with compound **178** (Figure 2-6), supported the proposed structure and the results of the molecular modeling experiment. The restricted rotation of catechol rings presumed that only one of the two non-equivalent protons H17's and only one out of H28 and H32 due to its restricted rotation might have cross peaks to the aromatic protons of the catechol rings. However, both the nonequivalent protons H17's gave correlations to H4 and H8, and the proton H16 correlated to the aromatic protons H28 and H32 simultaneously.

Acetylation of compound **178** yielded the expected octaacetate **351** [HRFABMS obsd. m/z 918.2186 $(M + H)^+$, $C_{48}H_{40}NO_{18}$, dev. -6.4 ppm]. The proton NMR spectrum of **178** recorded in DMSO-d_6 with a trace amount of TFA showed eight more sharp signals, each of which represented a OH proton (Table 2-3).

A trace amount of a methyl derivative of **178** was also detected in a semi-purified mixture, by a diode-array HPLC, however, no attempt was made to characterize the compound.

Ningalone (**179**) was obtained as a dark-red amorphous solid. The HRFAB mass spectrum of compound **179** established the molecular formula as $C_{40}H_{27}NO_{12}$ (28 degrees

Figure 2-6. NOESY correlations of ningalamide (**178**)[a,b]

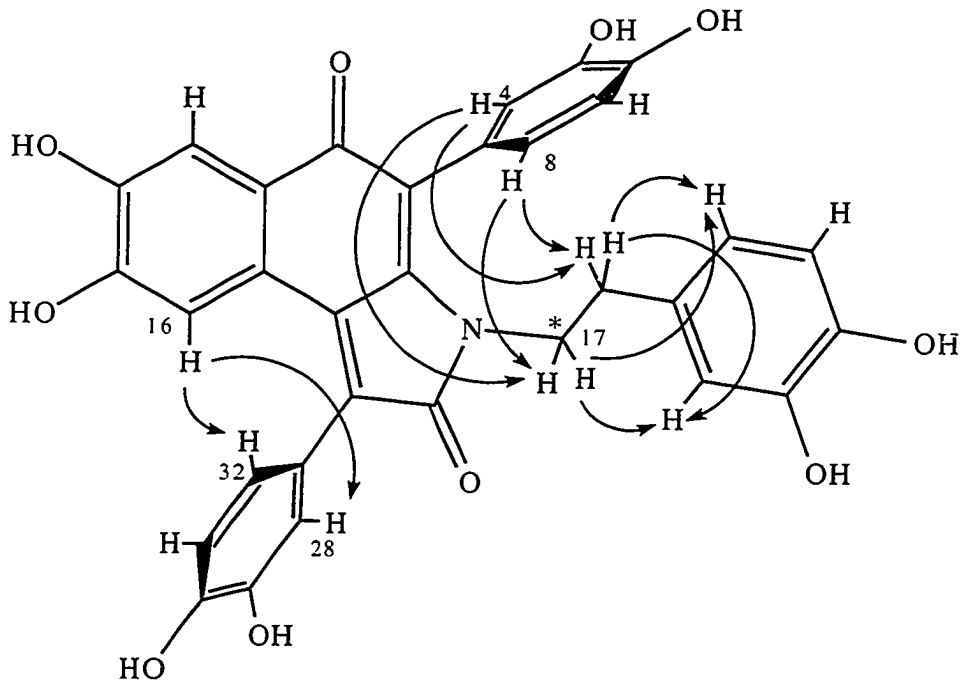

a) Although both the diastereotopic protons at C17 showed correlations to H4, H8, H20, and H25, only one nOe has been presented in the individual case for clarity.

b) Only one atropoisomer among four conformers is presented. The presented structure is not an energy-minimized strcture. The ethylene moiety of the dopamine including C17 is shown in an arbitary manner for clarity. To see the actual conformation in an energy-minimized state, see figure 2-5.

of unsaturation). The proton NMR spectrum of **179** showed only five signals, each of which represented two protons by integration, respectively, except for three one proton signals at δ 5.95 (dd, 1H, J = 7.5, 1.5 Hz), 6.12 (d, 1H, J = 1.5 Hz), and 6.30 (d, 1H, J = 7.5 Hz) in the aromatic region,. Moreover, only 24 signals were observed in the ^{13}C NMR spectrum. Eight of these signals could be assigned to a familiar N,N-disubstituted dopamine moiety (Table 2-4). These data indicated a symmetry plane was present in the molecule, which bissected the nitrogen atom. Half of the symmetric element, $C_{16}H_9O_5$, remained to be assigned. The IR spectrum showed a strong hydroxyl band at 3700-3000 cm^{-1} and a conjugated ketone at 1665 cm^{-1} by correlation with six resonances downfield of δ 140 and a carbon signal at δ 185.4 (s). The UV spectrum of **179** [(MeOH) λ_{max} : 508 nm (ε 9900), 404 (sh), 294 (17000), 276 (18000), and 206 (41000)] suggested a highly conjugated system. A bathochromic shift was observed upon addition of base (1N NaOH), suggesting a phenolic compound. Consistent with this conclusion, addition of acid (6N HCl) gave no change.

The presence of a dopamine moiety was evident from the ^1H NMR spectral data : two mutually coupled methylenes at δ 2.13 (t, 2H, J = 6.5 Hz) and 2.95 (t, 2H, J = 6.5 Hz), and three aromatic signals at δ 5.95 (dd, 1H, J =7.5, 1.5 Hz), 6.12 (d, 1H, J = 1.5 Hz), and 6.30 (d, 1H, J = 7.5 Hz). HMQC and HMBC experiments established the connectivity of C18 (δ 34.5) and C19 (δ 130.5) (Table 2-4). The proton signal at δ 2.95 (H17) coupled to a quaternary carbon at δ 156.4 (C9), via a $^3J_{CH}$ coupling through the nitrogen atom. A quaternary carbon C2 (δ 118.9) was connected to a 4-monosubstituted catechol ring (C3-C8), based on correlations of H4 (δ 6.82) and H8 (δ 6.68) to C2 (δ 118.9) in the HMBC spectra.

A 3,4-disubstituted catechol moiety (C11-C16) was identified by correlations of H13 (δ 7.45) to C1 (δ 185.4), C11 (δ 125.0) and C15 (δ 150.2), and H16 (δ 7.85) to C10 (δ 126.4), C12 (δ 132.2), C14 (δ 148.9) and C15 (δ 150.2) in the HMBC spectra.

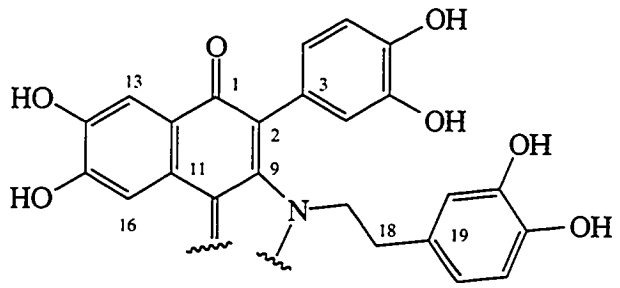

The large difference in chemical shift between C2 (δ 118.9) and C9 (δ 156.4) could

Table 2-4. Physical and spectral properties of ningalone (**179**)

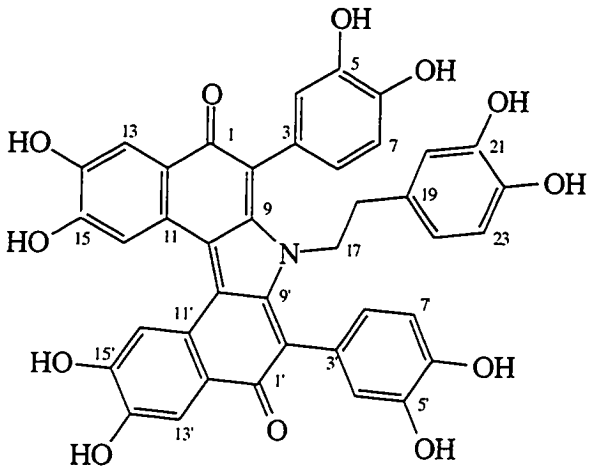

179. ningalone

Source: *Didemnum* sp.

Exmouth, Western Australia

Amorphous solid

Molecular formula: $C_{40}H_{27}NO_{12}$

LRFABMS (NBA matrix): obsd. *m/z* 714 $(M + H)^+$, *m/z* 736 $(M + Na)^+$

(SGly Matrix): obsd. *m/z* 715 $(M + 2H)^+$

UV (MeOH) λ_{max}: 508 (ε 9900), 404 (sh), 294 (17000), 276 (18000), 206 (41000) nm

IR (NaCl) ν_{max}: 3700-3000, 1665, 1562, 1296 cm^{-1}

$[\alpha]_D = 0^o$

NMR data

No	$^{13}C^a$	$^1H^{a,b}$	HMBC (8Hz)^{a,b}	NOESY^d
1, 1'	185.4 (2C)			
2, 2'	118.9 (2C)			
3, 3'	126.1 (2C)			
4, 4'	119.4 (2C)	6.82 (d, 2H, J = 1.5 Hz)^c	C2, C2', C5, C5' C6, C6', C8, C8'	H17, H18
5, 5'	146.1 (2C)			
6, 6'	146.5 (2C)			
7, 7'	116.2 (2C)	6.83 (d, 2H, J = 8)^c	C3, C3' C5, C5', C6, C6'	H8, H8'

Table 2-4 (continued).

No	$^{13}C^{a}$	$^{1}H^{a,b}$	HMBC (8Hz)[a,b]	NOESY[d]
8, 8'	124.2 (2C)	6.68 (dd, 2H, J = 8, 1.5)[c]	C2, C2', C4, C4', C6, C6'	H7, H7', H17, H18
9, 9'	156.4 (2C)			
10, 10'	126.4 (2C)			
11, 11'	125.0 (2C)			
12, 12'	132.2 (2C)			
13, 13'	115.0 (2C)	7.45 (s, 2H)	C1, C1', C11, C11', C15, C15'	
14, 14'	148.9 (2C)			
15, 15'	150.2 (2C)			
16, 16'	114.2 (2C)	7.85 (s, 2H)	C10, C10', C12, C12', C14, C14', C15, C15'	
17	47.5	2.95 (t, 2H, J = 6.5)	C9, C9', C18, C19	H4, H4', H8, H8', H18, H20, H24
18	34.5	2.13 (t, 2H, J = 6.5)	C17, C19, C20, C24	H4, H4', H8, H8', H17, H20, H24
19	130.5			
20	117.1	6.12 (d, 1H, J = 1.5)	C18, C21, C22, C24	H17, H18
21	145.5			
22	144.6			
23	115.7	6.30 (d, 1H, J = 7.5)	C19, C21, C22	H24
24	121.4	5.95 (dd, 1H, J = 7.5, 1.5)	C18, C20, C22	H17, H18, H23

^{13}C NMR was recorded at 125 MHz. Assignments were aided by a DEPT sequence experiment, a COSY experiment, and an HMQC experiment. [a] Spectra were obtained in MeOH-d_4. [b] Experiments were carried out at 500 MHz. [c] To facilitate NOESY experiment ^{1}H NMR spectrum was also recorded at 500 MHz in DMSO-d_6. Protons at positions H4, H7, and H8 appeared at δ 6.76 (s, 2H), 6.72 (d, 2H, J = 8 Hz), and 6.59 (d, 2H, J = 8), respectively. [d] NOESY experiment had been performed at 500 MHz in DMSO-d_6.

be rationalized if C2 was α and C9 was β to the conjugated carbonyl C1 (δ 185.4). Thus, having completed 16 carbons assignments, the complete assignment of the ^{1}H and ^{13}C NMR spectra had been achieved (Table 2-4).

Treatment of ningalone with acetic anhydride in pyridine yielded the expected decaacetate, **352** [HRFABMS obsd. m/z 1135. 2708 $(M + 2H)^+$, $C_{60}H_{49}NO_{22}$, dev. -3.4 ppm], which showed acetate methyl signals in an integrated ratio of 1:1:2:2:2:2 in the proton NMR spectrum.

The molecular modeling study of **179** showed that in a diastereomer of the energy-minimized structures of **179**, two 3,4-disubstituted catechol rings in the main pentacyclic skeleton were predicted to be twisted each other as much as 44 degrees out of the plane to avoid steric hindrance, and, as a result, the pentacyclic system had almost an one-half spiral conformation. The interproton distance between H16 and H16' was 2.5 Å. Therefore, each proton experienced a diamagnetic anistropic effect from the catechol ring, which was demonstrated in the proton spectrum of **179**. The protons H16 and H16' resonated at δ 7.85, a low field position which was in good agreement with the estimated value from the proton-benzene distance and the calculated diamagnetic anistropy of benzene with a function of hexagonal distance from the benzene ring (Johnson and Bovey, 1958). Two quinonoid groups and two catechol rings at C2 and C2' were of anti configuration against the planes of the pyrrole ring and the dopamine unit respectively. The catechol rings were juxtaposed at an 11 degree angle. Furthermore, the catechol rings were almost orthogonal (an 87 degree angle) to the plane of the pyrrole ring in the center of the pentacyclic system. The configuration adopted forced the catechol ring of the dopamine moiety into a semi-vertical configuration with respect to the plane of the overall pentacyclic system. As suggested by computer-generated perspective drawings of **179** (Figure 2-7), the rotational barrier about C2-C3 and C2'-C3' bonds were extremely high, up to 1200 Kcal/mole. Therefore, free rotation of the bonds appeared to be severely hindered. The energy barrier of rotation about C18-C19 bond was estimated to be only 8 Kcal/mole and thus its free rotation is assumed.

NOESY experiments supported the assignment of structure for ningalone. Both protons H17's (δ 2.95) and H18's (δ 2.13) showed enhancements with H4 and H4' (δ 6.82), and H8 and H8' (δ 6.68), indicating that the two catechol rings (C3-C8 and C3'-C8') were flanking the dopamine. The results of these experiments are summarized in Figure 2-8.

Ningalone has a unique functionality, a highly extended quinone methide, which is closely related to purpurone, a molecule from a sponge *Iotrochota* sp. (Chan *et al.* 1993).

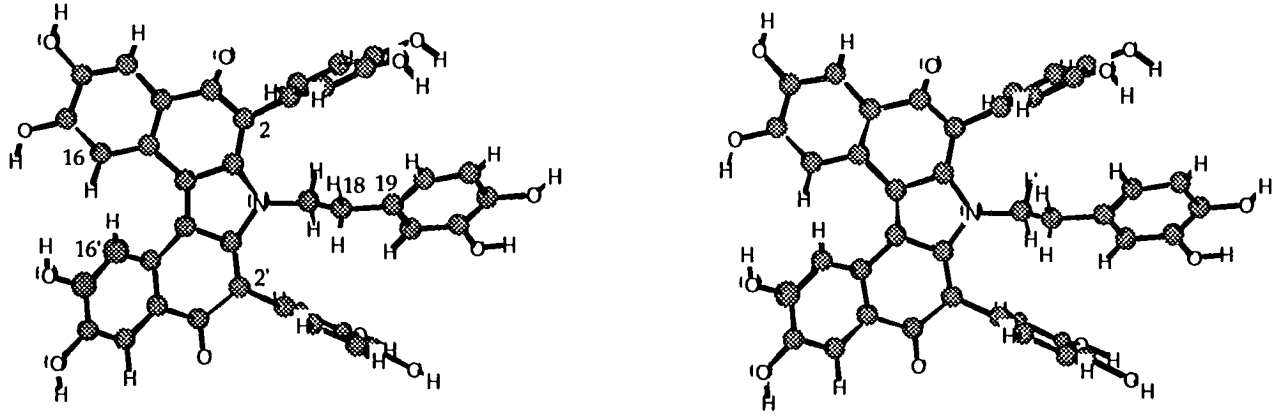

Figure 2-7. An energy-minimized structure of ningalone (**179**) in a stereo view. One possible diastereomer is presented. In a diastereomer of the energy-minimized structures of **179**, two 3,4-disubstituted catechol rings in the main pentacyclic skeleton were predicted to be twisted each other as much as 44 degrees out of the plane to avoid steric hindrance, and, as a result, the pentacyclic system had almost an one-half spiral conformation. Therefore, each proton (H16 or H16') might experience a diamagnetic anistropic effect from the catechol ring. Two quinonoid groups and two catechol rings at C2 and C2' were of anti configuration against the planes of the pyrrole ring and the dopamine unit respectively. The catechol rings were juxtaposed at an 11 degree angle. Furthermore, the catechol rings were almost orthogonal (an 87 degree angle) to the plane of the pyrrole ring in the center of the pentacyclic system. The configuration adopted forced the catechol ring of the dopamine moiety into a semi-vertical configuration with respect to the plane of the overall pentacyclic system. The rotational barrier about C2-C3 and C2'-C3' bonds were extremely high, up to 1200 Kcal/mole. Therefore, free rotation of the bonds appeared to be severely hindered. The energy barrier of rotation about C18-C19 bond was estimated to be only 8 Kcal/mole and thus its free rotation is assumed. The same methods described in Figure 18 were used for energy minimization and actual presentation of **179**.

Figure 2-8. NOESY correlations of ningalone (**179**)[a,b].

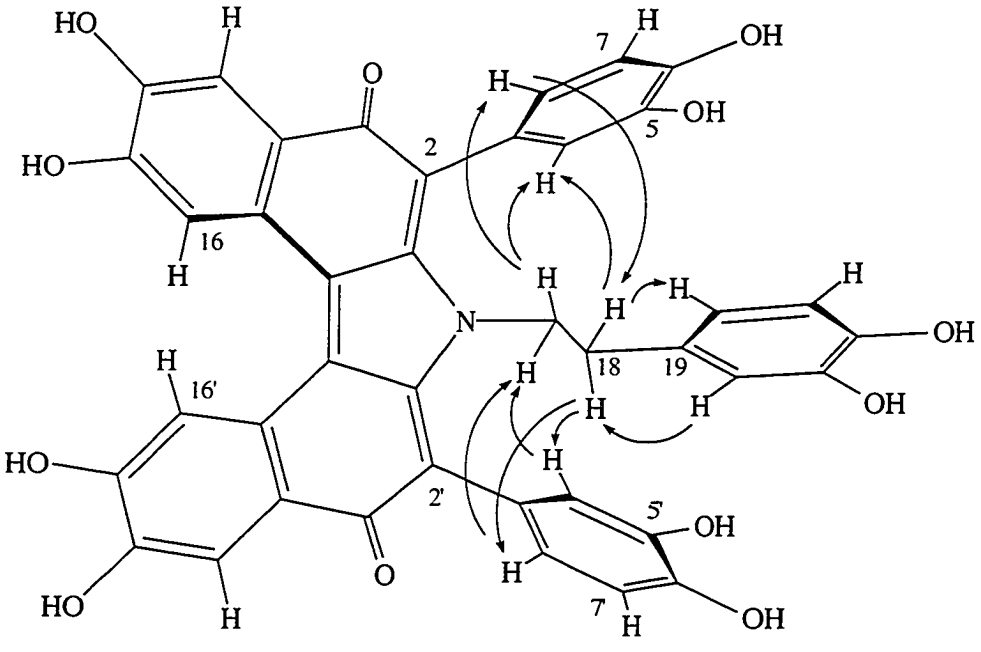

a) Only one atropoisomer among several conformers is presented. The presented structure is not an energy-minimized strcture. The ethylene moiety of the dopamine including C18 is shown in an arbitary manner for clarity. To see the actual conformation in an energy-minimized state, see figure 2-7.

b) Both protons H17's and H18's showed enhancements with H4 and H4', and H8 and H8', indicating that the two catechol rings (C3-C8 and C3'-C8') were flanking the dopamine. These experiments fully supported the proposed structure and the results of the molecular modeling study.

All of the alkaloids have a question of steric hindrance leading to restricted rotation of the catechol rings or twisting of the molecules. To understand that process, a molecular modeling program, pcmodel (a software released from the Serena Software), was utilized to investigate the most stable conformations of these alkaloids. Shown in Figure 2-9 are the space filling models of the four alkaloids in one of the their lowest energy forms. In order to avoid steric interactions, the pentacyclic systems of ningalactone (**176**) and ningalone (**179**) are severely twisted. In ningalin (**177**), ningalamide (**178**), and the largest alkaloid ningalone (**179**), all mono-substituted catechol rings (except for those of the dopamine units) were predicted to be almost orthogonal to the plane of gross structures. Based on the computer data it was clear the rotations of the catechol rings are highly restricted.

One interesting feature of these molecules shown in Figure 2-9 is the fact that they are possibly chiral by virtue of restricted rotation and consequent conformational helicity. By comparison with similar structures, this pentacyclic system was sufficient to lead to the helicity (Goedicke and Stegemeyer 1970, Liberko *et al.* 1993, Bestman and Both 1974a,b). However, no optical rotation was observed for these compounds.

The racemic mixture may be resolved by using a method developed Newman and Lendicer (1956). In this method, an optically active complex of an optical antipode and a chiral 2-(2,4,5,7-tetranitro-9-fluorenylideneaminooxy)-propionic acid, TAPA, is prepared by adding the optically active TAPA to a solution of racemates followed by boiling and standing overnight. The derived-optically active enantiomer is then separated from the complex by chromatographic methods. This method is one of the most interesting in the sense of chiral separation without using a chiral solvent.

The orthogonal presence of catechol rings in proximity to the dopamine moiety of **178** and **179** resulted in their shielding effect to the dopamine (Figure 2-10). The shielding and deshielding effect of the phenyl ring is a well known process (Johnson and Bovey 1958, Jackman and Sternhell 1969) which is also observed in the Mosher ester (Dale and Mosher 1973). The shielding of protons near a benzene ring is a function of distance along the orthogonal axis from the center of the ring, but the deshielding of the protons is a function of distance along the hexagonal axis (Johnson and Bovey 1958, Jackman and Sternhell 1969). The experimentally observed values were compared with the estimated resonances in Tables 2-5 - 2-7. To calculate the shielding effect on the dopamine unit in ningalamide (**178**) and ningalone (**179**), the chemical shifts in ningalin (**177**) were used as a reference.

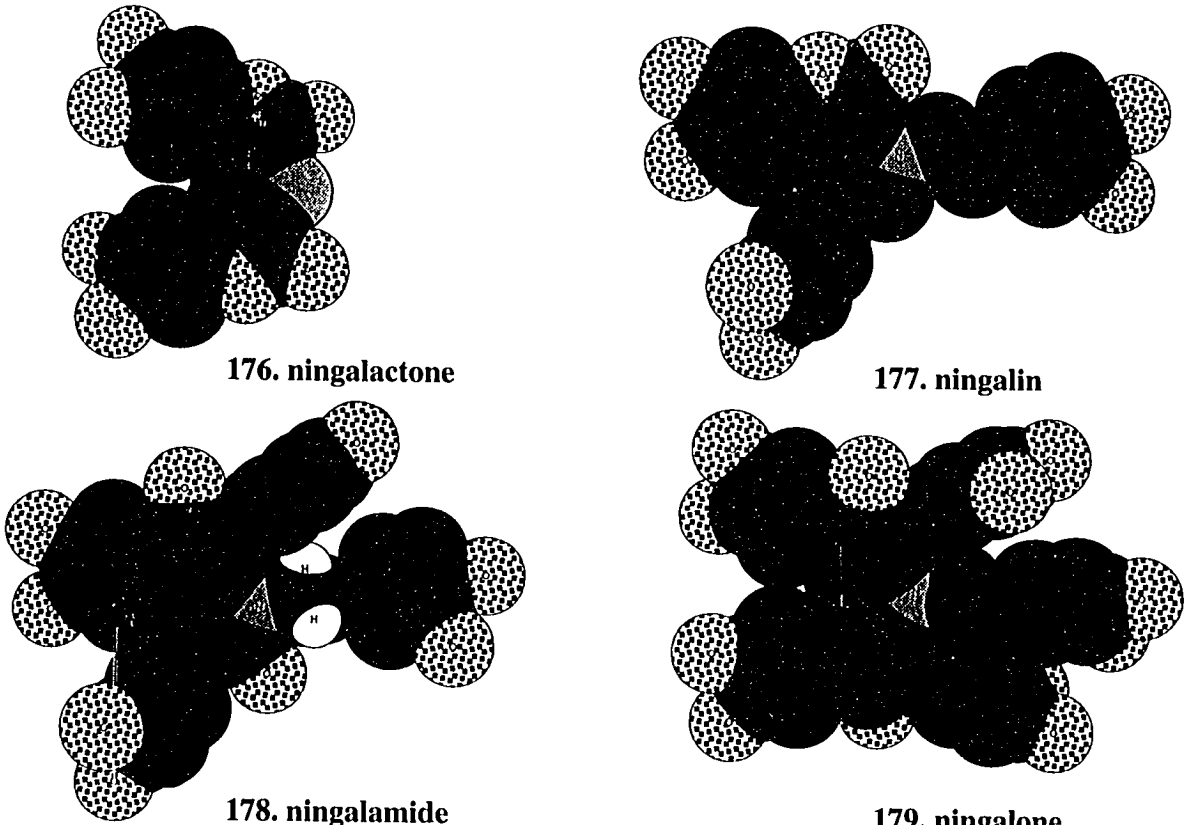

176. ningalactone

177. ningalin

178. ningalamide

179. ningalone

Figure 2-9. Computer-generated perspective drawings (space-filling models) of one of the lowest energy forms of alkaloids **176 - 179.** Hydrogen atoms except for H17's in the ningalamide (**178**) are omitted for clarity. The protons in the ningalamide are shown to perceive a diastereotopic nature each other (see text for detail). The remaining atoms are presented with arbitary radii. The energy-minimized conformers or atropoisomers have been obtained using a Serena software, pcmodel, which adopts a MMX force field, and the presented 3-dimensional strucutres were drawn using a Chem3D program released from Cambridge Scientific Computing, Inc..

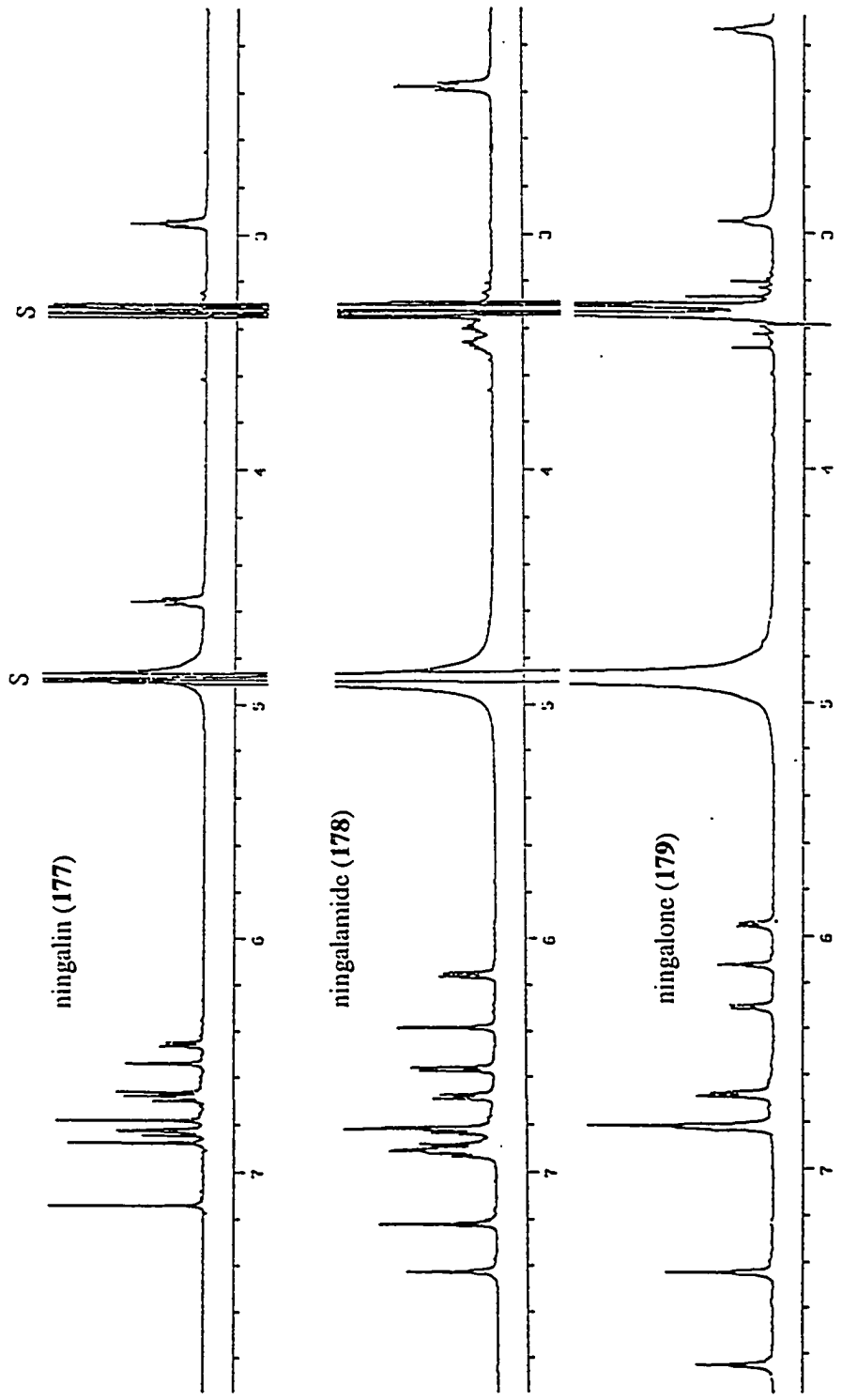

Figure 2-10. The shielding effect of phenyl rings to the dopamine moiety in ningalamide (178) and ningalone (179).

Tables 2-5 - 2-7. Theoretical and experimental values of the diamagnetic anistropy of the phenyl rings and carbonyl group in ningalamide (**178**) and ningalone (**179**)

Table 2-5. Distance between shielded protons and phenyl ring, and between the protons and amide carbonyl in ningalamide (**178**)

C# \ target group	catechol ring	amide carbonyl	phenyl of DOPA
17	2.46 (-0.9)	3.9 (0)[a]	2.8 (-0.44)[b]
18	3.08 (-0.38)	3.9 (-0.13)	no effect
20	6.19 (0)	3.85 (-0.15)	no effect
23	4.6 (-0.11)	7.87 (0)	no effect
24	2.91 (-0.4)	6.0 (0)	no effect

Table 2-6. Distance between shielded protons and phenyl rings in ningalone (**179**)

C# \target	catechol ring A	catechol ring A'	phenyl of DOPA
17	4.14 (-0.17)	2.43 (-0.9)	2.72 (-0.53)[b]
18	2.67 (-0.8)	4.59 (-0.11)	no effect
20	2.85 (-0.43)	6.01 (0)	no effect
23	4.24 (-0.17)	6.3 (0)	no effect
24	2.77 (-0.53)	5.6 (0)	no effect

Table 2-7. Comparison of experimental and theoretical shielding effects

C# \ cmpd	ningalamide (**178**)		ningalone (**179**)	
	calculated	experimental	calculated	experimental
17	-1.3	-1.1	-1.6	-1.6
18	-0.51	-0.58	-0.9	-0.82
20	-0.15	-0.17	-0.43	-0.42
23	-0.11	-0.12	-0.17	-0.36
24	-0.4	-0.31	-0.53	-0.51

All distances are presented in Angstrom. The shielding effects in parentheses of Tables 6 and 7 are shown in ppm unit. a) Since C-N bonds were located between C=O bond and the proton H17 and two bonds were in the same plane of the proton H17 in **178**, the shielding effect of the carbonyl might be negligible. b) The shielding effect may be overestimated.

In ningalin (**177**), two methylene units in the dopamine moiety resonated at δ 4.55 and 2.94, respectively. The same methylenes in ningalamide (**178**), however, appeared at δ 3.30 and 3.23, and 2.24. Two different chemical shifts of the protons of the methylene next to the nitrogen in ningalamide (**178**) are due to the fact that they are diastereotopic, which is obvious in the 3-dimensional drawing of the molecule (Figure 2-9). The shielding effect is mainly responsible for the contribution of the catechol ring flanking to the dopamine because a long-range shielding effect of the carbonyl group (ester and amide) to the methylene (H17's) in both ningalin (**177**) and ningalamide (**178**) is almost same amount due to identical geometry and the same inter-functional group distance in either case. However, that holds true for only one proton of the methylene in **178**. Since the C17-N bond of **178** was located between the amide C=O bond and the proton H17 orienting the flanking catechol ring, and three functional groups were in the same plane, the shielding effect of the carbonyl group on this proton might be negligible. One of the dominant contributions to the shielding of the proton was the phenyl ring of the dopamine. To avoid steric hindrance between the catechol ring at C2 and the dopamine moiety, the plane of the dopamine phenyl ring was 24 degrees out of the plane of the pyrrole ring, which forced the H17 proton above the phenyl ring. However, the proton was not situated directly above the phenyl ring. Because of this effect, the assessed shielding effect due to the phenyl group on the proton was overestimated (Tables 2-5 -2-7). All shielding effects observed in ningalamide (**178**) could be rationalized by the diamagnetic anistropy of catechol rings. The only exception was that of proton H20. Since the catechol ring was more than 6 Â away, the group did not affect the proton H20. Nevertheless, the carbonyl group of the amide was close enough to produce a long-range shielding effect (Jackman and Sternhill 1969). The value was obtained using Figure 2-2-12a in the book of Jackman and Sternhill (1969) from a distance between the carbonyl group and the proton.

The diamagnetic anistropic effect of the phenyl ring is most conspicuous in ningalone (**179**). Two flanking catechol rings resulted in the shielding on the methylenes as much as 1.60 ppm compared to those of ningalin (**177**). At a glance, the shielding effects induced by both catechol rings seemed to be same for each methylene proton. However, as shown earlier, the molecule was twisted to avoid a steric hindrance. Therefore, the effect given by each catechol ring was different. These results were presented in Table 2-6. Generally speaking, the estimated shielding effects on the protons of the dopamine in both ningalamide and ningalone were consistent with the predicted values (Table 2-7).

C. Structure Elucidation of Lamellarins O-T (168-173, Figure 2-11).

Lamellarin P (**169**, Table 2-8) was obtained as an amorphous solid. The high resolution desorption electron ionization mass spectrometry (HRDEIMS) established its molecular formula as $C_{26}H_{19}NO_8$ [obsd. *m/z* 471.0969 M^+, dev. -3.5 ppm]. The high degree of unsaturation (18 degrees) was evident from the molecular formula, and also supported by its UV spectrum [(MeOH) λ_{max}: 336 (ε 17000) , 315 (17000), 278 (22000), 265 (sh), and 205 (43000) nm]. A bathochromic shift (1N NaOH), a broad and strong IR absorption band at 3700 - 3000 cm^{-1}, and ^{13}C NMR data (8 signals downfield of δ 140) suggested the phenolic nature of the compound. A conjugated ester functional group was present, which was indicated by a strong IR band at 1690 cm^{-1} in combination with a carbon signal at δ 154.4.

The proton NMR spectrum showed seven aromatic signals and two mutually coupled methylene resonances [δ 2.94 (t, 2H, J = 7 Hz), 4.54 (dt, 1H, J = 13.5, 7 Hz), and 4.60 (dt, 1H, J = 13.5, 7 Hz)]. Among the aromatic signals, a 1,2,4-trisubstituted benzene ring was very obvious from analysis of coupling constants [δ 6.76 (dd, 1H, J = 8, 2 Hz), 6.75 (d, 1H, J = 2 Hz), and 7.09 (d, 1H, J = 8 Hz)]. Four aromatic singlets either came from four different spin systems or were para-positioned since there was no coupling among them.

In the HMBC spectrum of **169**, the proton signals at δ 7.09 (H21) and 6.75 (H24) were coupled to both quaternary carbon signals at δ 147.0 and 147.5. However, the carbon signal at δ 147.5 only correlated to the proton signal H25 at δ 6.76. Therefore, the carbon signal was assigned to C23, since $^4J_{CH}$ couplings were rarely observed in the HMBC experiments (8 Hz). The methoxy signal at δ 3.89 also coupled to the carbon signal at δ 147.5. Furthermore, a correlation between the methoxy signal and the proton signal H24 was observed in NOESY spectra. This allowed the position of the methoxy group to be assigned. The carbon signal C19 at δ 114.2 was long-range coupled to the proton H25 at δ 6.76, which resulted in assignment of subunit **A** (Scheme III).

Two protons H13 at δ 6.68 and H16 at δ 6.42 were para-positioned since there was no coupling in the proton spectrum of **169**. The assignment of two hydroxyl groups at the most deshielded carbons at δ 143.6 and 146.2 was supported by the up-field shifts of two adjacent carbon signals C13 (δ 115.1)and C16 (δ 113.2). Initially, the carbon signal at δ 125.7 was assigned as any carbon within a three-bond range such as C2, C12, or C18. The carbon signal gave two additional correlations to protons H11's (δ 2.94) and to proton H16 (δ 6.42). Hence, the possibility of the carbon being C18 was eliminated with the

Figure 2-11. Lamellarins and their derivatives **353** - **356**

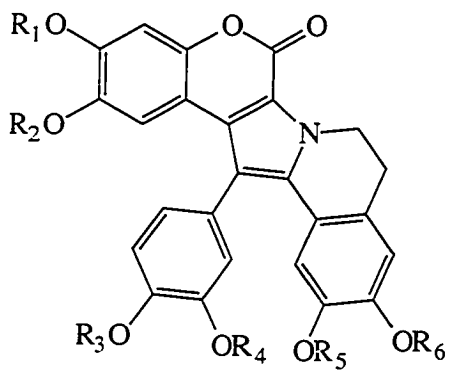

lamellarins

168.	O	$R_1 = R_2 = R_3 = R_4 = R_5 = R_6 = H$
169.	P	$R_1 = R_2 = R_4 = R_5 = R_6 = H$, $R_3 = Me$
170.	Q	$R_1 = Me$, $R_2 = R_3 = R_4 = R_5 = R_6 = H$
171.	R	$R_1 = R_2 = R_4 = R_6 = H$, $R_3 = R_5 = Me$
172.	S	$R_1 = R_3 = Me$, $R_2 = R_4 = R_5 = R_6 = H$
173.	T	$R_1 = R_5 = Me$, $R_2 = R_3 = R_4 = R_6 = H$
353.		$R_1 = R_2 = R_3 = R_4 = R_5 = R_6 = Ac$
354.		$R_1 = R_2 = R_4 = R_5 = R_6 = Ac$, $R_3 = Me$
355.		$R_1 = Me$, $R_2 = R_3 = R_4 = R_5 = R_6 = Ac$
356.		$R_1 = R_2 = R_4 = R_6 = Ac$, $R_3 = R_5 = Me$

Table 2-8. Physical and spectral properties of lamellarin P (**169**)

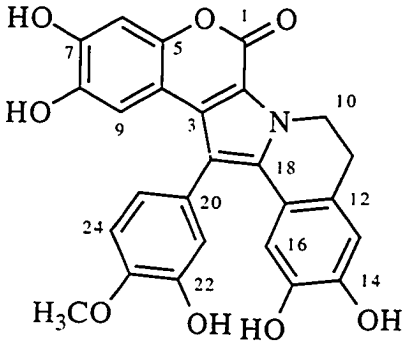

169. lamellarin P

Source: *Didemnum* sp.
Exmouth, western Australia
Amorphous solid
Molecular formula: $C_{26}H_{19}NO_8$
LRDEIMS: m/z 473 M^+
UV (MeOH) λ_{max}: 336 (ε 17000), 315 (17000), 278 (23000), 265 (sh), 205 (43000) nm.
IR (NaCl) ν_{max}: 3700 - 3000, 1690, 1595, 1420, 1285, 1250, 1187 cm^{-1}
$[\alpha]_D = 0°$

NMR data

No	$^{13}C^a$	$^1H^b$	HMBC (8 Hz)^b	NOESY^b
1	154.4			
2	112.2			
3	127.5			
4	108.9			
5	146.2			
6	103.2	6.72 (s, 1H)	C4, C5, C7, C8	
7	144.7			
8	142.1			
9	108.5	6.47 (s, 1H)	C3, C5, C7, C8	H21, H25
10	42.0	4.54 (dt, 1H, J = 13.5, 7 Hz) 4.60 (dt, 1H, J = 13.5, 7)	C2, C11, C12, C18	H11
11	27.8	2.94 (t, 2H, J = 7)	C10, C12, C13, C17	H10, H13
12	125.7			
13	115.1	6.68 (s, 1H)	C14, C15, C17	H11
14	146.2			
15	143.6			
16	113.2	6.42 (s, 1H)	C12, C14, C15, C18	H21, H25
17	118.3			
18	135.9			
19	114.2			
20	127.0			
21	117.4	6.75 (d, 1H, J = 2)	C22, C23, C25	H9, H16
22	147.0			
23	147.5			
24	112.9	7.09 (d, 1H, J = 8)	C20, C22, C23	H25
25	121.2	6.76(dd, 1H, J = 8, 2)	C19, C21, C23	H9, H16
OCH_3	55.4	3.89 (s, 3H)	C23	H24

All experiments were performed in DMSO-d_6. Chemical shifts are reported in δ units (downfield of TMS). All $^1J_{CH}$ correlations were determined by HMQC experiments at 500 MHz. a) ^{13}C NMR was obtained at 50 MHz. b) Spectra were acquired at 500 MHz.

Scheme III

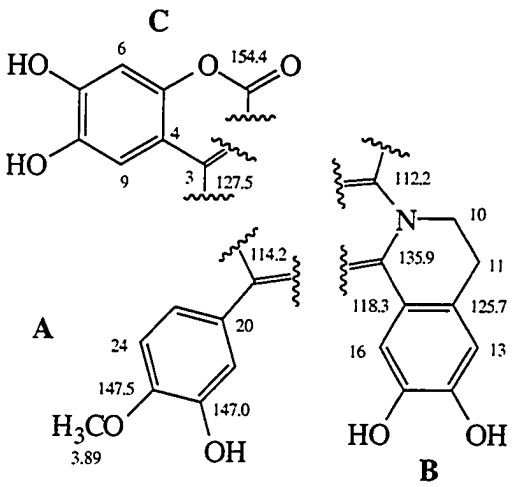

restriction of HMBC couplings within three-bond ranges. With a correlation of H13 (δ 6.68) to C17 (δ 118.3), a dihydroisoquinoline moiety, subunit **B**, was constructed.

From HMBC correlations by two para-positioned proton singlets (H6 and H9) and the ester functional group suggested by IR (1690 cm^{-1}) and the carbon signal at δ 154.4, the subunit **C** was very obvious.

Two bonds, C3-C19 and C18-C19, were established based on NOESY correlations: H9 to H21, H9 to H25, H16 to H21, and H16 to H25. The large difference in chemical shift between C2 (δ 112.2) and C3 (δ 127.5) could be rationalized if C2 and C3 were α and β to the ester carbonyl C1 (δ 154.4). These overall data explained the 18 unsaturations inherent in the molecular formula. The assignment was also supported by the shielding of two protons H9 (δ 6.47) and H16 (δ 6.42) induced by the catechol ring at C19.

Lamellarin O (**168**), the major metabolite, was obtained as an amorphous solid. The molecular formula $C_{25}H_{17}NO_8$ established by HRDEI (obsd. M^+ m/z 459.0942, dev. -2.7 ppm) indicated that **168** was a demethyl derivative of **169**. The UV spectrum of **168** was almost identical to that of **169** [(MeOH) λ_{max}: 337 (ε 17100), 317 (17100), 276 (21800), 268 (sh), and 205 (42400) nm]. All results obtained from 2-dimensional NMR analysis were fully consistent with the proposed structure (Table 2-9).

Table 2-9. Physical and spectral properties of lamellarin O (**168**)

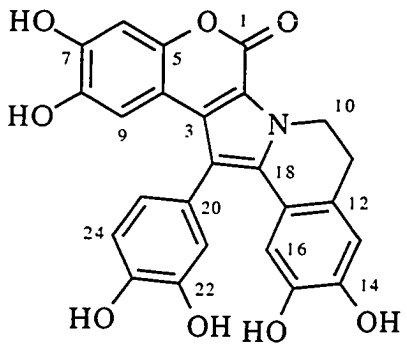

168. lamellarin O

Source: *Didemnum* sp.
Exmouth, western Australia
Amorphous solid
Molecular formula: $C_{25}H_{17}NO_8$
LRDEIMS: obsd. m/z 459 M^+
UV (MeOH) λ_{max}: 337 (ε 17100), 317 (17100), 276 (21800), 268 (sh), 205 (42400) nm.
IR (NaCl) ν_{max}: 3700-3000, 1686, 1597, 1423, 1282, 1252, 1191, 1158, 1023, 990 cm^{-1}
$[\alpha]_D = 0^o$

NMR data

No	$^{13}C^a$	$^1H^b$	HMBC (8 Hz)^b
1	154.5		
2	112.2		
3	127.5		
4	109.3		
5	145.9		
6	103.3	6.73 (s, 1H)	C4, C5, C7, C8
7	142.0		
8	144.7		
9	108.9	6.53 (s, 1H)	C3, C5, C7, C8
10	42.0	4.48 (dt, 1H, *J* = 14, 7 Hz) 4.57 (dt, 1H, *J* = 14, 7)	C11, C12, C18
11	27.9	2.90 (t, 2H, *J* = 7)	C10, C12, C13, C17
12	125.8		
13	115.1	6.68 (s, 1H)	C11, C14, C15, C17
14	146.0		
15	143.6		
16	113.5	6.46 (s, 1H)	C12, C14, C15, C18
17	118.5		
18	136.0		
19	114.7		
20	125.5		
21	117.5	6.69 (d, 1H, *J* = 2)	C19, C23, C25
22	146.1		
23	145.2		
24	116.8	6.90 (d, 1H, *J* = 8)	C20, C22, C23
25	121.3	6.62 (dd, 1H, *J* = 8, 2)	C19, C21, C23
OH		9.08 (bs, 6H)	

All experiments were performed in DMSO-d_6. All $^1J_{CH}$ correlations were determined by DEPT and XHCORR experiments at 50 MHz. a) ^{13}C NMR spectra were obtained at 50 and 125 MHz. b) Spectra were acquired at 500 MHz.

Lamellarin Q (**170**) was purified as an amorphous solid. The molecular formula $C_{26}H_{19}NO_8$, suggested from the HRDEI mass spectrum (M^+ obsd. *m/z* 473.1125, dev. 3.0 ppm) in conjugation with ^1H and ^{13}C NMR spectra, showed that **170** was a regio-isomer of **169** by placement of the methoxy group at δ 3.85 (instead of 3.89). The difference in chemical shift between the two methoxy groups in the ^1H NMR spectra of both compounds was only 0.04 ppm. HPLC analysis, using a diode-array detector, verified the proposal. The UV spectra of the compounds were exactly identical in all aspects. The placement of the methoxy at δ 3.85 of **170** at C14 was concluded by HMBC and NOESY experiments. Three protons H13 (δ 6.89), H16 (δ 6.45), and H26 (δ 3.85) were coupled to a quaternary carbon at δ 147.8. The carbon signal could thus be either C14 or C15. However, the proton signal H13 clearly showed a correlation to the methoxy proton in the NOESY spectra. Therefore, the methoxy group was placed to C14, and the structure was proposed as shown (Table 2-10).

Lamellarin R (**171**, Table 2-11) was obtained as an amorphous solid. The molecular formula, $C_{27}H_{21}NO_8$, determined by HRDEI (M^+ obsd. *m/z* 487.1258, dev. -1.9 ppm), revealed that **171** was a methyl derivative of **169**. The UV spectrum of **171** [(MeOH) λ_{max}: 336 (ε 17600), 315 (17600), 278 (22000), 265 (sh), and 205 (45000) nm] suggested the presence of the same chromophore as found in **169**. The presence of a methoxy group (δ 3.23) at C15 was indicated by its up-field shift compared to another methoxy signal at δ 3.84, which was induced by diamagnetic anistropy of the catechol ring at C19. Long-range HMBC coupling of the proton signal at δ 3.23 to C15 (δ 145.8), and a nuclear Overhauser enhancement (nOe) of H16 (δ 6.47) upon irradiation of the methoxy signal confirmed its placement at C15. Another methoxy was positioned at C23 based on a HMBC correlation and an nOe of H24 (δ 7.17) upon irradiation of this methoxy signal.

Lamellarins S (**172**) and T (**173**) could not be completely separated. The molecular ion observed in the HRDEI mass spectrum of the mixture was 487.1259 which was appropriate for the molecular formula $C_{27}H_{21}NO_8$ (dev. -1.7 ppm). The UV spectra, obtained by diode-array HPLC analysis using a reversed-phase column (ODS-silica), was perfectly matched to that of **169**. The ^1H NMR spectrum of the mixture showed four methoxy signals at δ 3.35, 3.86, 3.87, 3.95 in a ratio of 1:1:1:1. With standards of **168-171**, and lamellarins G (**160**) and L (**165**), the mixture eluted between **171** and **165**. Since **160** and **165** were also isolated from this study, the proton spectrum of the mixture was compared with those of **160** and **165** in exactly same condition. The methoxy at C23

Table 2-10. Physical and spectral properties of lamellarin Q (**170**)

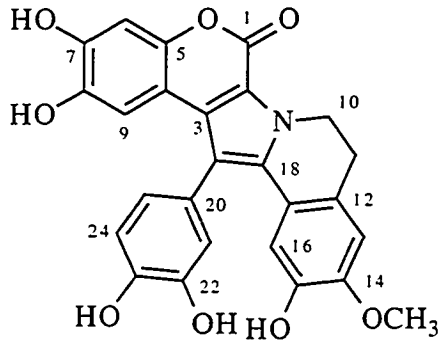

170. lamellarin Q

Source: *Didemnum* sp.
Exmouth, western Australia
Amorphous solid
Molecular formula: $C_{26}H_{19}NO_8$
LRDEIMS: m/z 473 M^+
UV (MeOH) λ_{max}: 336 (ε 16500), 315 (16500), 278 (21000), 265 (sh), 205 (44000) nm.
IR (NaCl) ν_{max}: 3700 - 3000, 1691, 1596, 1422, 1289, 1252, 1185 cm^{-1}
$[\alpha]_D = 0^o$

NMR data

No	$^{13}C^a$	$^1H^b$	HMBC (8 Hz)^b	NOESY^{b,c}
1	154.5			
2	112.4			
3	127.5			
4	108.6			
5	146.0			
6	103.2	6.70 (S, 1H)	C4, C5, C7, C8	
7	142.1			
8	144.7			
9	109.0	6.51 (s, 1H)	C3, C5, C7, C8	
10	42.0	4.53 (dt, 1H, *J* = 13.5, 7 Hz) 4.62 (dt, 1H, *J* = 13.5, 7)	C11, C12, C18	H11
11	28.1	3.00 (t, 2H, *J* = 7)	C10, C12, C13, C17	H10, H13
12	125.6			
13	111.7	6.69 (S, 1H)	C11, C12, C14, C15, C17	H11, H26
14	147.8			
15	144.6			
16	113.0	6.45 (S, 1H)	C12, C14, C15, C18	H21, H25
17	119.9			
18	135.5			
19	115.0			
20	125.3			
21	116.8	6.67 (d, 1H, *J* = 2)	C19, C22, C23, C25	H9, H16
22	146.3			
23	145.2			
24	117.4	6.88 (d, 1H, *J* = 8)	C20, C22, C23	H25
25	121.2	6.59(dd, 1H, *J* = 8, 2)	C19, C21, C23	
OCH_3	55.6	3.85 (s, 3H)	C23	H24

All experiments were performed in DMSO-d_6. Chemical shifts are reported in δ units (downfield of TMS). All $^1J_{CH}$ correlations were determined by HMQC experiments at 500 MHz. a) ^{13}C NMR was obtained at 50 MHz. b) Spectra were acquired at 500 MHz. c) Mixing time (0.1 sec) used in the NOESY experiment was not enough, resulted in lack of correlations (D1 =2 sec.).

Table 2-11. Physical and spectral properties of lamellarin R (**171**).

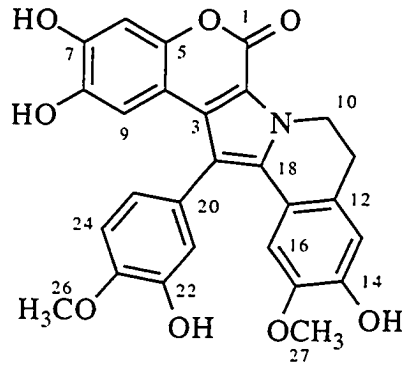

171. lamellarin R

Source: *Didemnum* sp.
Exmouth, western Australia
Amorphous solid
Molecular formula: $C_{27}H_{21}NO_8$
LRDEIMS: m/z 487 M^+
UV (MeOH) λ_{max}: 336 (ε 17600), 315 (17600), 278 (22000), 265 (sh), 205 (45000) nm.
IR (NaCl) ν_{max}: 3700 - 3000, 1692, 1595, 1422, 1288, 1250, 1186 cm^{-1}
$[\alpha]_D = 0°$

NMR data

No	$^{13}C^a$	$^1H^b$	HMBC (8 Hz)^b	NOEDS^b
1	~155			
2	~112			
3	127.0			
4	108.7			
5	146.8			
6	102.6	6.71 (s, 1H)	C4, C7, C8	
7	141.7			
8	144.0			
9	108.0	6.63 (s, 1H)	C3, C5, C7, C8	
10	41.8	4.51 (dt, 1H, J = 14, 7 Hz) 4.62 (dt, 1H, J = 14, 7)	C11, C12, C18	
11	27.0	2.95 (t, 2H, J = 7)	C10, C12, C13, C17	
12	127.0			
13	114.7	6.70 (s, 1H)	C15, C17	
14	146.8			
15	145.8			
16	108.6	6.47 (s, 1H)	C12, C14, C18	
17	117.7			
18	135.7			
19	113.7			
20	127.0			
21	117.3	6.79 (d, 1H, J = 2)	C23, C25	
22	147.6			
23	147.4			
24	113.7	7.17 (d, 1H, J = 8)	C20, C22	
25	121.4	6.80(dd, 1H, J = 8, 2)	C19, C21, C23	
26	55.1	3.84 (s, 3H)	C23	H24
27	54.4	3.23 (s, 3H)	C15	H16

All experiments were performed in DMSO-d_6. Chemical shifts are reported in δ units (downfield of TMS). All $^1J_{CH}$ correlations were determined by HMQC experiments at 500 MHz. a) ^{13}C NMR was obtained at 50 MHz. b) Spectra were acquired at 500 MHz.

was the most deshielded, while the methoxy at C15 was the most shielded. Normally the methoxy groups at C7, C8, C14, C15, C22, and C23 resonated at δ 3.81, 3.53, 3.67, 3.36, 3.75, 3.89 (3.92) in MeOH-d_4. Therefore, the two signal at δ 3.86 and 3.87 were assigned at C1. The proton signals at δ 3.35 and 3.95 were connected to C15 and C23, respectively. As a result, the lamellarins S and T were proposed as the structures **172** and **173** (Figure 2-11).

The structure of lamellarin L was identified as **165** by 2-dimensional NMR analysis in 1991. The same structure was reported recently by Carroll *et al.* (1993). In the purification of **169**, a trace amount of 3-methoxy derivative of lamellarin H (**161**) was also detected. The HRDEI mass spectrum showed a molecular ion at m/z 471.0969 [$C_{26}H_{17}NO_8$, dev. 3.1 ppm]. The ^1H NMR spectrum of the compound contained a characteristic signal at δ 9.00 (d, 1H, J = 7 Hz) and 3.95 (s, 3H) which are the proton next to the nitrogen and a methoxy signal at C23. However, the compound was not fully characterized.

As implied in the NOESY experiment of **169**, the catechol ring at C19 was predicted to be almost orthogonal to the rest of the molecule from molecular modeling studies (Figure 2-12). Due to the highly restricted rotation of the catechol ring, the molecule could be chiral. However, all lamellarins in this study were racemic as observed before in previous studies (Anderson *et al.* 1985, Lindquist *et al.* 1988, Carroll *et al.* 1993). Once again to obtain an optically active atropoisomer, Newman and Landicer's method (1956) could be applied.

Although there is no evidence defining the origin of these molecules, judging by their structures, all of these alkaloids appear to be condensation products of DOPA's derived from the amino acid tyrosines. Biosynthetically, the compounds might be produced from the condensation of two, three, four, and five DOPA molecules (Figure 2-13). Interestingly, these alkaloids had predictable mode of DOPA addition even though each had a completely different carbon skeleton. The numbering system for the lamellarins used in this study is different from that in previous studies because it was designed to illustrate their relatedness.

Closely related compounds isolated from ascidians are the lamellarins (Anderson *et al.* 1985, Lindquist *et al.* 1988, Carroll *et al.* 1993), polycitrins (Rudi *et al.* 1993), and lukianols (Yoshida *et al.* 1991). The intermediate **I**, a condensation product of two DOPA

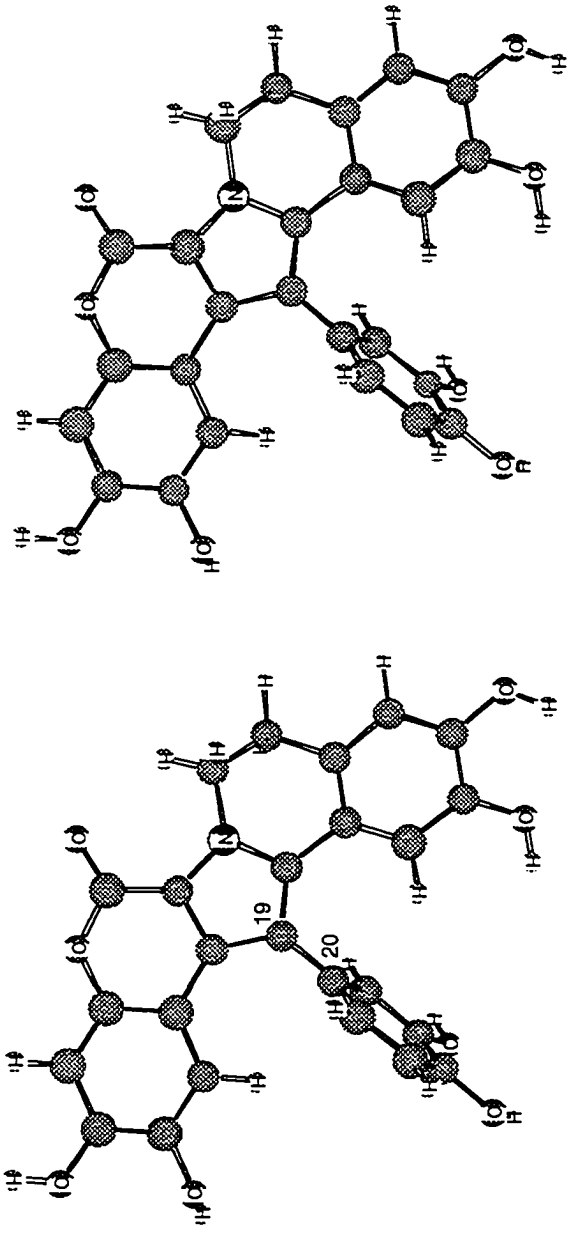

Figure 2-12. An energy-minimized structure of lamellarin O (**168**) in a stereo view. Due to the proximity of the coumarin and the isoquinoline moieties, free rotation of the catechol ring at C19 is seriously restricted. The rotational barrier of the bond between C19 and C20 was in excess of 800 kcal/mole. The catechol ring was 74 degrees out of the plane of the pyrrole ring since the isoquinoline ring was twisted about 20 degrees. The coumarin moiety and the pyrrole ring were perfectly co-planar. Energy minimization of **168** was performed using a Serena software, pcmodel, which adopts a MMX force field. The actual presentation of **168** was obtained using a combination of a Chem3D program and a ChemDraw software released from the Cambridge Scientific Computing, Inc.

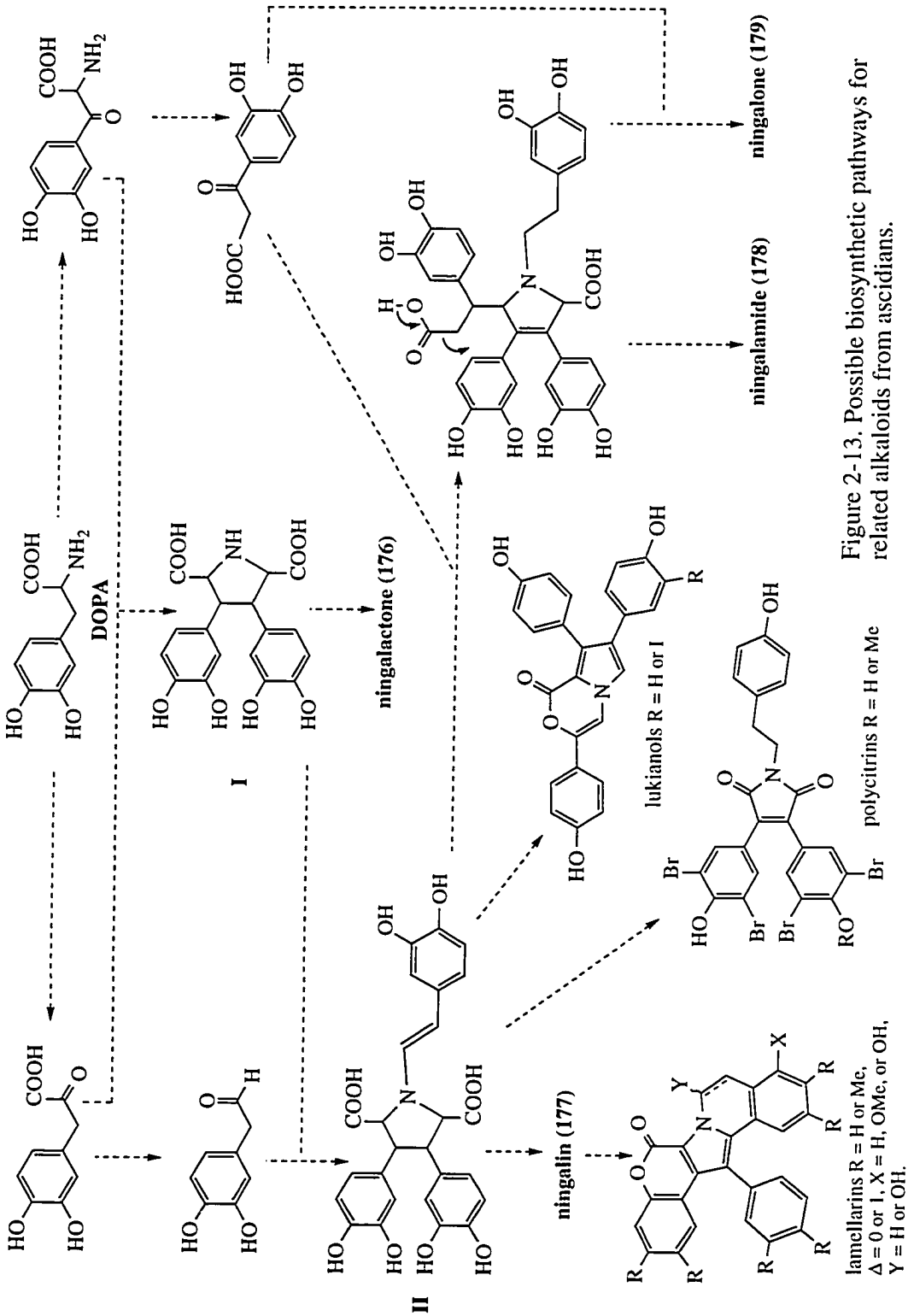

Figure 2-13. Possible biosynthetic pathways for related alkaloids from ascidians.

units, may be a key precursor to yield **II** which may be transformed into ningalin (**177**), lukianols (**174-175**), lamellarins (**154-173**), and polycitrins (**145-146**) through coupling and oxidative decarboxylation. Further addition of DOPA unit(s) leads to ningalamide and ningalone. The structural similarity between purpurone, a sponge-derived analog (Chan *et al.* 1993), and ningalone may lead to the hypothesis of the microbial origin of these compounds. However, the compounds may also be the result of convergent evolution of biosyntheses (Faulkner *et al.* 1993) due to the common presumptive precursor (DOPA).

All new compounds from this ascidian were tested for cytotoxicity against human colon cell line HCT 116 in culture. Ningalactone (**176**) and lamellarin O (**168**) showed cytotoxicity with IC_{50} of 3.3 and 1.4 μg/ml, respectively. None of these compounds isolated in this study were tested for antimicrobial properties. This aspect will be pursued in the future. Because ningalin (**177**) and lamellarin O (**168**) were isolated in sufficient quantities, these compounds were tested for antiinflammation *in vitro*. Ningalin exhibited a very strong antiinflammatory property.

D. Implication to biological roles of DOPA-originated alkaloids in ascidians

Ascidians are known to accumulate vanadium (V) at extremely high concentration up to 0.15 M (Marcara *et al.* 1979). This phenomenon is common only among the family Polycitoridae of Order Aplousobranchia and within the Order Phlebobranchia. However, for other ascidians, especially those of the Order Stolidobranchia, vanadium accumulation is negligible but iron is highly enriched. One noticeable observation is that sequestration of iron is a universal process among ascidians. Even though the families Polyclinidae and Didemnidae are rarely mentioned as iron accumulators, they sequester iron as much as 18 million times greater than that of seawater. In seawater, the average iron concentration is 1 nmole/kg (Chester 1991, Bruland 1983). The main species (at least 90 %) of iron in aerobic sea water is found as $Fe(OH)_3$ (Kester *et al.* 1975). Iron in the blood cells of ascidians is, however, present as iron (II), and 70 % of this iron is associated with cell membrane (Agudelo *et al.* 1983). In several species of the genus *Didemnum*, vanadium concentrations are less than 20 ppm dry wt (Parry 1984). But iron concentrations are 311 $\pm$ 177 ppm dry wt (5.6 mmole/kg, Stoecker 1980), a level of 5 million times greater than that present in seawater.

To explain these phenomena, several iron- and vanadium-reducing/binding proteins were proposed (Azumi *et al.* 1990, Pizarro *et al.* 1989, Agudelo *et al.* 1983, Clifford *et al.* 1983, Dorsett *et al.* 1987, Michibata *et al.* 1991, Michibata and Uyama 1990, Uyama *et al.* 1991). These proteins contained high proportions of 3,4-dihydroxyphenylalanine (DOPA) and other aromatic residues. An alternative approach yielded many organic ligands, such as tunichromes (Bruening *et al.* 1985 and 1986, Oltz *et al.* 1988) and halocyamines (Azumi *et al.* 1990), which showed *in vitro* and *in vivo* binding and reducing activities against iron and vanadium (Ryan *et al.* 1992). One mechanism that has been recognized for the compounds involves the chelation of metals such as Fe^{3+} and V^{5+} by DOPA or 3,4,5-trihydroxypheylalanine (TOPA) residues (Avdeef *et al.* 1978).

In this study, 1.55 kg (wet weight) animals yielded 343 (269 + 74) g freeze-dried tissues. With 35.7 g of total organic extract, solvent partitioning gave the following fractions: n-butanol (3 g), EtOAc (2.8 g), hexane, and water fractions. Total quantity of alkaloids (1.7 g = 4991 ppm, dry wt.) present in the ethyl acetate fraction was estimated from the amount of the isolated compounds from the second extraction (74 g, dry wt.), since the first attempt to isolate the alkaloids was unsuccessful. By this method, the average concentration of these alkaloids is approximately 10. 8 mmole/kg. The molar ratio between iron and these alkaloids is 1 to 2. This result is consistent with a preferred

stoichiometry of tunichrome-vanadium complexation (Oltz *et al.* 1988) since iron and vanadium have the same valence orbital. Therefore, these alkaloids may serve as chelators for the sequestration of iron. However, the majority of the butanol fraction also contained DOPA-derived alkaloids (based on Sephadex LH-20 columns and ^{1}H NMR experiments of fractions), although complete characterization of those compounds was hampered by their awkward solubility. Since the butanol fraction was almost equal in mass to the ethyl acetate fraction, DOPA-derived alkaloids exist far in excess of the molar amounts requiredto explain the sequestration of iron in this ascidian. The abundance of these alkaloids suggests another reason for their synthesis.

A characteristic feature of ascidians is that they possess tunics. The tunic is composed of three structural components, the hyaline ground substance (mainly muco-polysaccharides), the fiber, and the cuticle at the surface of the tunic (Krishnan 1975, Smith 1970a,b). The cuticle contains a very high proportion of the total protein of the tunic, amounting to 85 % of its protein nitrogen in *Halocynthia* species (Stievenart 1971).

The deep purple color of the ascidians in this study, devoid of any conspicuous symbiotic algae , suggested that there could be an extensive quinone tanning process in the cuticle of this animal.

The sclerotization process is basically governed by three different chemical reactions: oxidations, Michael additions, and radical couplings (Figure 2-14). During tanning, catechol groups of these alkaloids may be enzymatically (phenoloxidase) or non-enzymatically (chelation with iron) activated to form *o*-quinones that undergo rapid Michael 1,4-addition reaction with cuticular nucleophiles, such as thiols, amines, and phenols (Peter 1989) to form the corresponding catechol ring adducts, generating both protein-catechol and chitin-catechol conjugates that undergo further oxidation and coupling to generate the cross-links necessary for the hardening of cuticle. Alternatively, quinone methides, generated by tautomerase (Saul and Sugumaran 1989a,b) from *o*-quinones, leads to sclerotization via non-enzymatic Michael 1,6-addition of cuticular nucleophiles, thus forming side chain adducts and initiating quinone methide sclerotization (Anderson 1979a, Anderson *et al.* 1980, Suguramaran *et al.* 1989). Catechol groups of these alkaloids may also serve as substrates for quinone methides of cuticular proteins to generate benzodioxan dimers through 1,3-cycloaddition (Anderson 1972, Suguramaran *et al.* 1992). The formation of dimers and trimers (Krishnan *et al.* 1972) through free radical coupling of the alkaloids capable of cross-links may often be the favored mechanism (Pau *et al.* 1971). Any nonacetylated glucosamine in chitin would permit direct cross-linking to tanning quinones since sulfated glycosaminoglycans are very abundant in the tunics of ascidians

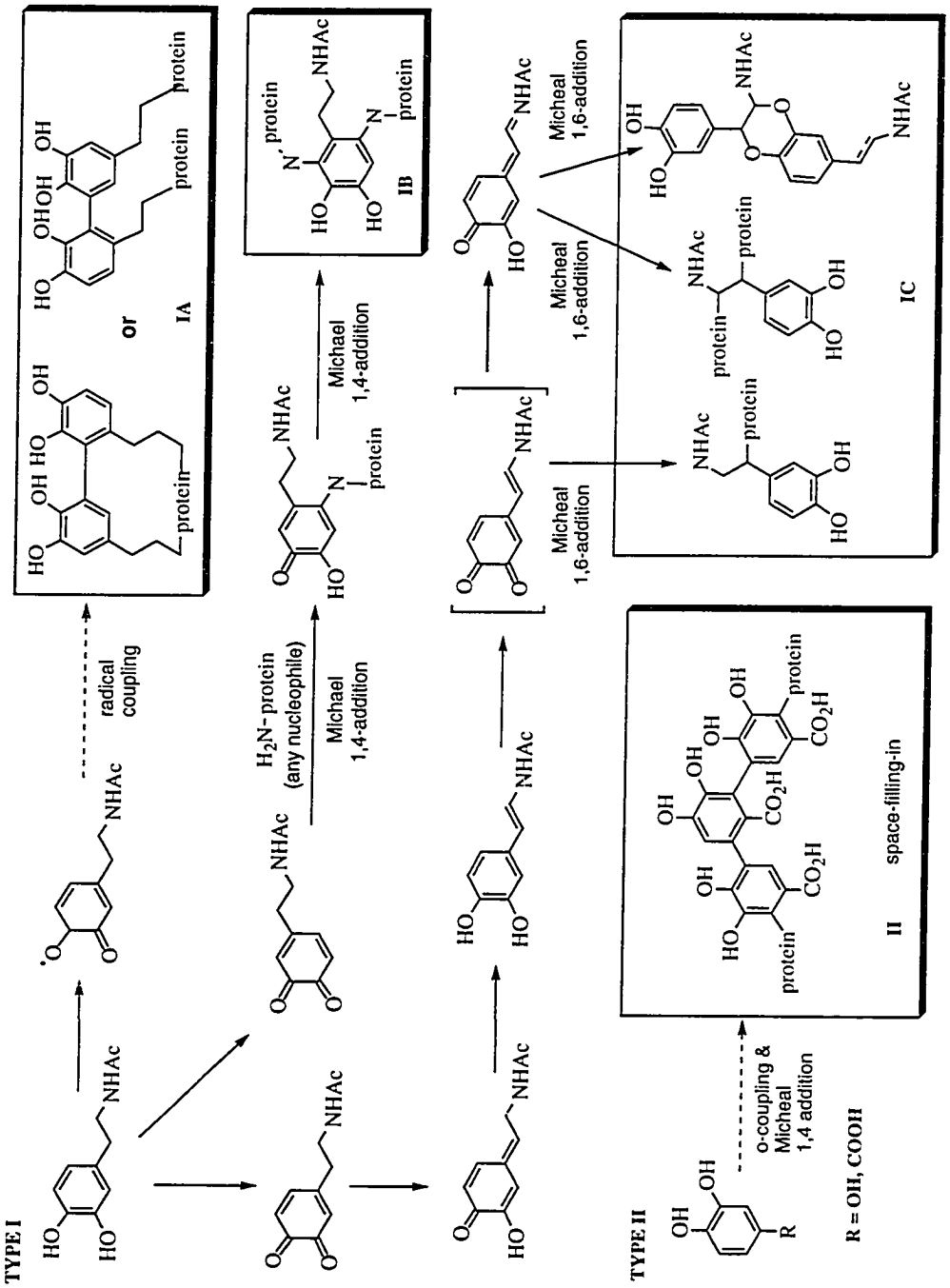

Figure 2-14. Known tanning mechanisms of cuticular protein in insects.

(Anno *et al.* 1974). If these alkaloids (**176-179**) are present in excess, their self-polymerization may occur to fill in space between protein chains or sulfated glycans (Santos *et al.* 1992, Albano *et al.* 1990, Pavao *et al.* 1989a,b) since structural analysis of the DOPA-derived alkaloids in terms of biosynthesis (Figure 2-13) elicited a predictable manner of DOPA-condensation. If the same manner of addition continued, heptomer and nanomer could be formed. Due to the steric hindrance, these polymers can not be planar. The polymers have to be twisted-helical shaped. Thus, the condensation may result in the formation of helical polymers. This condensation reaction may be a novel mechanism of biopolymerization in some ascidians. This hypothesis is summarized in Figure 2-15. The presence of a heptomer (**III**) was confirmed by ^{1}H NMR of a semi-purified fraction [δ 2.1 (t, 2H, J = 7 Hz), 2.9 (t, 2H, J = 7 Hz), 5.9 (dd, 1H, J = 8, 2 Hz), 6.1 (d, 1H, J = 2 Hz), 6.3 (d, 1H, J = 8 Hz), 6.67 (d, 2H, J = 8 Hz), 6.8 (d, 2H, J = 2 Hz), 6.81 (dd, 2H, J = 2 Hz), 7.22 (s, 2H), 7.42 (s, 2H), 7.6 (s, 2H), and 7.9 (s, 2H)]. However, full characterization of the compound has yet to be completed.

Interestingly, the alkaloids identified in this study showed no optical activity. This may be originated from enzymatic hydrolysis of these compounds during extraction which are attached to the cellular celluloses or proteins. In consequence, there may be racemization. Indirect support of this hypothesis came from a distantly-related organism, sponge *Iotrochota* sp. Mild acid hydrolysis of aqueous ethanol extract, followed by reversed-phase HPLC, yielded a polyphenolic compound, purpurone (Chan *et al.* 1993), which is closely related to ningalone (**179**). It suggested that purpurone was linked to polysaccharides (by NMR).

Now, the question is whether real conjugates of these alkaloids and biopolymers, such as celluloses and proteins, exist. During solvent partitioning of crude extract, a black precipitate was obtained from the intermediate layer between n-butanol and water. The substance was not soluble in any solvent, even in DMSO. When the material was dissolved in a mixture of D_2O and DMSO-d_6 with 10 % trifluoroacetic acid-d, the ^{1}H NMR spectrum revealed characteristic aromatic signals. This experiment indicated that these alkaloids might exist as protein-alkaloid conjugates or glycan-alkaloid adducts.

Finally, the tanning process by DOPA-derived alkaloids may be related with iodine accumulation (Thorndyke 1973, Barrington 1975). Catechol oxidases catalyze the oxidation of catechols to the corresponding quinones. Certain qunones are capable of stimulating the iodination of protein *in vitro*, suggesting that the iodination of scleroprotein *in vivo* may be mediated by the oxidation of iodide by quinones (Tong and Chaikoff 1961). Alternatively, quinones may act indirectly in the iodination process by generating hydrogen

Figure 2-15. A proposed "space filling" mechanism of sclerotization in tunic formation of the *Didemnum* ascidian in this study. Each compound may serve as a cross-link between proteins. Compounds **IV** and **V** are purely hypothetical.

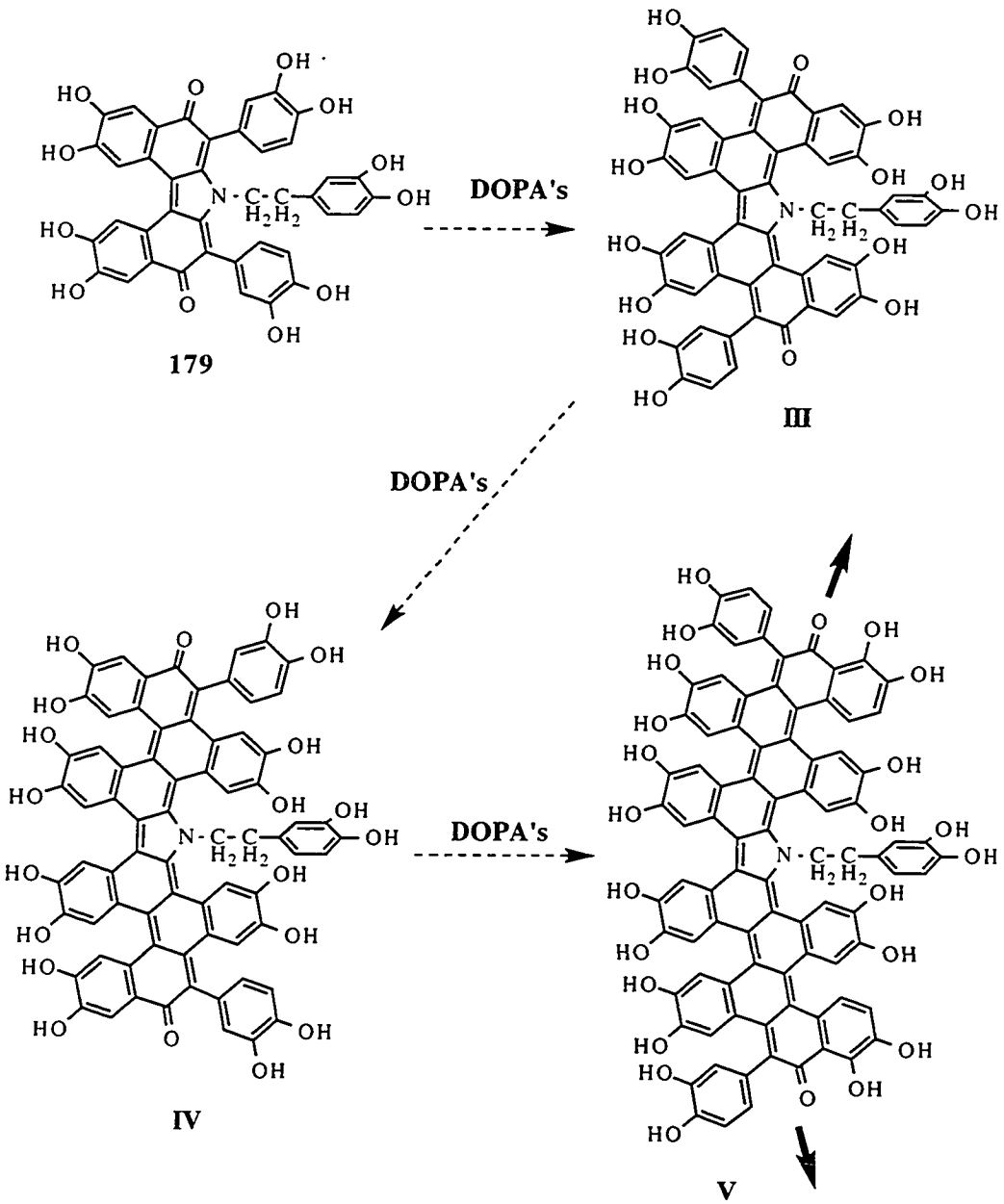

peroxide. In this scheme, iodination of protein would then occur either spontaneously in the presence of high concentrations of hydrogen peroxide or enzymatically through the action of a peroxidase (Taurog 1974). The catechol compounds are possibly converted to the respective quinones by catechol oxidase or metals, such as vanadium and iron, and as a result, they may serve as oxidants for iodide or substrates for tanning process which are essential for the formation of the tunic.

In conclusion, these alkaloids may have an important functional role in tunic formation. Iron and vanadium accumulation may be facilitated by these DOPA-derived compounds. In this process, quinones or quinone methides are formed through semiquinone radicals as a result of chelation between metals and catechols, which are indispensable for iodination or the tunic formation through tanning processes. These alkaloids may serve as cross-links to fill in space between other structure molecules. The structural analysis of these alkaloids revealed a novel condensation mechanism of amino acids, DOPA's.

These compounds also implicate defensive roles of secondary metabolites in direct and indirect ways: chemicals themselves as anti-feedants and formation of polymers which are resistant to digestion by predators (low nutritional value).

The vanadium accumulating ascidians are also good sequesters of iron. The iron accumulation is a universal process in the ascidians. In this respect, what's the difference in chemistry in terms of metal sequestration between species of the family Polycitorridae and species of the families Polyclinidae and Didemnidae? If the transport mechanism of the metals are not active (as described in chapter I), how is one of the metals preferred to the other? Of course, the physiological effects of the molecules will be of prime interest as well as the biochemistry of their production. But, all of these questions are dependent on the goal of this study, namely the identification of novel secondary metabolites.

E. Experimental General

Infrared spectra were recorded on a Perkin Elmer FT-IR spectrophotometer Model 1600 and ultraviolet spectra on a Perkin Elmer Model Lambda 3B and on a Hewlett-Packard diode array detector of Hewlett-Packard HPLC Model 1090 series II. NMR spectra were recorded on a Varian UN-500 instrument at 500 MHz (^1H) and 125 MHz (^{13}C), respectively. Double Quantum Filtered Correlation SpectroscopY (DQFCOSY), Total Correlation SpectroscopY (TOCSY), Nuclear Overhauser Exchange Correlation SpectroscopY (NOESY), ^1H-detected Heteronuclear Multiple-Quantum ^1H-^{13}C Coherence (HMQC), and ^1H-detected Heteronuclear Multiple-Bond ^1H-^{13}C Correlation (HMBC) experiments were performed using a Varian UN-500 spectrometer. A Brucker WP-200SY spectrometer was used for ^{13}C detected X-H CORRelation (XHCORR) and COrrelation by LOng range Coupling (COLOC) experiments. All chemical shifts were reported with respect to TMS (δ 0). Typical d1 delay of 0.65-1 sec was used for DQFCOSY, TOCSY experiments. For NOESY experiments, 3-4 sec d1 delay and 600-1000 msec mixing time were utilized. The homonuclear 2-dimensional NMR spectra were acquired and processed in phase-sensitive modes, such as phase = 1,2 or 3. Both Gaussian and sinebell functions were used for weighting. The heteronuclear correlation expeiments (HMBC) were optimized at 130 and 160 Hz's for aliphatic and aromatic compounds, respectively, to suppress $^1J_{CH}$ couplings. Typical d1 delay of 0.7-1.0 sec was utilized for proton-detected heteronuclear 2-dimensional NMR experiments. For processing of those spectra, sine bell and Gaussian weighting functions were used for HMBC and HMQC experiments, respectively.

Low resolution electron ionization and chemical ionization mass spectra were recorded at 70 eV on a Hewlett-Packard Model 5930A mass spectrometer. High and low resolution FAB, DEI, and DCI mass measurements were supplied by the Mass Spec. Facility at the University of California , Riverside. Electron dispersive spectroscopy established the presence of heavy atom, such as sulfur and chlorine in some natural products. Optical rotations were measured on a Roudolf polarimeter with a 10-cm cell. Melting points were determined using a Fisher-Johns apparatus and were reported uncorrected. Final purifications of secondary metabolites and reaction products were accomplished by preparative high-performance liquid chromatography on reversed-phase (ODS-silica), NH_2, and CN columns. Some separations were also achieved by high-speed counter-current liquid partition chromatography using various solvent mixtures.

F. Experimental, Chapter II

Collection, Extraction, and Isolation Procedures.

The purple encrusting ascidian, *Didemnum* sp. (WA-90-19 and 58), was collected by hand using SCUBA (-10 m) near Exmouth, Western Australia in the Indian Ocean, in December 1990. The specimens were immediately frozen after collection. The lyophilized animal (343 g, dry weight) was extracted twice each with 70% MeOH/$CHCl_3$ and methanol. The combined extract was concentrated and partitioned between hexane and methanol. The methanol-soluble material was further partitioned between ethyl acetate and water. The extremely polar nature of the alkaloids made separation by TLC unsuccessful. The original purification, mediated by silica at certain steps during the separation, resulted in almost complete loss of **176**, and **178-9**. However, diode-array HPLC analysis using various several solvents (analytical ODS-silica and NH_2 columns) facilitated the finding of a perfect condition for the separation of the alkaloids. First, a mixture in 2 mg/ml concentration was chromatographed using a linear gradient mode. The compound to be isolated was located in the chromatogram by its UV spectrum. The approximate condition, determined from the chromatogram, was used as a reference for the isocratic mode separation. Subtle changes of the conditions were performed several times to optimize the separation. Gel-filtration of the ethyl acetate-solubles through Sephadex LH-20 and Spectra Gel HW-40 with methanol gave a semi-pure compound **176**, pure **161** and **168**, and several fractions which contained compounds **177-9**, **160-1**, **165**, and **168-173.** Compound **176** was obtained pure as a precipitate from the methanol solution of the impure fraction in the freezer. Further purification of other alkaloids was accomplished by reversed-phase HPLC (ODS-silica). To purify compounds **177-8**, **160**, **165**, and **171-3,** 35 % CH_3CN-5 % methanolic water was used as the eluting solvent. The most polar compound **179** and **169-170** were also purified by ODS-HPLC using 30 % CH_3CN-5% methanolic water. Yields of compounds **168-173**, and **176-9** were 854 mg, 10 mg, 7 mg, 5 mg, 5.6 mg (**172** & **173**), 20 mg, 60 mg, 23.4 mg, and 36 mg, respectively. A fraction containing a 1:1 mixture of **169** and **170** (160 mg) was not purified further. Known compounds **160-1** and **165** were also separated as much as 5, 8, and 93 mg, respectively.

Ningalactone(176) : an amorphous solid (DMSO); $[\alpha]_D = 0^o$; HRFABMS, $(M + H)^+$ obsd. *m/z* 368.0420, $C_{18}H_{10}NO_8$. dev.3.7 ppm; IR (NaCl) ν_{max}: 3377, 3186, 1702, 1617, 1494, 1375, 1256, 1153 cm^{-1}; UV (10 % DMSO/MeOH) λ_{max}: 370 nm (ε 2160), 325 (sh), 303 (8450), 262 (8650), 235 (10000); UV (10 % DMSO/MeOH + NaOH) λ_{max}: 393 nm (ε 1970), 350 (sh), 314 (9150), 274 (8450), 235 (10600).

Ningalin(177): an amorphous solid (DMSO-MeOH); $[\alpha]_D = 0^o$; HRFABMS, $(M + H)^+$ obsd. *m/z* 462.1189, $C_{25}H_{20}NO_8$. dev. -0.109 ppm; IR (NaCl) ν_{max}: 3700-3000, 1698, 1602, 1561, 1527, 1414, 1281, 1158, 1023, 984 cm^{-1}; UV-Vis (MeOH) λ_{max}: 332 nm (ε 8700), 289 (10000), 236 (sh), 204 (46000); UV-Vis (MeOH+NaOH): 363 nm (ε 8100), 292 (10000), 245 (sh), 204 (62000).

Ningalamide(178): a dark-red amorphous solid; $[\alpha]_D = 0^o$; HRFABMS, $(M + H)^+$ obsd. *m/z* 582.1385, $C_{32}H_{24}NO_{10}$. dev. -2.6 ppm; IR (NaCl) ν_{max}: 3700-3000, 1699, 1623, 1593, 1515, 1431, 1393, 1360, 1292, 1200, 1117, 1022, 983 cm^{-1}; UV-Vis (MeOH) λ_{max}: 450 nm (sh), 355 (ε 5800), 301 (sh), 289 (9400), 204 (34000); UV-Vis (MeOH + NaOH): 530 nm (sh), 351 (sh), 309 (ε 12000), 204 (43000).

Ningalone(179): a dark-red amorphous solid; $[\alpha]_D = 0^o$; HRFABMS (thioglycerol): $(M + 2H)^+$ obsd. *m/z* 715.1718, $C_{40}H_{29}NO_{12}$, dev. -3.9 ppm); LRFABMS (NBA): $(M + H)^+$ obsd. *m/z* 714 and $(M + Na)^+$ *m/z* 736; IR (NaCl) ν_{max}: 3700-3000, 1665, 1562, 1296 cm^{-1}; UV-Vis (MeOH) λ_{max}: 508 nm (ε 9900), 404 (sh), 294 (17000), 276 (18000), 206 (41000); UV-Vis (MeOH + NaOH): 518 nm (ε 4800), 314 (17000), 274 (19000), 206 (98000).

Lamellarin O (168): an amorphous solid; $[\alpha]_D = 0^o$; HRDEIMS: M^+ obsd. *m/z* 459.0942, $C_{25}H_{17}NO_8$, dev.-2.7 ppm; UV (MeOH) λ_{max}: 337 nm (ε 17100), 317 (17100), 276 (21800), 268 (sh), 205 (42400); UV (MeOH + NaOH) λmax: 363 nm (ε 14900), 323 (17000), 287 (23900), 205 (67700); IR (NaCl) ν_{max}: 3700 - 3000, 1686, 1597, 1423, 1282, 1252, 1191, 1158, 1023, 990 cm^{-1}.

Lamellarin P (169): an amorphous solid; $[\alpha]_D = 0^o$; HRDEIMS: M^+ obsd. *m/z* 473.1094, $C_{26}H_{19}NO_8$, dev. -3.5 ppm; UV (MeOH) λ_{max}: 336 nm (ε 17000), 315 (17000), 278 (23000), 268 (sh), 205 (43000); UV (MeOH + NaOH) λ_{max}: 362 nm (ε

15800), 322 (17600), 287 (23000), 205(60000); IR (NaCl) ν_{max}: 3700 - 3000, 1690, 1595, 1420, 1285, 1250, 1187 cm^{-1}.

Lamellarin Q (170): an amorphous solid; $[\alpha]_D = 0^o$; HRDEIMS: M^+ obsd. *m/z* 473.1125, $C_{26}H_{19}NO_8$, dev. 3.0 ppm; UV (MeOH) λ_{max}: 336 nm (ε 16500), 315 (16500), 278 (21000), 265 (sh), 205 (44000); UV (MeOH + NaOH) λ_{max}: 362 nm (ε 15000), 322 (15700), 287 (23600), 205 (57700); IR (NaCl) ν_{max}: 3700 - 3000, 1691, 1596, 1422, 1289, 1252, 1185 cm^{-1}.

Lamellarin R (171): an amorphous solid; $[\alpha]_D = 0^o$; HRDEIMS: M^+ obsd. *m/z* 487.1258, $C_{27}H_{21}NO_8$, dev. -1.9 ppm; UV (MeOH) λ_{max}: 336 nm (ε 17600), 317 (17600), 278 (22000), 265 (sh), 205 (45000); UV (MeOH + NaOH) λ_{max}: 363 nm (ε 14200), 322 (16000), 286 (23000), 205 (65000); IR (NaCl) ν_{max}: 3700-3000, 1692, 1595, 1422, 1288, 1250, 1186 cm^{-1}.

Lamellarin S (172) and **T (173)**: HRDEIMS: M^+ obsd. *m/z* 487.1259, $C_{27}H_{21}NO_8$, dev. -1.7 ppm; UV (Diode-Array Detector) λ_{max}: 332, 315, 278, 265, 220 nm; IR (NaCl) ν_{max}: 3700-3000, 1686, 1597, 1423, 1282, 1252, 1191, 1158, 1023, 990 cm^{-1}.

Preparation of Acetate Derivatives 349-356.

In a typical procedure, acetic anhydride (0.5 ml) was added to a solution of alkaloid (5 mg) in pyridine and stirred for 2 hours at room temperature. The reaction was monitored by TLC. Reagents were evaporated under high vacuum and partitioned sequentially between ethyl acetate and ice water, between ethyl acetate and 0.1 $NaHCO_3$ solution, and ethyl acetate and brine. Finally the product was dried with $MgSO_4$ and filtered. The solvent was evaporated under vacuum, and the residue was purified by reverse-phased HPLC (ODS-silica) using acetonitrile-methanolic water to give the acetate derivative.

Tetraacetate 349: an amorphous solid; $[\alpha]_D = 0^o$; LRFABMS, $(M + H)^+$ obsd. *m/z* 536, $(M + Na)^+$ m/z 558; HRFABMS, $(M + H)^+$ obsd. *m/z* 536.0837, $C_{26}H_{18}NO_{12}$, dev. 1.5 ppm; ^1H NMR (500 MHz, CD_2Cl_2/MeOH-d_4 = 3:2): 2.37 (s, 6H), 2.39 (s, 6H), 7.38 (s, 2H), 8.32 (s, 2H).

Hexaacetate 350: a yellow oil ($CDCl_3$); $[\alpha]_D = 0^o$; HRFABMS, $(M + H)^+$ obsd. *m/z* 714.1811, $C_{37}H_{32}NO_{14}$, dev. -1.7 ppm); ^1H NMR (500 MHz, $CDCl_3$): 2.26 (s, 6H), 2.28 (s, 3H), 2.29 (s, 3H), 2.31 (s, 3H), 2.32 (s, 3H), 3.16 (t, 2H, *J* = 8 Hz), 4.67 (t, 2H, *J* = 8 Hz), 6.83 (s, 1H), 6.97 (d, 1H, *J* = 8 Hz), 6.98 (s, 1H), 7.09 (d, 1H, *J* = 8 Hz), 7.21 (d, 1H, *J* = 8 Hz), 7.25 (d, 1H, *J* = 8 Hz), 7.27 (s, 2H), 7.62 (s, 1H); ^{13}C NMR (50 MHz, $CDCl_3$): 20.6 (6C), 37.4, 50.8, 112.4, 115.8, 116.4, 117.9, 118.9, 123.6, 123.9 (2C), 124.7, 125.5, 127.1, 127.7, 132.0, 132.3, 136.4, 138.3, 141.0, 141.4 , 141.7, 142.0, 142.1, 148.9, 154.5, 168.0 168.2 (2C), 168.3 (2C), 168.6.

Octaacetate 351: a yellow-green amorphous soild ($CDCl_3$); $[\alpha]_D = 0^o$; HRFABMS, $(M + H)^+$ obsd. *m/z* 918.2186, $C_{48}H_{40}NO_{18}$, dev. -6.4 ppm; ^1H NMR (500 MHz, $CDCl_3$); 2.15 (s, 3H), 2.17 (s, 3H), 2.18 (s, 3H), 2.22 (s, 3H), 2.23 (s, 3H), 2.24 (s, H), 2.26 (s, 3H), 2.27 (s, 3H), 2.46 (t, 2H, *J* = 8 Hz), 3.60 (t, 2H, *J* = 8 Hz), 6.16 (dd, 1H, *J* = 8, 2 Hz), 6.66 (d, 1H, *J* = 2 Hz), 6.95 (d, 1H, *J* = 8 Hz), 7.18 (dd, 1H, *J* = 8, 2 Hz), 7.20 (d, 1H, *J* = 2 Hz), 7.25 (d, 1H, *J* = 8 Hz), 7.31 (d, 1H, *J* = 8 Hz), 7.38 (d, 1H, *J* = 2 Hz), 7.42 (dd, 1H, *J* = 8, 2 Hz), 7.66 (s, 1H), 7.89 (s, 1H); ^{13}C NMR (125 MHz, $CDCl_3$): 20.5 (4C), 20.6$_2$, 20.6$_5$, 20.6$_9$, 20.7$_3$, 34.4, 42.8, 121.5, 123.3, 123.5, 123.7, 124.2, 125.3, 126.5, 127.3, 127.6, 127.9, 128.2, 128.6, 128.8, 129.0, 129.1, 130.1, 130.6, 133.7, 136.1, 140.7, 141.7, 141.8, 142.2, 142.6, 143.6, 144.1, 145.5, 147.4, 167.6, 167.7$_2$(2C), 167.7$_6$, 167.8$_2$, 168.1 (2C), 168.3, 169.6, 181.6.

Decaacetate 352: a dark-green noncrystalline solid (from ethyl acetate); $[\alpha]_D = 0^o$; HRFABMS, $(M + 2H)^+$ obsd. *m/z* 1135.2708, $C_{60}H_{49}NO_{22}$, dev. -3.4 ppm; ^1H NMR (500 MHz, $CDCl_3$): 2.13 (s, 3H), 2.14 (s, 3H), ~2.24 (2H), 2.28 (s, 6H), 2.30 (s, 6H), 2.33 (s, 6H), 2.35 (s, 6H), 3.23 (m, 2H), 6.43 (d, 1H, *J* = 1.5 Hz), 6.49 (dd, 1H, *J* = 8, 1.5 Hz), 6.75 (d, 1H, *J* = 8 Hz), 7.26 (d, 2H, *J* = 1.5 Hz), 7.28 d, 2H, *J* = 8 Hz), 7.29 (dd, 2H, *J* = 8, 1.5 Hz), 7.98 (s, 2H), 8.18 (s, 2H).

Calculation of shielding effects of phenyl rings in 178 and 179.

Estimated internuclear distances were obtained using a computer-molecular modeling program, pcmodel. Figure 2-2-12a in Jackman and Sternhill's book (1969) and Figure 1 in Johnson and Bovey (1958) were used to estimate long-range shielding values of the protons. For calculating shielding effects of phenyl rings and amide carbonyl group to the dopamine of **178** and **179** experimentally, chemical shifts obtained in the ^1H NMR

spectrum of ningalin (**177**) were utilized as references.

Methylation of ningalactone (176).

A solution of **176** (5 mg) in 2 ml methanol was put into the outer tube of a micro-scale diazomethane generation apparatus (from Aldrich), and 14 mg (0.09 mmol) of 1-methyl-3-nitro-1-nitrosoguanidine (MNNG) into the inner tube. The bottom half of the apparatus was cooled with ice in water to prevent vigorous reaction. Diazomethane was generated by dropwise addition of 1 ml 6 N NaOH solution into the inner tube by using a syringe. After 1 hour, the solvent was removed under vacuum. The products were unstable and resulted in a mixture not to be separated by HPLC. No further attempt was made to characterize the products.

Chapter III

The Natural Products Chemistry of a Brown/Purple *Didemnum* sp. (WA90122, WA90129, and WA9204)

A. Introduction to Chapter III

Ascidians shelter many symbiotic and parasitic organisms, including bacteria, protozoans, algae, and small invertebrates both inside and out. Two kinds of symbiotic unicellular algae are known, the procyanophyte, *Synechocystis* (Lafargue and Duclaux 1979), and the prochlorophyte, *Prochloron* (Lewin 1975). *Prochloron* lives on or near the surface of didemnids, and also lives in the cloacal cavities of didemnids. This association is very common in several genera of didemnids, such as *Tridemnum, Didemnum, Lissoclinum, Diplosoma, Leptoclinides, and Atriolum. Synechocystis* has been also known as a symbiont of *Lissoclinum bistratum* and other didemnids (Monniot *et al.* 1990).

A few studies have demonstrated the close association of microorganisms and marine invertebrates (Gil-Turnes 1988 and 1989). This may be also true of ascidians. The frequent association of ascidians and microorganisms suggests that some natural products from ascidians may have alternative sources, namely microbial origins. The production of secondary metabolites by symbionts of an ascidian was proposed in the case of cyclic peptides, bistratamides (**203 -204**), isolated from *Lissoclinum bistratum* (Degnan *et al.* 1989). The cyclic peptides were reportedly found in the algal symbionts when the obligate algal symbionts of the genus *Prochloron* were removed from the host ascidian and extracted. However, it was not clear whether they were made by the ascidian and transferred to the algal cells or synthesized by the algal symbiont itself. In my study, a specific ascidian, *Didemnum sp.*, was encountered, which might demonstrate the importance of symbionts in the production of secondary metabolites isolated from ascidians.

Two distinct *Didemnum* species were collected by hand using SCUBA (-8 m) in the Exmouth region of Western Australia in December of 1990 and 1992. A brown morph, a thin encrusting colonial ascidian, possessed small bumps (WA-90-122) while a shiny dark purple morph, a thin encrusting colonial ascidians, had a smooth surface showing matted

pattern.

The study of chemical constituents of these*Didemnum* species, WA90-129 (also WA-90-122), revealed very interesting results. Seven different natural products, including enterocin (**193**), 5-deoxyenterocin (**192**), and didemnocins A and B (**194-195**), were isolated (Figure 3-1). When the structural work was completed, a library search, using Chemical Abstracts (CAS) on-line database, revealed that two of metabolites were originally known from *Streptomyces* spp. isolated from soil samples. These compounds were known as enterocin (Miyairi *et al.* 1976, Tokuma *et al.* 1976) [or vulgamycin (Seto *et al.* 1976)] and 5-deoxyenterocin (Yaginuma *et al.* 1987).

The results strongly suggested that these compounds might be produced by microbial symbionts. To clarify whether the compounds are microbial products or not, microscopic examination of this ascidian and biological investigation of microorganisms isolated from the ascidian were carried out.

For this study, the second collection of the same ascidians was conducted in December of 1992. The specimen was carefully examined by visual comparison with a voucher and co-development of its crude extract on TLC with standard compounds. Two strains of bacteria were isolated in the collection site and frozen in sterilized sea water and glycerol for laboratory experiment, nine strains were isolated from the frozen ascidian in the laboratory. Nine isolates were fermented and their cultures were chemically investigated.

In the following section, each identified compound will be discussed in terms of structure elucidation and its microbial origin.

Figure 3-1. 5-Deoxyenterocin, enterocin, didemnocins A and B.

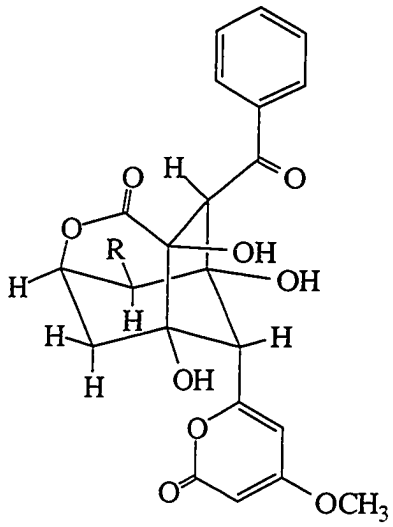

192. 5-deoxyenterocin R = H

193. enterocin (or vulgamycin) R = OH

194. didemnocin A R = 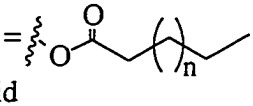

n = 18, behenic acid

195. didemnocin B R = 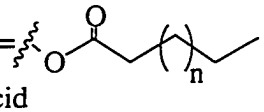

n =16, arachidic acid

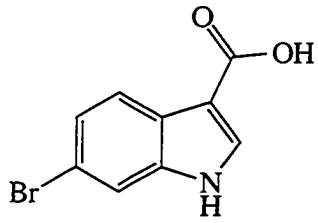

348. 6-bromoindole-3-carboxylic acid

B. The Isolation and Structure Elucidation of Deoxyenterocin (192) and Didemnocins A (194) and B (195).

The frozen ascidians (WA-90-122/129) were lyophilized and extracted twice with 70 % methanol/ dichloromethane. The combined extract was concentrated under vacuum and partitioned successively bewteen hexane and methanol, between ethyl acetate and water, and between n-butanol and water. Using vacuum flash chromatography followed by reversed-phase HPLC, enterocin (**193**, 0.11 % dry wt.), deoxyenterocin (**192**, 3.5 % dry wt.), didemnocins A (**194**, 0.026 % dry wt.) and B (**195**, 0.011 % dry wt.), three additional didemnocin derivatives, and a bromoindole derivative were isolated.

Deoxyenterocin (**192**) was obtained as a white solid, mp 220-222 °C. The molecular formula, $C_{22}H_{20}O_9$, established by HRFABMS [$(M + H)^+$ obsd. *m/z* 429.1205, dev. 4.53 ppm], showed 13 degrees of unsaturation. A strong IR absorption at 3404 cm^{-1}, in conjugation with three D_2O-exchangeable proton signals at δ 5.49 (s, 1H), 5.83 (s, 1H), and 5.92 (s, 1H), suggested the presence of three tertiary alcohols.

The proton spectrum of compound **192** showed the presence of two methylenes [(δ 1.62, bd, *J* = 14.5 Hz, and 2.22, dd, *J* = 14.5, 2 Hz) and (δ 2.06, bd, *J* = 14.5 Hz, and 2.65, dd, *J* = 14.5, 4 Hz)], a methoxy (δ 3.82, s, 3H), two *meta*-coupled heteroaromatic protons (δ 5.61, d, and 6.26, d, *J* = 2.5 Hz), a mono-substituted benzene ring (δ 7.49, t, 2H, 7.59, t, 1H, and 7.78, d, 2H, *J* = 8 Hz), and three protons (δ 4.00, s, 4.61, bs, and 4.83, m).

From COSY and ^{13}C NMR spectral analysis, a 4-methoxy-α-pyrone (**A**, δ 162.0, 105.6, 170.7, 87.8, 163.5, and 56.3) and a benzoyl moiety [**B**, 195.1, 139.4, 128.0 (2C), 128.5 (2C), and 132.7] were identified (Table 3-1).

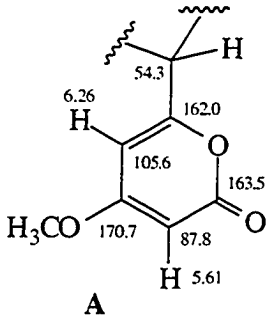

A

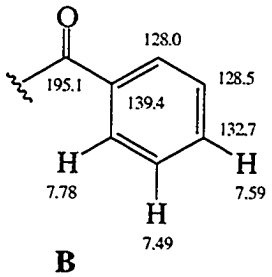

B

The meta-coupled proton signals at δ 6.26 and δ 5.61 directly correlated to

Table 3-1. Physical and spectral properties of 5-deoxyenterocin (**192**).

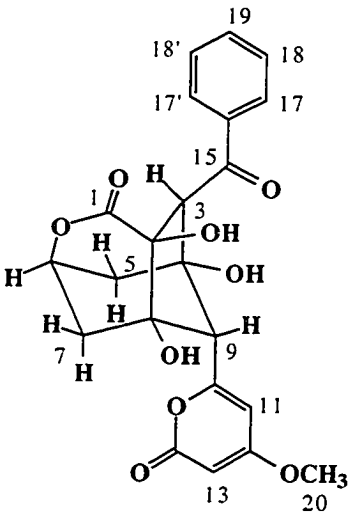

192. 5-deoxyenterocin

Source: *Didemnum* sp. (WA-90-129)
Exmouth, Western Australia
Solid, mp 218 - 220 °C
Molecular formula: $C_{22}H_{20}O_9$
HRFABMS: $(M + H)^+$ obsd. *m/z* 429.1205
$C_{22}H_{21}O_9$, dev. 4.53 ppm
LRFABMS: $(M + H)^+$ obsd. *m/z* 429.2
LREIMS: *m/z* 428, 348, 323, 269, 243, 235, 185, 167, 140, 125, 105, 77, 69, 44
UV (MeOH) λ_{max}: 284 (ε 5650), 248 (8110), 203 (24900) nm
IR (NaCl) ν_{max}: 3404, 1751, 1716, 1691, 1640, 1564, 1458, 1410, 1375, 1336, 1295, 1226, 1224, 1153, 1134, 1025, 1005 cm^{-1}
$[\alpha]_D = -31.5°$ (c 1.0, MeOH)

NMR data

No.	^{13}C	$^{1}H^a$	COSY[a]	HMBC[a] (8 Hz)	NOESY[a]
1	174.1				
2	79.7	5.80(s, OH)		C3, C2, C1	
3	61.0	4.00 (s, 1H)		C5, C9, C4, C8, C2, C1, C15	H5, H17, H17'
4	75.9	5.49 (s, OH)		C5, C9, C4, C3	
5	39.5	2.06 (bd, $1H_{eq}$, J = 15)[b]	H6, H9, $H5_{ax}$	C7, C9, C3, C6, C4	H3, $H5_{ax}$, H6 $H5_{eq}$, H6, H11
		2.65 (dd, $1H_{ax}$, J = 15, 4)[b]	H6, $H5_{eq}$	C3, C4, C9	
6	72.6	4.83 (m, 1H)	H5, H7	C7, C5, C4, C8, C1	H5, H7
7	36.8	1.62 (bd, $1H_{eq}$, J = 14)[b]	H6, H9, $H7_{ax}$	C5, C9, C6, C8	H6, $H7_{ax}$ H6, H_{eq}
		2.22 (dd, $1H_{ax}$, J = 14, 3)[b]	H6, $H7_{eq}$	C9, C8, C2	
8	77.1	5.91 (s, OH)		C7, C9, C8	
9	54.3	4.61 (bs, 1H)	$H5_{eq}$, $H7_{eq}$	C7, C5, C4, C8, C11, C10	H11
10	162.0				

Table 3-1. (continued)

No.	^{13}C	$^{1}H^{a}$	COSY[a]	HMBC[a] (8 Hz)	NOESY[a]
11	105.6	6.26 (d, 1H, J = 2.5)	H13	C12, C10, C13, C9	$H5_{ax}$, H9, H20
12	170.7				
13	87.8	5.61 (d, 1H, J = 2.5)	H11	C12, C14, C11	H20
14	163.5				
15	195.1				
16	139.4				
17, 17'	128.0	7.78(d, 2H, J = 8)	H18, H18'	C15, C19, C17'	H3, H18, H18'
18, 18'	128.5	7.49 (t, 2H, J = 8)	H17, H17', H19	C16, C18'	H17, H17', H19
19	132.7	7.59 (t, 1H, J = 8)	H18, H18'	C17, C17'	H18, H18'
20	56.3	3.81(s, 3H)		C12	H11, H13

All spectra, except for NOESY (MeOH-d_4), were recorded in DMSO-d_6. Assignments were aided by DEPT and HMQC experiments. Chemical shifts are reported in δ units (down field of TMS). Coupling constants are presented in Hz units. ^{13}C NMR experiments were performed at 125 MHz. [a] Spectra were obtained at 500 MHz. [b] In MeOH-d_4, each signal resonated at δ 2.17 (dd, 1H, J = 15, 1.5 Hz), 2.82 (dd, 1H, J = 15, 4.5 Hz), 1.82 (dd, 1H, J = 15, 2 Hz), and 2.55 (dd, 1H, J = 15, 3 Hz), respectively.

carbon signals at δ 87.8 and 105.6, respectively. In the HMBC spectrum of **192**, the proton signal at δ 5.61 coupled to two quarternary carbon signals at δ 163.5 and 170.7. The proton signal at δ 6.26 correlated to a quarternary carbon signal at δ 162.0 as well as the carbon signal at δ 170.7. Since $^4J_{CH}$ couplings are rarely observed in HMBC (8Hz) spectra, the carbon signal at δ 170.7 had to be within three bonds. Therefore, this carbon signal was assigned to C12. A methoxy group was connected to this carbon based on a correlation of H20 (δ 3.81) and C12 (δ 170.7). The carbon signal at either δ 162.0 or 163.5 could be assigned to the ester carbonyl of the α-pyrone. However, this ambiguity was resolved by a correlation between H11 (δ 6.26) and a methine carbon signal at δ 54.3 (C9). The presence of 4-methoxy-α-pyrone was also supported by strong IR absorptions at 1716 and 1564 cm^{-1}.

The presence of the phenyl ketone moiety was indicated by the downfield shift of the proton signal at δ 7.80 and a strong IR absorption at 1691 cm^{-1}. An HMBC correlation of an aromatic signal at δ 7.78 with the carbonyl signal at δ 195.1 confirmed the assignment.

Since there are no methods to differentiate between $^2J_{CH}$ and $^3J_{CH}$ couplings in HMBC spectra, the rest of structure identification was quite challenging. Three OH groups were very useful because they gave correlations to assign their respective carbons, one or two bonds away. By using this method, the following partial structures, **C-E**, were identified.

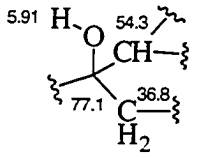

C

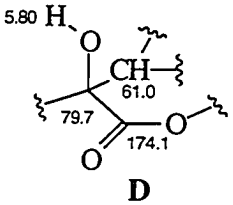

D

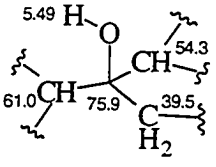

E

Substructures **C-E** were then linked by NMR correlation methods. A carbon signal at δ 61.0 was coupled to both hydroxy protons at δ 5.49 and 5.80. Thus, two hyroxylated carbons, resonated at δ 75.9 and 79.7, was connected through a methine carbon C3 (δ 61.0). A carbon signal at δ 54.3 was common in both partial strcutures **C** and **E**. The above led to the assignment of partial structure **F**.

Two geminally-coupled methylenes (δ 1.66 and 2.22; 2.06 and 2.65) were coupled to an oxygenated methine proton (δ 4.83) in the COSY spectrum (Table 3-1). These results led to the assignment of partial structure **G**. From partial structures **F** and **G**, a

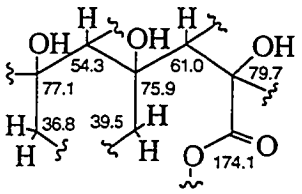

F

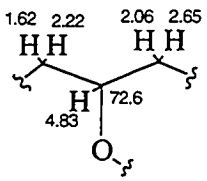

G

substituted cyclohexane moiety was identified. This assignment was also confirmed by HMBC correlations of H6 (δ 4.83) and C4 (δ 75.9), C5 (δ 39.5), C7 (δ 36.8), and C8 (δ 77.1). In addition to these correlations, the proton signal at δ 4.83 also coupled to an ester carbonyl at δ 174.1. As implicated by molecular formula of **192**, C6 (δ 72.6) was, as a result, attached to C1 (δ 174.1) through an oxygen (**H**). The lactone functionality was also supported by a strong IR absorption at 1751 cm^{-1}. Since C9 (δ 54.3) was already connected to the 4-methoxy-α-pyrone, C8 (δ 77.1) could be connected to either C3 (δ 61.0) or C2 (δ 79.7). However, an HMBC correlation of H7 (δ 2.22) and C2 (δ 79.7) could be explained only if connectivity between C2 and C8 was established. Therefore, a unique tricyclic structure, **I**, was revealed as the carbon skeleton of **192**.

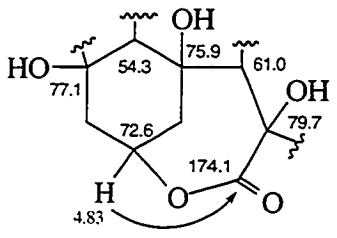

H

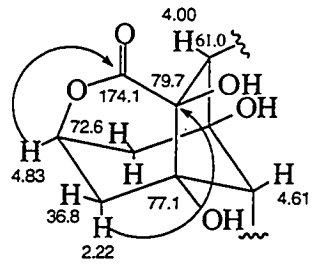

I

Finally, the phenyl ketone was attached to C3 (δ 61.0) on the basis of a correlation between H3 (δ 4.00) and C15 (δ 195.1). The relative stereochemistry of cyclohexane ring (C4 - C9) remained to be assigned. Since H9 (δ 4.61) was coupled to only one of the protons at C5 (δ 2.06) and C7 (δ 1.62) and not to the others (δ 2.65 at C5 and 2.22 at C7), H9 and the former two protons (δ 2.06 and 1.62) must be in 1,3-diequatorial relationships. The ^1H decoupling and COSY experiments clearly demonstrated W-couplings, although, as expected, the coupling constants were less than 1 Hz in the proton NMR spectrum of **192**. Thus, the 4-methoxy-α-pyrone was placed in an axial position at C9. However, the relative stereochemistry at C3 (δ 61.0) was assignable only when NOESY correlations were used. If the stereochemistry at C3 were as shown in Table 3-1,

a NOESY correlation of H3 (δ 4.00) and $H5_{eq}$ (δ 2.06) could be expected. However, if the opposite stereochemistry at that carbon was assumed, the proton H3 would yield an nOe enhancement of H9 (δ 4.61) in the NOESY spectrum of **192**. The NOESY spectrum of **192** clearly showed the relative stereochemistry at C3 as drawn in Table 3-1. Since the X-ray structure of an analog, enterocin or vulgamycin (**193**), was known from previous work, optical rotations of both compounds, **192** and **193**, were compared to assign the absolute stereochemistry at C3. Because the measured optical rotation of **192** ($[\alpha]_D$ = -31.3 °) was the same sign as that of **193** ($[\alpha]_D$ = -18.7 °, measured in this study), the absolute configuration at C3 was assigned as **S**.

The assignment of **192** was also supported by mass fragments in the HREIMS. The presence of the phenyl ketone subunit was demonstrated by two ions observed at *m/z* 77.0392 (C_6H_5, dev. 0.43 ppm) and 105.0323 (C_7H_5O, dev. -16.9 ppm). The cleavage of this subunit resulted in a daughter ion at *m/z* 323.0760 (M - C_7H_5O, $C_{15}H_{15}O_8$, dev. -2.17 ppm). The mass ion observed at *m/z* 125.0240 ($C_6H_5O_3$, dev. 0.71 ppm) was assigned to the methoxy-α-pyrone functionality in 5-deoxyenterocin.

The molecular modeling experiment of **192** (Figure 3-2), using pcmodel 4.51, was conducted to estimate coupling constants between H6 and H5's, and between H6 and H7's. Since only two hydroxyl groups at C2 and C5 were acetylated in **193**, hydrogen bondings were considered between an oxygens at C2 and an OH proton at C8, and between the carbonyl oxygen at C15 and the hydroxyl group at C4. This configuration was also supported by a NOESY correlation of H3 and H17/H17'. In an energy-minized structure of **192**, the dihedral angles of H6 and $H5_{eq}/H7_{eq}$ and H6 and $H5_{ax}H7_{ax}$ are 72, 68, 43, and 49 degrees, respectively. The calculated coupling constants based on these dihedral angles were 0.87, 1.06, 4.17, and 3.29 Hzs, respectively. Although the coupling constants, less than or equal to 1 Hz, were poorly resolved in the proton spectrum of **192** due to digital resolution of the spectrometer used in this study, the measured values were in good agreement with the predicted values (Table 3-1).

Didemnocin A (**194**) was obtained as an white amorphous soild. The molecular formula, $C_{44}H_{62}O_{11}$, was established by HRFABMS [$(M + H)^+$ obsd. *m/z* 767.4354 dev. -2.14 ppm]. The UV spectrum of **194** [(MeOH) λ_{max}: 284 (ε 12700), 249 (19100), and 203 (58000) nm] suggested **194** had the same chromophores as in enterocin. In the ^1H NMR and COSY spectra of **194**, three proton signals at δ 1.90 (ddd, 1H, *J* = 15, 3, 2 Hz), 2.70 (dd, 1H, *J* = 15, 3 Hz), and 5.84 (d, 1H, *J* = 5 Hz) coupled to a proton signal at δ 4.94 (ddd, 1H, *J* = 5, 3, 3 Hz), while the proton signal at δ 1.90 only coupled to a

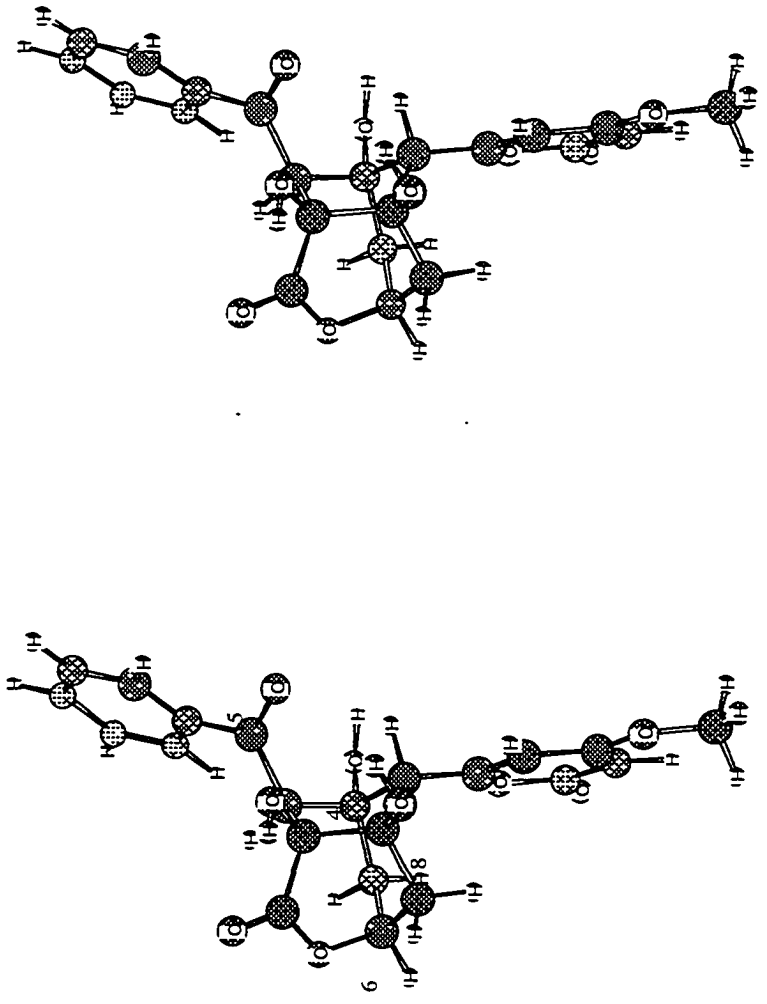

Figure 3-2. An energy-minimized strcuture of 5-deoxyenterocin (**192**) in a stereo view. Energy minimization of **192** was performed using a Serena software, pcmodel, which adopts a MMX force field. The actual presentation of **192** was obtained using a combination of a Chem3D program and a ChemDraw software released from the Cambridge Scientific Computing, Inc.

Table 3-2. Physical and spectral properties of didemnocin A (**194**).

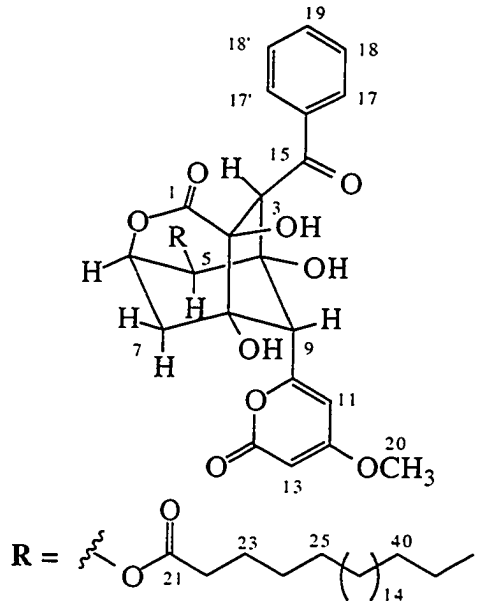

194. didemnocin A

Source: *Didemnum* sp. (WA-90-129) Exmouth, Western Australia
Amorphous solid
Molecular formula: $C_{44}H_{62}O_{11}$
HRFABMS: $(M + H)^+$ obsd. *m/z* 767.4354, $C_{44}H_{63}O_{11}$, dev. 2.14 ppm
LRFABMS: $(M + Na)^+$ obsd. *m/z* 789.5, $(M + H)^+$ obsd. m/z 767.5
LREIMS:obsd. *m/z* 341,340, 297, 288, 259, 241, 211, 185, 167, 140, 129, 125, 115, 111, 105, 97, 85, 83, 77, 73, 71, 69, 60, 57, 55, 43, 41
UV (MeOH) λ_{max}: 284 (ε 12700), 249 (19100), 203 (58000) nm
IR (NaCl) ν_{max}: 3385, 2915, 2848, 1740, 1694, 1643, 1564, 1465, 1378, 1254, 1223, 1125, 1019 cm^{-1}
$[\alpha]_D = -75.5^\circ$ (c 0.19, MeOH)

NMR data

No.	^{13}C	^1H[a]	COSY[a]	HMBC[a] (8 Hz)	NOESY[a]
1	175.1				
2	80.9	6.08 (s, OH)[b]		C1, C3	H9
3	55.9	4.59 (S, 1H)		C1, C2, C4, C5, C8, C9, C15	4-OH, H17, H17'
4	78.8	5.87 (s, OH)[b]		C4, C9	H3, H9
5	73.2	5.84 (d, 1H, J = 5)	H6	C3, C4, C21	H6, $H7_{ax}$
6	74.4	4.94 (ddd, 1H, J = 5, 3, 3)	H5, H7	C1, C4, C5, C8	H5, H7
7	36.5	1.90 (ddd, $1H_{eq}$, J = 15, 3, 2)	H6, $H7_{ax}$, H9		H6, $H7_{ax}$
		2.70 (dd, $1H_{ax}$, J = 15, 3)	H6, $H7_{eq}$	C2, C8, C9	H5, H6, $H7_{eq}$
8	77.5	6.06 (s, OH)[b]		C7, C8	H9
9	56.8	4.81 (d, 1H, J = 2)	H7eq	C4, C5, C7, C8, C10, C11	4-OH, 8-OH, H11
10	161.6				

Table 3-2. (continued)

No.	^{13}C	$^{1}H^{a}$	COSY[a]	HMBC[a] (8 Hz)	NOESY[a]
11	107.3	6.40 (d, 1H, J = 2)	H13	C10, C12, C13	H9, H20
12	173.3				
13	89.2	5.65 (d, 1H, J = 2)	H11	C11, C12	H20
14	166.7				
15	196.7				
16	140.8				
17, 17'	129.5	7.89 (d, 2H, J = 8)	H18, H18'	C15, C19, C17', C17	H3, H18, H18'
18, 18'	129.6	7.48 (t, 2H, J =8)	C16, H18', H18	C16, C18', C18	H17, H17', H19
19	134.2	7.59 (t, 1H, J = 8)	H18, H18'	C17, C17'	H18, H18'
20	57.0	3.89 (s, 3H)		C12	H11, H13
21	174.2				
22	35.0	2.42 (dt, 1H, J = 14, 7) 2.46 (dt, 1H, J = 14, 7)	H23	C21, C23, C24	H23
23	26.1	1.63 (q, 2H, J =7)	H22, H24	C21, C22, C25	H22
24	30.1	1.33 (m, 2H)	H23, H25		
25	30.5	1.30 (m, 2H)	H24, H26		
26	30.6	1.30 (m, 2H)		C27	
27-39	30.8	1.30 (s, 26H)		C27- C39	
40	33.1	1.30 (m, 2H)			
41	23.7	1.30 (m, 2H)			
42	14.4	0.89 (t, 3H, J =7)	H41	C40, C41	H41

All spectra, except for HMBC and NOESY spectra (DMSO-d_6), were recorded in MeOH-d_4. Assignments were aided by HMQC experiments. Chemical shifts are reported in δ units (down field of TMS). Coupling constants are presented in Hz units. ^{13}C NMR experiments were performed at 50 MHz. [a] Spectra were obtained at 500 MHz. [b] Signals were observed in DMSO-d_6. They were exchanged with H_2O in NOESY spectra.

proton signal at δ 4.81 (d, 1H, J = 2Hz). These results suggested that the protons at δ 1.90 and δ 4.81 had a 1,3-diequatorial relationship (W-coupling). The lackn of coupling of the proton at δ 4.81 with the protons at δ 5.84 and 2.70 indicated that the latter were in axial configurations. The same coupling pattern was revealed in the proton NMR spectrum of enterocin (**193**). However, the proton signal (δ 5.84) of a hydroxylated carbon at δ 73.2 was shifted downfield, compared with the same proton signal (δ 4.64) in **193**. It was thus reasonable that the deshielding effect was exerted by a carbonyl group of a fatty acid ester that was attached to that carbon (C5, δ 73.2). The assignment was also supported by an HMBC correlation. The proton signal at δ 5.84 (H5) correlated to the carbonyl carbon at δ 174.2 (C21) in the HMBC spectrum of **194** (Table 3-2).

The proton NMR spectrum of **194** showed several characteristic signals for a long-chain fatty acid [δ 2.42 (dt, 1H, J = 14, 7 Hz), 2.46 (dt, 1H, J = 14, 7 Hz), 1.63 (q, 2H, J = 7 Hz), 1.33 (m, 2H), 1.30 (s, 26H), and 0.89 (t, 3H, J = 7Hz)]. A methoxy-α-pyrone and the phenyl ketone were identified by similar spectral features. Since there was no additional unsaturation observed in the proton spectrum of **194**, the fatty acid must be fully saturated. Because the measurement of proton numbers of the fatty acid in the proton spectrum of **194,** by integration, was not accurate, the identity of the fatty acid was revealed from the molecular formula of **194**. The saturated fatty acid was identified as behenic acid (22:0), based on the number of carbons (22) in the fatty acid chain. However, the most conclusive evidence came from the LREIMS experiments of **194**. Since **194** had a γ-proton, H6, to the fatty acid ester carbonyl, the major fragment in the mass spectrum of **194** was arisen from the rearrangement of the γ-proton, followed by α-cleavage of the fatty acid ester (Figure 3-3). The mechanism is called the "McLafferty + 1" rearrangment (McLafferty 1980). The LREIMS spectrum showed the base peaks of *m/z* 340 (Type **I**). The type **II** fragment resulted in a minor mass ion at *m/z* 341. The presence of a 4-methoxy-α-pyrone and the phenyl ketone was also demonstrated by mass fragments at *m/z* 125, 105, and 77 in the LREIMS spectrum of **194**.

The absolute stereochemistry at C3 was assigned as the same configuration as that of 5-deoxyenterocin (**192**), based on the measured optical rotation of **194** ($[\alpha]_D$ = -75.7°).

Didemnocin B (**195**) was obtained as an amorphous solid. The proton NMR andUV spectra of **195** were almost identical (Tablc 3-3). Thus, **195** was a derivative of **194**. With aid of HRFABMS, the molecular formula, $C_{42}H_{58}O_{11}$, was established. The structure was, therefore, identified as the arachidic acid (20:0) ester of enterocin, which was confirmed by LREIMS experiments. The LREI mass spectrum of **195** showed the

Figure 3-3. The mass fragment pattern of didemnocin A (**194**).

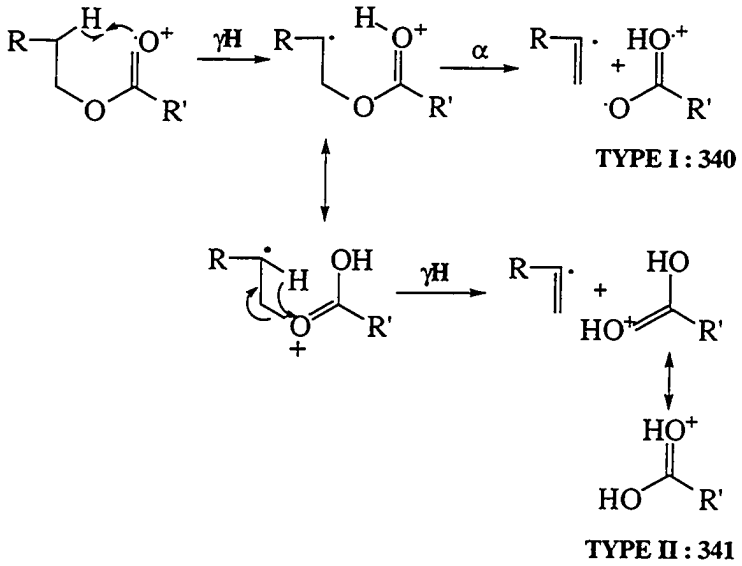

base peak at *m/z* 312 which was a rearranged fragment of arachidic acid. A minor mass ion at *m/z* 313 was also observed. The optical rotation ($[\alpha]_D$ = -81°) of **195** suggested the same stereochemistry as that of deoxyenterocin (**192**).

Several additional derivatives of didemnocin were isolated from the ethyl acetate fraction. The diode-array HPLC analysis of these derivatives showed they possessed the same enterocin carbon skeletons. Since one of them eluted between didemnocin A (**194**) and B (**195**) in the reversed-phase HPLC, it was tentatively assigned as an unusual fatty acid (21:0) ester of enterocin.

A bromoindole derivative (**348**) was also isolated as a yellow amorphous solid. Molecular formula, $C_9H_6NO_2Br$, was established by HRDEIMS [obsd. *m/z* 221.9555 $(M-OH)^+$, dev. 0.2 ppm]. The mass spectrum of this compound exhibited chracteristic ions (*m/z* 224 and 222) for the presence of a bromine. A carboxylic acid functionality was evident from strong IR absorptions at 3399 and 1600 cm^{-1} in conjugation with a carbon NMR signal at δ 169.2.

The proton spectrum of compound **348** showed the presence of 1,2,4-trisubstituted benzene ring [δ 7.25 (dd, 1H, *J* = 8.5, 1.5 Hz), 7.63 (d, 1H, *J* = 1.5 Hz), and 8.07 (d, 1H, *J* = 8.5 Hz)] and a aromatic singlet [δ 8.11 (bs, 1H)]. ^1H-^{13}C

Table 3-3. Physical and spectral properties of didemnocin B (**195**)

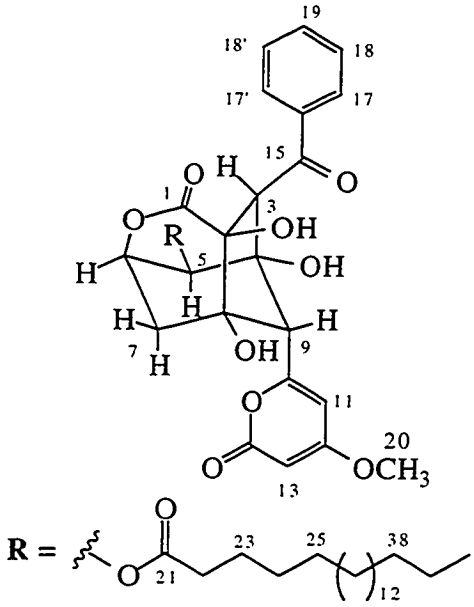

195. didemnocin B

Source: *Didemnum* sp. (WA-90-129)
Exmouth, Western Australia
Amorphous solid
Molecular formula: $C_{42}H_{58}O_{11}$
HRFABMS: $(M + H)^+$ obsd. *m/z* 739.4052
$C_{42}H_{59}O_{11}$, dev. -0.73 ppm
LRFABMS: $(M + Na)^+$ obsd. *m/z* 761.4,
$(M + H)^+$ obsd. *m/z* 739.5
LREIMS: *m/z* 313, 312, 269, 221, 185, 149, 147, 129, 125, 105, 97, 85, 83, 77, 73, 69, 60, 57, 43
UV (MeOH) λ_{max}: 284 (ε 12900), 247 (20400), 203 (57200) nm
IR (NaCl) ν_{max}: 3376, 2922, 2852, 1741, 1694, 1638, 1453, 1253, 1224, 1119 cm^{-1}
$[\alpha]_D = -81^\circ$ (c 0.15, MeOH)

NMR data

No	^1H (500 MHz, MeOH-d_4)
3	4. 59 (s, 1H)
5	5.84 (d, 1H, J = 4.5 Hz)
6	4.94 (m, 1H)
7	1.90 (ddd, $1H_{eq}$, J = 15, 3, 2 Hz)
	2.70 (dd, $1H_{ax}$, J = 15, 3 Hz)
9	4. 81 (d, 1H, J = 2 Hz)
11	6.40 (d, 1H, J = 8 Hz)
13	5.65 (d, 1H, J = 2Hz)
17, 17'	7.89 (t, 2H, J = 8 Hz)
18, 18'	7. 48 (t, 2H, J = 8 Hz)
19	7.59 (t, 1H, J = 8 Hz)
20	3.89 (s, 3H)
22	2.42 (dt, 1H, J = 14, 7 Hz)
	2.46 (dt, 1H, J =14, 7 Hz)
23	1.63 (q, 2H, J = 7 Hz)
24	1.33 (m, 2H)
25-38	1.30 (s, 28H)
39	1.30 (m, 2H)
40	0.89 (t, 3H, J = 7 Hz)

Chemical shifts are given in δ units (downfield of TMS). Assignments were based on a comparison of ^1H NMR assignments for didemnocin A (**194**).

Table 3-4. Physical and spectral properties of 6-bromoindole-3-carboxylic acid (**348**).

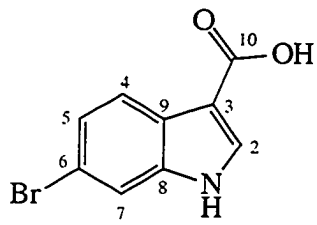

348. 6-bromoindole-3-carboxylic acid

Source: *Didemnum* sp.
Exmouth, Western Australia
Amorphous solid
Molecular formula: $C_9H_6NO_2Br$
LRDEIMS: obsd. *m/z* 224, 222, 197, 195, 116, 89, 63
UV (diode-Array HPLC) λ_{max}: 308, 273, 250 nm
IR (NaCl) ν_{max}: 3399, 1600, 1515, 1392, 1342, 1242, 1120, 1040, 798 cm^{-1}.

NMR data

No	^{13}C	^{1}H	HMBC (8 Hz)
N		11.9 (bs, 1H)	
2	136.5	8.11 (bs, 1H)	C3, C8, C9
3	114.0		
4	122.8	8.07 (d, 1H, J = 8.5 Hz)	C5, C6, C8
5	124.0	7.25 (dd, 1H, J = 8.5, 1.5 Hz)	C7, C9
6	114.8		
7	114.7	7.63 (d, 1H, J = 1.5 Hz)	C5, C6, C9
8	137.4		
9	125.0		
10	169.2		
OH			

All spectra were obtained in DMSO-d_6. Assignments were aided by HMQC experiments. Chemical shifts are reported in d units (downfield of TMS). ^{1}H and ^{13}C NMR experiments were performed at 500 MHz and 50 MHz, respectively.

correlation experiments with the compound resulted in the assignment of 6-bromoindole subunit (Table 3-4). The UV spectrum of this compound suggested an extended conjugation [(Diode-array HPLC) λ_{max}: 320, 273, and 250 nm]. Therefore, the structure of this compound was proposed as 6-bromoindolic-3-acid.

The possibility of **348** being 5-bromoindole-3-carboxylic acid was ruled out based on the followings: i) in the HMBC spectra of **348**, a correlation between a proton signal at δ 7.25 and a carbon signal at δ 125.0 is not likely since $^{4}J_{CH}$ couplings (a coupling between H6 and C9) are hardly observed in the HMBC spectra using 8 Hz-coupling constant. ii)

because of the presence of the carboxylic group at C3, the proton signals at C2 and C4 have to be much more deshielded than those at C5, C6, and C7. However, in the case of 5-bromoindole-3-carboxylic acid, H7 (δ 8.07) is much more deshielded than H4 (δ 7.63). Therefore, compound **348** was assigned as 6-bromoindole-3-carboxylic acid.

However, there were some questions to be considered. First of all, in the mass spectrum of aromatic acid, the molecular ion is normally observed. But, this was not the case. Secondly, the LRFAB mass spectrum of **348** gave several mass ions at *m/z* 327 (27 %), 314 (16) and 312 (19), 295 (27), 279 (100), 224 (27) & 222 (27), and 221 (57). One of the possibilties is that 6-bromoindole-3-carboxylic acid may be a degradation product of unknown compound with molecular weight of 313 and 311.

6-bromoindole-3-carboxylic acid was previously isolated from the sponge *Pseudosuberites hyalin*us (Rasmussen *et al.* 1993).

C. Potential Microbial Origins of secondary metabolites

A major concern in marine natural products research is the presence of symbiotic organisms, which make it difficult to accurately identify the source of secondary metabolites. The isolation of identical compounds, such as cycloxazoline (Hambley *et al.* 1992) or westiellamide (Princep *et al.* 1992), tetrapyrrole (Lindquist and Fenical 1991, Carté and Faulkner 1983, Kazlauskas *et al.* 1982), tambjamines (Paul *et al.* 1990), and dercitamide or kuanoniamine D (Carroll and Scheuer 1990, Gunawardana *et al.* 1992), or closely related compounds [lissoclinolide (Davidson and Ireland 1990) /tetrenolin (Pagani *et al.* 1973, Gallo *et al.* 1969), saframycin B (Arai et al. 1979) /renieramycin E (He and Faulkner 1989) /ecteinascidins (Wright *et al.* 1990, Rinehart *et al.* 1990a,b,c), and staurosporine derivatives (Kinnel and Scheuer 1992, Omura *et al.* 1977, Tsubotani *et al.* 1991)] from at least two different sources evokes the question of the potential microbial biosyntheses of the compounds.

The known compound, enterocin (**193**), was originally isolated from three strains of soil bacteria, *Sterptomyces candidus var. enterostaticus,* S. *viridochromogenes,* and S. *hygroscopicus* (Miyairi *et al.* 1976, Tokuma *et al.* 1976, Seto *et al.* 1976). The compound had bacteriostatic activities against gram-positive and gram-negative bacteria but no activity against fungi and yeast. Recently, deoxyenterocin (**192**) was filed for a Japanese patent (Yaginuma et al. 1987). The compound had very potent activity against *Sarcina lutea, Staphylococcus aureus, Klebsiella pneumoniae,* and *Vibrio percolans.* Deoxyenterocin was also isolated from a marine bacterium, PG-19 (unpublished work). These microbial metabolites, and the compounds isolated from *Didemnum* sp. in this study, had the same absolute configuration. These results strongly suggest the compounds isolated in this study might have microbial origins. To test this hypothesis, microscopic examination of this ascidian and chemical investigation of microorganisms in culture isolated from this ascidian were carried out.

The visual examination of the ascidian tissue using light microscope showed massive numbers of hook-shaped bacteria on and in the tissue of this ascidian. Eleven different strains of bacteria were isolated from the ascidian, but one did not survive transit from Australia to laboratory. Nine of them have been fermented in different media. The broths were extracted with ethyl acetate and then analyzed by TLC and by NMR methods.

None of the bacteria isolated from this ascidian produced the enterocin derivatives isolated here. There are several factors which may affect the results. Two strains of bacteria were originally isolated from the ascidian before freezing the sample. One of them

did not survive transit from Australia to the laboratory. The majority of the strains were isolated from the frozen ascidian long time after collection. Thus, the responsible strains might not survive the freezing process. Alternatively, the symbionts of this ascidian may not have been isolated. It would not be uncommon for symbionts to require specialized media and conditions which were not met here. Therefore, none of the enterocin-producing bacteria might grow in the culture media. The culture medium often changes the characteristic of the symbionts since the environment they experience has shifted from oligotrophic to eutrophic conditions. As a result, there was no need of competition among microorganisms. That might be why the microorganisms did not produce the isolated compounds from this ascidian. Another possibility was that the ascidian could be a real producer of these natural products.

In conclusion, enterocins and didemnocins could be microbial metabolites since both terrestrial and marine bacteria produced the compounds. None of the results, however, were conclusive. Nevertheless, the microscopic study showed that massive amounts of specific, hook-shaped microorganisms were present on and in the ascidian. An interesting fact was that the ascidian contained the major compound, deoxyenterocin, in as much as 4 % of dried animal. Despite of the fact that I could not prove the source of the natural products, this research has demonstrated an interesting possibility of the microbial origin of enterocin derivatives. Since *Vibrio* species are important pathogens in the marine environment (Trischman 1993), the strong potency of 5-deoxyenterocin against this microorganism suggests the host ascidian may have an advantage of an infection-free surface.

D. Experimental, Chapter III

Collection, Extraction, and Isolation Procedures.

The brown and purple encrusting ascidians, *Didemnum* spp. (WA-90-122 and WA-90-129), were collected by hand using SCUBA near Exmouth, Western Australia in the Indian Ocean in December 1990 and 1992. Since both species had the same chemistry, the collections were combined. For chemical investigation, the specimens were immediately frozen after collection. The lyophilzed animals (26.6 g dry wt) were extracted twice with 70 % methanol/ dichloromethane. The combined extract was concentrated and partitioned between hexane and methanol. The methanol fraction was further fractionated between ethyl acetate and water. The silica flash chromatography ($MeOH/CHCl_3$), followed by reversed-phase HPLC (25 % MeCN/ 2 % $MeOH/H_2O$), yielded deoxyenterocin (935 mg, 3.5 % dry wt), enterocin (30 mg, 0.11 % dry wt), and a mixture of didemnocins. The mixture was furhter purified by using successive reversed-phase HPLC (100 % MeOH and 2 % H_2O/MeOH) to give didemnocins A (6.8 mg, 0.026 % dry wt), B (3 mg, 0.011 % dry wt), several didemnocin dervatives, and a bromoindole derivative (2 mg, 0.008 %).

Isolation and Chemical Investigation of Microorganisms from ascidians.

For microbial study of this ascidian, a second collection was made in December of 1992. Specimens (WA-92-04) were carefully compared with a previous voucher. The presence of deoxyenterocin in the crude extract of WA-90-4 was examined with standards by thin layer chromatogrphy. Once the ascidian was confirmed as the same species as WA-90-122/129, a small piece of the ascidian was frozen in sterile sea water and glycerol. Water extract of the animal was prepared by chopping a small piece, adding sterile sea water, and sterile filtering. The extract was serially diluted with sterile sea water (approximately 10 fold dilutions). The isolates were stored at -80 °C with 10 % glycerol added to the usual culture media in 2 ml cryovials. The following media were used in microbiological methods:

A-1 media: starch (10 g), yeast extract (4 g), peptone (2 g), Tris 1M ph 8.0 (10 ml), Sea water (750 ml), and deionized water (250 ml); B-1 Media: peptone (2.5 g), yeast extract (1.5 g), 50 % glycerol 3.0 ml, sea water (750 ml), deionized water 250 ml.

Cultures were extracted twice with ethyl acetate. The crude extracts were concentrated under vacuum. Partial purification was conducted using vacuum silica flash chromatography and preparative thin layer chromatography (TLC). The crude extracts and

each fraction were carefully examined for the enterocins utilizing TLC and ^{1}H NMR analysis.

Deoxyenterocin (192): white solid, mp 218-220 °C; $[\alpha]_D$ = -31.5 °C; HRFABMS: (M + H)$^+$ obsd. *m/z* 429.1205, $C_{22}H_{21}O_9$, dev. 4.53 ppm; IR (NaCl) ν_{max}: 3404, 1751, 1691, 1640, 1564, 1458, 1410, 1375, 1336, 1295, 1226, 1224, 1153, 1134, 1025, 1005 cm^{-1}; UV (MeOH) λ_{max}: 284 (ε 5650), 248 (8110), 203 (24900) nm; UV (MeOH + NaOH) λ_{max}: 385 (ε 1710), 284 (5600), 244 (8800), 205 (70000) nm; LREIMS: obsd. *m/z* 428, 348, 323, 269, 243, 235, 185, 167, 140, 125, 105, 77, 69, 44.

Didemnocin A (194): amorphous solid; $[\alpha]_D$ = -75.5 °C; HRFABMS: (M + H)$^+$ obsd. *m/z* 767.4354, $C_{44}H_{63}O_{11}$, dev. -2.14 ppm; IR (NaCl) ν_{max}: 3385, 2915, 2848, 1740, 1694, 1643, 1564, 1465, 1378, 1254, 1223, 1125, 1019 cm^{-1}; UV (MeOH) λ_{max}: 284 (ε 12700), 248 (19100), 203 (58000) nm; UV (MeOH + NaOH) λ_{max}: 385 (ε 3010), 282 (11600), 246 (19600), 205 (57000) nm; LREIMS: obsd. *m/z* 341, 340, 297, 288, 259, 241, 211, 185, 167, 140, 129, 125, 115, 111, 105, 97, 85, 83, 77, 73, 71, 69, 60, 57, 43, 41.

Didemnocin B (195): amorphous solid; $[\alpha]_D$ = -81 °C; HRFABMS: (M + H)$^+$ obsd. m/z 739.4052, $C_{42}H_{59}O_{11}$, dev. -0.73 ppm; IR (NaCl) ν_{max}: 3376, 2922, 2852, 1741, 1694, 1638, 1453, 1253, 1224, 1119 cm^{-1}; UV (MeOH) λ_{max}: 284 (ε 12900), 247 (20400), 203 (57200) nm; UV (MeOH + NaOH) λ_{max}: 382 (ε 4000), 282 (12000), 244 (19800), 205 (78000) nm; LREIMS: obsd. *m/z* 313, 312, 269, 221, 185, 149, 147, 129, 125, 105, 97, 85, 83, 77, 73, 69, 60, 57, 55, 43.

6-brmoindole-3carboxylic acid (348): amorphous solid, HRDEIMS: (M-OH)+ obsd. m/z 221.9555, C9H6NO2Br, dev. 0.2 ppm; IR (NaCl) ν_{max}: 3399, 1600, 1515, 1392, 1342, 1242, 1120, 1040, 798 cm-1; UV (diode-array HPLC) λ_{max}: 308, 273, 250 nm; LRDEIMS: obsd. *m/z* 224, 222, 197, 195, 116, 89, 63.

Chapter IV

The Natural Products Chemistry of an Unidentified *Aplidiopsis* sp. (WA-90-47)

A. Introduction to Chapter IV

The genus *Aplidiopsis* is massive colonial ascidians with common cloacal cavities, found in many reef habits throughout New Caledonia (Monniot *et al.* 1990) and the Antarctic (Kott 1969, Monniot *et al.* 1990). The genus is often confused with related genus *Synoicum* (Kott 1969). Both *Synoicum* and *Aplidium* have a wide connection between the abdomen and the post-abdomen, but they can be differentiated by the shape of the cloacal siphon and the character of the stomach (Monniot *et al.* 1990).

An interesting ascidian, an *Aplidiopsis* sp. (WA-90-47, 5 kg, wet weight) was collected about 3 km north of Town Beach at Exmouth, Western Australia in December of 1990. The ascidian lives on sandy bottom at -7 m. The ascidian is a massive, soft, and convoluted colonial polyclinid with a rather semitransluscent tuinic. The colony was gelatinous and fixed by the whole extent of its basal surface. The semitransparent tunic was sometimes associated with sand adhering externally. The surface of the colony was raised into rounded areas over the system. The ascidians were highly exposed to predators. However, they were very abundant in this predator-rich environment. It was suspected that these ascidians are chemically defended.

Part of the collection (3.5 kg, wet wt) was lyophilized. The dried animal (332 g) was extracted three times with 70 % methanol / dichloromethane. The combined extract was concentrated under vacuum and partitioned into the following fractions: hexane, ethyl acetate, n-butanol, and water. Gel filtration of the ethyl acetate fraction (2.3 g) through a Sephadex LH-20 column, followed by vacuum flash chromatography, gave pure aplidiamines A (**1**, 20 mg) and B (**2**, 2 mg) (Figure 4-1).

Figure 4-1. Aplidiamines A (**1**) and B (**2**) and methyl derivatives, **357-360**

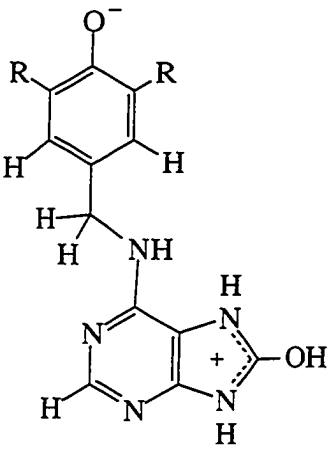

1. aplidiamine A R = Br
2. aplidiamine B R = H

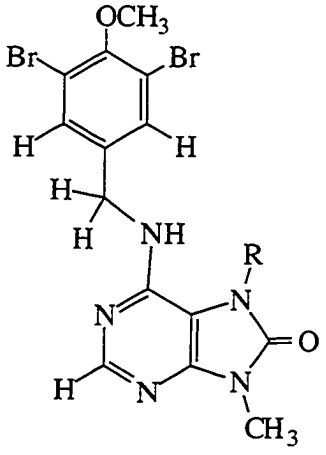

357. R = CH_3
358. R = H

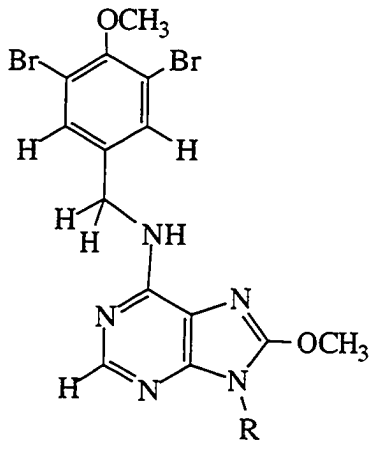

359. R = CH_3
360. R = H

B. The Structure Elucidation of Aplidiamines A (1) and B (2)

Aplidiamine A (**1,** Table 4-1) was obtained as a white solid, mp 241-243 °C. The molecular formula, $C_{12}H_9N_5O_2Br_2$, showed 10 degrees of unsaturation. Since only six proton resonances in the proton NMR spectrum of **1** were observed, the molecule had an element of symmetry. A bathochromic shift upon addition of base (NaOH), in conjunction with a strong IR absorption at 3159 cm^{-1}, suggested the phenolic nature of the compound.

The proton spectrum of **1** revealed a disubstituted amino methylene moiety (**A**) [δ 4.54 (d, 2H, J = 5.5 Hz) and 6.87 (t, 1H, J = 5.5 Hz)], two aromatic singlets (δ 7.52 and 8.04), and two exchangeable protons [δ 9.87 (2H) and 11.3]. The proton signal at δ 8.04 directly coupled to a carbon signal at δ 150.8. In the HMBC spectrum of **1**, the measured $^1J_{CH}$ coupling constant between these proton and carbon was 200 Hz. When only the coupling constant was concerned, there were three possible structures: furan ($^1J_{C\text{-}2H\text{-}2}$ = 202 Hz), imidazole ($^1J_{C\text{-}2H\text{-}2}$ = 208 Hz), and pyrimidine ($^1J_{C\text{-}2H\text{-}2}$ = 203 Hz) (Breitamaier and Voelter 1987). However, the pyrimidine structure was the most consistent based on both the proton and carbon chemical shifts. Thus, this carbon had to be connected to two nitrogens (**B**).

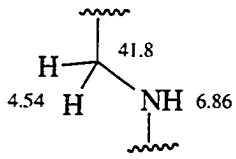

A

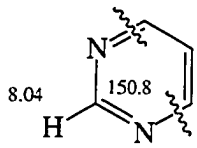

B

The proton signal at δ 7.52 (H3/H3') directly coupled to a carbon signal at δ 131.2 (C3/C3') in the HMQC spectra. In addition, this proton (H3/H3') also correlated the carbon signal at δ 131.2 (C3'/C3) in the HMBC spectrum. These results established a 1,2,3,5-tetrasubstituted benzene ring. This proton signal coupled to two quaternary carbon signals at δ 149.9 (C1) and 111. 9 (C2/C2'). Because of the symmetric nature the benzene ring moiety, two bromines and an oxygen were placed to the two shielded carbons (δ 111. 9) and the most deshielded carbon (δ 149.9) in the benzene ring. This benzene ring was connected to partial structure **A** based on HMBC correlations of a proton signal at δ 4.54 (H5's) and two carbon signals at δ 131.2 (C3/C3') and 134.0 (C4). These resulted in partial structure **C**. The dibromophenolic moiety is a well known system in the bastidin and the purealidin carbon skeletons (Pordesimo and Schmitz 1990, Ishibashi *et al.* 1991, Kobayashi *et al.* 1991). The assignment was fully consistent with the previously reported chemical shift data.

Table 4-1. Physical and spectral properties of aplidiamine A (**1**)

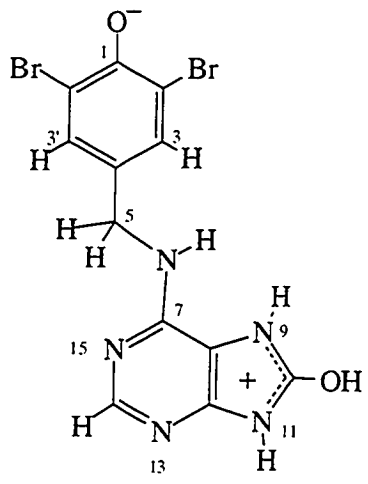

1. aplidiamine A

Source: *Aplidiopsis* sp. (WA-90-47)
Exmouth, Western Australia
White solid, mp 241-243 °C
Molecular formula: $C_{12}H_9N_5O_2{}^{79}Br_2$
HRFABMS: $(M + H)^+$ obsd. *m/z* 413.9189, $C_{12}H_{10}N_5O_2Br_2$, dev. -3.0 ppm
LRFABMS: $(M + H)^+$ obsd. *m/z* 418 (62), 416 (100), 414 (69); $(M - Br + H)^+$: 338 (20), 336 (21); 279, 265, 237, 214, 165, 151, 149
UV (50 % MeOH/CH_2Cl_2) λ_{max}: 273 (ε 15800), 221 (17300) nm
IR (NaCl) ν_{max}: 3159, 1701, 1682 (sh), 1634, 1472, 1405, 1339, 1139, 1006 cm^{-1}

NMR data

No.	^{13}C	^{1}H	HMBC (8 Hz)	NOESY
1	149.9			
2, 2'	111.9			
3, 3'	131.2	7.52 (s, 2H)	C1, C2, C2', C3', C3, C5	H5
4	134.0			
5	41.8	4.54 (d, 2H, J = 5.5 Hz)	C3, C3', C4, C7	H3, H3', H6
6		6.87 (t, 1H, J = 5.5 Hz)	C5, C7, C8	H5
7	145.2			
8	104.7			
9		9.87 (s, 1H)	C8, C10	
10	152.7	9.87 (s, OH)	C10	H11
11		11.3 (s, 1H)	C10, C12	H10
12	147.7			
13				
14	150.8	8.04 (s, 1H)	C8, C12	

All spectra were recorded in DMSO-d_6 at 500 MHz (^{1}H) and 125 MHz (^{13}C). Chemical shifts are reported in δ units (downfield of TMS). Assignments were aided by HMQC experiments.

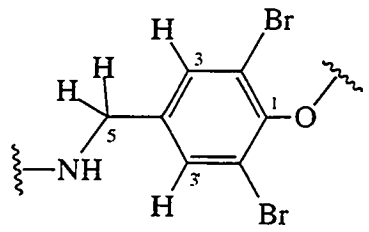

C

A quaternary carbon at δ 145.2 (C7) was coupled to the both proton signals at δ 4.54 (H5) and 6.87 (H6), while a quaternary carbon at δ 104.7 (C8) was only correlated to the proton signal at δ 6.87. Furthermore, the former carbon signal was coupled to a singlet aromatic proton at δ 8.04 (H14). Since $^{4J}_{CH}$ coupling was not plausible in the HMBC (8 Hz) spectrum, the carbon signal at δ 145.2 was assigned to C7 (Table 4-1). The proton signal at δ 8.04 gave an additional coupling to a quaternary carbon at δ 147.7 (C12). Therefore, a 2-amino-3,4-disubstituted pyrimidine structure (**D**) was identified. In the HMBC spectrum of **1**, both $^{3}J_{H\text{-}14C\text{-}7}$ and $^{3}J_{H\text{-}14C\text{-}12}$ coupling constants were accurately measured in the proton domain since the carbon domain was not decoupled. Both coupling constants were 9.5 Hz. The result was very consistent with literature values (Breitamaier and Voelter 1987).

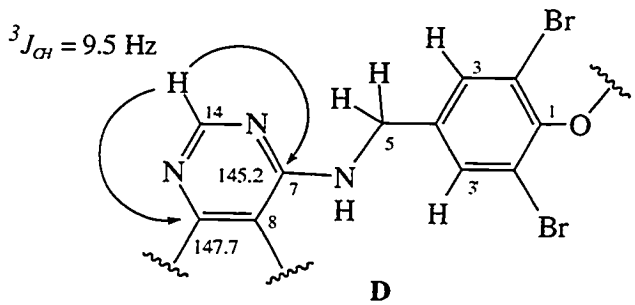

D

A carbon signal at δ 152.7 (C10), in conjugation with strong IR absorptions at 1705 and 1681 cm^{-1}, suggested the presence of a ureide moiety. However, this was not consistent with HMBC results. Three exchangeable protons at δ 9.87 (2H) and 11.3 and three carbon signals at δ 104.7, 147.7, and 152.7 composed a spin system, based on analysis of the HMBC spectrum of **1**.

To clarify the ambiguity, **1** was methylated with diazomethane in methanol/ dichloromethane. The reaction yielded four methylated products, **357-360** (Figure 4-2). Further characterization of **1** involved the methyl derivative **357** and **359** since N-methyl signals provided additional information about structure of aplidiamine A.

Figure 4-2. Methylated derivatives of aplidiamine A (**1**).

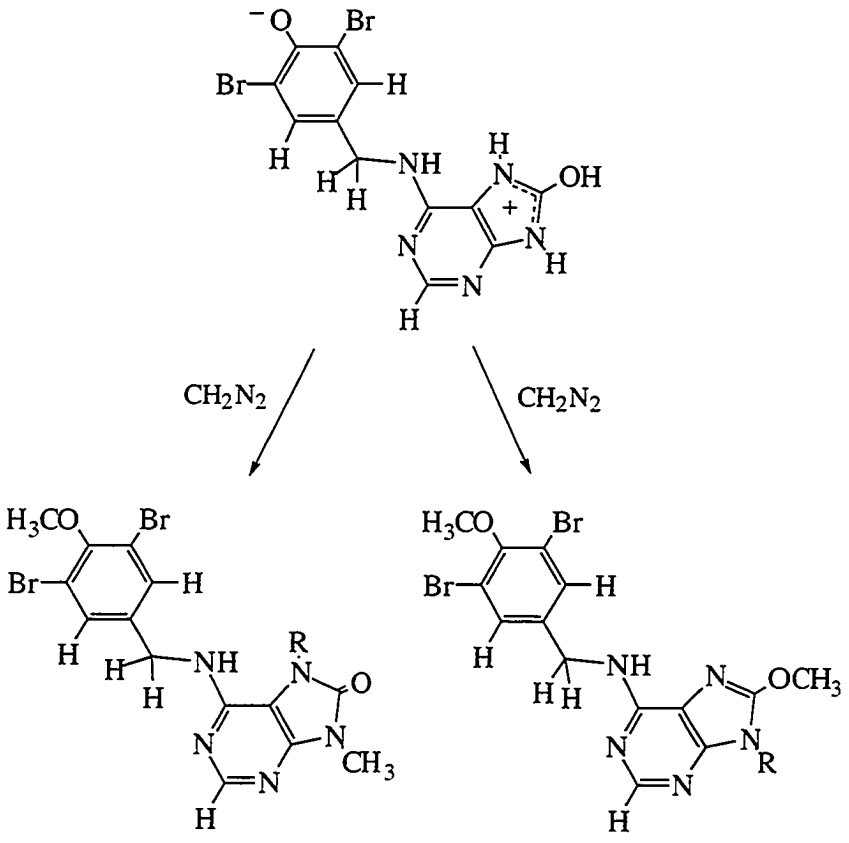

357. R = CH_3
358. R = H

359. R = CH_3
360. R = H

Compound **357** was obtained as an amorphous solid. The molecular formula, $C_{15}H_{15}N_5O_2Br_2$, established by HRDEIMS (M^+ obsd. *m/z* 458.9547 dev. -1.0 ppm), and its UV spectrum (diode-array HPLC: 275 and 220 nm) confirmed that **357** was a trimethyl derivative of **1** (Table 4-2). An N-methyl signal (δ 3.65) at N9 coupled to C8 (δ 105.6) and C10 (δ 153.0). An N-methyl signal (δ 3.45) at N11 also showed two correlations of H17 (δ 3.45)/C10 (δ 153.0) and H17/C12 (δ 147.4) in the HMBC spectrum of **357**. Therefore, an imidazol-2-one moiety was revealed (Table 4-2).

Table 4-2. Physical and spectral properties of methyl derivative (**357**).

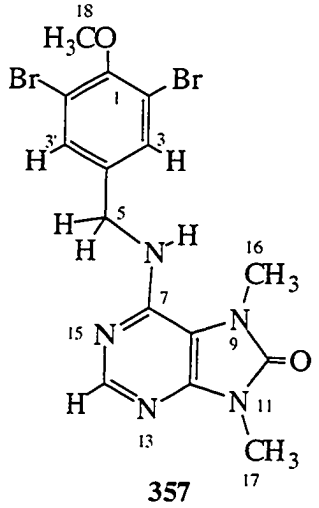

357

Source: synthetic product of **1**
Amorphous solid
HRFABMS: $(M + H)^+$ obsd. *m/z* 458.9547,
$C_{15}H_{15}N_5O_2{}^{81}Br_2$, dev. -1.0 ppm
UV (Diode-Array) λ_{max}: 275, 220 nm

NMR Data

No	^{13}C	^{1}H	HMBC
1	153.4		
2, 2'	117.9		C1, C2 (C2'), C3'(C3), C5
3, 3'	131.5	7.51 (s, 2H)	
4	137.4		
5	42.6	4.71 (d, 1H, J = 6)	C3 (C3'), C4, C7
6		4.99 (t, 1H, J = 6)	C4, C7
7	145.7		
8	105.6		
10	153.0		
12	147.4		
14	150.6	8.27 (s, 1H)	C7, C12
16	29.0	3.65 (s, 3H)	C8, C10
17	26.3	3.45 (s, 3H)	C10, C12
18	60.3	3.88 (s, 3H)	C1

All spectra was recorded in $CDCl_3$. Chemical shifts are reported in δ units (downfield of TMS). All ^{1}H NMR experiments were performed at 500 MHz. ^{13}C assignments were based on HMQC and HMBC experiments.

An additional methylated product **359** was obtained as an amorphous solid. The molecular formula, $C_{15}H_{15}N_5O_2Br_2$, established by HRDEIMS (M^+ obsd. *m/z* 458.9568 dev. 3.6 ppm), suggested that **359** was a regioisomer of **357**. The proton spectrum of compound **359** was almost identical to that of compound **357**, except for the presence of a methoxy signal at δ 4.15 (s, 3H) instead of a N-methyl at δ 3.65 (s, 3H). The methoxy proton signal at δ 4.15 gave an HMBC correlation to C10 (δ 155.4). A methoxy imine functionality was thus evident from these results. Therefore, compound **359** was identified as the structure presented in Table 4-3. Two additional products **358** and **360** were characterized based on a comparison of ^{1}H NMR assignment for **357** and **359**. All spectral data (experimental section) were consistent with the proposed structures **358** and **360** (Figure 4-2).

Aplidiamine A (**1**) had to be a zwitterion structure, as proposed in Table 4-1, because the OH proton at δ 9.87 coupled to C10 (δ 152.7) not to C1 (δ 149.9) in the HMBC spectra of aplidiamine (**1**). Furthermore, the methylation of compound **1** yielded four products which were consistent with this proposition. If aplidiamine (**1**) would exist as a ureide phenol in neutral form, the methylation of **1** with diazomethane could yield products **357-8** only. However, the reaction gave two additional products **359-360**, all of which were proofs of the existence of **1** as a zwitterion structure. However, aplidiamine exists in a neutral from in the solid state, as indicated by its IR absorptions at 1701 and 1682 cm^{-1}.

The mass fragment pattern of **1** supported the proposed structure (Figure 4-3). The LRFABMS spectrum of **1** showed a nice triplet as indication of two bromine atoms [$(M + H)^+$ obsd. *m/z* 418 (62 %), 416 (100), and 414 (69)]. The loss of a bromine atom was indicated by a doublet at *m/z* 338 and 336. A fragment ion of *p*-hydroxy dibromobenzylic subunit was observed as a triplet at *m/z* 277, 279, and 281. The presence of adenin-8-one moiety was demonstrated by a mass ion at *m/z* 152.

The $^1J_{CH}$ and $^3J_{CH}$ coupling constants were measured in the HMBC spectrum of **357** (Table 4-4). As expected, the aromatic proton signal at δ 7.51 showed $^1J_{CH}$ equal to 161.8 Hz which is characteristic of the benzene ring. The experimental value of $^1J_{CH}$ (209 Hz) of chloroform was perfectly matched with the literature value (Breitamaier and Voelter 1987). Once again, $^1J_{CH}$ (200 Hz) and $^3J_{CH}$'s (9.52 Hz) for the proton signal at δ 8.27 were the same as those of **1** (data not shown here).

Table 4-3. Physical and spectral properties of methyl derivative of aplidiamine A (**359**).

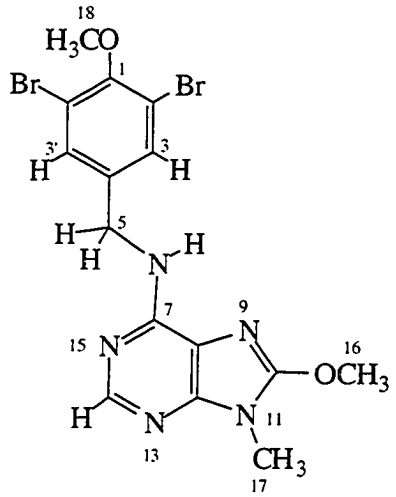

359

Source: synthetic product of **1**
Amorphous solid
Molecular formula: $C_{15}H_{15}N_5O_2Br_2$
HRFABMS: M^+ obsd. m/z 458.9568, $C_{15}H_{15}N_5O_2{}^{81}Br_2$, dev. 3.6 ppm
UV (Diode-Array) λ_{max}: 275, 220 nm

NMR Data

No	^{13}C	^1H	HMBC
1	152.9		
2, 2'	117.9		C1, C2 (C2'), C3'(C3), C5
3, 3'	131.7	7.53 (s, 2H)	
4	137.9		
5	42.9	4.79 (d, 1H, J = 6.5 Hz)	C3 (C3'), C4, C7
6		5.80 (bs, 1H)	
7	151.7		
8	ND		
10	155.4		
12	149.5		
14	151.0	8.31 (s, 1H)	C7, C12
16	56.7	4.15 (s, 3H)	C10
17	27.0	3.56 (s, 3H)	C10, C12
18	60.4	3.86(s, 3H)	C1

All spectra was recorded in $CDCl_3$. Chemical shifts are reported in δ units (downfield of TMS). All ^1H NMR experiments were performed at 500 MHz. ^{13}C assignments were based on HMQC and HMBC experiments.

Figure 4-3. Mass fragment pattern of aplidiamine A (**1**) in its LRFABMS spectrum.

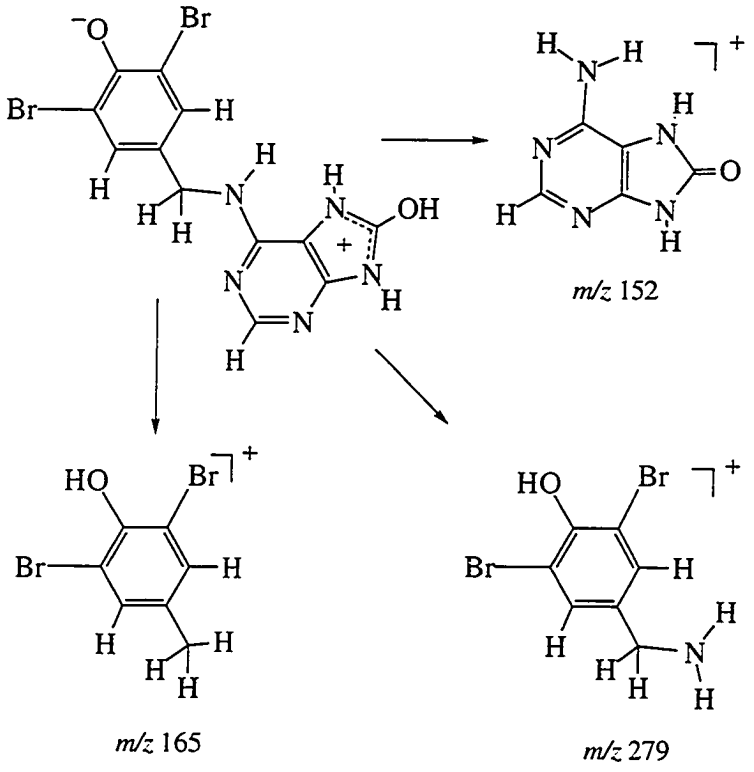

Table 4-4. $^{1}J_{CH}$ and $^{3}J_{CH}$ coupling constants of methyl derivative (**357**).

^{1}H (500 MHz, $CDCl_3$)	^{13}C (125 MHz, $CDCl_3$)	$^{1}J_{CH}$ (Hz)	$^{3}J_{CH}$ (Hz)
3.45	26.3	142.8	
3.65	29.0	138.0	
3.88	60.3	147.5	
4.71	42.6	148.0	
$CHCl_3$	77.0	209.0	
7.51	131.5	161.8	
8.27	150.6	200.0	
8.27	145.7		9.52
8.27	147.4		9.52

Aplidiamine B (**2**) was obtained as an amorphous solid. The UV spectrum of **2** [(MeOH) λ_{max}: 275 (ε 12000) and 220 (15300) nm] showed the same chromophore as that of **1**. The proton NMR spectrum of **2** revealed the presence of disubstituted benzene ring. On the basis of this, **2** was tentatively assigned as a debromo derivative of **1**. But, because of sample size limitations, aplidiamine B (**2**) was not completely characterized.

These compounds are unusual in terms of their biosynthesis. Most compounds possessing a dibromophenol subunit (Pordesimo and Schmitz 1990, Ishibashi *et al.* 1991, Kobayashi *et al.* 1991) seem likely to be derived from tyrosine. However, one carbon seems missing in the case of the aplidiamines.

The aplidiamines are interesting examples of ascidian metabolites which can be easily neglected by chemists by virtue of their simplicity of the spectral data and polarity. This work may provide an example of a possible defensive adaptation of an *Aplidiopsis* species.

C. Experimental, Chapter IV

Collection, Extraction, and Isolation procedure

The ascidian (WA-90-47) was collected by hand using SCUBA (-7 m) approximately 1 mile north of Town Beach at Exmouth, Western Australia in December of 1990. The specimens were preserved in the freezer (-40 °C) until used. The lyophilized animals were extracted with three times with 70 % methanol/ dichloromethane. The extract was filtered and concentrated under vacuum. The combined extract was partitioned between haxane and methanol. The methanol soluble fraction was further partitioned into ethyl acetate- and water-soluble fractions. Sephadex LH-20 gel filtration of the ethyl actate fraction (MeOH), followed by vacuum silica flash chromatography, yielded pure compounds **1** and **2**. Since aplidiamine A (**1**) had a limited solubility in cold methanol, the semi-purified compound in methanol was cooled, and the solvent was decanted and the precipitate was washed with cold methanol several times to give a pure aplidiamine A (**1**, 20 mg, 0.006 % dry wt).

Aplidiamine A (1): white solid, mp 241-243 °C; HRFABMS: $(M + H)^+$ obsd. *m/z* 413.9189, $C_{12}H_{10}N_5O_2Br_2$, dev. -3.0 ppm; IR (NaCl) ν_{max}: 3159, 1701, 1682, 1634, 1472, 1405, 1339, 1139, 1006 cm^{-1}; UV (50 % $MeOH/CH_2Cl_2$) λ_{max}: 273 (ε 15800), 221 (17300) nm; UV ($MeOH/CH_2Cl_2$ + HCl) λ_{max}: 290 (ε 15200), 223 (19000) nm; UV ($MeOH/CH_2Cl_2$ + NaOH) λ_{max}: 377 (sh), 313 (sh), 283 (ε 30700), 250 (sh), 223 (52500) nm.

Aplidiamine B (2): an amorphous solid; UV (50 % $MeOH/CH_2Cl_2$) λ_{max}: 275 (ε 12000) and 220 (15300) nm.

Methylation

Aplidiamine A (**1**, 18 mg) was dissolved in 8 ml of a 25 % methanol / dichloromethane solution. The solvent was reduced to 4 ml by purging with nitrogen. Excess diazomethane (4 ml) in ether solution was added and the solution was stirred at room temperature. The reaction was monitored by thin layer chromatography. When the reaction was complete, the solvent was removed under vacuum. Reversed-phase HPLC (ODS, 20 % H_2O/MeCN) of the product mixture yielded four methylated derivatives **357** (5 mg), **358** (3mg), **359** (5 mg), and **360** (3 mg).

Trimethyl derivative (357): amorphous solid, HRDEIMS: M^+ obsd. *m/z* 458.9547, $C_{15}H_{15}N_5O_2{}^{81}Br_2$, dev. -1.0 ppm; LRDEIMS: obsd. *m/z* 459, 457 455, 296, 294, 292, 281, 279, 277, 164; UV (diode-array HPLC) λ_{max}: 275, 220 nm.

Dimethyl derivative (358): amorphous solid, HRDEIMS: M^+ obsd. *m/z* 440.9467, $C_{14}H_{13}N_5O_2Br_2$, dev. 7.0 ppm; LRDEIMS: obsd. *m/z* 445, 443, 441, 282, 279, 277, 165, 150, 96; UV (diode-array HPLC) λ_{max}: 275, 220 nm; ^1H NMR (500MHz, $CDCl_3$): δ 3.28 (s, 3H), 3.86 (s, 3H), 4.75 (d, 2H, J = 5.8 Hz), 6.73 (bs, 1H), 7.50 (s, 2H), 8.28 (s, 1H).

Trimethyl derivative (359): amorphous solid, HRDEIMS: M^+ obsd. *m/z* 458.9568, $C_{15}H_{15}N_5O_2Br_2$, dev. 3.6 ppm; LRDEIMS: obsd. *m/z* 459, 457 455, 363, 361, 296, 294, 292, 281, 279, 277, 164, 150; UV (diode-array HPLC) λ_{max}: 275, 220 nm.

Dimethyl derivative (360): amorphous solid, HRDEIMS: M^+ obsd. *m/z* 440.9449, $C_{14}H_{13}N_5O_2Br_2$, dev. 3.0 ppm; LRDEIMS: obsd. *m/z* 445, 443, 441, 282, 279, 277, 165, 150, 96, 94; UV (diode-array HPLC) λ_{max}: 275, 220 nm; ^1H NMR (500MHz, $CDCl_3$ w/ MeOH-d_4): δ 3.84 (s, 3H), 3.86 (s, 3H), 4.65 (s, 2H), 7.49 (s, 2H), 7.89 (s, 1H).

Chapter V

The Natural Product Chemistry of an Unidentified *Eudistoma* sp. (WA-92-67)

A. Introduction to Chapter V

The genus *Eudistoma* contains diverse forms, including thin or thick encrusting species, mounds, ball-like cushions, and erect lobes. A branchial sac with three rows of stigmata is characteristic of this genus (Monniot *et al.* 1990). The classification of the genus *Eudistoma* at the species level is dependent upon the precise form of the gut-tract, gonadal traits, and larval structure (Plough 1978).

Eudistoma is a highly chemically-rich genus. So far, 14 % of known compounds from ascidian sources are isolated from species of the genus *Eudistoma.* However, the chemistry reported is rather simple. Almost 70 % of the *Eudistoma* metabolites are based on β-carbolines. Most are brominated β-carbolines with a substituent at C1, such as isopentyl (Adesanya *et al.* 1992), pyrrol derivatives (Kobayashi *et al.* 1984), and phenethyl derivatives (Kobayashi *et al.* 1990a, Kinzer and Cadellina 1987). Some are 1,2,3,4-tetrahydro-β-carbolines with an oxathiazepine ring fused at C1 and N2 (Rinehart *et al.* 1984, 1987). Only two compounds, eudistomidins E (**107**) and F (**108**), possess a tetrahydropyrimidine ring fused to the β-carboline system (Murata *et al.* 1991). Despite their rather simple structures, these compounds exhibit a variety of bioactivities, such as antiviral, antifungal, antibacterial, antileukemic, calmodulin antagonistic, and sarcoplasmic reticulum Ca^{2+}-inducing activities as well as rabbit heart muscle actomyosin ATPase inhibitory activity (see Chapter I).

Eight pyridoacridine polyaromatic alkaloids have also been isolated from this source (Rudi *et al.* 1988a,b, Rudi and Kashman 1989). Six possess potent growth regulatory properties (Schochet *et al.* 1993). This class of compound is very common in both ascidian and sponge chemistry (Molinski 1993).

In addition to β-carbolines and pyridoacridines, a tyrosine-derived alkaloid, rigidin (Kobayashi *et al.* 1990b), and a derivative of well-known microbial metabolite, 11-hydroxystaurosporine (Kinnel and Scheuer 1992), are natural products from *Eudistoma* spp. Calmodulin antagonistic and protein kinase C inhibitory activities are their reported pharmacological activities.

Apart from typical *Eudistoma* metabolites reported to date, 24-membered macrolides, iejimalides (Kobayashi *et al.* 1988, Kikuchi *et al.* 1991), are one of the most peculiar molecules isolated from this genus. These unusual macrolides are extremely potent cytotoxic agents against murine leukemia cell lines, L1210 and L5178Y, and human epidermoid carcinoma cells.

For this investigation, an unidentified *Eudistoma* sp. was collected by hand using SCUBA (-8 m) from Western Australia in the Indian Ocean in December of 1992. *Eudistoma* sp. is an orange colored colonial polycitorid. The tunic was soft and gelatinous. The color of this thick encrusting ascidian changed to brown upon the death of the colony.

Specimens of the ascidians were immediately frozen after collection and stored for several months at -40 °C. The sample was lyophilized and extracted twice with 70 % methanol/ dichloromethane. The combined extract was concentrated under vacuum. Solvent partitioning and size exclusion chromatography, followed by reversed-phase vacuum flash chromatography and reverse and normal mode HPLC with an amino column, yielded eudisins A (**141**, 0.07 % dry wt), B (**142**, 0.02 % dry wt), and C (**143**, 0.02 % dry wt) (Figure 5-1).

This chapter describes the structure elucidation of these compounds using spectroscopic methods, including the extensive use of 2-dimensional NMR correlation experiments. Molecular modeling studies were also conducted to explain the UV spectrum of these compounds and to clarify the stereochemistry of the only chiral center in eudisin C (**143**).

Figure 5-1. Eudisins A, B, C, and methyl derivative **361**

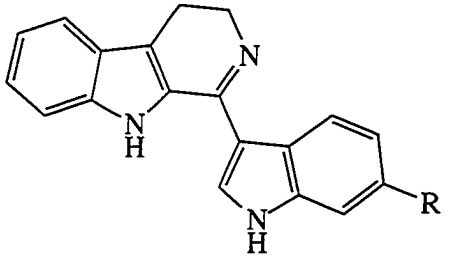

141. eudisin A R = Br
142. eudisin B R = H

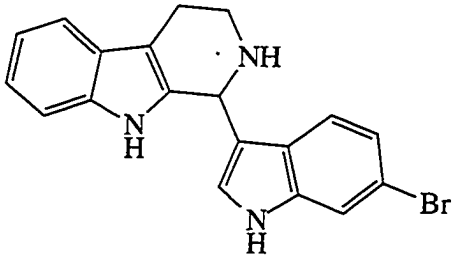

143. eudisin C

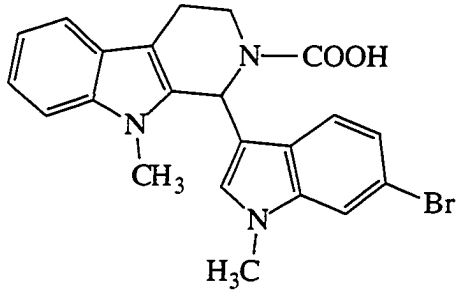

361

B. Structure elucidation of Eudisins A (141), B (142), and C (143)

Eudisin A (**141**, Table 5-1) was obtained as an amorphous yellow-green solid. The presence of bromine was obvious in the LRFABMS spectrum of **141** [$(M + H)^+$ obsd. *m/z* 366 (86 %) and 364 (100)]. The molecular formula, $C_{19}H_{14}N_3Br$, established by HRFABMS [$(M + H)^+$ obsd. *m/z* 364.0424, dev. -7.0 ppm] in conjugation with ^1H and ^{13}C NMR data, showed 14 degrees of unsaturation. The extended conjugation of **141** was evident from its UV absorptions [(MeOH) λ_{max}: 396 (ε 10400), 325 (20700), 290 (17500), 250 (sh), 220 (56600) nm]. Strong IR absorptions at 3406 and 1581 cm^{-1}, two proton NMR signals at δ 11.5 (bs, 1H) and 12.1 (bs, 1H), and a carbon NMR signal at δ 158.5 suggested that this molecule possessed two NH's and an imine (C=N) functionality. The destruction of the 396 nm-UV chromophore in **141** upon addition of base (NaOH) [(MeOH + NaOH) λ_{max}: 315(ε 9020), 292 (7040), 245 (sh), 206 (70000) nm] indicated that **141** was unstable under these conditions.

The proton NMR spectrum of **141** revealed four different spin systems: a 1,2-disubstituted and 1,3,4-trisubstituted benzene rings [δ 7.18 (t, 1H, *J* = 8.3 Hz), 7.36 (t, 1H, *J* = 8.3 Hz), 7.38 (dd, 1H, *J* = 8.3, 1.5 Hz), 7.50 (d, 1H *J* = 8.3 Hz), 7.72 (d, 1H *J* = 8.3 Hz), 7.74 (d, 1H, *J* = 1.5 Hz), and 7.84 (d, 1H, *J* = 8.3 Hz)], mutually coupled ethyl amine moiety [δ 3.18 (t, 2H, *J* = 8.3 Hz) and 4.00 (t, 2H, *J* = 8.3 Hz)], and an aromatic singlet [δ 8.09 (s, 1H)]. COSY experiments unambiguously resolved two substituted benzene systems. The *ortho*-coupled proton signals at δ 7.36 (H5) and 7.18 (H6) correlated with the two aromatic doublets at δ 7.50 (H4) and 7.72 (H7), respectively. The proton signal at δ 7.38 (H20) also coupled to the two proton signals at δ 7.74 (H18) and 7.84 (H21). Thus, seven aromatic signals were clearly assigned as in partial structures **A** and **B**.

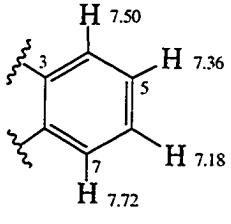

A

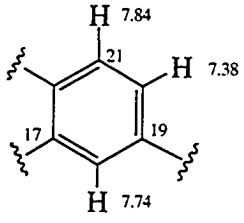

B

Further structural assignment of **141** was facilitated by HMBC experiments (Table 5-1). A proton signal at δ 3.18 (H10's) was correlated to three quaternary carbon signals at δ 124.2 (C9), 127.0 (C8), and 128.3 (C1), while a proton signal at δ 4.00 (H11's)

Table 5-1. Physical and spectral properties of eudisin A (**141**)

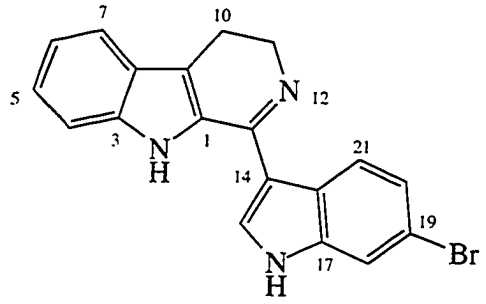

141. eudisin A

Source: *Eudistoma* sp. (WA-92-67)
Exmouth, Western Australia
Yellow-green amorphous solid
Molecular formula: $C_{19}H_{14}N_3Br$
HRFABMS: $(M + H)^+$ obsd. *m/z* 364.0424
$C_{19}H_{15}N_3{}^{79}Br$, dev. -7.0 ppm
LRFABMS: $(M + H)^+$ obsd. *m/z* 366 (86), 364 (100), 306, $(M - Br + H)^+$ 286
UV (MeOH) λ_{max}: 396 (ε 10400), 325 (20700), 290 (17500), 250(sh), 220 (56600) nm
IR (NaCl) ν_{max}: 3406, 3157, 1581, 1515, 1442, 1334, 1196, 981, 890, 800, 745 cm^{-1}

NMR data

No	^{13}C	^{1}H	COSY	HMBC
1	128.3			
2		12.1 (bs, 1H)[a]		
3	142.0			
4	114.6	7.50 (d, 1H, *J* = 8.3)	H5	C6, C8
5	128.5	7.36 (t, 1H, *J* = 8.3)	H4, H6	C3, C7
6	122.7	7.18 (t, 1H, *J* = 8.3)	H5, H7	C4, C8
7	122.3	7.72 (d, 1H, *J* = 8.3)	H6	C3, C5
8	127.0			
9	124.2			
10	21.0	3.18 (t, 2H, *J* = 8.3)	H11	C1, C8, C9, C11
11	45.5	4.00 (t, 2H, *J* = 8.3)	H10	C9, C10, C13
13	158.5			
14	110.6			
15	135.8	8.09 (s, 1H)		C13, C14, C17, C22
16		11.5 (bs, 1H)[a]		
17	140.4			
18	117.1	7.74 (d, 1H, *J* = 1.5)	H20	C19, C20, C22
19	118.6			
20	126.7	7.38 (dd, 1H, *J* = 8.3, 1.5)	H18, H21	C18, C22
21	123.4	7.84 (d, 1H, *J* = 8.3)	H20	C14, C17, C19, C22
22	125.9			

All spectra were recorded in MeOH with reference to TMS. ^{13}C NMR data were obtained at 125 MHz. All ^{1}H NMR experiments were performed at 500 MHz. Coupling constants are presented in Hz units. [a] The chemical shifts of the two exchangeable proton were acquired from the proton NMR spectrum of **141** in DMSO-d_6.

correlated to the carbon signal at δ 124.2 only. Thus, the carbon signal at δ 124.2 was assigned to C9. Two proton signals at δ 7.50 (H4) and 7.18 (H6) were also coupled to a carbon signal at δ 127.0. Since $^4J_{CH}$ couplings are not likely in the HMBC experiment, this carbon was assigned to C8. Since both proton signals at δ 7.18 (H6) and 3.18 (H10's) coupled to the carbon signal at δ 127.0 (C8), the connectivity between C8 and C9 was established. These results gave rise to assignment of the carbon signal at δ 128.3 to C1. The alternative assignment (as C13) was ruled out because $^4J_{CH}$ couplings were not likely. The proton signal at δ 4.00 (H11's) gave an additional correlation to the imino carbon at δ 158.5. Similarly, a carbon signal at δ 142.6 was assigned to C3, based on correlations of H5 (δ 7.36) and C3, and of H7 (δ 7.72) and C3. An NH group was placed at the most deshielded carbon, C3. The assignment was also supported by the upfield shift of adjacent carbon C4 (δ 114.6). Therefore, partial structure **C** was assigned.

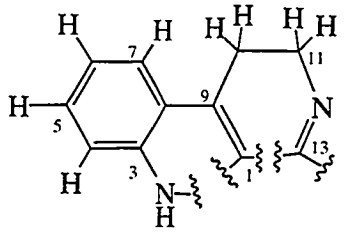

C

A proton signal at δ 7.38 (H20) coupled to a carbon signal at δ 125.9. This carbon signal could be assigned to either C19 or C22. However, the carbon signal was also correlated to an aromatic singlet at δ 8.09 (H15) which was directly coupled to a carbon signal at δ 135.8 (C15). As a result, that signal was assigned to C22. Since both proton signals at δ 8.09 and 7.84 (H21) gave cross peaks with two quaternary carbon signals at δ 110.6 and 140.4, these carbon signals were assigned to C14 and C17, respectively. Therefore, a bromoindole moiety (**D**) was revealed.

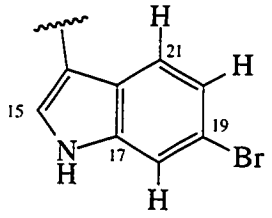

D

Finally, the two partial structures (**C** and **D**) were combined, based on a correlation of H15 (δ 8.09) and C13 (δ 158.5). To meet the molecular formula, connectivites of C1-N2 and C1-C13 were established.

At this point, regiochemistry of the bromoindole had to be clarified. There were two possible ways to prove the proposed structure. First of all, because of the presence of the nitrogen in the indole system, C17 (δ 140.4) and C22 (δ 125.9) had to be assigned as proposed (Table 5-1). In the alternative structure (5-bromoindole, **E**, rather than 6-bromoindole), the two correlations [cross peaks of H6 (δ 7.38)-C9 (δ 125.9) and H7 (δ 7.84)-C3 (δ 110.6)], observed in the HMBC spectrum of **141**, could not be explained.

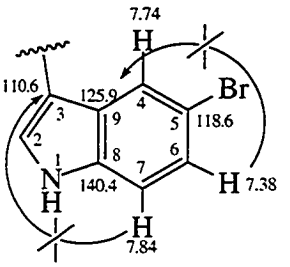

E

The second approach is based on NOEDS experiment with a methylated derivative. Eudisin A (**141**) was methylated with methyl iodide and potassium carbonate in acetone to give a single product (**361**) which is a very unusual product (Scheme I).

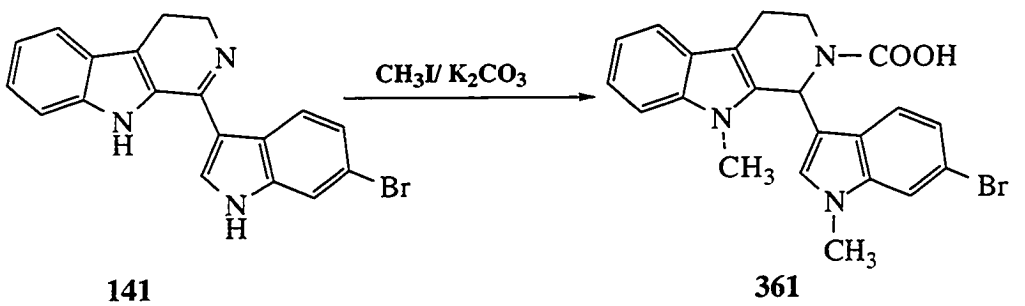

141 **361**

Scheme I

The proton spectrum of **361** showed two methyl groups [δ 3.86 (s, 3H) and 4.01 (s, 3H)], a bromoindole [δ 7.86 (d, 1H, J = 7.8 Hz), 7.20 (t, 1H, J = 7.8), 7.38 (t, 1H, J = 7.8), and 7.53 (d, 1H, J = 7.8)], a 2,3-disubstituted indole [δ 7.47 (dd, 1H, J = 8.3, 2 Hz), 8.18 (d, 1H, J = 8.3), and 7.84 (d, 1H, J = 2)], a mutually coupled ethyl [δ 3.55 (m, 2H) and 3.86 (m, 2H)], and an additional singlet at δ 5.62 (s, 1H) which was assigned a methine proton at C13. Strong IR absorptions at 3430, 1732, and 1221 cm^{-1} suggested the

presence of an N-COOH group. The LRCI mass spectrum of **361** gave the molecular ion at *m/z* 438 (30 %) and 440 (29). Therefore, the reaction product of **141** was assigned as N,N-dimethyl-eudisin A-N-carboxylic acid, **361**. The mass fragments in the LRCIMS spectrum of **361** supported the proposed structure (Figure 5-2). Loss of the carboxyl group was observed at *m/z* 394 and 392. The base peak was $(M - Br)^+$ at *m/z* 360 (100 %). Further loss of the acid group from $(M - Br)^+$ ion yielded a mass ion at *m/z* 315.

Extensive NOEDS experiments with **361** established the substitution pattern of the bromoindole moiety in **141** and the assignment of the methyl groups. The results from these NOEDS experiments are summarized in Scheme II. Irradiation of a methyl signal at δ 4.01 enhanced the two proton signals at δ 8.03 (s, 1H) and 7.84 (d, 1H, J = 2 Hz) by 2 % each, respectively, assigning this methyl group to N16. Irradiation of the other methyl signal at δ 3.77 produced a 1 % enhancement at the proton signals at δ 8.03, and in addition, a 2 % enhancement of the δ 7.53 (d, 1H, J = 7.8 Hz). This methyl signal was assigned to N2. These results unambiguously established the regiochemistry of the bromoindole, completing the assignment of eudisin A (**141**).

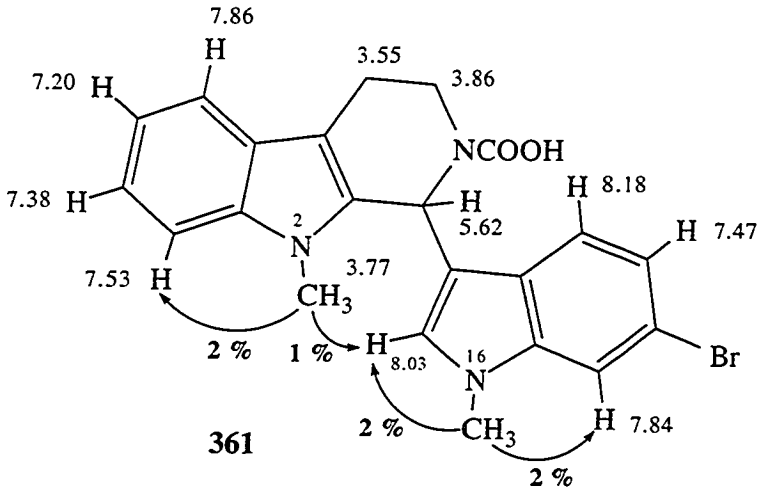

361

Scheme II

The molecular modeling study of **141** showed that the molecule was a planar structure in an energy-minimized structure (Figure 5-3). In this conformation, the imine group was perfectly aligned with the indole moiety. The bromoindole ring was twisted at only 22 degrees. Therefore, all π electrons seem completely conjugated. This conformation explained the UV spectrum of eudisin A (**141**).

Figure 5-2. Proposed fragment pattern in the LRCIMS of **361**.

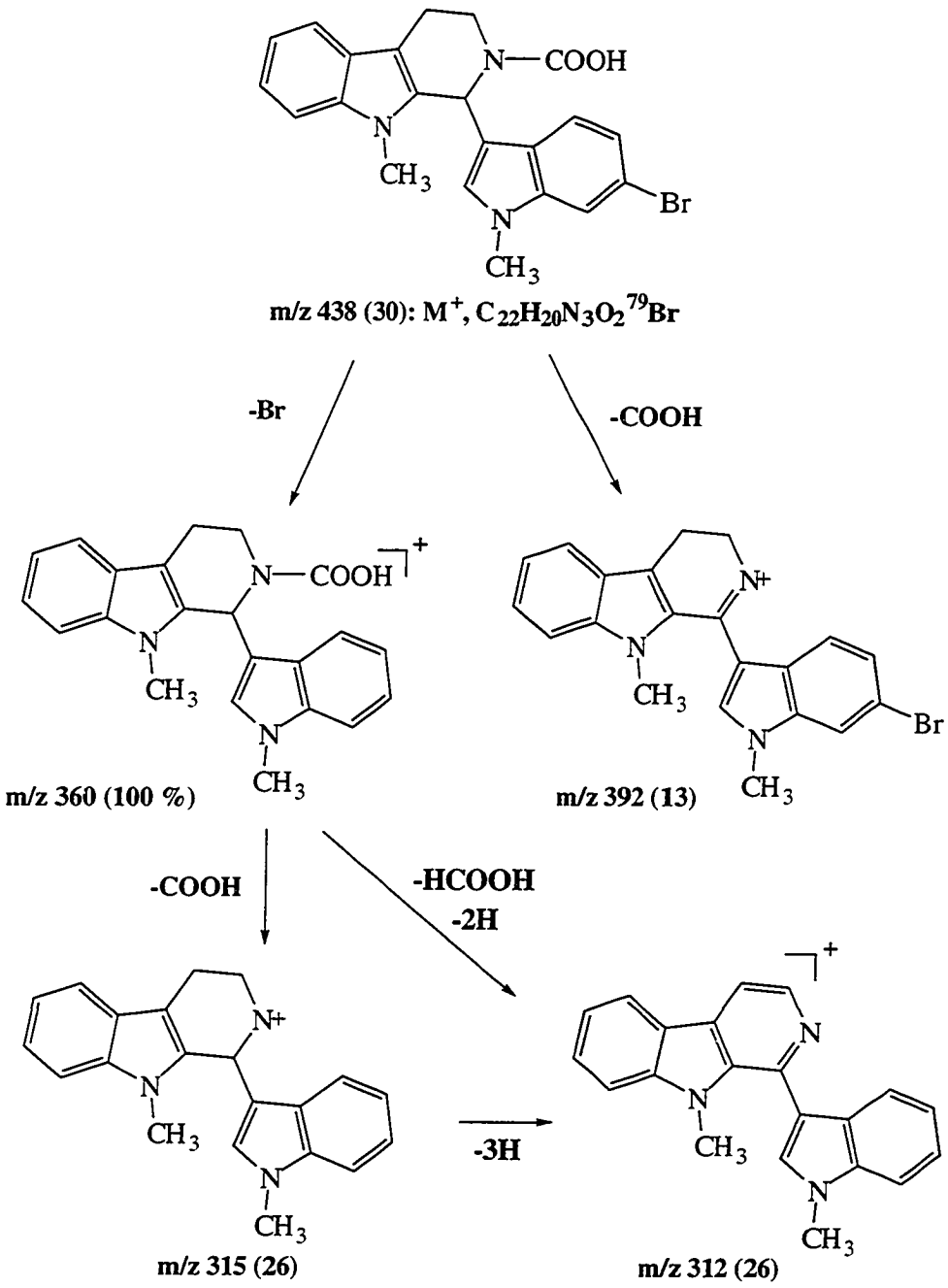

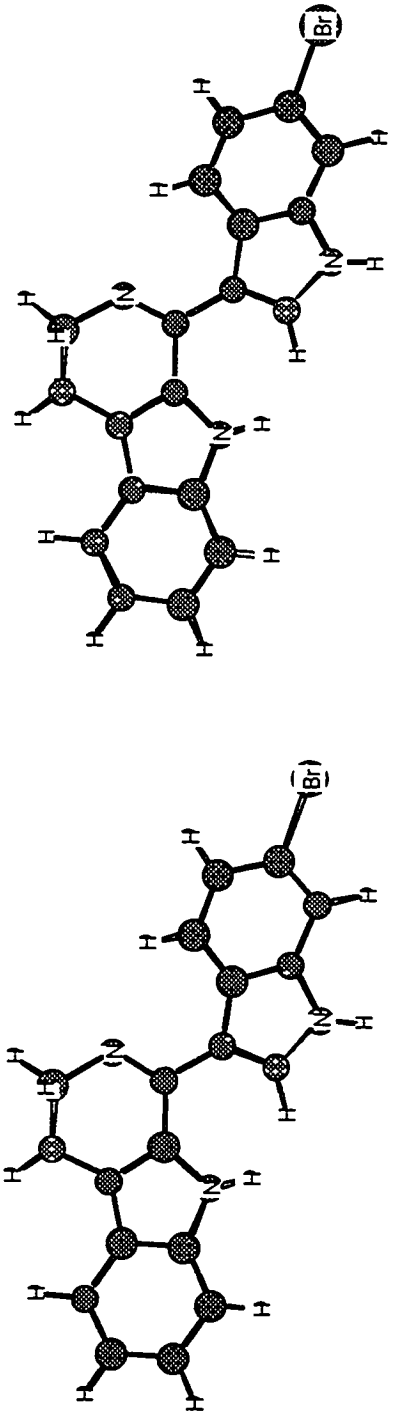

Figure 5-3. An energy-minimized structure of eudisin A (**141**) in a stereo view. The 3,4-dihydro-β-carboline ring and the bromoindole ring were almost coplanar and, in consequence, extended conjugation was achieved, resulting in the UV spectrum of **141**. Energy minimization of **141** was performed using a Serena software, pcmodel, which adopts a MMX force field. The actual presentation of **141** was obtained using a combination of a Chem3D program and a ChemDraw software released from the Cambridge Scientific Computing, Inc.

Eudisin B (**142**) was obtained as an amorphous solid. The molecular formula, $C_{19}H_{16}N_3$, suggested that **142** is a debromo derivative of **141**. The IR spectrum of **142** revealed the presence of an imino group and NH protons, based on strong absorptions at 3387, 3252, and 1591 cm^{-1}. The UV spectrum of **142** [(MeOH) λ_{max}: 397 (ε 9530), 330(9560), 282 (6010), 274 (6010), 248 (11200), and 208 (27500) nm] contained the same chromophore as that of **141**. The proton NMR spectrum of **142** also supported the proposed structure. There were two 1,2-disubstituted benzene rings [δ 7.23 (t, 1H, J = 8 Hz), 7.35 (t, 1H, J = 8), 7.40 (t, 1H, J = 8), 7.54 (d, 1H, J = 8), 7.62 (d, 1H, J = 8), 7.78 (d, 1H, J = 8), and 7.97 (d, 1H, J =8)], an ethyl [δ 3.28 (t, 2H, J = 7.5 Hz) and 4.05 (t, 2H, J = 7.5)], and an aromatic singlet [δ 8.27 (s, 1H)]. All results obtained from 2-dimensional NMR experiments were fully consistent with the presented structure (Table 5-2).

Eudisin C (**143**) was obtained as a white amorphous solid. The molecular formula, $C_{19}H_{16}N_3Br$, showed 13 degrees of unsaturation. The UV spectrum of **143** [(Diode-Array HPLC) λ_{max}: 280 and 225 nm], in conjugation with the molecular formula, suggested that **143** is a dihydro derivative of **141**. An additional signal at δ 5.57 (s, 1H), the absence of the imino carbon resonance at ca. δ 160, and a new methine carbon signal at δ 51.5 also supported the proposed structure. The assignment of **143** was based on comparison of its carbon data with those of **141** (Table 5-3).

The molecular modeling study of **143** showed that two epimers at C13 adopted completely different conformation (Figure 5-4). In the case of epimer-**I**, interproton distances of H13-H21 and H13-H10 are 2.4 Å and 2.6 Å, respectively. However, interproton distance between H13 and H14 were more than 4 Å. Furthermore, the maxium barrier to rotation about C13-C14 bond was estimated to be in excess of 300 Kcal/mole, thus free rotation of that bond appeared highly restricted. In the epimer-**II**, proton H9 is 2.8 Å away from proton H13. Almost the same distance was predicted between H13 and H14. Once again, free rotation about the C13-C14 bond was unlikely at room temperature. Therefore, the stereochemistry at C13 could be determined based on NOEDS experiments with **143**. However, eudisin C was racemic. As expected from no optical activity, the irradiation of H13 (δ 5.57) yielded 3.5 % nOe enhancements of both H15 (δ 7.18) and H21 (δ 7.14).

Eudisins A (**141**) and B (**142**) are the first examples of 3,4-dihydro-β–carbolines from marine sources. In the plant biosynthesis of β-carbolines, tetrahydro-β-carbolines are

Table 5-2. Physical and spectral properties of eudisin B (**142**)

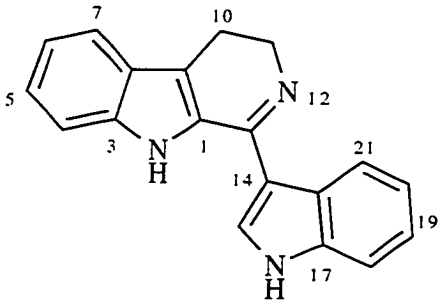

142. eudisin B

Source: *Eudistoma* sp. (WA-92-67)
Exmouth, Western Australia
Yellow-green amorphous solid
Molecular formula: $C_{19}H_{15}N_3$
HRFABMS: $(M + H)^+$ obsd. *m/z* 286.1353
$C_{19}H_{17}N_3$, dev. 3.1 ppm
LRFABMS: $(M + H)^+$ obsd. *m/z* 286
UV (MeOH) λ_{max}: 397 (ε 9530), 330 (9560), 282 (6010), 274(6010), 248 (11200), 208 (27600) nm
IR (NaCl) ν_{max}: 3387, 3252, 1591, 1538, 1520, 1448, 1375, 1261, 1243 cm^{-1}

NMR data

No	^{13}C	^{1}H	COSY	HMBC
1	127.5			
2				
3	142.6			
4	114.5	7.54 (d, 1H, *J* = 8)	H5	C6, C8
5	129.2	7.43 (t, 1H, *J* = 8)	H4, H6	
6	123.0	7.23 (t, 1H, *J* = 8)	H5, H7	C4, C8
7	122.5	7.78 (d, 1H, *J* = 8)	H6	C3, C5, C9
8	126.7			
9	125.8			
10	20.7	3.28 (t, 2H, *J* = 7.5)	H11	C1, C9, C11
11	43.5	4.05 (t, 2H, *J* = 7.5)	H10	C9, C10, C13
13	158.7			
14	108.3			
15	136.8	8.27 (s, 1H)		C14, C17, C22
16				
17	139.5			
18	114.1	7.62(d, 1H, *J* = 8)	H19	C20, C22
19	125.8	7.40 (t, 1H, *J* = 8)	H18	C17
20	124.2	7.35 (t, 1H, *J* = 8)	H21	C18, C22
21	123.4	7.97 (d, 1H, *J* = 8)	H20	C17, C19
22	126.1			

All spectra were recorded in MeOH with reference to TMS. ^{13}C NMR data were obtained at 125 MHz. All ^{1}H NMR experiments were performed at 500 MHz. Coupling constants are presented in Hertz.

Table 5-3. Physical and spectral data of eudisin C (**143**).

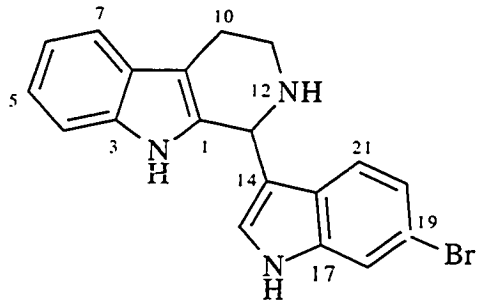

143. eudisin C

Source: *Eudistoma* sp. (WA-92-67)
Exmouth, Western Australia
White amorphous solid
Molecular formula: $C_{19}H_{16}N_3Br$
HRDEIMS: M^+ obsd. *m/z* 365.0533
$C_{19}H_{16}N_3{}^{79}Br$, dev. 1.5 ppm
LRDEIMS: M^+ obsd. *m/z* 367 (15), 365 (17), 338, 286, 256, 197 (93), 195 (100), 169, 143, 116, 89, 84, 63
UV (MeOH) λ_{max}: 280, 225 nm
IR (NaCl) ν_{max}: 3390, 3214, 2925, 2842, 1579, 1450, 1342, 804, 739 cm^{-1}
Specific rotation: $[\alpha]_D = 0°$ (c 0.14, MeOH)

NMR data

No	^{13}C	^{1}H	COSY	HMBC
1	133.5			
2				
3	139.7*			
4	112.7	7.19(bd, 1H, *J* = 8)	H5	
5	120.5	7.03(td, 1H, *J* = 8, 1.5)	H4	
6	123.2	6.99 (td, 1H, *J* = 8, 1.5)	H5	
7	119.4	7.47 (bd, 1H, *J* = 8)	H6	
8	126.9			
9	116.9			
10	22.1	2.87 (m, 1H)	H11	
		2.95 (m, 1H)		
11	43.3	3.14 (m, 1H)	H10	
		3.35 (m, 1H)		
13	51.5	5.57 (s,1H)		C1, C9, C11, C14, C15
14	109.3			
15	128.4	7.18 (s, 1H)		
16				
17	138.5*			
18	116.0	7.62 (d, 1H, *J* = 2)	H20	
19	114.2			
20	124.2	7.01 (dd, 1H, *J* = 8, 2)	H18, H21	
21	121.8	7.14 (d, 1H, *J* = 8)	H20	
22	126.9			

All spectra were recorded in MeOH with reference to TMS. ^{13}C NMR data were obtained at 125 MHz. All ^{1}H NMR experiments were performed at 500 MHz. Coupling constants are presented in Hertz. * Signals may be interchanged.

Figure 5-4. Results of molecular modeling study of two epimers at C13 of **143**.

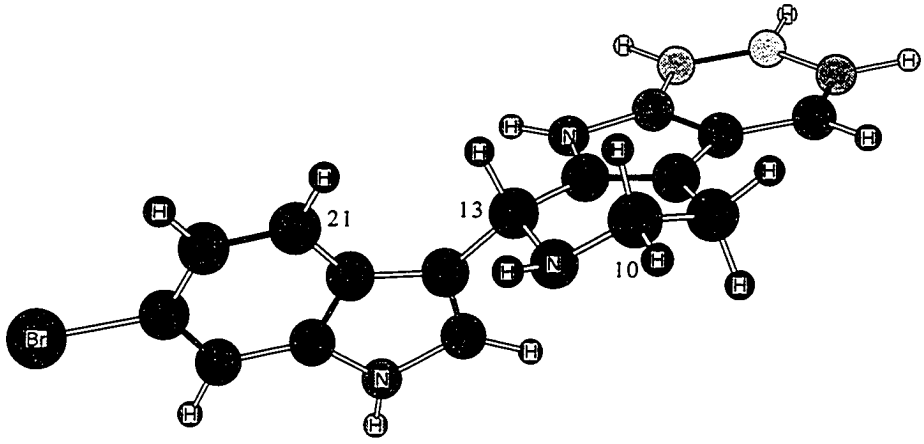

Epimer -I

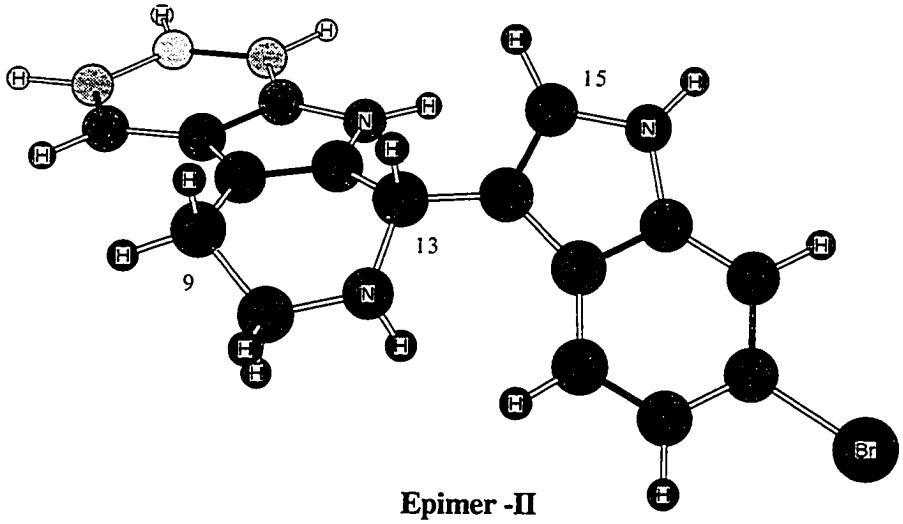

Epimer -II

dehydrogenated to β-carbolines via dihydro-β-carbolines (Slaytor and McFarlane 1968). Numerous β-caroline alkaloids (Adesanya *et al.* 1992, Kobayashi *et al.* 1984, 1990a, Kinzer and Cadellina 1987) were isolated from many ascidians, while only a few tetrahydro-β-carbolines (Rinehart *et al.* 1984, 1987) were identified. However, none of dihydro-β-carbolines were isolated from marine sources to date. In the partially purified fractions of this ascidian in this study, 10,11-dehydroeudisin A was also detected by diode-array HPLC analysis, based on their UV chromophores (λ_{max}: 335 nm). Therefore, it is not unreasonable to presume that biosyntheses of these compounds may follow the track of plant metabolic pathways.

C. Experimental, Chapter V

Collection, Extraction, and Isolation procedure

An unidentified *Eudistoma* sp. was collected by hand using SCUBA (-8 m) from Western Australia in the Indian Ocean in December of 1992. The *Eudistoma* sp. is an orange colored colonial polycitorid. The tunic was soft and gelatinous. The color of this thick encrusting ascidian changed to brown upon the death of the colony.

Specimens of the ascidians were immediately frozen after collection and stored for several months at -40 °C. The sample was lyophilized and extracted twice with 70 % methanol/ dichloromethane. The combined extract was concentrated under vacuum. Solvent partitioning of the crude extract into hexane and methanol and subsequent fractionation of the methanol solubles into ethyl acetate and water were conducted. Size exclusion chromatography on Sephadex LH-20 (MeOH), followed by reversed-phase (C-18) vacuum flash chromatography (MeOH/H_2O) and reversed mode HPLC with an amino colmn (5 % H_2O/ MeOH), yielded eudisins A (**141**, 0.07 % dry wt), B (**142**, 0.02 % dry wt), and semi-pure C (**143**) . The impure eudisin C (**143**) was finally purified by using an NH_2-column (12 % MeOH/ $CHCl_3$) to give pure eudisin C (**143**, 0.02 % dry wt).

Eudisin A (141): an amorphous yellow-green solid; HRFABMS: $(M + H)^+$ obsd. *m/z* 364.0424, $C_{19}H_{15}N_3{}^{79}Br$, dev. -7.0 ppm; IR (NaCl) ν_{max}: 3406, 3157, 1581, 1515, 1442, 1334, 1196, 981, 890, 800, 745 cm^{-1}; UV (MeOH) λ_{max}: 396 (ε 10400), 325 (20700), 290 (17500), 250 (sh), 220 (56600) nm; UV (MeOH + NaOH) λ_{max}: 315 (ε 9020), 292 (7040), 245 (sh), 206 (70000) nm.

Eudisin B (142): an amorphous yellow-green solid; HRFABMS: $(M + H)^+$ obsd. *m/z* 286.1353, $C_{19}H_{16}N_3$, dev. 3.1 ppm; IR (NaCl) ν_{max}: 3387, 3252, 1591, 1538, 1520, 1375, 1261, 1243 cm^{-1}; UV (MeOH) λ_{max}: 397 (ε 9530), 330 (9560), 282 (6010), 274 (6010), 248 (11200), 208 (27800) nm; UV (MeOH + NaOH) λ_{max}: 314 (ε 9340), 243 (sh), 210 (60000) nm.

Eudisin C (143): an amorphous solid; $[\alpha]_D = 0$ °; HRDEIMS: M^+ obsd. *m/z* 365.0533, $C_{19}H_{16}N_3{}^{79}Br$, dev. 1.5 ppm; IR (NaCl) ν_{max}: 3390, 3214, 2925, 2842, 1579, 1450, 1342, 804, 739 cm^{-1}; UV (diode-Array) λ_{max}: 280, 225 nm

Methylation of Eudisin A (141) to yield 361

Excess methyl iodide (1 ml) was added to a stirred solution of **141** (3 mg) and excess potassium carbonate in acetone (5 ml) under nitrogen. The reaction mixture was stirred for 12 hours at room temperature. Upon workup, 1.5 ml of methanol was added and then potassium carbonate was removed by filtration through a sintered-glass filter. The solvent was removed under vacuum. The residue was reconstituted in dichloromethane and the solvent was removed under vacuum. The product, a single compound (**361**), was used for ^{1}H NMR and other spectral analyses without further purification.

Dimethyl eudisin carboxylic acid (361): amorphous solid; LRCIMS: *m/z* 440(29 %), 438 (30), 394 (12), 392 (13), 360 (100), 315 (26), 312 (26); IR (NaCl) IR (NaCl) ν_{max}: 3430, 2925, 2854, 1732, 1604, 1523, 1464, 1366, 1221, 1129, 1078, 899, 819, 747 cm^{-1}; UV (MeOH) λ_{max}: 325 (ε 9868), 274 (11200), 245(sh), 227 (32800) nm; ^{1}H NMR (500 MHz, acetone-d_6): 3.55 (m, 2H), 3.77 (s, 3H), 3.86 (m, 2H), 4.01 (s, 3H), 5.62 (s, 1H), 7.20 (t, 1H, J = 7.8 Hz), 7.38 (t, 1H, J = 7.8), 7.47 (dd, 1H, J =8.3, 2), 7.53 (d, 1H, J = 7.8), 7.84 (d, 1H, J = 8.3), 7.86 (d, 1H, J = 7.8), 8.03 (s, 1H), 8.18 (d, 1H, J = 8.3).

Chapter VI

The Isolation of Kuanoniamine D from an Unidentified Ascidian (WA-90-59)

A. Introduction to Chapter VI

Pyridoacridines are highly condensed polyaromatic alkaloids mainly isolated from sponges and ascidians (Molinski 1993). Compounds of this class have, however, been isolated from the anemone, *Calliactis parastica* (Cimino *et al.* 1987), and the prosobranch mollusc, *Chleynotus semperi* (Carroll and Scheuer 1990).

Structurally, a variety of pyridoacridine carbon skeletons are known from ascidians. They range from simple side chain adducts to highly condensed octacyclic alkaloids. Often the additional ring present was a thiazinone, thiazole, or pyridine derivative.

Although over 30 compounds were isolated from ascidian sources, this class of compound was confined to a few genera of ascidians, such as *Cystodytes, Eudistoma, Didemnum, Diplosoma, Leptoclinides, Lissoclinum, Trididemnum*, and *Amphicarpa*. The ascidian *Cystodytes dellechiajei*, and an unidentified species of *Cystodytes*, were found to synthesize nine tetracyclic alkaloids, cystodytins A-I (**84-92**, Kobayashi *et al.* 1988 and 1991), and pentacyclic compounds, kuanoniamines A-D (**95-98**, Carroll and Scheuer 1990; Gunawardana *et al.* 1992), respectively. Studies of *Eudistoma* species yielded various carbon skeletons in the pyridoacridine class. A tetracyclic alkaloid, norsegoline (**135**), the hexacyclic alkaloids, segolines A-B (**132-133**), isosegoline (**134**), and shermilamine B (**137**), the hepatacyclic alkaloid, eilatin (**136**), and the octacyclic alkaloids, eudistones A-B (**138-139**), were isolated (Rudi *et al.* 1988a-b; Rudi and Kashman 1989; He and Faulkner 1991). A class of closely-related compounds containing a thiomethyl, the varamines A-B (**241-242**) and diplamine (**198**), were identified from two didemnids, L. *vareau* and a *Diplosoma* sp. (Charyulu *et al.* 1989; Molinski and Ireland 1989). Ascididemin (**186**), 11-hydroxyascididemin (**200**), 2-bromoleptoclinidione (**199**), and meridine and another isomer (**310-311**) were ring-fusion products of pyridine derivatives of the pyridoacridine ring system. These compounds were described from two

unidentified species of the genera *Didemnum* and *Leptoclinides* (Kobayashi *et al.* 1988, Bloor and Schmitz 1987, de Guzman and Schmitz 1989, Schmitz *et al.* 1991a-b). Pentacyclic pyridoacridine-thiazinone alkaloids, such as shermilamines A-B (**265**, **137**), were isolated from an unidentified *Tridemnum* species (Cooray *et al.* 1988, Carroll *et al.* 1989).

Cystodytins A-B (**84-85**) were found to be potent Ca^{2+} release agents (Kobayashi *et al.* 1988). Shermilamine B (**137**) and ascididemin (**186**) inhibited Topoisomerase II (Schmitz *et al.* 1991). A Ru (II) complex of 2-bromoleptoclinidione (**199**) intercalated into DNA and induced single strand cleavage of supercoiled pBR322 DNA (Goulle *et al.* 1991). In addition, most pyridoacridines showed *in vitro* cytotoxicity generally against tumor cells.

A chemical investigation, reported here, of an unidentified purple thin encrusting ascidian (WA-90-59) resulted in the isolation of kuanoniamine D (**98**) salt (Figure 6-1) as the major compound. Thymidine and 2'-deoxyuridine were also isolated. The presence of kuanoniamine D (**98**) was determined by mass spectral analysis and 2-dimensional NMR correlation methods.

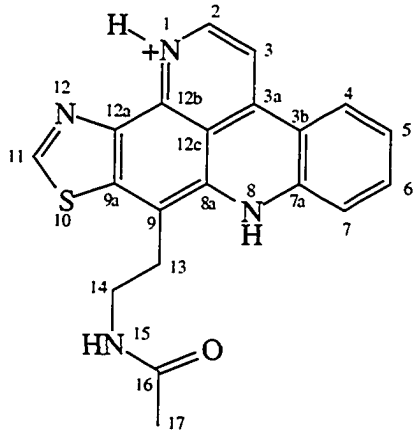

98. kuanoniamine D salt

Figure 6-1. Kuanoniamine D (**98**) salt from an unidentified ascidian.

B. Identification of Kuanoniamine D (98) salt

The major compound was obtained as an pink amorphous solid. The HRFAB mass spectral analysis of the compound exhibited a parent ion (M^+) at m/z 361.1139 which analyzed for $C_{20}H_{17}N_4OS$, in conjugation with ^1H and ^{13}C NMR data (Table 6-1). Since the ^{13}C NMR data were so different from those of most known compounds, extensive 2-dimensional NMR experiments were conducted. This compound was, however, identified as kuanoniamine D (**98**) salt by analysis of its HMQC and HMBC spectra. Complete comparisons of the ^1H and ^{13}C NMR data for **98** in this study with the previously reported values in the literature (Carroll and Scheuer 1990) are presented in Table 6-1.

Table 6-1. Comparison of ^1H and ^{13}C NMR data for **98** from an unidentified ascidian collected in Western Australia with the previously reported values.

	previously reported values[b] (free base)		data from this study (salt)	
No.	^{13}C	^1H	^{13}C	^1H
2	151.0	8.70 (d, 1H, *J* = 5.1)	143.0	8.49 (d, 1H, *J* = 6)
3	108.6	7.73 (d, 1H, *J* = 5.1)	107.7	7.91 (d, 1H, *J* = 6)
3a	139.3		148.9	
3b	115.8		114.3	
4	124.0	8.11 (d, 1H, *J* =8.1)	125.7	8.30[a] (d, 1H, *J* =8)
5	121.1	7.06 (dt, 1H, *J* = 8.1, 3.9)	123.3	7.29[a] (dd, 1H, *J* = 8, 4)
6	131.9	7.45 (dt, 1H, *J* = 8.1, 3.9)	135.0	7.73[a] (d, 1H, *J* = 4)
7	116.3	7.45 (d, 1H, *J* = 3.9)	117.8	7.73[a] (s, 1H)
7a	139.3		140.6	
8		10.15 (s, 1H)		11.6 (s, 1H)
8a	133.5		133.0	
9	104.6		108.4	
9a	139.6		143.3	
11	149.0	9.09 (s, 1H)	152.9	9.44 (s, 1H)
12a	139.9		133.0	
12b	143.6		132.0	
12c	117.7		118.5	
13	31.1	3.07 (t, 2H, *J* = 7.2)	31.0	3.07 (t, 2H, *J* = 6)
14	36.7	3.27 (td, 2H, *J* = 7.2, 5.2)	36.2	3.29 (td, 2H, *J* = 6, 5.5)
15		8.39 (t, 1H, *J* =5.2)		8.44(t, 1H, *J* =5.5)
16	171.0		171.3	
17	22.5	1.87 (s, 3H)	22.4	1.84(s, 3H)

All spectra were recorded in DMSO-d_6 at 500 MHz. The assignment of ^{13}C NMR signals was based on HMQC and HMBC experiments. Chemical shifts are reported in δ units (downfield of TMS). Coupling constants are shown in Hertz. [a] Coupling constants were well observed in the proton spectrum of the salt in MeOH-d_4: δ 8.20 (d, 1H, J = 8 Hz), 7.95 (d, 1H, J = 8), 7.82 (t, 1H, J = 8), and 7.50 (t, 1H, J = 8). [b] NMR data reported by Carroll and Scheuer (1991).

C. Experimental, Chapter VI

Collection and Isolation

Specimens of an unidentified ascidian (WA-90-59) were collected at -7 m depth by using SCUBA at Exmouth in the western Australia in December 1990. The colonies of this ascidian were immediately frozen and preserved at -40 °C. The lyophilized ascidian (80 g) was exhaustively extracted with 70 % methanolic chloroform. The combined extract was concentrated by rotary evaporation and partitioned into hexane, ethyl acetate, n-butanol, and water. Gel filtration of the ethyl acetate soluble compounds with Sephadex LH-20 using methanol as the eluting solvent, followed by HPLC on an amino bonded phase of with 10 % MeOH/$CHCl_3$, yielded 15 mg (0.02 %) of the major compound as well as thymidine and 2'-deoxyuridine.

Kuanoniamine D salt: M+ obsd. *m/z* 361.1139, $C_{20}H_{17}N_4OS$ requires 361.1123, dev. 4.4 ppm; ^1H NMR (500MHz, MeOH-d_4): δ 2.16 (s, 3H), 3.42 (m, 4H), 7.41 (t, 1H, J = 8 Hz), 7.79 (d, 1H, J = 6.5), 7.81 (t, 1H, J = 8), 7.95 (d, 1H, J =8.5), 8.21 (d, 1H, J = 8.5), 8.41 (d, 1H, J = 6.5), 9.13 (s, 1H).

Chapter VII

The Natural Products Chemistry of *Polycarpa clavata* (WA-90-06)

A. Introduction to Chapter VI

Polycarpa clavata is one of the largest ascidians, reaching up to 20 cm high when its long stalk is included. The tunic is thick and leathery. When the animal was dissected, the mantle of the branchial sac inside the tunic was pale orange-colored and the guts was deep orange-colored. Chemical investigations of *Polycarpa* species are very limited. A study of the related ascidian, *P. auzata*, resulted in the isolation of polycarpamines A - E (**330-334**), each of which contained a high percentage of sulfur and novel functional groups (Lindquist and Fenical 1990).

The chemistry of *Polycarpa clavata*, a solitary ascidian living conspicuously on shallow sandy reef flats highly exposed to carnivorous predators, was examined. The specimen was collected just north of twin rocks at approximately 2 km south of Town Beach at Exmouth, Western Australia in December of 1990. This ascidian lives on sand at the collection site. This stalked solitary ascidian is very abundant in Western Australia. The collections of *P. clavata* were frozen immediately and preserved in the freezer at -40 °C until used.

Clavatamine (**335**, Figure 7-1) was extremely difficult to separate from other compounds present in *P. clavata*. The simplicity of its NMR spectra hampered the structural elucidation. After several unsuccessful trials of different chromatogrphic techniques, high speed countercurrent liquid-liquid chromatography was utilized to purify **335**. Clavatamine was identified by combined HRMS, NMR, and molecular modeling experiments.

In addition to a description of the isolation and structural elucidation, this chapter will discuss the significance of these compounds based on their localization with the animal.

Figure 7-1. Clavatamine, Related Compounds, and their Acetylated Derivatives **362-364**.

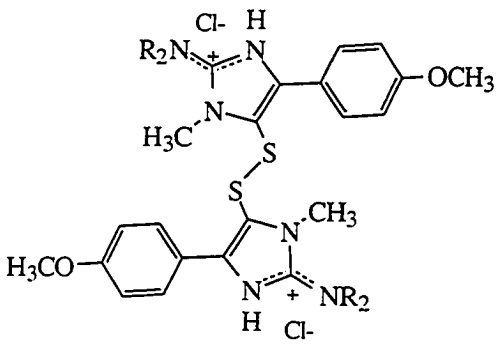

335 R = H
362 R = H, X = OAc

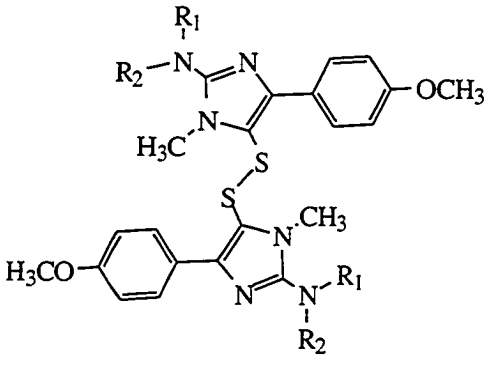

336 $R_1 = R_2 = H$
363 $R_1 = H, R_2 = Ac$
364 $R_1 = R_2 = Ac$

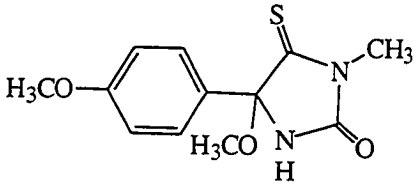

337

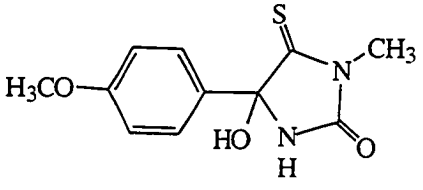

338

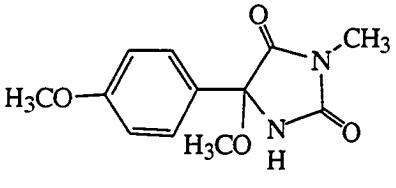

339

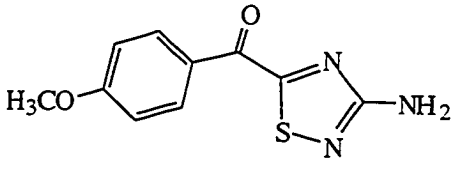

340

B. The Isolation and Structural elucidation of clavatamine (335) and related compounds (336-340)

The freeze-dried animals (1.7 kg, wet weight) were extracted twice with 70 % methanolic methylene chloride. The combined extract was concentrated under vacuum and partitioned into four fractions: hexane, ethyl acetate, n-butanol, and water. Gel-filtration of the n-butanol fraction through Sephadex LH-20, followed by high speed countercurrent chromatography, gave clavatamine (**335**, 0.016 % wet weight) and semi-pure carpaphenol (**365**). The fraction containing **365** (0.002 %) was further purified by using seccessive size exclusion chromatography on Sephadex LH-20 and non-ionic polmeric absorbent XAD-2. The ethyl acetate fraction was subjected to size-exclusion chromatography and reversed-phase HPLC to yield **337** (0.0046 %), **338** (0.0006 %), **339** (0.0008 %), **340** (0.0004 %), and **341** (0.0006 %). A separation scheme, with the same n-butanol fraction, using silica flash chromatography and reversed-phase HPLC, gave **336** (0.0008 %) only.

Clavatamine (**335**) was obtained as an orange crystal (rod, MeOH), mp 201-203 °C. The molecular formula, $C_{22}H_{24}N_6O_2S_2$, established by HRFABMS (M^+ obsd. *m/z* 469.1503, dev. 4.8 ppm), showed 13.5 degrees of unsaturation. Since only 11 carbon signals were observed, there was a symmetry element in the molecule. The high content of nitrogen suggested the presence of guanidinium groups, which was supported by IR absorptions at 3351(NH_2), 2833, 2762, 2704 (NH_2^+, ammonium bands, Nakanishi, 1964), 2390 - 2000 (immonium bands), 1673 (C=N), 1503 (Ar-NH_2), and 1256 (C-N) cm^{-1} (Nakanishi 1962).

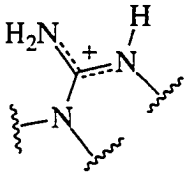

from IR absorption bands
(see text for detail)

The proton NMR spectrum of **335** (methanol-d_4) showed only four signals which were assigned to an O-methyl [δ 3.85 (s, 6H)], an N-methyl [δ 3.16 (s, 6H)], and a para-substituted benzene ring [δ 6.98 (d, 4H, J = 8.5 Hz) and 7.40 (d, 4H, J = 8.5 Hz)] (Table 7-1). The carbon NMR spectrum of **335** supported the presence of the para-substituted benzene ring (δ 113.9, 117.3, 127.4, and 160.3), the O-methyl (δ 55.5), and the N-methyl groups (δ 28.8).

Table 7-1. Physical and spectral properties of clavatamine (**335**).

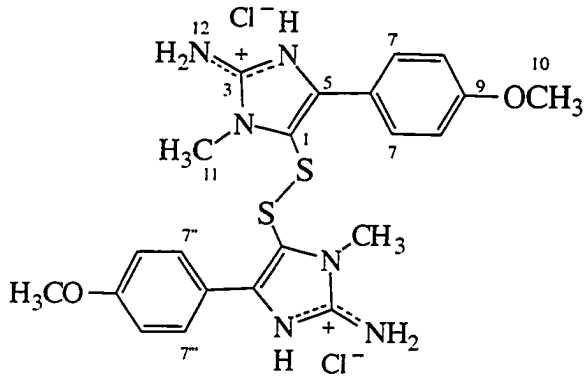

335. clavatamine

Sourece: *Polycarpa clavata*
Exmouth, Western Australia
orange solid, mp 193-195°C
Molecular formula: $C_{22}H_{24}N_6O_2S_2$
HRFABMS: M^+ obsd. *m/z* 469.1503, $C_{22}H_{24}N_6O_2S_2$, dev. 4.8 ppm
LRFABMS: $(M + Na)^+$ obsd. *m/z* 491, $(M+H)^+$ obsd. *m/z* 469, $(1/2\ M + 2H)^+$ obsd m/z 236
UV (MeOH) λ_{max}: 394 (ε 3810), 259 (19400), 202 (28400) nm
IR (NaCl) ν_{max}: 3351, 3267, 3097, 2762, 2704, 2390-2000 (w), 1673, 1606, 1503, 1435, 1292, 1256, 1182, 1023, 987, 834 cm^{-1}

NMR data

No.	^1H[a]	^{13}C[b,c]	HMBC[a] (8 Hz)
1 (1')		108.7	
2 (2')			
3 (3')		147.2	
4 (4')	13.5 (bs, 2H)		
5 (5')		137.1	
6 (6')		117.3	
7 (7', 7", 7"')	7.42 (bd, 4H, *J* = 8.5 Hz)	127.4	C5 (C5'), C7' (C7, C7"', C7"), C9 (C9')
8 (8', 8", 8"')	6.98 (d, 4H, *J* = 8.5 Hz)	113.9	C6 (C6'), C8' (C8, C8"' , C8"), C9 (C9')
9 (9')		160.3	
10 (10')	3.87 (s, 6H)	55.5	C9 (C9')
11 (11')	3.20 (bs, 6H)	28.8	C1 (C1'), C3 (C3')
12 (12')	7.68 (bs, 4H)		

All spectra were recorded in DMSO-d_6. [a] All experiments were performed at 500 MHz. [b] ^{13}C NMR experiments were was recorded at 50 MHz. [c] Assignment of signals was assisted by HMQC experiments.

In the HMBC spectra of **335**, the proton signals at δ 6.98 and 7.42 were coupled to quaternary carbon signals at δ 117.3 and 137.1, respectively, while both protons were correlated to a quaternary carbon signal at δ 160.3. The proton signal at δ 3.87 was also coupled to the quaternary carbon signal at δ 160.3. As a result, the quaternary carbon at δ 137.1 could be assigned to either C5 (C5') or C6 (C6'). The issue, however, was clarified by an nOe enhancement of the proton signal at δ 6.98 upon irradiation of the proton signal at δ 3.87 in the NOEDS experiments. Therefore, the quaternary carbon signal at δ 137.1 was assigned to C5 (C5'). The quaternary carbon signal at δ 160.3 was assigned to C9 (C9'), which was supported by the upfield shift of two adjacent carbon signals at δ 113.9 (**A**). From the HMBC spectra of **335**, the N-methyl protons (δ 3.20) coupled to two quaternary carbon signals at δ 108.7 (C1 and C1') and 147.2 (C3 and C3') (**B**).

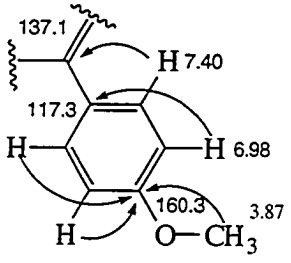

A

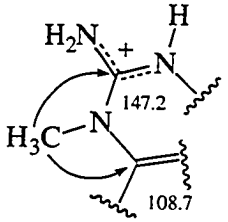

B

Because of the extended conjugation of **335**, indicated by its UV spectrum [(MeOH) λ_{max}: 394 (ε 3810) , 259 (19400), and 202 (28400) nm], two connectivities of C1 (C1')-C5 (C5') and N4 (N4')-C5 (C5') were established (Table 7-1). To meet the molecular formula, a disulfide bridge was connected between C1 and C1'.

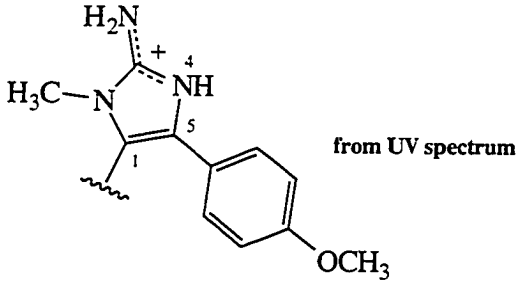

from UV spectrum

There was no model compound for spectral comparison with **335**. However, all lamellarins have an isoquinoline moiety which is similar to part of **335**. Since lamellarin P (**169**) has a fully conjugated system, two carbons (δ 114.2 and 118.3) next to a carbon

resonated at δ 135.9 are very shielded. The similar phenomenon was observed in **335**.

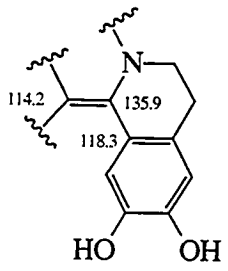

from lamellarin P (169)

The presence of two sulfur atoms was demonstrated by isotope cluster abundance analysis in the LRFAB mass spectrum of **335**. The estimated isotope cluster abundance from the molecular formula of **335** was the following: *m/z* 469 (100 %), 470 (29.1), 471 (13.4), and 472 (3). The actual isotope pattern measured from the LRFAB mass spectrum of **335** completely matched the theoretically calculated isotope distribution for the M^+ ions: *m/z* 469 (100%), 470 (30), 471 (15), and 472 (4). Thus, the presence of the two sulfur atoms in **335** was confirmed.

Electron dispersive spectroscopy (EDS) of clavatamine crystals established the presence of sulfur and chlorine. Therefore, the anions were identified as chlorides.

Raney nickel reduction of clavatamine in methanol was conducted to yield a sulfur-free monomer. The reaction in the refluxed methanol gave several products. Aromatic rings in clavatamine were completely reduced into an aliphatic rings. Several chromatographic methods were, however, failed to purify the products. Another reduction of clavatamine in methanol with Raney-Nickel at room temperature yielded three major products, based on ^1H NMR of the mixture. Once again, separation of those compounds was unsuccessful. In constrast, these compounds had an intact phenol ring.

Clavatamine (**335**) was fully soluble in water. To demonstrate the ionic character of **335**, The chloride ions were replaced by two acetates by treatment with NH_4OH and EtOAc in H_2O. The proton spectrum of the product, **362**, contained an additional signal at δ 2.00 (s, 6H). Once again the IR spectrum of **362** showed ammonium bands at 2833, 2762, and 2704 cm^{-1}. Two additional strong bands at 1558 and 1335 cm^{-1} revealed the presence of the acetate groups (Nakanishi 1962). As expected, the HRFAB mass spectrum of **362** provided the same molecular ion (M^+ obsd. *m/z* 469.1475, $C_{22}H_{25}N_6O_2S_2$, dev. -1.2 ppm).

Computer-assisted molecular modeling experiments with clavatamine, using "pcmodel" from Serena Software, were conducted. Because the charges of clavatamine

made its energy-minimization difficult to converge, a neutral form of clavatamine was used for the modeling study instead. The results showed that the two N-methyl groups were at 2.6 Å to the four protons (which resonated at δ 7.42) of the phenyl rings (Figure 7-2). Irradiation of the aromatic proton signal at δ 7.42 yielded a 1% nOe enhancement of the methyls (δ 3.20). Two parallel planes of phenyl rings were linked through a disulfide bridge, mediated by two coplanar imidazolium groups, of which planes were not parallel to the phenyl rings. The ^{13}C chemical shifts of the imidazolium rings were significantly different from those values reported in other natural products (Palumbo *et al.* 1984, Pathirana and Anderson 1986) since the imidazolium and the phenyl rings presumably form a molecular orbital in one-half of the molecule. In fact, the imidazolium ring is 36 degrees out of the plane of the phenyl ring in one-half of the molecule in an energy-minimized structure. The proposal was also supported by the long wavelength UV absorption of clavatamine indicative of extended conjugation.

The positive charges, stabilized through NH_2-C3 (C3')-N4 (N4') bonds in **335**, were found to be completely delocalized in MeOH-d_4 since there was no broadening of any signals in its proton spectrum. The presence of two exchangeable proton signals at δ 7.68 (s, 4H) and 13.5 (bs, 2H) in the proton spectrum of **335** in DMSO-d_6 supported this proposal and its ionic nature. Acetylation of **335** with Ac_2O/pyridine gave a major product **364**, a tetraacetate [HRFABMS: $(M + H)^+$ obsd. *m/z* 637.1867, $C_{30}H_{33}N_6O_2S_2$, dev. -5.7 ppm]. Presumably, compound **335** was neutralized in pyridine before acetylation by acetic anhydride. Later, upon addition of acetic anhydride, the imines of the imidazole rings might be acetylated first and then the newly generated imine protons (C3=NH) could be acetylated. The broadening of acetamide signal at δ 2.20 (bs, 12H) suggested tautomerization of the acetyl groups. A strong IR (NaCl) absortption at 1734 cm^{-1} indicated that **364** existed as an imide in the solid state (Nakanishi 1962).

Compound **336**, the free base form of clavatamine, was obtained as an orange solid. The proton NMR spectrum of **336** suggested that the molecule was virtually identical with **335** (Table 7-2). This was supported by both the FAB mass spectrum (*m/z* 469), which indicated the same molecular formula as that of **335**, and the UV spectrum of **336** [(MeOH) λ_{max}: 370 (ε 3300) , 260 (13200), 222 (sh), and 202 (31600) nm], which showed the same chromophore that is present in clavatamine. However, there were a few differences between **335** and **336**. The proton NMR spectrum of **335** showed significant broadening of two signals at δ 3.14 (bs, 6H) and 7.37 (bs, 4H). Only seven resonances were observed in the ^{13}C NMR spectrum of **336**. These results suggested that **336** was

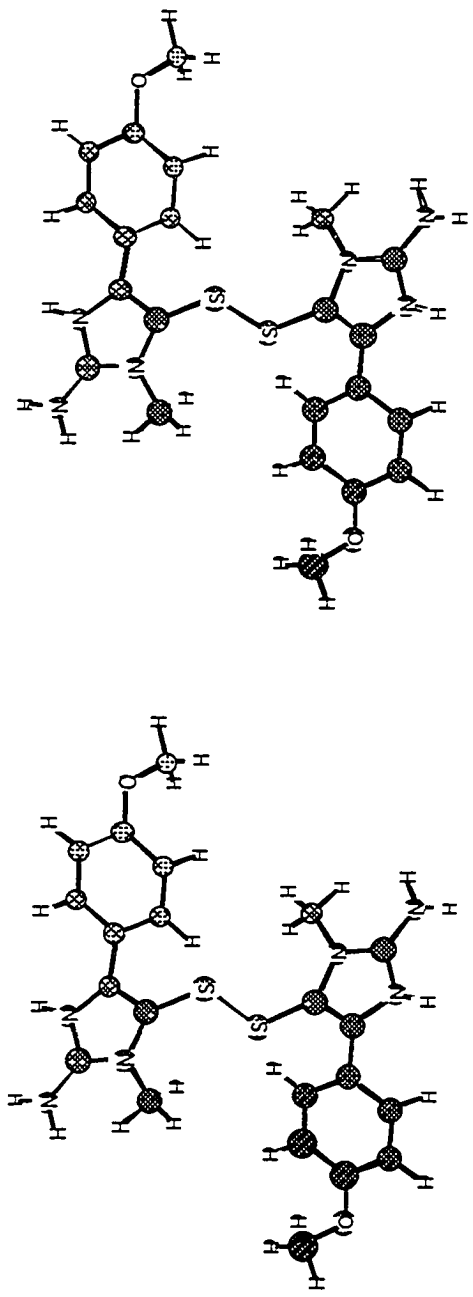

Figure 7-2. An energy-minimized conformer of clavatamine (**335**) in a stereo view. The imidazolium ring and the phenyl ring in half of the molecule were 36 degrees out of the plane to avoid steric hindrance. The protons H7's (δ 7.42) were predicted to be in proximity to N-methyl groups. Energy minimization of **335** was performed using a Serena software, pcmodel, which adopts a MMX force field. The actual presentation of **335** was obtained using a combination of a Chem3D program and a ChemDraw software released from the Cambridge Scientific Computing, Inc.

Table 7-2. Physical and spectral properties of **336**.

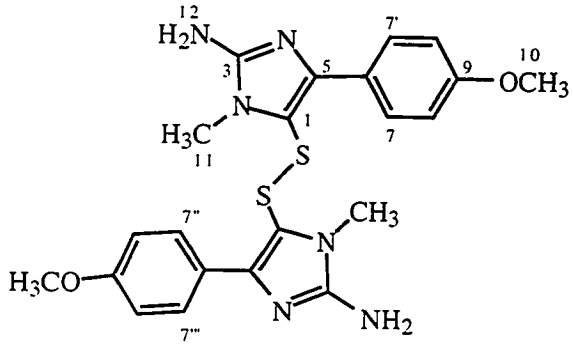

336

Sourece: *Polycarpa clavata*
Exmouth, Western Australia
orange solid
Molecular formula: $C_{22}H_{24}N_6O_2S_2$
HRFABMS (thioglycerol): $(1/2\ M + 2H)^+$
obsd. *m/z* 236.0856, $C_{11}H_{14}N_3OS$,
dev. -0.7 ppm
LRFABMS (glycerol): $(M + H)^+$ obsd.
m/z 469, 437, 236, 204
UV (MeOH) λ_{max}: 370 (ε 3680), 260 (13200), 220 (sh), 202 (35700) nm
IR (NaCl) ν_{max}: 3330, 1663, 1629, 1607, 1549, 1498, 1440, 1411, 1329, 1244, 1174, 1024, 833 cm^{-1}

NMR data

No.	^1H[a]	^{13}C[b]	HMBC[a] (8 Hz)
1 (1')		110.1	
3 (3')		152.3	
4 (4')			
5 (5')		ND	
6 (6')		124.6	
7 (7', 7", 7"')	7.37 (bs, 4H)	129.2	C7' (C7, C7"', C7"), C9 (C9')
8 (8', 8", 8"')	6.86 (d, 4H, *J* = 8.5 Hz)	114.7	C6 (C6'), C8' (C8, C8"' , C8"), C9 (C9')
9 (9')		161.6	
10 (10')	3.83 (s, 6H)	56.3	C9 (C9')
11 (11')	3.14 (bs, 6H)	29.3	C1 (C1'), C3 (C3')

All spectra were recorded in MeOH-d_4. [a] All experiments were performed at 500 MHz. [b] Assignment of signals was based on HMQC and HMBC experiments.

tautomerized rapidly in solution. During long ^{13}C NMR acquisition times, the compound decomposed into several monomeric derivatives. The assignment of ^{13}C NMR data for **336** was futile because its ^{13}C NMR spectrum contained signals from **336** and more than two other decomposion products. Therefore, the ^{13}C signals were assigned solely by using HMBC correlations. Three carbon signals at δ 110.1, 152.3, and 124.6 were assigned to C1 (C1'), C3 (C3'), and C6 (C6'), respectively, based on HMBC correlations (Table 7-2). However, C5 (C5') was not observed due to severe signal broadening of a proton signal at δ 7.37, which was induced by tautomerization of **336**. Mass fragmentation in the LRFAB mass spectrum of **336** is presented in Figure 7-3. The LRFAB mass spectrum of **336**, using a glycerol matrix, showed two base peak ions at m/z 204 and 236, except for the molecular ion at *m/z* 469. The 236 and 204 ions corresponded to $(M/2 + H)^+$ and an ion which lost a sulfur atom from the 236 ion, respectively. The HRFAB mass spectrum of **336**, utilizing a thioglycerol matrix, provided further support for the presence of the disulfide bridge. During the ionization of **336**, the thioglycerol matrix completely reduced the disulfide group into thiols. The highest mass ion observed was therefore at *m/z* 236, which was the base ion peak. The intensity of the ion peak at *m/z* 204 was greatly diminished. Analysis of the HRFAB mass spectrum of **336** gave a partial molecular formula as $C_{11}H_{14}N_3OS$ [$(M/2 + H)^+$ obsd. *m/z* 236.0856 dev. -0.7 ppm]. Irradiation of the proton signal at δ 7.37 of **336** yielded an expected nOe enhancement at δ 3.14.

A bathochromic shift of the UV chromophore (λ_{max} 394 nm) in **335**, in comparison with that (λ_{max} 370 nm) in **336**, was consistent with the fact that **335** is in the ionic form. In the IR spectrum of **336**, the ammonium bands (2833, 2762, and 2704 cm^{-1}) and immonium bands (2390-2000 cm^{-1}) were not observed . Instead, there were two additional absorptions at 1629 and 1549 cm^{-1} due to the tautomerization of **335** between imino- and enamino-forms. Furthermore, the carbon signal at δ 152.3 [C3 (C3')] in **336**, in comparison with that of **335**, shifted downfield since C3 (C3') of **336** was more deshielded than the same carbon of **335**. In clavatamine, electrons of NH_2-C3 (C3')-NH bonds were completely delocalized. However, those bonding electrons of **336** were localized around either the nitrogen N4 or the nitrogen N-C3. The proposed structure was confirmed by conversion of **335** into **336** with silica in chloroform and methanol. Acetylation of compound **336** gave the expected diacetate **361** [HRFABMS: $(M + H)^+$ obsd. *m/z* 553.1700, $C_{26}H_{29}N_6O_4S_2$, dev. -1.5 ppm].

To demonstrate that clavatamine was the natural product, this ascidian was extracted with solely methanol. The proton NMR of crude extract of the branchial sac clearly

Figure 7-3. The mass fragmentation of compound **336**.

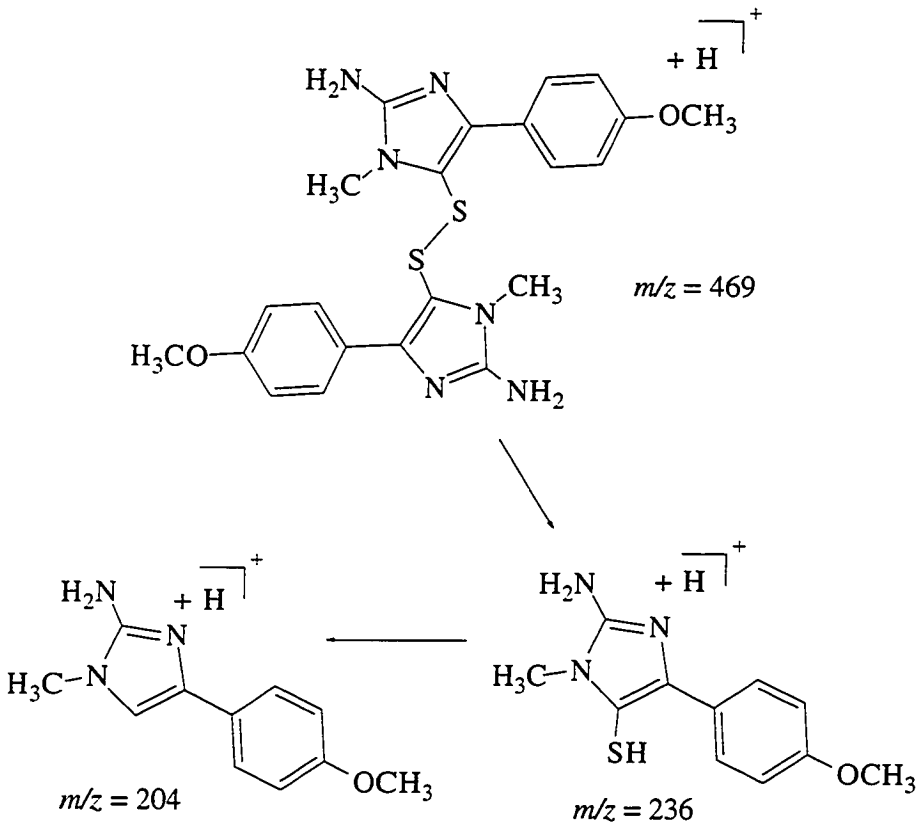

showed that clavatamine was present as a dication with chloride counter ions in this ascidian.

Compound **337** (Table 7-3) was obtained as needles, mp 127-129 °C. A parent ion at *m/z* 267.0821 in the HRFAB mass spectrum of **337** was appropriate for the molecular formula of $C_{12}H_{14}N_2O_3S$ (dev. 6.6 ppm). Strong IR absorptions at 1313 and 1755 cm^{-1}, in conjugation with ^{13}C NMR resonances at δ 202.5 and 155.6, suggested that there were a thioimide and a ureide group. Two methoxys [δ 3.15 (s, 3H) and 3.74 (s, 3H)], a N-methyl [δ 3.19 (s, 3H)], a para-substituted benzene ring [δ 6.91 (d, 2H, J = 8.5 Hz) and 7.38 (d, 2H, J = 8.5 Hz)], and one exchangeable [NH, δ 9.75 (bs, 1H)] were identified from the ^1H NMR spectrum of **337**. The presence of aminal was indicated by a carbon signal at δ 93.6, which was assigned to C5 based on the HMBC correlation of H7 (H7') at δ 7.38 to C5. The position of the exchangeable proton (δ 9.75) was clearly established by HMBC correlations of H11 to C1 and C3. To meet the molecular formula,

Table 7-3. Physical and spectral properties of **337**.

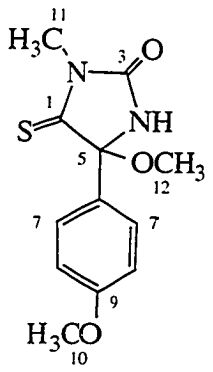

337

Sourece: *Polycarpa clavata*
Exmouth, Western Australia
crystal (needle), mp 127-129 °C
Molecular formula: $C_{12}H_{14}N_2O_3S$
HRFABMS: $(M + H)^+$ obsd. *m/z* 267.0821, $C_{12}H_{15}N_2O_3S$, dev. 6.6 ppm
LRFABMS (+): $(M + H)^+$ obsd. *m/z* 267, 235, 192, 176; **LRFABMS** (-): *m/z* 265, 166
UV (MeOH) λ_{max}: 279 (ε 12800), 222 (14800), 203 (14100) nm
IR (NaCl) ν_{max}: 3287, 1755, 1609, 1511, 1465, 1313, 1252, 1175, 1075, 1027, 835 cm^{-1}
$[\alpha]_D = 0^o$

NMR data

No.	$^1H^a$	$^{13}C^b$	HMBC[a] (8 Hz)
1		202.5	
3		155.6	
4	9.75 (bs, 1H)		
5		93.6	
6		130.0	
7 (7')	7.38 (d, 2H, *J* = 8.5 Hz)	127.6	C5, C7' (C7), C9
8 (8')	6.91 (d, 2H, *J* = 8.5 Hz)	113.4	C6, C8' (C8), C9
9		159.7	
10	3.74 (s, 3H)	55.2	C9
11	3.19 (s, 3H)	28.8	C1, C3
12	3.15 (s, 3H)	49.8	C5

All spectra were recorded in DMSO-d_6. The assignment of signals was based on HMQC and HMBC experiments. [a] All experiments were performed at 500 MHz. [b] ^{13}C NMR experiment was acquired at 125 MHz.

an additional ring must be present.

Compound **338** was obtained as an amorphous solid. The molecular formula, $C_{11}H_{12}N_2O_3S$, established by HRFABMS [$(M + H)^+$ obsd *m/z* 253.0649, $C_{11}H_{13}N_2O_3S$, dev. 0.8 ppm], suggested that **338** is a demethyl derivative of **337**. The UV spectrum [(MeOH) λ_{max}: 202 (ε 9900), 220 (8260), and 278 (7530) nm] and IR spectrum of **338** were almost identical to those of **337**. The proton signal at δ 3.15 in **337** was replaced by a new signal at δ 7.28 in **338**, which was a benzylic alcohol. Compound **338** lost a H_2O molecule readily even in the FAB mass spectrum [$(M - H_2O + H)^+$ obsd. *m/z* 235], which was an indication of the benzyl functional group. All spectral data were fully consistent with the proposed structure (Table 7-4).

Compound **339** was obtained as an amorphous solid. The molecular formula, $C_{12}H_{14}N_2O_4$, indicated that a carbonyl functional group was substituted for the thiocarbonyl group of the compound **337**. An imide and a ureide functionalities were evident from strong IR absorptions at 1783 and 1713 cm^{-1}. Once again the position of an exchangeable proton at N4 (δ 9.32) was clarified by HMBC correlations of H11 to C1 and C3 (Table 7-5). The carbon resonances at δ 169.9 and 154.9 agreed perfectly with the proposed functional groups, such as the imide and the ureide.

Compound **340** (Table 7-6) was obtained as an orange amorphous solid. The molecular formula, $C_{10}H_9N_2O_3S$, was determined by HRDEIMS (M^+, obsd. *m/z* 235.0337, dev. 9.2 ppm). The extended conjugation of **340** was apparent from its UV spectrum [(MeOH) λ_{max}: 320 (ε 9280), 223 (9750), and 200 (44900) nm]. A *p*-methoxy benzoyl group was identified from the proton NMR spectrum of **340** [δ 7.05 (d, 2H, J = 8.5 Hz), 8.56 (d, 2H, J = 8.5 Hz), and 3.91 (s, 3H)]. The downfield shift of a doublet at δ 8.56 indicated the presence of ketone adjacent to the phenyl ring. This was supported by an HMBC correlation of H8 (H8') to a carbon signal at δ 180.9 and a base ion peak at *m/z* 135. 0442($C_8H_7O_2$, dev. -3.0 ppm) in the high resolution desorption electron ionization (HRDEI) mass spectrum of **340**. A guanidine group was suggested by IR absorptions at 3439, 3332, 1646, and 1629 cm^{-1}. Moreover, the HRDEI mass spectrum of **340** provided a mass fragment ion at *m/z* 73.9949 (CH_2N_2S, dev. 11.2 ppm, the only match within 50 ppm), which was a very distinctive daughter ion of 1,2,4-thiadiazole (Porter 1985). Mass fragmentation of **340** in the DEI mass spectrum was fully consistent with the proposed structure (Figure 7-4). One interesting feature of **340** was illuminated by two

Table 7-4. Physical and spectral properties of **338**.

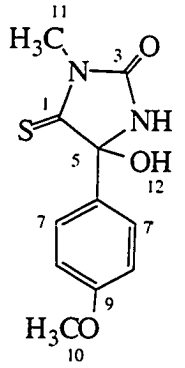

338

Sourece: *Polycarpa clavata*

Exmouth, Western Australia

amorphous solid

Molecular formula: $C_{11}H_{12}N_2O_3S$

HRFABMS: $(M + H)^+$ obsd. *m/z* 253.0649, $C_{11}H_{13}N_2O_3S$, dev. 0.8 ppm

LRFABMS (thioglycerol): obsd. *m/z* 362 $(M + SGLY)^+$, 253, 235; **LRFABMS** (NBA): *m/z* 406 $(M + NBA)^+$, 253, 235

UV (MeOH) λ_{max}: 278 (ε 7530), 220 (8260), 202 (9900) nm

IR (NaCl) ν_{max}: 3285, 1736, 1610, 1511, 1461, 1306, 1249, 1170, 1019 cm^{-1}

$[\alpha]_D = 0°$

NMR data

No.	^1H[a]	^{13}C[b]	HMBC[a] (8 Hz)
1		206.7	
3		155.3	
4	9.60 (bs, 1H)		C1, C3, C5
5		89.5	
6		131.7	
7 (7')	7.36 (d, 2H, *J* = 8.5 Hz)	127.5	C5, C7' (C7), C9
8 (8')	6.89 (d, 2H, *J* = 8.5 Hz)	113.2	C6, C8' (C8), C9
9		159.4	
10	3.73 (s, 3H)	55.1	C9
11	3.16(s, 3H)	28.8	C1, C3
12	7.28 (bs, 1H)		

All spectra were recorded in DMSO-d_6. The assignment of signals was based on HMQC and HMBC experiments. [a] All experiments were performed at 500 MHz. [b] ^{13}C NMR experiment was acquired at 50 MHz.

Table 7-5. Physical and spectral properties of **339**.

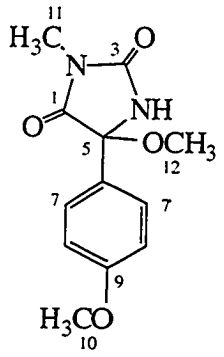

339

Sourece: *Polycarpa clavata*

Exmouth, Western Australia

amorphous solid

Molecular formula: $C_{12}H_{14}N_2O_4$

HRFABMS: $(M + H)^+$ obsd. *m/z* 251.1038, $C_{12}H_{15}N_2O_4$, dev. 2.5 ppm

LRFABMS: obsd. *m/z* 251 $(M + H)^+$, 219

UV (MeOH) λ_{max}: 292 (ε 1560), 277 (1910), 225 (6320), 203 (10200) nm

IR (NaCl) ν_{max}: 3239, 1783, 1713, 1608, 1510, 1452, 1390, 1303, 1249, 1174, 1067, 1026, 995 cm^{-1}

$[\alpha]_D = 0°$

NMR data

No.	^1H[a]	^{13}C[b]	HMBC[a] (8 Hz)
1		169.9	
3		154.9	
4	9.32 (bs, 1H)		C1, C3, C5
5		87.8	
6		126.7	
7 (7')	7.40 (d, 2H, *J* = 8.5 Hz)	127.6	C5, C7' (C7), C9
8 (8')	6.95 (d, 2H, *J* = 8.5 Hz)	113.7	C6, C8' (C8), C9
9		158.8	
10	3.75 (s, 3H)	55.2	C9
11	2.87 (s, 3H)	24.1	C1, C3
12	3.16(s, 3H)	50.7	C5

All spectra were recorded in DMSO-d_6. The assignment of signals was based on HMQC and HMBC experiments. [a] All experiments were performed at 500 MHz. [b] ^{13}C NMR experiment was acquired at 50 MHz.

Table 7-6. Physical and spectral properties of **340**.

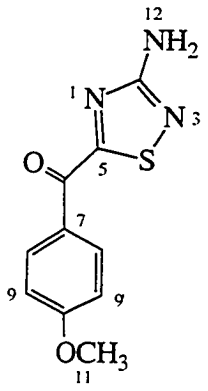

340

Sourece: *Polycarpa clavata*

Exmouth, Western Australia

amorphous orange solid

Molecular formula:

HRDEIMS: M^+ obsd. m/z 235.0337, $C_{10}H_9N_2O_3S$, dev. 9.2 ppm

LRDEIMS: obsd. m/z 237 (2 %), 236 (6), 235 (35), 207, 193, 166, 135 (100), 121, 107, 92, 77, 74, 64, 63, 50

UV (MeOH) λ_{max}: 320 (ε 9280), 223 (9750) 200 (44900) nm

IR (NaCl) ν_{max}: 3439, 3332, 3214, 1738, 1646, 1629, 1589, 1530, 1298, 1266, 1175, 1121, 1018, 873, 856, 838, 758, 738 cm^{-1}

NMR data

No.	^1H[a]	^{13}C[b]	HMBC[a] (8 Hz)
2		171.8	
5		185.4	
6		180.9	
7	7.37 (bs, 4H)	126.6	
8 (8')	8.43 (d, 4H, J = 8.5 Hz)	133.3	C6, C8' (C8), C9' (C9), C10
9 (9')	7.18 (d, 2H, J = 8.5 Hz)	114.3	C7, C9 (C9'), C10
10		164.6	
11	3.91(s, 3H)	55.8	C10
12	7.11 (bs, 2H)		

All spectra were recorded in MeOH-d_4. [a] All experiments were performed at 500 MHz. [b] Assignment of signals was based on HMQC and HMBC experiments.

Figure 7-4. Mass fragments of compound **340** in the HR/LRDEI mass spectra.

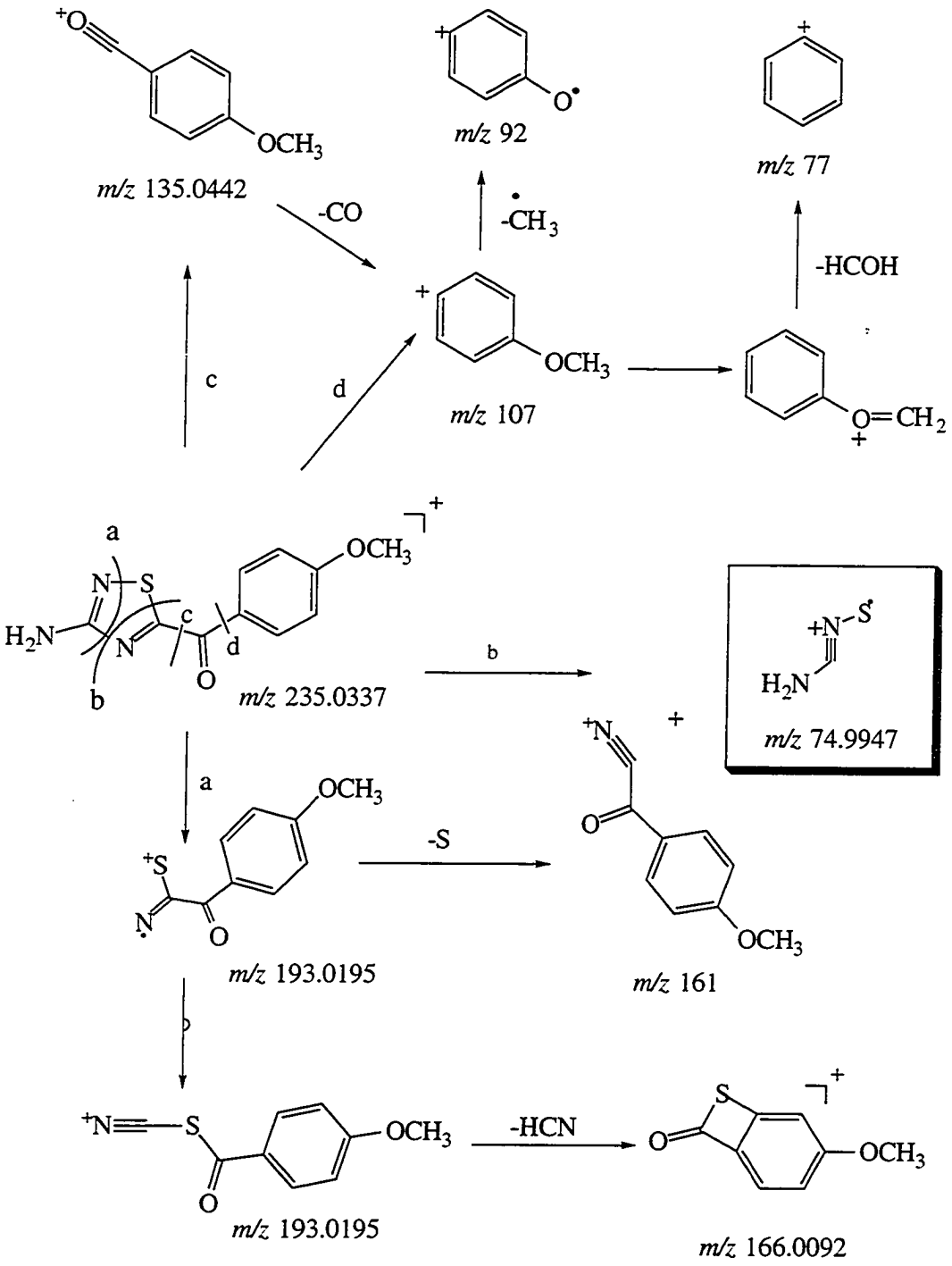

extra signals at 3214 and 1738 cm^{-1} in the IR spectrum. It suggested that the molecule might exist in the solid state as a mixture of imine/enamine. A related compound containing a 1,2,4-thiadiazole, dendrodoine (**318**), was isolated from the tunicate *Dendrodoa grossularia* (Heitz et al. 1980).

Compound **341** was obtained as an amorphous solid. The proton NMR spectrum revealed the presence of a *p*-methoxy benzoyl moiety [δ 3.90 (s, 3H), 7.95 (d, 2H, J = 8.5 Hz), and 7.07 (d, 2H, J = 8.5 Hz)] and a methoxy group [δ 3.94 (s, 3H)]. The assignment was also supported by an HMBC correlation of the proton signal at δ 7.95 and a carbon signal at δ 185.0, and by a mass ion at *m/z* 135 in the LRDEI mass spectrum of **341**. A strong IR absorption at 1672 cm^{-1} suggested a Ar-CO-S-R functionality (Nakanishi 1962). A strong IR absorption at 1731 cm^{-1}, in conjugation with a carbon signal at δ 164.5, suggested the presence of a ureide group. The HMBC spectrum of **341** showed a correlation of the proton signal at δ 3.94 and the carbon signal at δ 164.5. Thus, a methoxy ureide moiety was identified. The methyl group (at δ 3.94, H11) slowly tautomerized from an oxygen to a nitrogen atom (N2) in MeOH-d_4, generating a newly proton signal at δ 3.34 (s, 1H) as well as the proton signal at δ 3.94 (s, 2H) in the proton spectrum of **341**. The proposition was also supported by appearance of a carbon signal at δ 43.8 in MeOH-d_4. However, this carbon signal completely disappeared in the carbon spectrum of **341** in DMSO-d_6. These results yielded two partial subunits **A** and **B**.

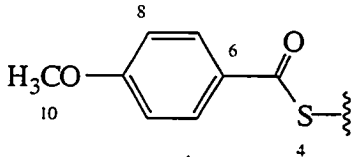

A

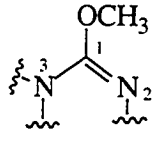

B

The negative LRFAB mass spectrum of **341** showed the molecular ion $(M - H)^-$ at *m/z* 237 (65 %). As a result, the presence of an S-N bond was established. Based on these results, the following structure (**C**) was proposed. The LRDEI mass spectrum of **341** supported the assignment. Mass ions at *m/z* 135 and 103 indicated the presence of *p*-methoxy benzoyl and the rest of structure. Because the carbon signal at δ 185.0 was not appropriate for an amide carbonyl, the alternative (**D**) was rejected. However, the exact mass could not be obtained from the mass spectrum of **341** because the only useful mass reference compound had a peak which coincided with the molecular ion.

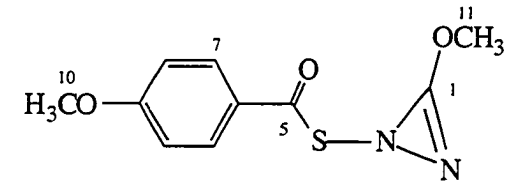

C

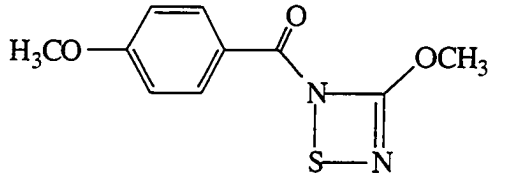

D

An intriguing aspect of compounds **337-339** was that they are racemic. This suggested the possibility that compounds **337-339** could be artifacts produced during extraction or purification steps. To test this hypothesis, the free base **336** was freshly generated by silica flash chromatography of clavatamine and monitored by ^{1}H NMR for several days. After 1 day, two additional monomeric derivatives were already produced *in situ* from **336** in a NMR tube. Another fraction from silica flash chromatography of **335** contained more than 20 decomposed products. Since purification of each compounds was not possible, HMBC experiments were carried out with the former mixture to identify the decomposed products. Indeed, the products had a thiocarbonyl and a ureide functional group which gave ^{13}C signals at δ 209 and 159, obtained in the HMBC spectrum of the mixture. In addition, treatment of clavatamine with mild base (NH_4OH) in a H_2O/MeOH mixture yielded the same results. This phenomenon could be rationalized by acid- or base-catalyzed hydrolysis of guanidine, followed by cleavage of the disulfide bridge, to give several monomeric derivatives upon extraction or isolation. The hypothesis was indirectly supported by the lack of optical activity of compounds **337-339** and relative abundance of each compound [**335** (270 mg), **336**, (13 mg), **337** (78 mg), **338** (10 mg), **339** (13 mg), and **340** (6.8 mg)].

Most of clvatamine was localized in the mantle of the branchial sac and the gut when the frozen ascidian was carefully dissected and different tissues of the ascidian extracted and analyzed (Table 7-7). The concentration of clavatamine in the branchial sac was 24 times higher than that in the tunic. Although the gill structure showed to contain a lower enrichment ratio, this result was attributed to the presence of most ice of this ascidian in this tissue. Thus, the enrichment ratio in the gills could be almost same as that in the

Table 7-7. Analysis of clavatamine in the different tissues of *Polycarpa clavata.*

	tunic	mantle(sac)	gills	guts
wet weight (g)	83.4	6.66	23	15
crude extract (g)	3.66	0.57	0.63	0.29
clavatamine total (mg)	6.2	12.2	3.77	3.85
clavatamine/g of wet tissue (μg)	74	1830	164	257
enrichment ratio	1	24	2.2	3.5

branchial sac.

The mantle (body wall) lines the enveloping tunic. It is composed of two epithelial layers. Between them lies muscular fibers. The musculature comprises smooth muscle and shoes two arrangements: a fine, felt-like coating of short fibers, variously distributed within the mantle, around guts, and elsewhere; and juxtaposed circular and longitudinal bundles of long fibers. Strong sphincters encircle the siphons. Circular muscles wrap the entire body elsewhere. These longitudinal bundles of muscle fibers enable either siphon to close and can contract the body itself either partially or completely (Monniot *et al* 1991). The distribution of clavatamine led to some perpectives about the roles of the compound. An ATP regeneration system, permitting a sudden use of large amounts of energy related with a rapid muscular contraction, is composed of a phosphagen (phosphoguanidine) and its kinases (Lehninger 1982, Watts 1975). The phosphagen kinase catalyses the transfer of a phosphate from ATP to a guanidine group of substrate. The contractile system is capable of break-down ATP to ADP faster than it can be generated by the normal available metabolic pathways. Regeneration of ATP from the phosphagen store bridges the gap until full capacity of normal metabolic pathways, such as glycolysis and citric acid cycle, can be achieved. Ascidians, especially *Polycarpa* spp., have a very powerful muscular system capable of instantaneous contraction of its siphons and the whole body to keep them from clogging or according to environmental disturbance (Kott 1989). The clavatamine may act as a substrate for the phosphagen kinase along with known substrates of the enzyme, such as arginine and creatine which were known from the ascidian, *Styela mammiculata* (Watts 1975).

These compounds may also explain elaboration of sophisticated nature in chemical adaptation. When predators attack the ascidian, the localization of the compound near the tunic may immediately deters the animals, only if the level of clavatamine concentration

observed in the tunic is effective enough. However, since clavatamine is water-soluble, exudation of the compound from the branchial sac can be also possible to deter predators.

These alkaloids (**335-340**) were tested for cytotoxicity against human colon tumor cell line in culture. Clavatamine and its free base (**336**) showed moderate cytoxicities with IC_{50} of 1.9 and 0.9 μg/ml respectively. Compound **336** was a powerful inhibitor (IC_{50} = 15 nM) for the enzyme, inosine monophosphate dehydrogenase, which is essential in the *de novo* synthesis of guanidine nucleotides and present in high level in tumor cells (personal communication).

This work is an interesting example of ascidian chemistry and a nice demonstration of how isolation procedures affect the isolation of secondary metabolites.

Experimental, Chapter VII

Collection, Extraction, and Isolation Procedures.

The solitary ascidian, *Polycarpa clavata*, was collected by hand using SCUBA (-10 m) at Exmouth, Western Australia in the Indian Ocean, in December of 1990. The specimens were immediately frozen after collection. The lyophilized animals (from 1.7 kg frozen animals) were extracted twice with 70% MeOH/CH_2Cl_2. The combined extract was concentrated and partitioned between hexane and methanol. The methanol-soluble material was then partitioned between ethyl acetate and water. The water-solubles were further partitioned between n-butanol and water. Gel-filtration of the n-butanol fraction through Sephadex LH-20 (MeOH/DCM = 1:1), followed by high speed countercurrent chromatography ($CHCl_3$/MeOH/H_2O = 4:4:3), gave a pure compound **335** (270 mg). Succesive size exclusion chromatography on Sephadex LH-20 (MeOH) and chromatography on non-ionic polymeric absorbent, XAD-2 (H_2O/MeOH/Acetone), of the butanol soluble fraction yielded a deep orange alkaloid, carpaphenol **365** (30 mg). Further purification of the alkaloids **337-341** from the ethyl acetate fraction was accomplished by size-exclusion chromatography LH-20 (50 % MeOH/DCM) and reverse-phased HPLC(ODS-silica) with 45 % H_2O/MeOH and 30 % H_2O/MeOH. A separation scheme, with the same n-butanol fraction, using silica flash chromatography (DCM/MeOH gradient) and repeated reverse-phased HPLC(ODS-silica) (20, 25, and 40 % aqueous methanol), gave only compound **336**. Yields of compounds **335-341** were 270 mg (0.016 % wet wt), 13 mg (0.0008%), 78 mg (0.0046 %), 10 mg (0.0006 %), 13 mg (0.0008 %), 6.8 mg (0.0004 %), and 10 mg (0.0006 %), respectively.

Crystalization of clavatamine

Clavatamine (40 mg), isolated by successive size-exclusion chromatography, was dissolved in methanol (10 ml). The solution was transferred in a test tube with an aluminum-foil cover. The solvent was very slowly evaporated in the cold room. Orange crystaline rods were generated after a month. This crystal was used to measure its melting point.

Clavatamine (335): orange crystal (rod from MeOH); mp 201-203 °C; LRFABMS: obsd. *m/z* 491 $(M + Na)^+$, 469 $(M + H)^+$, 437, 236; LRFAMS: Isotope Cluster Abundance: obsd. *m/z* 469 (100%), 470 (30), 471 (15), 472 (4); calc: obsd. *m/z* 469 (100), 470 (29.1), 471 (13.4), 472 (3); HRFABMS: $(M + H)^+$ obsd. *m/z* 469.1475,

$C_{22}H_{25}N_6O_2S_2$, dev. −1.2; UV (MeOH) λ_{max}: 202 (ε 28400), 259 (19400), 394 (3810) nm; UV (MeOH + NaOH) λ_{max}: 203 (ε 42500), 224 (sh), 278 (12400) nm ; UV (MeOH + HCl) λ_{max}: 202 (ε 28200), 255 (21300), 354 (4760) nm; IR (neat, NaCl) ν_{max}: 3351, 3267, 3097, 2833, 2762, 2704, 2390-2000 (w), 1673, 1606, 1503, 1435, 1292, 1256, 1182, 1023, 987, 834 cm^{-1}; NOEDS: 3.87 ppm (irrad.): 6.98 ppm (1 %); 3.20ppm (irrad.): 7.42 ppm (1 %), 7.68 (4.2); ^{13}C NMR (MeOH-d_4): δ 29.9, 56.7, 111.7, 115.9, 129.6, 139.2, 149.1, 163.4.

Compound 336: orange solid; LRFABMS (glycerol): obsd. *m/z* 469 $(M + H)^+$, 437, 236 (100), 204 (98); HRFABMS (thioglycerol): $(M + H)^+$ obsd. *m/z* 236.0856, $C_{11}H_{14}ON_3S$, dev. -0.7 ppm; UV (MeOH) λ_{max}: 202 (ε 31600), 222(sh), 260 (13200), 370 (3680) nm; UV (MeOH + NaOH) λ_{max}: 205 (ε 182000), 280 (11000) nm; UV (MeOH + HCl) λ_{max}: 202 (ε 35700), 222 (sh), 256 (15400), 357 (3300) nm; IR (neat, NaCl) ν_{max}: 3330, 1663, 1629, 1607, 1549, 1498, 1459, 1440, 1411, 1329, 1244, 1174, 1024, 833 cm^{-1}; NOEDS: 7.37 (irrad.): 6.86 (8.9 %), 3.12 (1).

Compound 337: crystal (needle); mp 127-129 °C; $[\alpha]_D$ 0°; LRFABMS (+): obsd. *m/z* 267, 235, 192, 176; LRFABMS (-): obsd. *m/z* 265, 166; HRFABMS: $(M + H)^+$ obsd. *m/z* 267.0821 , $C_{12}H_{15}N_2O_3S$, dev. 6.6 ppm; UV (MeOH) 203 (ε 14100), 222 (14800), 279 (12800) nm; IR (neat, NaCl) ν_{max}: 3287, 1755, 1609, 1511, 1465, 1313, 1252, 1175, 1075, 1027, 832 cm^{-1}.

Compound 338: amorphous solid; $[\alpha]_D$ 0°; LRFABMS (MeOH/SGLY): obsd. *m/z* 362 $(M + SGLY)^+$, 253, 235; LRFABMS (MeOH/NBA): 406 $(M + NBA)^+$, 253, 235; HRFABMS: $(M + H)^+$ obsd. *m/z* 253.0649, $C_{11}H_{13}N_2O_3S$, dev. 0.8 ppm; UV (MeOH) λ_{max}: 202 (ε 9900), 220 (8260), 278 (7530) nm; IR (neat, NaCl) ν_{max}: 3285, 1736, 1610, 1511, 1461, 1306, 1249, 1170, 1019 cm^{-1}.

Compound 339: amorphous solid; $[\alpha]_D$ 0°; LRFABMS: obsd. *m/z* 251, 219; HRFABMS $(M + H)^+$ obsd. *m/z* 251.1038, $C_{12}H_{15}N_2O_4$, dev. 2.5 ppm; UV (MeOH) λ_{max}: 203 (ε 10200), 225 (6230), 277 (1910), 292 (1560) nm; IR (neat, NaCl) ν_{max}: 3239, 1783, 1713, 1608, 1510, 1452, 1390, 1303, 1249, 1174, 1067, 1026, 995 cm^{-1}.

Compound 340: amorphous orange solid; LRDEI obsd. *m/z* 237 (2 %), 236 (6), 235 (35), 207, 193, 166, 161, 135 (100), 121, 107, 92, 77, 74, 64, 63, 50; Isotope cluster

distribution: theoretical *m/z* 235 (100 %), 236 (13.4), 237 (5.7); obsd. *m/z* 235 (100), 236 (18), 237 (7); HRDEI: M^+ obsd. *m/z* 235. 0337, $C_{10}H_9N_2O_3S$, dev.9.2 ppm; *m/z* 207.0453, $C_9H_9N_3OS$, dev. -6.3; *m/z* 193.0195, $C_9H_7NO_2S$, dev. −1.3; *m/z* 166.0092, $C_8H_6O_2S$, dev. 2.1; *m/z* 135. 0442, $C_8H_7O_2$, dev. -3.0; *m/z* 73.9947, CH_2N_2S, dev. 11.2; UV (MeOH) λ_{max}: 200 (ε 44900), 223 (9750), 320 (9280) nm; IR neat, NaCl) ν_{max}: 3439, 3332, 1738, 1646, 1629, 1589, 1530, 1298, 1266, 1175, 1121, 1018, 873, 856, 838, 758, 738 cm^{-1}.

Compound 341: amorphous solid; LRFABMS (-): $(M - H)^-$ obsd. *m/z* 237 (65 %); LRDEIMS: *m/z* 236, 218, 217, 203, 144, 135, 134, 133, 107, 103, 92, 90, 77, 63, 55; UV (MeOH) λ_{max}: 288 (ε 15700), 234 (9140), 200 (14900) nm; IR (NaCl) ν_{max}: 1731, 1672, 1600, 1508, 1395, 1268, 1220, 1164, 1025, 845 cm^{-1}; ^1H NMR (500 MHz, MeOH-d_4): δ 3.90 (s, 3H), 3.94 (s, 3H), 7.07 (d, 2H, *J* = 8.5 Hz), 7.95 (d, 2H, *J* = 8.5 Hz); 3.34 (s, 1H), 3.90 (s, 3H), 3.94 (s, 2H), 7.07 (d, 2H, *J* = 8.5 Hz), 7.95 (d, 2H, *J* = 8.5 Hz); ^1H NMR (500 MHz, DMSO-d_6): δ 3.88 (s, 3H, H11), 3.92 (s, 3H, H10), 7.13 (d, 2H, *J* = 8 Hz, H8/8'), 7.93 (d, 2H, *J* = 8 Hz, H7/7'); ^{13}C NMR (125 MHz, DMSO-d_6): δ 185.0 (C5), 165.0 (C9), 164.5 (C1), 132.2 (2C, C7/7'), 124.5 (C6), 114.7 (2C, C8/8'), 55.9 (C10), 52.8 (C11).

carpaphenol 365: red amorphous solid; LRFABMS (+): *m/z* 419, 397, 379; UV (MeOH) λ_{max}: 468 (ε 4330), 345 (5550), 276 (13900), 205 (32500) nm; UV (MeOH + NaOH) λ_{max}: 507 (ε 3780), 362 (6050), 289 (11800), 203 (45300) nm; IR (NaCl) ν_{max}: 3345, 3172, 2760, 2350-2000 (w), 1689, 1630, 1570, 1438, 1347, 1291, 1198, 1136, 1003, 989 cm^{-1}; EDS (crystal): S and Cl; ^1H NMR (500 MHz, DMSO-d_6 + trace TFA): δ 6.10 (dd, 1H, J =8, 2 Hz), 6.30 (s, 1H), 6.60 (d, 1H, J = 8), 7.00 (s, 1H), 7.38 (s, 1H), 7.50 (bs, 2H), 9.00 (s, 1H), 9.10 (bs, 2H), 9.30 (s, 1H), 9.80 (bs, 1H), 10.6 (s, 1H); ^{13}C NMR (125 MHz, DMSO-d_6): δ 77.2, 111.5, 112.1, 114.2, 114.5, 115.0, 115.4, 118.3, 132.0, 134.4, 144.7, 144.9, 145.1, 146.5, 158.2, 159.9, 169.6, 179.7.

Preparation of 362

NH_4OH (0.3 ml) was added to a solution of **335** (7 mg) in water (15 ml), and immediately the solution was extracted with EtOAc (20 ml) three times. The solvent was evaporated under vacuum. The product **362** was used for ^1H NMR spectral analysis without further purification.

Compound 362: orange solid; HRFABMS: M^+ obsd. *m/z* 469.1475, $C_{22}H_{25}N_6O_2S_2$, dev.-1.2 ppm; IR (NaCl) ν_{max}: 3312, 3124, 2840, 2787, 2702, 1673, 1607, 1558, 1504, 1415, 1335, 1251, 1179, 1026, 833 cm^{-1}; ^1H NMR (200 MHz, MeOH-d_4): δ 2.00 (s, 6H), 3.14 (bs, 6H), 3.85 (s, 6H), 6.87 (d, 4H, J = 8.5 Hz), 7.37 (bd, 4H, J = 8.5 Hz); ^{13}C NMR (50 MHz, MeOH-d_4): δ 22.7, 29.3, 56.3, 115.0, 129.7, 162.1.

In situ generation of monomeric derivatives

NH_4OH (0.3 ml) was added to a solution of **335** (15 mg) in aqueous methanol (3 ml H_2O/10 ml MeOH). After 10 minutes, solvent was evaporated under vacuum using n-butanol to produce an azotrophe. The residue then was dissolved in methanol and used for ^1H NMR spectral analysis without further purification.

Preparation of Acetates 363 and 364

In a typical procedure, acetic anhydride (0.5 mL) was added to a solution of **335** (50 mg) in pyridine and stirred for 12 hours at room temperature. The reaction was monitored by TLC. Reagents were evaporated under high vacuum and partitioned sequentially between ethyl acetate and ice water, between ethyl acetate and 0.1 N $NaHCO_3$ solution, and between ethyl acetate and brine. Finally, the product was dried with $MgSO_4$ and filtered. The solvent was evaporated under vacuum, and residue was purified by reverse-phased HPLC (ODS-silica) using 37 % aqueous acetonitrile to give the tetraacetate **364** (7 mg) as a orange powder.

Compound 363: HRFABMS: $(M + H)^+$ obsd. *m/z* 553.1700, $C_{26}H_{29}N_6O_4S_2$, dev. -1.5 ppm; ^1H NMR ($CDCl_3$ with a few drops of MeOH-d_4): δ 2.20 (s, 6H), 3.20 (bs, 6H), 3.85 (s, 6H), 6.90 (d, 4H, J = 8.5 Hz), 7.65 (bs, 4H).

Compound 364: orange solid; mp 193-195 °C; LRFABMS: obsd. *m/z* 637, 595, 553, 522, 319, 276, 234, 192; HRFABMS: $(M + H)^+$ obsd. *m/z* 637.1867, $C_{30}H_{33}N_6O_2S_2$, dev. -5.7 ppm; UV (CH_2Cl_2) λ_{max}: 250 (ε 33000), 360 (9600) nm; IR (neat, NaCl) ν_{max}: 1734, 1611, 1496, 1367, 1249, 1224, 1201, 1176, 1031, 837 cm^{-1}; ^1H NMR ($CDCl_3$): δ 2.20 (bs, 12H), 3.32 (s, 6H), 3.83 (s, 6H), 6.88 (d, 4H, J = 8Hz), 7.95 (d, 4H, J = 8Hz); ^{13}C NMR ($CDCl_3$): δ 25.7, 30.4, 55.3, 113.9, 117.6, 125.3, 128.8, 141.9, 146.9, 159.9, 171.7; NOEDS: δ 7.95 (irrad.): δ 6.88 (12.9 %), 3.83 (~ 3), 3.32 (1).

Conversion of clavatamine (335) into free base (336)

Chromatographic grade silica gel, (mesh), was added into methanol solution (25 ml) of clavatamine (**335**, 11 mg). The solvent was next removed under vacumm. The remaining silica phase was loaded on a silica column (3.2 X 7.5 cm), and solvents [dichloromethane (60 ml), 20 % methanolic dichloromethane (100 ml), and 60 % methanolic dichloromethane (100 ml)] used to elute an orange band. The orange fractions were combined and the solvent evaporated under vacuum to give a clean product (11 mg), identical in all aspects with **336**

Analysis of clavatamine in the different tissues.

The frozen ascidian, *Polycarpa clavata*, was carefully dissected with a scalpel. The wet tissue were extracted with methanol once. The presence of clavatamine was monitored by TLC on silica plate (20 % MeOH/DCM). Each crude extract was quantitatively diluted with MeOH/H_2O in sequential manner. The quantitative analysis of clavatamine was performed with diode-array reversed-phase HPLC (ODS-silica) by using gradient elution of 50 % MeCN/H_2O to 100 MeCN within 20 minutes. The absolute concentration was obtained from the standard curve which was obtained by using standard solutions.

To demonstrate that clavatamine was the natural product, crude extract of the branchial sac was examined by ^1H NMR in MeOH-d_4.

Chapter VIII

Summary

Natural products chemistry is a multidisciplinary science which adopts ecology, pharmacology, separation science, spectroscopy, and synthetic chemistry. The characterization of compounds provides a basis for several sciences. The natural products themselves are often synthetic and biosynthetic targets. Still, medicinal and pharmaceutical sciences heavily depend on natural products for lead compounds to design new drugs. Natural products chemistry often leads to new reactions and molecular probes for biological studies. Contemporary collaborations, which center increasingly on molecules rather than systems, yield data for chemosystematic and ecological studies. In the current organic chemical literature, the prominence of ideas associated with conformation analysis is very striking. Sometimes, the structure of a molecule in solution is very different from that of crystal. The study is normally guided by NMR spectroscopy and molecular modeling. It must still be emphasized that these studies are initiated by the discovery of biologically and structurally interesting natural products. In marine natural products chemistry, the isolation of new marine secondary metabolites illustrates novel aspects of marine metabolism. First of all, in numerous instances novel skeletons of natural products are encountered which are of great biogenetic interest and which have not yet been found in terrestrial systems. The second feature of marine natural products chemistry is that the biosynthetic studies are just beginning to be performed. This is not only due to the complications associated with radioactive precursor incorporation, but also because it is frequently obscure where and by whom the natural product is biosynthesized. Most invertebrates (especially those of the benthos) are filter-feeders, and many have associated some microorganisms. Therefore, secondary metabolites may be produced by microbial symbionts, or derived from exogenous dietary sources.

Marine ascidians are a genetically-distinct group of invertebrates in marine environments. They are sedentary filter-feeders and often called sea-quirts. Ascidians are chordates because they possess a notocord and pharyngeal clefts in their larval stage. Ascidians possess the tunic. The tunic that envelops the ascidian body is composed mainly

of sulfated glycans. Ascidians are divided into three Orders depending upon the structure of the adult's branchial sac and the relative position of their gonads and gut-loop to the branchial sac. These animals are known to bind environmental iodine and to accumulate iron and vanadium at extremely high levels. Normally the gradient between ascidians and seawater is 10^6 to 10^7. In the field of marine natural products chemistry, ascidians are broadly divided into two groups: solitary and colonial ascidians, although that notation is not consistent with classical systematics. In between these two groups, compound ascidians lie. In the colonial organization, groups of zooids share a common cloacal chamber while retaining their individual oral siphons. In the compound ascidians, each zooid is independent but stalks are in common.

Prior researches demonstrated the importance of secondary metabolites in the survival of ascidians in the sense of chemical defense. Although almost 400 secondary metabolites were isolated from ascidians, most of them were relatively non-polar compounds. Furthermore, the aquatic environment implicates the significance of hydrophilic molecules in defensive adaptations. Therefore, the main objective of this research was to investigate biosynthetic diversity and limitation of ascidian secondary metabolism with emphasis of identification of hydrophilic bioactive molecules and unprecedented carbon skeletons. In this way, a broader understanding of ascidian secondary metabolism, and a chemical data base for studies of chemical ecology, could be established.

For this research, 220 collections of ascidians were made from the Exmouth region in Western Australia in 1990 and 1992. Among them, 15 projects were selected on the basis of TLC analysis (100 % CH_2Cl_2, 5-20 % MeOH/ CH_2Cl_2), ^1H NMR analysis, and biotesting.

Structural elucidation was conducted using a combination of chemical and spectral methods: various methods of mass spectrometry (MS), infrared (IR), ultraviolet and visible (UV-Vis), and proton and carbon nuclear magnetic resonance (NMR) spectroscopy. Most of structural information was, however, obtained from 2-dimensional NMR experiments.

In total, 25 new secondary metabolites in 11 different structural classes were isolated, including 8 new carbon skeletons. In addition, 13 previously reported compounds were also isolated. All of the compounds isolated from this study are listed in

Figure 8-1.

Aplidiamines (**1-2**) were isolated from an unidentified ascidian, an *Aplidiopsis* sp. These compounds were the first examples of zwitterion compounds ever isolated from an ascidian source.

The eudisin class compounds (**141-142**) are very interesting in terms of their biosynthesis. They are the first example of dihydro-β-carbolines from marine sources. The isolation of the compounds implicated that biosynthetic route of β-carbolines in ascidians may follow similar plant metabolic pathways.

The chemical investigation of a brown *Didemnum* sp. gave two new compounds (**194-195**). The isolation of these compounds along with two known compounds, enterocin and deoxyenterocin (**192-193**) isolated originally from cultures of soil bacteria, suggested a microbial origin of these metabolites. In fact, one of these compounds (deoxyenterocin) was also isolated from a marine bacterium, PG-19. The presence of massive number of hook-shaped bacteria in the tissue of this ascidian supported this hypothesis. Chemical investigation of nine microbial isolates from this ascidian was conducted. However, none of them produced enterocin or related compounds. Alternatively, the symbionts of this ascidian might not have been isolated. It would not be uncommon for symbionts to require specialized media and conditions which were not met in this research. Or, the culture media changed the characteristic of the symbionts because of highly nutrient-rich environment. Although chemical investigation of these microorganisms in culture did not yield any enterocin class compounds, this research has demonstrated an interesting possibility of the microbial origin of these enterocin derivatives.

From a purple *Didemnum* ascidian, 13 phenolic compounds, including 3 previously reported molecules, were isolated in five different classes, three of which were new carbon skeletons. The smallest molecule, ningalactone (**176**), had eighteen carbons and the largest one, ningalone (**179**), had forty carbons. The average number of unsaturation was 20. The increase of unsaturation number was also reflected in their color and UV chromophores. The bathochromic shifts in the UV spectra and 7 or 8 carbon unit difference implicated the potential DOPA-addition. One of the interesting features of these molecules is the fact that all of alkaloids suffer severe steric hindrance leading to the restricted rotation of the catechol rings. To help me understand that process, I utilized a molecular modeling program, called "pcmodel", to investigate the most stable conformations of these alkaloids. In ningalactone and ningalone, the two disubstituted catechol rings lie out of the plane in order to avoid steric clouding. Also in ningalin,

Figure 8-1. Secondary metabolites isolated from ascidians in this study.

Class I

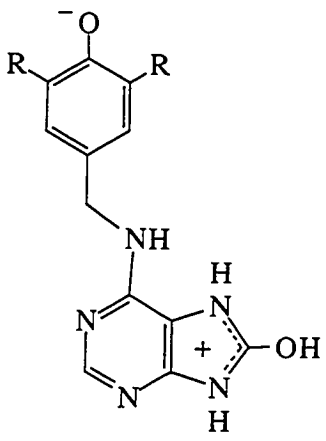

1. aplidiamine A R = Br
2. aplidiamine B R = H

Class II

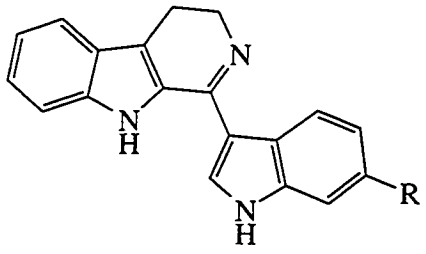

141. eudisin A R = Br
142. eudisin B R = H

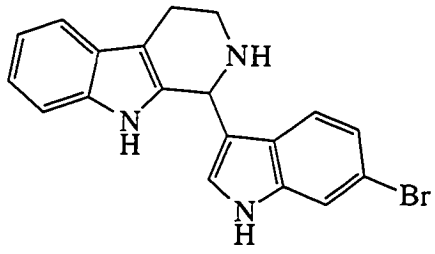

143. eudisin C

Class III

195. didemnocin B

R = 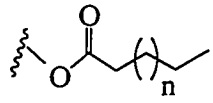 n = 18

194. didemnocin A

R = 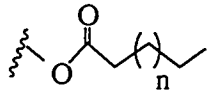 n = 16

192. deoxyenterocin R = H (known)
193. enterocin R = OH (known)

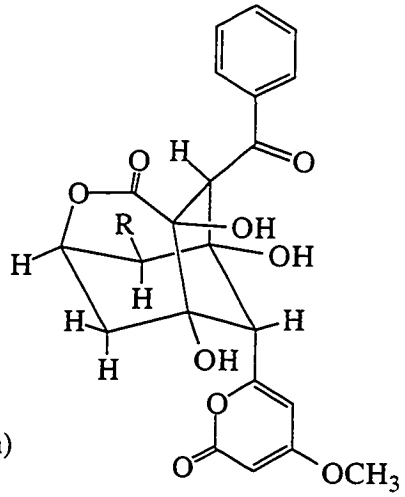

Figure 8-1. (continued)

Class IV

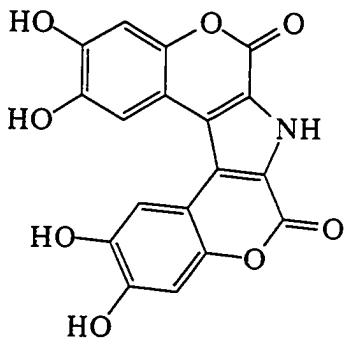

176. ningalactone

Class V

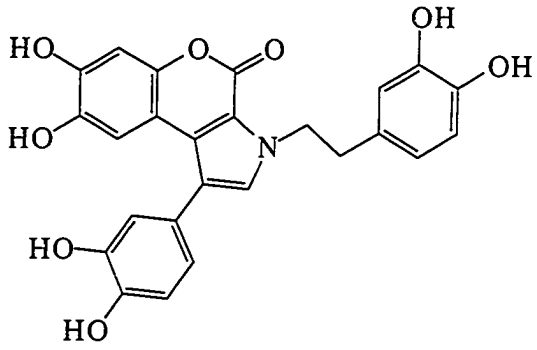

177. ningalin

Class VI

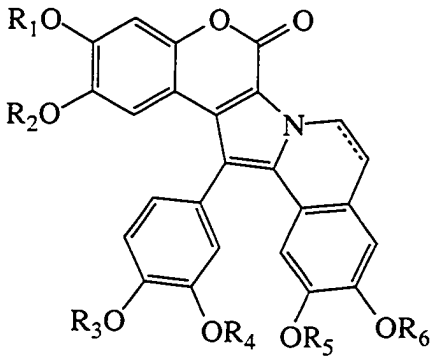

168-173. lamellarins O-T

168. $R_1 = R_2 = R_3 = R_4 = R_5 = R_6 = H$
169. $R_1 = R_2 = R_4 = R_5 = R_6 = H$, $R_3 = Me$
170. $R_1 = Me$, $R_2 = R_3 = R_4 = R_5 = R_6 = H$
171. $R_1 = R_2 = R_4 = R_6 = H$, $R_3 = R_5 = Me$
172. $R_1 = R_3 = Me$, $R_2 = R_4 = R_5 = R_6 = H$
173. $R_1 = R_5 = Me$, $R_2 = R_3 = R_4 = R_6 = H$

160-161, 165. lamellarins G-H, L (previously described)

160. $R_1 = R_3 = R_5 = Me$, $R_2 = R_4 = R_6 = H$
165. $R_2 = R_3 = R_5 = Me$, $R_1 = R_4 = R_6 = H$
161. $R_1 = R_2 = R_3 = R_4 = R_5 = R_6 = H$, $\Delta = 1$

Figure 8-1. (continued)

Class VII

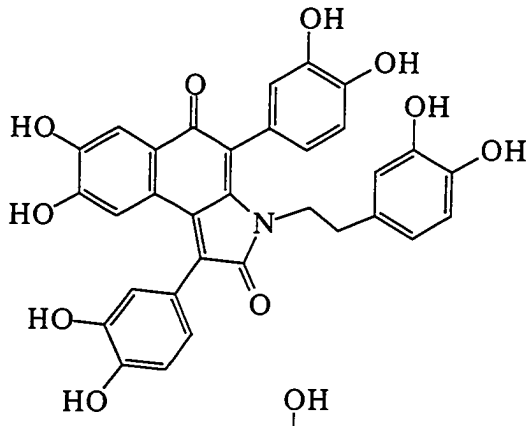

178. ningalamide

Class VIII

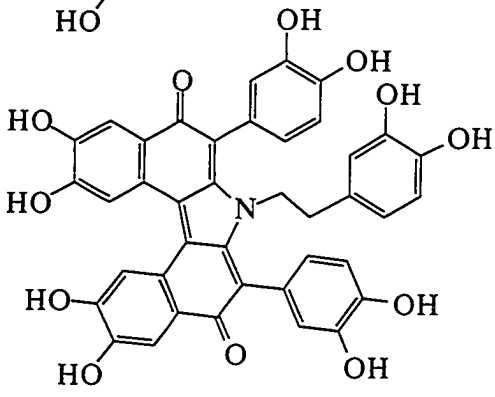

179. ningalone

Class IX

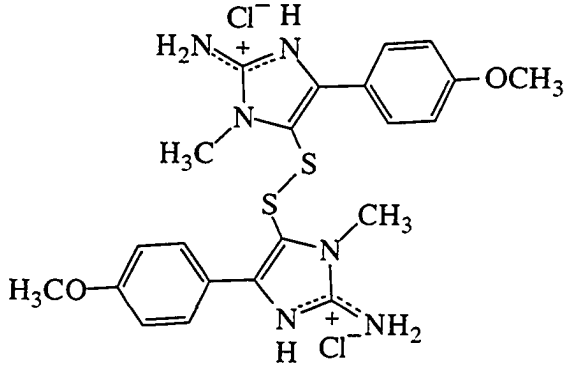

335. clavatamine

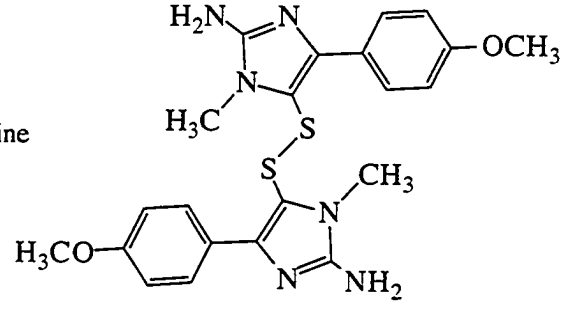

336. free base of clavatamine

Figure 8-1. (continued)

Class Xa

337. clavatamine monomer

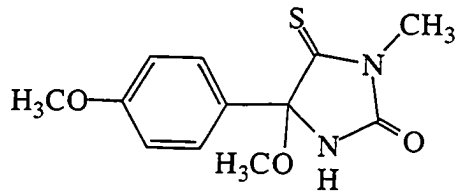

338. clavatamine monomer

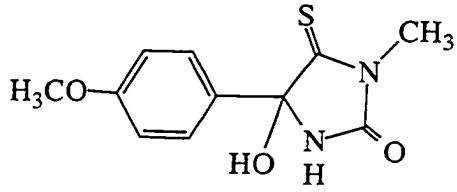

339. clavatamine monomer

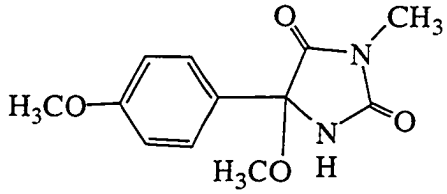

Class Xb

340.

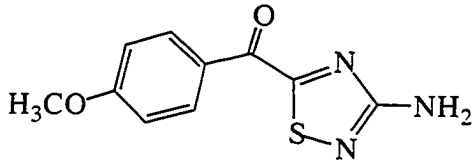

341.

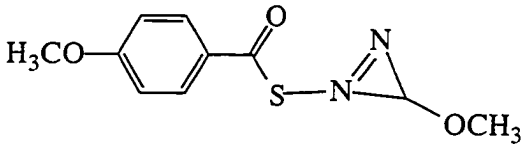

Class XI (tentatively assigned)

364. carpaphenol

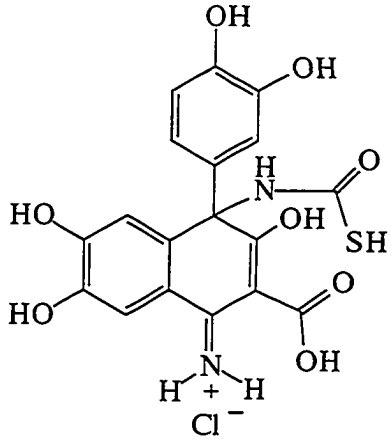

Figure 8-1. (continued)

Known compounds

66. tambjamine F

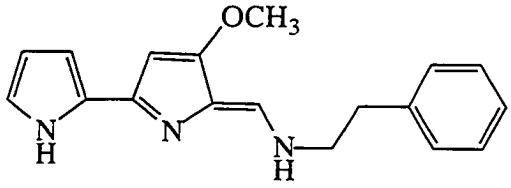

68. tetrapyrrole

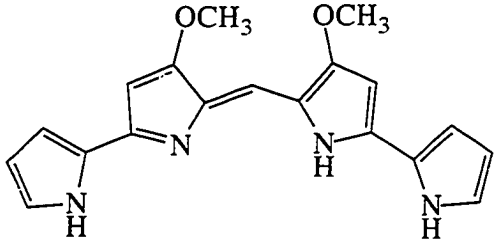

98. kuanoniamine D salt

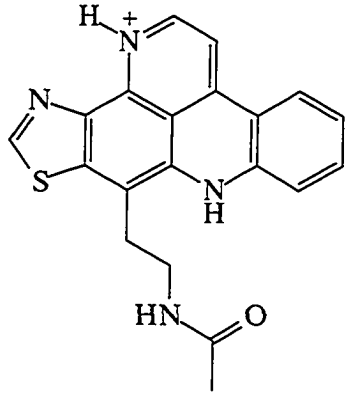

187.

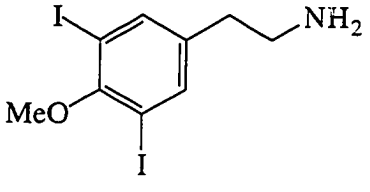

Figure 8-1. (continued)

Known compounds

247-248.

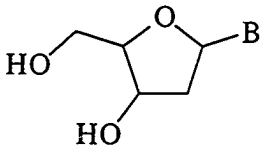

B =

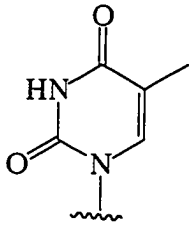

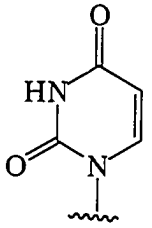

348. 6-bromoindole-3carboxylic acid

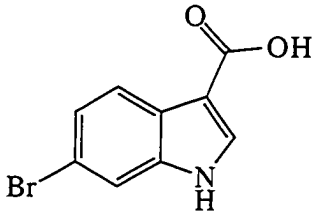

349. methyl (4-hydroxyphenyl) acetate

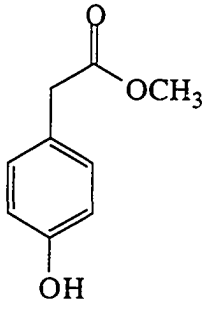

lamellarins, ningalamide, and ningalone, all of the momo-substituted catechol rings, by calculations, are predicted to be at almost 90 degree of the basic skeleton of molecule. NMR analysis using NOESY experiments also illustrated these features. Based on these results, the compounds may be chiral by virtue of restricted rotation and conformation effect. However, none of them were optically active. A remarkable feature of ningalamide and ningalone were the ^1H NMR shielding effects of the phenyl rings. The protons of the dopamine moiety of ningalamide and ningalone were significantly shielded. For example, the signal of protons next to the nitrogen appeared 1.3 and 1.6 ppm upfield compared with the same proton signal in ningalin. What's the potential role of these alkaloids? First of all, they can be considered in terms of metal sequestration, especially iron. In the didemnid ascidians, vanadium accumulation is negligible but iron accumulation is extremely high upto 10^7. Since iron is known to chelate with catechols, these compounds may have a suggestive role in the iron accumulation. The other one could be their involvement in tunic formation. All of these compounds have elements for tanning which is common in insects. One exception could be "space filling" mechanisms. In this sense, a completely different mechanism was proposed based on possible their biosynthesis. Judging by their structures, all of theses alkaloids appeared to be condensation products of DOPA derived from amino acid tyrosine in various reasonable manners. If the same manner of addition were continued, heptomer and nanomer could be possible. By ^1H NMR analysis of a semi-purified fraction, the presence of heptomer was proposed. Another feature of condensation is the formation of helical polymers. Because of the steric hindrance the polymer can not be planar. Therefore, the polymer has to be twisted helical-shaped. This may be a novel mechanism of biopolymerization in ascidians.

Over the past decades, rapid developments of separation methods have been achieved. The choice of method totally depends on the solubility and polarity of the natural product. Clavatamine (**335**) is a good example of how isolation methods affects the nature of natural products in marine natural products chemistry. Even with the technological advance of chromatography, a mistake in the selection of separation methods results in an artifact. Solvent partition and size exclusion chromatography on Sephadex LH-20 column, followed by high speed countercurrent chromatography, gave clavatamine (**335**), while silica flash chromatography and successive reversed-phase high performance liquid chromatography yielded an artifact, the free base (**336**). In addition to these compounds, several additional compounds, monomeric derivatives (**337-341**), were isolated. From ^1H NMR analysis of the free base and HMBC experiments with the newly generated

mixture from the free base, all monomeric derivatives were proposed to be produced *in situ* from decomposition of clavatamine. The HMBC experiments with the mixture clearly showed the presence of two monomeric derivatives which in turn might yield **337-339** upon addition of methanol or water. This phenomenon suggested acid- or base-catalyzed hydrolysis of guanidine, followed by cleavage of disulfide bridge, could give several monomeric derivatives upon extraction or isolation.

Perhaps one of the most interesting secondary metabolites isolated in this study is carpaphenol (**364**). Although the structure presented here was tentatively assigned, the presence of three oxygens in the right side of the molecule could give an extremely interesting property. Because of the hydrophilic and highly acidic nature of this compound, it may conjugate with Fe^{3+} due to the presence of two acid and one enol functional groups. These compounds may be the responsible ligands for iron sequestration of the styelid ascidian *Polycarpa clavata.*

Several previously reported compounds were also characterized in this study. Among them, 6-bromoindole-3-carboxylic acid (**348**) and methyl (4-hydroxyphenyl) acetate (**348a**), previously known as a synthetic compound, were the first isolation from ascidian sources. Compound **348a** was present in extremely high yield (0.3 %, dry wt).

In summary, this research resulted in a high diversity of novel secondary metabolites from marine ascidians. In total, 25 new natural products in 11 different class, including 8 new carbon skeletons, were isolated in this study. Many of them are interesting examples of ascidian metabolites which could easily be neglected by chemists by virtue of simplicity of their ^1H NMR spectra, lack of proton signals, and awkward solubilities. The isolation of the enterocin class compounds and the presence of a massive number of bacteria strongly suggested the potential microbial origin of these molecules, even though chemical investigation of bacterial isolates in culture could not prove this hypothesis. Furthermore, the majority of molecules characterized in this study are hydrophilic. Since there is a growing interest of hydrophilic secondary metabolites from ascidians and sponges, the methods utilized in this study can be applied to isolation of water-soluble molecules in the future. Especially, solvent partitioning and size exclusion chromatography using Sephadex LH-20 or Spectra Gel TSK HW-40, followed by chromatography on ion exchange resins or high speed countercurrent chromatography, can be widely utilized in a variety of systems. As previous studies indicated, this study also demonstrated that ascidians are producers of a large number of amino acid-derived compounds with only few exceptions. The compounds isolated in this research showed

various bioactivity such as antiinflammation, antimicrobial activity and cytotoxicity. Some of them may be involved in the tunic formation and metal accumulation. The structural analysis of DOPA-derived alkaloids revealed a novel condensation mechanism of amino acids. This may be a new polymerization and tanning mechanism in some ascidians. This work also presents examples of possible defensive adaptations within this chemically-prolific group of marine invertebrates.

REFERENCES

Adesanya, S. A., Chbani, M., Pais, M., and Debitus, C. 1992. *J. Nat. Prod.* **55**, 525.

Agudelo, M. I., Kustin, K., and McLeod, G. C. 1983.*Comp. Biochem. Phsiol.*, **75A**, 211-214.

Agudelo, M. I., Kustin, K., McLeod, G. C., Robinson, W. E., and Wang, R. T. 1983. *Biol. Bull.* **165**, 100-109.

Aguliar, E. and Meyers, A. I. 1994a. Tetrahedron Lett. **35**, 2473-2476.

Aguliar, E. and Meyers, A. I. 1994b. *Tetrahedron Lett.* **35**, 2477-2480.

Albano, R. M. and Mouroa, P. A. 1986. *J. Biol. Chem.* **261**, 758-765.

Albano, R. M., Pavao, M. S. G., and Mouroa, P. A. S. 1990. *Carbohydr. Res.* **208**, 163-174.

Anderson, R. J., Faulkner, D. J., Cun-heng, He, Van Duyne, G. D., and Clardy, J. 1985. *J. Am. Chem. Soc.* **107**, 5492-5495.

Anderson, R. S. 1971. *Biol. Bull.* **141**, 91-98.

Anderson, S. O. 1972. *J. Insect. Physiol.* **18**, 527-540.

Anderson, S. O. 1979. *Ann. Rev. Ent.* **24**, 29-61.

Anderson, S. O. 1985. In: Comprehensive insect physiology biochemistry and Pharmacology. Vol. 3. G. A. Kerkut and L. I. Gilbert eds. Pergamon Press, New York, 59-74.

Anderson, S. O., Jacobson, J. P., and Roepstorff, P. 1980. *Tetrahedron* **36**, 3249-3252.

Anno, K., Ostuka, K., and Seno, N. 1974. *Biochim. Biophys. Acta* **362**, 215-219.

Anthoni, U., Nielson, P. H., and Christopherson, C. 1991. *Tetrahedron Lett.* **32**, 7303-304.

Arabshahi, L. and Schmitz, F. J. 1988. *Tetrahedron Lett.* **29**, 1099-1102.

Aracil, J. M., Badre, A., Fadli, G., Jeanty, G., Banaigs, B., Francisco, C., Lafargue, F., Heitz, A., and Aumelas, A. 1991. *Tetrahedron Lett.* **32**, 2609-2612.

Arai, T. 1979. *Tetrahedron Lett.* 2355-2358.

Arai, T. in: Natural products isoaltion, separation methods for antimicrobials, antivirals, and enzyme inhibitors. Wagman, G. and Cooper, R. eds. Elservier, Amsterdam, 1989.

Avdeef, A., Sofen, S. R., Bregante, T. L., and Raymond, K. N. 1978. *J. Am. Chem.*

Soc. **100**, 5362-5370.

Azmi, K., Yokosawa, H., and Ishii, S.1990. *Biochem*istry **29**, 159-165.

Azumi, K., Satoh, N., and Yokosawa, H. 1993. *J. Exp. Zool.* **265**, 309-316.

Azumi, K., Yokosawa, H., and Ishii, S. 1990a. *Biochemistry* **29**, 159-165.

Azumi, K., Yokosawa, H., and Ishii, S. 1990b. *Experientia* **46**, 1020-1023.

Azumi, K., Yokosawa, H., and Ishii, S.1990a. *Biochemistry* **29**, 159.

Azumi, K., Yoshimizu, M., Suzuki, S., Ezura, Y., and Yokosawa, H. 1990b. *Experientia* **46**, 1066 - 1068.

Banaigs, B., Jeanty, G., Francisco, C., Joulin, P., Poncet, J., Heitz, A., Cave, A., Prome, J. C., Wahl, M., and Lafargue, F. 1989. *Tetrahedron* **45**, 181-190.

Barrington, E. J. W. 1975. *Symp. Zool. Soc. Lond.* **36**, 129-158.

Barrington, E. J. W. and Thorpe, A. 1968. *Proc. R. Soc. (B)* **171**, 91-109.

Barrow, R. A. and Capon, R. J. 1992. *J. Nat. Prod.* **55**, 1330-1331.

Bax, A. and Freeman, R. 1981. *J. Magn. Reson.* **44**, 542.

Bax, A., Griffery, R. G., and Hawkins, B. L. 1983. *J. Am. Chem. Soc.* **105**, 7188.

Bayer, E., Schiefer, G., Waidelich, D., Scippa, S., and de Vincentiis, M. 1992. *Angwe. Chem. Int. Ed. Engl.* **31**, 52-54.

Beak, G., Vasta, G. R., Marchalonis, J. J., and Habicht, G. S. 1989. *Comp. Biochem. Physiol.* **92B**, 93-98.

Beauge, L. A., and Glynn, I. M. 1977. *Nature* **268**, 355-356.

Belaud, C. and Guyot, M. 1984. *Tetrahedron Lett.* **25**, 3087-3090.

Benslimane, A. F., Pouchus, Y. F., Le Boterff, J., Verbist, J. F., Roussakis, C., and Monniot, F. 1988. *J. Nat. Prod.* **51**, 582-583.

Berrill, N. J. 1950. The tunicata with An account of the British species. Bernard Quaritch, Ltd. London, 354 pp.

Bestmann, H. J. and Both, W. 1974a. *Chem. Ber.* **107**, 2923-2925.

Bestmann, H. J. and Both, W. 1974b. *Chem. Ber.* **107**, 2926-2930.

Biard, J. F., Guyot, S., Roussakis, C., Verbist, J. F., Vercauteren, J., Weber, J. F., and Bourkef, K. 1994. *Tetrahedron Lett.* **35**, 2691-2694.

Bible, K. C., Buytendrop, M., Zierath, P. D., and Rinehart, K. L. Jr. 1988. *Proc. Natl.*

Acad. Sci. **85**, 4582-4586.

Bishop, M. J. and Ciufonlini, M. A. 1992. *J. Am. Chem. Soc.* **114**, 10081-10082. Biskuiak, J. E. and Ireland, C. M. 1983. *J. Org. Chem.* **48**, 2304-2306.

Blackman, A. J., Li, C., Hockless, D. C. R., Skelton, B. W., and White, A. H. 1993. *Tetrahedron* **49**, 8645-8656.

Bloor, S. J. and Schmitz, F. J. 1987, *J. Am. Chem. Soc.* **109**, 6134-6136.

Blunt, J. W., Lake, R. L., Munro, M. H. G., and Toyokuni, T. 1987. *Tetrahedron Lett.* **28**, 1825-1826.

Brand, S. G., Hawkins, C. J., Marshall, A. T., Nette, G. W., and Parry, D. L. 1989. *Comp. Biochem. Physiol.* **93B**, 425-436.

Breitmaier, E. and Voelter, W. 1987. Carbn-13 NMR specrtoscopy: high- resolution methods and applications in organic chemistry and biochemistry. VCH publishers, New York, 515 pp.

Bruening, R. C., Oltz, E. M., Furukawa, J., Nakanishi, K., and Kustin, K. 1985. *J. Am. Chem. Soc.* **107**, 5298-5300.

Bruening, R. C., Oltz, E. M., Furukawa, J., Nakanishi, K., and Kustin, K. 1986. *J. Nat. Prod.* **49**, 193-204.

Bruland, K. W. 1983. In: Trace elements in sea water in Chemical Oceanography J. P. Riley & R. Chester (eds) Vol. 8, Academic Press, London, 157 - 220.

Cantley, L. C., Jr., Ferguson, J. H., and Kustin, K. 1978.*J. Am. Chem. Soc.* **100**, 5210-5212.

Carlson, R. M. K. 1975. *Proc. Natl. Acad. Sci.* **72**, 2217-2221.

Carroll, A. R. and Scheuer, P. J. 1990. *J. Org. Chem.* **55**, 4426-4431.

Carroll, A. R. Bowden, B. F., and Coll, J. C. 1993a. *Aust. J. Chem.* **46**, 489-501.

Carroll, A. R., Boden, B. F., and Coll, J. C. 1993b. *Aust. J. Chem.* **46**, 1079-1083.

Carroll, A. R., Bowden, B. F., and Coll, J. C. 1993c. *Aust. J. Chem.* **46**, 825-832.

Carroll, A. R., Bowden, B. F., Coll, J. C., Hockless, D. C., Skeleton, B. W., and White, A. H. 1994. *Aust. J. Chem.* **47**, 61-69.

Carroll, A. R., Cooray, N. M., Poiner, A., and scheuer, P. J. 1989. *J. Org. Chem.* **54**, 4231-4232.

Carté, B. and Faulkner, D. J. 1982. *Tetrahedron Lett.* **23**, 3863-3866.

Carté, B. and Faulkner, D. J. 1983. *J. Org. Chem.* **48**, 2314-2318.

Carter, G. T. and Rinehart, Jr. K. L. 1978. *J. Am. Chem. Soc.* **100**, 7441-7442.

Cary, S. C., Warren, W., Anderson, E., and Giovannoni, S. J. 1993. *Molecular Mar. Biol. Biotech.* **2**, 51-62.

Chan, G. W., Francis, T., Thurean, D. R., Offen, P. H., Pierce, N. J., Westley, J. W., and Johnson, R. K. 1993. *J. Org. Chem.* **58**, 2544-2546.

Charyulu, G. A., McKee, T. C., and Ireland, C. M. 1989. *Tetrahedron Lett.* **30**, 4201-4202.

Chbani, M., Pais, M., Delauneux, J.-M., Debitus, C. 1993. *J. Nat. Prod.* **56**, 99-104.

Cheng, M. T. and Rinehart, K. L., Jr. 1978. *J. Am. Chem. Soc.* **100**, 7409-7411.

Chester, R. 1991. In: Trace elements in the oceans in Marine Geochemistry, Unwin Hyman, London, 346- 421.

Cimino, G., Crispino, A., De Rosa, S., De Stefano, S., Gavagnin, M., Sodano, G. 1987. *Tetrahedron* **43**, 4023-4030.

Clifford, J. H., Parry. D. L., Wood, B. J., and Clark, P. 1983. *Inorganica Chim. Acta* **78**, L29-L31.

Cole, P. C., Eckert, J. M., and Williams, K. L. 1983. *Anal. Chim. Acta* , 153, 61-67.

Collier, R. W. 1984. *Nature* **309**, 441-444.

Congreve, M. S., Holmes, A. B., Hughes, A. B., and Looney, M. G. 1993. *J. Am. Chem. Soc.* **115**, 5815-5816.

Cooper, R and Unger, S. 1985. *J. Antibiot.* **38**, 24.

Cooray, N. M., Scheuer, P. J., Parkanyl, L., and Clardy, J. 1988. *J. Org. Chem.* **53**, 4619-4620.

Copp, B. R., Blunt, J. W., and Munro, M. H. 1989. *Tetrahedron Lett.* **30**, 3703-3706.

Copp, B. R., Ireland, C. M., and Barrows, L. R. 1991. *J. Org. Chem.* **56**, 4596-4597.

Corley, D. G. and Moore, R. E. 1988. *J. Am. Chem. Soc.* **110**, 7920-7922.

Cotelle, N., Moreau, S., Bernier, J. L., Catteau, J. P., and Henichart, J. P. 1991. *Free Radical Biol. Med.* **11**, 63-68.

Cox, G. C., Hiller, R. G., and Larkman, A. W. D. Mar. Biol. 1985, 89, 149-163.

Cox, G., 1983. *J. Mar. Biol. Assoc. U. K.* **63**, 195.

Csaba, F. S. 1987. *Acta Morphol. Hung.* **35**, 105-110.

Dale, J. A. and Mosher, H. S. 1973 *J. Am. Chem. Soc.* **95**, 512-519.

Davidson, B. S. 1993. *Chem. Rev.* **93**, 1771-1791.

Davidson, B. S. and Ireland, C. M. 1990. *J. Nat. Prod.* **53**, 1036-1038.

Davidson, B. S., Molinski, T. F., Barrows, L. R., and Ireland, C. M. 1991. *J. Am. Chem. Soc.* **113**, 4709-4710.

Davis, A. R. 1991. *Mar. Biol.* **111**, 375-379.

Davis, A. R. and Wright, A. E. 1990. *J. Chem. Ecol.* **16**, 1349-1357.

Davis, A. R. and Wright, A. E.1989. *Mar. Biol.* **102**, 491-497.

De Leo, G. 1992. *Boll. Zool.* **59**, 195-213.

De Leo, G., Parrinello, N., DiBella, M. A. 1987. *Arch. Biol. (Bruxelles)* **98**, 35 -52.

De Leo, G., Patricolo, E., and Frittitta, G. 1981. *Acta Zool. (Stockh.)* **62**, 259-271.

de Guzman, F. S. and Schmitz, F. J. 1989. *Tetrahedron Lett.* **30**, 1069-1070.

de Silva, E. D., Miao, S., Anderson, R. J., Schultz, L. W., and Clardy, J. 1992. *Tetrahedron Lett.* **33**, 2917-2920.

Debitus, C., Laurent, D., and Pais, M. 1988. *J. Nat. Prod.* **51**, 799-801.

Degnan, B. M., Hawkins, C. J., Lavin, M. F., McCaffrey, E. J., Parry, D. L., and Watters, D. J. 1989a. *J. Med. Chem.* **32**, 1354-1359.

Degnan, B. M., Hawkins, C. J., Lavin, M. F., McCaffrey, E. J., Parry, D. L., van den Brenk, A. L., and Watters, D. J. 1989b. *J. Med. Chem.* **32**, 1349-1354.

Dematte, N., Guerriero, A., De Clauser, R., De Stanchina, G., Larfague, F., Cuomo, V., and Pietra, F. 1985. *Comp. Biochem. Physiol.* **81B**, 479-484.

Dematte,N. Guerriero, A., Lafargue, F., and Pietra, F. 1986, *Comp. Biochem. Physiol.* **84B**, 11-13.

Dingley, A. L., Kustin, K., Marcara, I. G., and McLeod, G. C. 1981. *Biochem. Biophys. Acta.* **649**, 493-502.

Do Amaral, A. D., Morris, R., and Barrington, E. J. W. 1972. *Gen. Comp. Endocrinol.* **19**, 370-372.

Dorsett, L. C., Hawkins, C. J., Grice, J. A., Lavin, M. F., Merefield, P. M., Parry, D. L., and Ross, I. L. 1987. *Biochemistry* **26**, 8078-8082.

Dunn, A. D. 1974. *J. Exp. Zool.* **188**, 103-124.

Dunn, A. D. 1975. *Gen. Comp. Endocrinol.* **25**, 83-95.

Dunn, A. D. 1980a. *Gen. Comp. Endocrin.* **40**, 484 - 493.

Dunn, A. D. 1980b. *Gen. Comp. Endocrinol.* **40**, 473-483.

Ehde, P., Andersson, I., and Pettersson, L. 1986. *Acta Chem. Scand.* **A40**, 489-499.

Ehde, P., Andersson, I., and Pettersson, L. 1989. *Acta Chem. Scand.* **43**, 136-143.

Eldridge, L. G. 1966. *Micronesica* **2**, 161-261.

Endean, R. 1961. *Q. Jl microsc. Sci.* **102**, 107-117.

Enders, D. and Finkam, M. 1993. *Liebigs Ann. Chem.*, (5), 551-5.

Fahy, E., Potts, B. C. M., Faulkner, D. J., and Smith, K. 1991. *J. Nat. Prod.* **54**, 564-569.

Faulkner, D. J. 1984. *Nat. Prod. Rep.* **1**, 551-598.

Faulkner, D. J. 1986. *Nat. Prod. Rep.* **3**, 1-33.

Faulkner, D. J. 1987. *Nat. Prod. Rep.* **4**, 539-576.

Faulkner, D. J. 1988. *Nat. Prod. Rep.* **5**, 613-663.

Faulkner, D. J. 1990. *Nat. Prod. Rep.* **6**, 269-309.

Faulkner, D. J. 1991. *Nat. Prod. Rep.* **7**, 97-147.

Faulkner, D. J. 1992. *Nat. Prod. Rep.* **8**, 323-364.

Faulkner, D. J. 1993. *Nat. Prod. Rep.* **9**,

Faulkner, D. J., He, H.-Y., Unson, M. D., Bewley, C. A., and Garson, M. J. 1993. *Gazz. Chim. Ital.* **123**, 301-307.

Fenical, W. 1974. In: Food-drugs from the sea conference, Proceedings, Marine Technology Society. Webber, H. H., and Ruggieri, G. D. eds. 388-394.

Ferguson, J. H. and Kustin, K. 1979. *Inorg. Chem.* **18**, 3349-3357.

Fluke, M. T. 1979. *Bull. Mar. Biol. Stn. Asmushi* **16**, 143-159.

Ford, P. W. and Davidson, B. S. 1993. *J. Org. Chem.* **58**, 4522-4523.

Forsyth, C. J. and Clardy, J. 1990. *J. Am. Chem. Soc.* **112**, 3497-3505.

Foster, M. P. and Ireland, C. M. 1993. *Tetrahedron Lett.* **34**, 2871-2874.

Foster, M. P., Concepcion, G. P., Caraan, G. B., nd Ireland, C. M. 1992b. *J. Org. Chem.* **57**, 6671-6675.

Foster, M. P., Mayne, C. L., Dunkel, R., Pugmire, R. J., Grant, D. M., Kornprobst, J.-M., Verbist, J.-F., Biard, J.-F., and Ireland, C. M. 1992. *J. Am. Chem. Soc.*

114., 1110-1111.

Frank, P., Carlson, R. M. K., and Hodgson, K. O. 1986. *Inorg. Chem.* **25**, 470-478.

Frank, P., Carlson, R. M. K., and Hodgson, K. O. 1988. *Inorg. Chem.* **27**, 118-122.

Frank, P., Hedman, B., Carlson, R. M. K., Tyson, T. A., Roe, A. L., and Hodgson, K. O. 1987. *Biochemistry* **26**, 4975.

Fredriksson, G., Ofverholm, T., and Ericson, L. E. 1988. *Cell Tissue Res.* **253**, 403-411.

Furusaki, A., Hashiba, N., Matsumoto, T., Hirano, A., Iwai, Y., and Omura, S. 1978. *J. Chem. Soc. Chem. Commun.* 800-801.

Gail, F. and Lafont, R. 1978. *Experientia* **34**, 1028-1029.

Gaill, F. and Momzikoff, A. 1975. *Mar. Biol.* **29**, 315-319.

Gallo, G. G., Coronelli, C., Vigevani, A., and Lancini, G. C. 1969. *Tetrahedron* **25**, 5677.

Gil-Turnes, M. S. 1988. *Ph. D. Dissertation*, UCSD, San Diego.

Gil-Turnes, M. S., Fenical, W., and Hay M. 1989.*Science* **246**, 116.

Goedicke, C. and Stegemeyer, H. 1970. *Tetrahedron Lett.* 937-940.

Goodbody, I., 1974. *Adv. Mar. Biol.* **12**, 1-149.

Gouffies, D., Juge, M., Grimaud, N., Welin, L., Sauviat, M. P., Barbin, Y., Laurent, D., Roussakis, C., Henichart, J. P., and Verbist, J. F. 1988. *Toxicon* **26**, 1129-1136.

Gouffies, D., Moreau, S., Helbecque, N., Bernier, J. L., Henichart, J. P., Barbin, Y., Laurent, D., and Verbist, J. F. 1988. *Tetrahedron* **44**, 451-458.

Goulle, V., Lehn, J. M., Schoenties, B., Schmitz, F. J. 1991. *Helv. Chim. Acta* **74**, 1471-1476.

Griffiths, D. J., and Thinh, L.-V. 1983. *Aust. J. Mar. Freshwat. Res.* **34**, 431-440.

Guan, Y., Sakai, R., Rinehart, K. L. Jr., and Wang, A. H.-J. 1993. *J. Biomolecular Str. Dynm.* **10**, 793-818.

Guella, G., Mancini, I., and Pietra, F. 1987. *Helv. CHim. Acta* **70**, 621-626.

Gunawardana, G. P., Koehn, F. E., Lee, A. Y., Clardy, J., He, H., and Faulkner, D. J. 1992. *J. Org. Chem.* **57**, 1523-1526.

Gupta, K. C., Miller, R. L., Williams, J. R., Gagosian, R. B., and Heinzer, F. 1979. *J. Nat. Prod.* **42**, 305-306.

Guyot, M. and Durgeat, M. 1981. *Tetrahedron Lett.* **22**, 1391-1392.

Guyot, M. and Meyer, M. 1986. *Tetrahedron Lett.* **27**, 2621-2622.

Guyot, M., Davoust, D., and Belaud, C. 1982. *Tetrahedron Lett.* **23**, 1905-1906.

Hamad, Y., Kondo, Y., Shibata, M., and Shioiri, T. 1989. *J. Am. Chem. Soc.* **111**, 669-673.

Hamada, Y., Kato, S., and Shioiri, T. 1985a. *Tetrahedron Lett.* **26**, 3223-3226.

Hamada, Y., Kondo, Y., Shibata, M., and Shioiri, T. 1987. *Peptide Chem.* 359-362.

Hamada, Y., Shibata, M., and Shioiri, T. 1985b, *Tetrahedron Lett.* **26**, 5155-5158.

Hamada, Y., Shibata, M., and Shioiri, T. 1985c, *Tetrahedron Lett.* **26**, 5159-5162.

Hamada, Y., Shibata, M., and Shioiri, T. 1985d, *Tetrahedron Lett.* **26**, 6501-6504.

Hamamoto, Y., Endo, M., Nakagawa, M., Nakanishi, T., and Mizukawa, K. 1983. *J. Chem. Soc. Chem. Commun.* 323-324.

Hambley, T. W., Hawkins, C. J., Lavin, M. F., van Den Brenk, A., and Watters, D. J. 1992. *Tetrahedron* **48**, 341-348.

Harris, B. D., Bhat, K. L., and Joullie, M. M. 1987. *Tetrahedron Lett.* **28**, 2837-2840.

Hawkins, C. J., Lavin, M. F., Marshall, K. A., van den Brenk, A. L., and Watters, D. J. 1990. *J. Med. Chem.* **33**, 1634-1638.

He, H. and Faulkner, D. J. 1991. *J. Org. Chem.* **56**, 5369-5371.

He, X., Kustin, K., Parry, D. L., Robinson, W. E., Ruberto, G., and Nakanishi, K. 1992. *Experientia* **48**, 367-371.

He. H. and Faulkner, D. J. 1989. *J. Org. Chem.* **54**, 5822.

Heitz, S., Durgeat, M., and Guyot, M. 1980. *Tetrahedron Lett.* **21**, 1457.

Heitz, S., Guyot, M., Brassy, C., and Bachet, B. 1980. *Tetrahedron Lett.* **21**, 1457-1458.

Helbecque, N., Moquin, C., Bernier, J.-L., Morel, E., Guyot, M., and Henichart, J.-P. 1987. *Cancer Biochem. Biophys.* **9**, 271-279.

Hirata, Y. 1979. *Pure Appl. Chem.* **51**, 1875.

Hirose, E., Saito, Y., and Watanabe, H. 1990. *Invertebrate Reprod. Develop.* **17**, 159-164.

Hirsch, S. Miroz, A., McCarthy, P. and Kashman, Y. 1989. *Tetrahedron Lett.* **30**, 4291-4294.

Hochachka, P.W. and Mommsen, T. P. 1983. *Science* **219**, 1391.

Hogan, I. T. and Sainabury, M. 1984. *Tetrahedron* **40**, 681-682.

Horenstein, B. A. and Nakanishi, K. 1989. J. Am. Chem. Soc. 111, 6242-6246.

Hossain, M. B., van der Helm., D., Antel, J., Sheldrick, G. M., Sanduja, S. K., and Weinheimer, A. J. 1988, *Proc. Natl. Acad. Sci. USA* **85**, 4118-4122.

Howard, B. M., Clarkson, K., and Berstein, R. L. 1979. *Tetrahedron Lett.* 4449-4452.

Hudson, J. B. and Towers, G. H. N. 1988. *Photochem. Photobiol.* **48**, 289-296.

Hudson, J. B., Saboune, H., Aramowski, Z., Towers, G. H. N., Rinehart, Jr. K. L. 1988. *Photochem. Photobiol.* **47**, 377-381.

Ikeda, Y, Mastuki, H., Ogawa, T., and Munakata, T. 1983. *J. Antibiot.* **36**, 1284.

Ireland, C. M. and Scheuer, P. J. 1980. *J. Am. Chem. Soc.* **102**, 5691-5692.

Ireland, C. M., Durso, A. R. Jr., Newman, R. A., and Hacker, M. P. 1982. *J. Org. Chem.* **47**, 1807-1811.

Ireland, C. M., Durso, Jr. A. R., Scheuer, P. J. 1981. *J. Nat. prod.* **44**, 360-361.

Ishibashi, M., Ohizumi, Y., Sasaki, T., Nakamura, H., Hirata, Y., and Kobayashi, J. 1987. *J. Org. Chem.* **52**, 450-453.

Ishibashi, M., Tsuda, M., Ohizumi, Y., Sasaki, T., and Kobayashi, J. 1991. *Experientia* **47**, 299-300.

Ishida, T., In, Y., Doi, M., Inoue, M., Hamada, Y., and Shioiri, T. 1992. *Biopolymers* **32**, 131-143.

Ishida, T., Inoue, M., Hamada, Y., Kato, S., and Shioiri, T. 1987a. *J. Chem. Soc. Chem. Commun.* 370-371.

Ishida, T., Ohishi, H., Inoue, M., Kamigauchi, M., Sugiura, M., Takao, N., Kato, S., Hamada, Y., and Shioiri, T. 1989. *J. Org. Chem.* **54**, 5337-5343.

Ishida, T., Tanaka, M., Nabae, M., Inoue, M., Kato, S., Hamada, Y., and Shioiri, T. 1988. *J. Org. Chem.* **53**, 107-112.

Ishida, T., Tanaka, M., Nabae, M., Inoue, M., Kato, S., Hamada, Y., Shioiri, T. 1987b. *Peptide Chem.* T. Shiba & S. Sakakibara eds. 67-70.

Jackman, L. M. and Strenhill, S. 1969. Applications of nuclear magnetic resonance spectroscopy in organic chemistry. Pergomon Press, Oxford, 61-113.

Jameson, R. F. and Kiss, T. 1986. *J. Chem. Soc. Dalton Trans.* 1833.

Jares-Erijman, E. A., Bapat, C. P., Lithgow-Bertelli, A., Rinehart, Jr. K. L., and Sakai, R. 1993. *J. Org. Chem.* **58**, 5732-5737.

Jerlov, N. G. 1976. Marine optics. 2nd ed. Elsevier Oceanography Series, No. 14., Elsevier, Amsterdam, 231 pp.

Jiang, T. L., Liu, R. H., and Salmon, S. E. 1983. *Cancer Chemother. Pharmacol.* **11**, 1-4.

Jimenez, C., Quinoa, E., Castedo, L., and Riguera, R. 1986. *J. Nat. Prod.* **49**, 905-909.

Johnson, C. E. Jr. and Bovey, F. A. 1958. *J. Chem. Phys.* **29**, 1012-1014.

Jouin, P., POncet, J., Dufour, M.-N., Pantaloni, A., and Castro, B. 1989. *J. Org. Chem.* **54**, 617-627.

Karuso, P. 1987. Chemical ecology of the nudibranchs. In: Bio-organic marine chemistry. Scheuer, P. J. ed., Springer-Verlag, Berlin, Germany, 31-60.

Kato, S. Sugiura, T., Hamada, Y., and Shiori, T. 1986b. *Peptide Chem.* T. Miyazawa ed. 285-290.

Kato, S., Hamada, Y., and Shiori, T. 1986a. *Tetrahedron Lett.* **27**, 2653-2556.

Kato, S., Kondo, Y., Sugiura, T., Hamada, Y., and Shioiri, T. 1985. *Peptide Chem.* Y. Kiso ed. 67-72.

Kazlauskas, R., Marwood, J. F., Murphy, P. T., and Wells, R. J. 1982. *Aust. J. Chem.* **35**, 215-7.

Kennedy, G. R. 1966. *Gen. Comp. Endocrinol.* **7**, 500-511.

Kessler, H., Mronga, S., Will, M., and Schmidt, U. 1990. *Helv. Chim. Acta* **73**, 25-47.

Kessler, H., Will, M., Antel, J., Beck, H., and Sheldrick, G. M. 1989. *Helv. Chim. Acta* **72**, 530-555.

Kester, D. R., Byrne, R. H. Jr., and Liang, Y. I. 1975. Redox reactions and soluion complexes of iron in marine systems. In: Marine Chemistry in the coastal environment. T. M. Church ed. ACS Symposium Series. No. 18.,56-79 .

Kikuchi, Y., Ishibashi, M., Sasaki, T., and Kobayashi, J. 1991. *Tetrahedron Lett.* **32**, 797-798.

Kim, D., Li, Y., and Nakanishi, K. 1991. J. Chem. Soc. Chem. Commun. 9-10.

Kim. D., Li, Y., Horenstein, B. A., and Nakanishi, K. 1990. *Tetrahedron Lett.* **31**, 7119-7122.

Kim. J., Pordesimo, E. O., Toth, S. I., Schmitz, F. J., and Altena, I. V. 1993. *J. Nat. Prod.* **56**, 1813-1816.

Kinnel, R. B. and Scheuer, P. J. 1992. *J. Org. Chem.* **57**, 6327-6329.

Kinzer, K. F. and Cardellina, II J. H. 1987. Tetrahedron Lett. 28, 925-926.

Kitahara, Y., Nakahara, S., Yonezawa, T., Nagatsu, M., and Kubo, A. 1993. *Heterocycles* **36**, 943-946.

Klavins, J. V. 1986. *J. Tumor Marker Oncol.* **1**, 3-12.

Kljaic, Z., Dogovic, N., and Gasic, M. J. 1983. *Comp. Biochem. Physiol.* **75B**, 519-521.

Kobayashi, J. Doi, Y., and Ishibashi, M. *J. Org. Chem.* **59**, 255-257.

Kobayashi, J. Nakamura, H., and Hirata, Y. 1981.*Tetrahedron Lett.* **22**, 3001-3002.

Kobayashi, J., Cheng, J-f., Kikuchi, Y., Ishibashi, M., Yamamura, S., Ohizumi, Y., Ohta, T., and Nozoe, S. 1990. *Tetrahedron Lett.* **31**, 4617-4620.

Kobayashi, J., Cheng, J., Walchi, M. R., Nakamura, H., Hirata, Y., Saaki, T., Ohizumi, Y., 1988. *J. Org. Chem.* **53**, 1800-1804.

Kobayashi, J., Cheng, J.-f., Nakamura, H., Ohizumi, Y., Hirata, Y., Sasaki, T., Ohta, T., and NOzoe, S. 1988. *Tetrahedron Lett.* **29**, 1177-1180.

Kobayashi, J., Cheng, J.-f., Ohta, T., Nakamura, H., Nozoe, S., Hirata, Y., Ohizumi, Y., and Sasaki, T. 1988. *J. Org. Chem.* **53**, 6147-6150.

Kobayashi, J., Cheng, J.-f., Ohta, T., Nozoe, S., Ohizumi, Y., and Sasaki, T. 1990. *J. Org. Chem.* **55**, 3666-3670.

Kobayashi, J., Harbour, G. C., Gilmore, J., and Rinehart, Jr. K. L. 1984. *J. Am. Chem. Soc.* **106**, 1526-1528.

Kobayashi, J., Ishibashi, M., Nagai, U., and Ohizumi, Y. 1989. *Experientia* **45**, 782-783.

Kobayashi, J., Nakamura, H., Ohizumi, Y., Hirata, Y. 1986, *Tetrahedron Lett.* **27**, 1191-1194.

Kobayashi, J., Tsuda, M., Agemi, K., Shigemori, H., Ishibashi, M., Sasaki,T., and Mikami, Y. 1991. *Tetrahedron* **47**, 6617-6622.

Kobayashi, J., Tsuda, M., Tanabe, A., Ishibashi, M., Chenh, J.-F., Yamamura, S., and Sasaki, T. 1991. *J. Nat. Prod.* **54**., 1634-1638.

Kogler, H., Sorensen, O. W., Bodenhausen, G., Ernst, R. R. 1983. *J. Magn. Reson.* **55**, 157.

Kohmoto, S., Kashman, Y., McConnell, O. J., Rinehart, Jr., K. L., Wright, A., and Koehn, F. 1988. *J. Org. Chem.* **53**, 3116.

Kong, F, and Faulkner, D. J. 1991. *Tetrahedron Lett.* **32**, 3667-3668.

Kott, P. 1969. Antarctic Ascidiacea, American Geophysical Union, Baltimore, 239 pp.

Kott, P. 1977. Algal supporting didemnid ascidians of the Great Barrier Reefs. In: Proceedings Third International coral reef symposium, Miami, Vol.1, 616-622.

Kott, P. 1989. Bull. Mar. Sci. **45**, 253.

Kott, P., Parry, D. L., and Cox, G. C. 1984. *Bull. Mar. Sci.* **34**, 308-312.

Krishnan, G. 1975. *Indian J. Exp. Biol.* **13**, 172-176.

Krishnan, G. and Ravindravanath, M. H. 1972. *Acta Histochem. Bd.* **44**, 348-364.

Lafargue, F. et Duclaux, G. 1979. *Annls. Inst. Ocenaogr., Paris (N. S.)* **55**, 163-184.

Lake, R. J., Blunt, R. L., and Munro, M. H. G. 1989. *Aust. J. Chem.* **42**, 1201-1206.

Lake, R. L., Brennan, M. M., Blunt, R. L., Munro, M. H. G., and Pannell, L. K. 1988. *Tetrahedron Lett.* **29**, 2255-2256.

Lake, R. L., McCombs, J. D., Blunt, R. L., Munro, M. H. G., and Robinson, W. T. 1988. *Tetrahedron Lett.* **29**, 4971-4972.

Lamas, L., Dorris, M. L., and Taurog, A. 1972. *Endocrinology* **90**, 1417-1426.

Larkum, A. W. D., Cox, G. C., Hiller, R. G., Parry, D. L., and Dibbayawan, T. P. 1987. *Mar. Biol.* **95**, 1-13.

Lee, S., Kustin, K., Robinson, W., Frankel, R., and Spartalian, K. 1988. *J. Inorg. Biochem.* **33**, 183-192.

Lee, S., Nakanishi, K., Chiang, M. Y., Frankel, R. B., and Spartalian, K. 1988, *J. Chem. Soc. Chem. Commun.*, 785-786.

Leninger, A. L. 1982a. Principles of biochemistry, Worth Publishing Inc., New York, 721-749.

Lehninger, A. L. 1982b. Principle of biochemistry, Worth Publishers, Inc., New York, 361-396.

Levine, L., Fujiki, H., Yamada, K., Ojika, M., Gjika, H. B., and van Vunakis, H. 1988. *Toxicon* **26**, 1123-1128.

Levitt, M. H., Nguyen, K. T., Hartzell, C. J., and Eaton, H. L. 1984. *J. Magn. Reson.* **58**, 462.

Lewin, R. A. 1977. *Phycologia* **16**, 217.

Lewin, R. A. 1984. *Phycologia* **23**, 203-208.

Li, W.-R., Ewing, W. R., Harris, B. D., and Joullie, M. M. *J. Am. Chem. Soc.* **112**, 7659-7672.

Liberko, C. A., Miller, L. L., Kartz, T. J., and Liu, L. 1993. *J. Am. Chem. Soc.* **115**, 2478-2482.

Lindquist, N. 1989. Ph.D. dissertation, UCSD, San Diego.

Lindquist, N. and Fenical, W. 1989. *Tetrahedron Lett.* **30**, 2735-2738.

Lindquist, N. and Fenical, W. 1990a. *Tetrahedron Lett.* **31**, 2389-2392.

Lindquist, N. and Fenical, W. 1990b. *Tetrahedron Lett.* **31**, 2521-2524.

Lindquist, N. and Fenical, W. 1991. *Experientia* **47**, 504-506.

Lindquist, N., Fenical, W., Parkanyl, L., and Clardy, J. 1991. *Experientia* **47**, 503-504.

Lindquist, N., Fenical, W., Sesin, D. F., Ireland, C. M., Forsyth, C. J., Clardy, J. 1988. *J. Am. Chem. Soc.* **110**, 1308-1309.

Lindquist, N. Fenical, W., Van Duyne, G. D., and Clardy, J. 1991. *J. Am. Chem. Soc.* **113**, 2303-2304.

Lindquist, N., Fenical, W, Van Duyne, G. D., and Clardy, J. 1988. *J. Org. Chem.* **53**, 4570-4574.

Lindquist, N., Fenical, W., Van Duyne, G. D., and Clardy, J. 1988. *J. Org. Chem.* **53**, 4570-4574.

Lindquist, N., Hay, M. E., and Fenical, W. 1992. *Ecological Monographs.* **62**, 547-568.

Litaudon, M. and Guyot, M. *Tetrahedron Lett.* **32**, 911-914.

Liu, J., Nakagawa, M., Ogata, K., and Hino, T. 1991. *Chem. Pharm. Bull.* **39**, 1672-1676.

Macara, I. G. 1980. *Trends Biochem. Sci.* **5**, 92.

Macara, I. G., McLeod, G. C., and Kustin, K. 1979. *Biochem. J.* **181**, 457-465.

Maki, J. S., Rittschof, D., Costlow, J. D., and Mitchell, R. 1988. *Mar. Biol.* **97**, 199-206.

Malochet-Grivois, C., Cotelle, P., Biard, J. F., Henichart, J. P., Debitus, C., Roussakis, C., and Verbist, J. F. 1991. *Tetrahedron Lett.* **32**, 6701-6702.

Marcara, I. G.; McLeod, G. C.; Kustin, K. 1979. *Comp. Biochem. Physiol. B: Comp. Biochem.* **63B**, 299.

Mastunaga, S., Fusetani, N., and Hashimoto, K. 1986. *Experientia* **42**, 84.

Mastuno, T. and Ookubo, M. 1981. *Tetrahedron Lett.* **22**, 4659-4660.

Mastuno, T. and Ookubo, M. 1982. *Chem. Lett.* 1605-1606.

Mastuno, T., Ookubo, M., and Komori, T. 1985. *J. Nat. Prod.* **48**, 606-613.

McDonald, L. A. and Ireland, C. M. 1992. *J. Nat. Prod.* **55**, 376-379.

McDonald, L. A., Foster, M. P., Phillips, D. R., Ireland, C. M., Lee, A. Y., and Clardy, J. 1992. *J. Org. Chem.* **57**, 4616-4624.

McKee, T. C., Ireland, C. M., Lindquist, N., and Fenical, W. *Tetrahedron Lett.* **30**, 3053-3056.

McLafferty, F. W. 1980. Interpretation of mass spectra. University Sciences Books, Mill Valley, California, 303 pp.

Meyers, A. I. and Tavares, F. 1994. *Tetrahedron Lett.* **35**, 2481-2484.

Miao, S. and Anderson, R. J. 1991. *J. Org. Chem.* **56**, 6275-6280.

Michbata, H. and Uyama, T. 1991. *J. Exp. Zool.* **254**, 132-137.

Michibata, H. 1989. *Zool. Sci.* **6**, 639-647 and references there in.

Michibata, H., Hirata, J., Unesaka, M., Numakunai, T., and Sakurai, H. 1987. *J Exp. Zool.* **244**, 33-38.

Michibata, H., Hirose, H., Sugiyama, K., Ookubo, Y., and Kanamori, K. 1990. *Biol. Bull.* **179**, 140-147.

Michibata, H., Morita, A., and Kanamori, K. 1991. *Biol. Bull.* **181**, 189-194.

Michibata, H., Uyama, T., and Hirata, J. 1990. *Zool. Sci.* **7**, 55-61.

Michibata, H., Zenko, Y., Yamada, K., Hasegawa, M., Terada, T., and Numakuani, T. 1989. *Zool. Sci.* **6**, 289-293.

Milanesi, C. and Burighel, P. 1978. *Acta Zool (Stockh.)* **59**, 135-147.

Millar, R. H. 1971. *Adv. Mar. Biol.* **9**, 1-100.

Mimura, T., Okabe, M., Satake, M., Nakanishi, T., Inada, A., Fujimoto, Y., Hata, F., Mastumura, Y., and Ikekawa, N. 1986. *Chem Pharm. Bull.* **34**, 4562-4568.

Mitchell, P. 1961. *Nature* **191**, 144.

Miyairi, N., Sakai, H.-I., Konomi, T., and Imanaka, H. 1976. *J. Antibiotics* **29**, 227-235.

Molina, P., Fresneda, P. M., and Canovas, M. 1992. *Tetrahedron Lett.* **33**, 2891-2894.

Molinski, T. F. 1993. *Chem. Rev.* **93**, 1825-1838.

Molinski, T. F. and Ireland, C. M. 1989. *J. Org. Chem.* **54**, 4256-4259.

Momzikoff, A. and Gaill, F. 1973. *Experientia* **29**, 1438-1439.

Monniot, C., Monniot, F., and Laboute, P. 1990. Coral reef ascidians of New Caledonia, Orstom, Paris, 131-233.

Moody, C. J., Rees, C. W., and Thomas, R. *Tetrahedron* **48**, 3589-3602.

Moquin, C. and Guyot, M. 1984. *Tetrahedron Lett.* **25**, 5047-5048.

Moquin-Pattery, C. and Guyot, M. 1989. *Tetrahedron* **45**, 3445-3450.

Mori, K. and Umemura, T. 1981a. *Tetrahedron Lett.* **22**, 4429-4432.

Mori, K. and Umemura, T. 1981b. *Tetrahedron Lett.* **22**, 4433-4436.

Mori, K. and Umemura, T. 1982. *Tetrahedron Lett.* **23**, 3391-3394.

Moriarty, R. M., Roll. D. M., Ku, Y.-Y., Nelson, C., and Ireland, C. M. 1987. *Tetrahedron Lett.* **28**, 749-752.

Moroz, S. V., Kurika, A. V., and Pavlenko, A. F. 1993. *Pure Appl. Chem.* **65**, 1253-1264.

Morris, R. J. 1983. *Lipids* **18**, 900-901.

Mukai, H. and Watanabe, H. 1976. *J. Morphol.* **148**, 337-362.

Murata, O., Shigemori, H., Ishibashi, M., Sugama, K., Hayashi, K., and Kobayashi, J. 1991. *Tetrahedron Lett.* **32**, 3539-3542.

Nakagawa, M., Liu, J.-J., Ogata, K., and Hino, T. 1986. *Tetrahedron Lett.* **27**, 6087-6090.

Nakamura, A., Ashino, T., and Yamamoto. 1991. *Tetrahedron Lett.* **32**, 4355-4358.

Nakamura, A., Masuda, H., Hamda, N. and Koizumi, A. 1992. *Toxicology Lett.* **60**, 257-262.

Nakamura, Y., Kobayashi, J., Gilmore, J., Mascal, M., Rinehart, Jr. K. L., Nakamura, H., and Ohizumi, Y. 1986. *J. Biol. Chem.* **261**, 4139-4142.

Nakanishi, K. 1964. Infrared absorption spectroscopy, Holden-Day, Inc., San Francisco, 233 pp.

Neville, A. C. 1975. Biology of the arthropod cuticle. Springer-Verlag, New York, 125-158.

Newman, M. S. and Lednicer, D. 1956. *J. Am. Chem. Soc.* **78**, 4765-4770.

Nilsson,O., Fredriksson, G., Ofverholm, T., and Ericson, L. E. 1988. *Cell Tissue Res.* **253**, 137-143.

Niwa, H., Inagaki, H., and Yamada, K. 1991. *Tetrahedron Lett.* **32**, 5127-5128.

Niwa, H., Yoshida, Y., and Yamada, K. 1988. *J. Nat. Prod.* **51**, 343-344.

Nybakken, J. W., 1982 Marine biology. An ecological approach, New York, Harper and Row, Publishers.

Ohtani, I., Kusumi, T., Kashman, Y., and Kakisawa, H. 1991. *J. Am. Chem. Soc.* **113**, 4092-4096.

Olson, R. R., and McPherson, R. 1987. *J. Exp. Mar. Biol. Ecol.* **110**, 245-256.

Oltz, E. M., Bruening, R. C., Smith, M. J., Kustin, K., and Nakanishi, K. 1988, *J. Am. Chem. Soc.* **110**, 6162-6172.

Oltz, E. M., Pollack, S., Delohery, T., Smith, M. J., Ojika, M., Lee, S., Kustin, K., and Nakanishi, K. **1989**. *Experientia* **45**, 186-190.

Omura, S, Iwai, Y., Hirano, A., Nakagawa, A. Awaya, J., Tsuchiya, H. Takahashi, Y., and Masuma, R. 1977. *J. Antibiot.* **30**, 275-282.

Osborne, N. N., Neuoff, V., Ewers, E., and Robertson, H. A. 1979. *Comp. Biochem. Physiol.* **63**, 209-213.

Pagani, H., Giancarlo, L., Tamoni, G., and Coronelli, C. 1973. J. Antibiot. 26, 1.

Pardy, R. L. and Lewin, R. A. 1981. *Bull. Mar. Sci.* **31**, 817-823.

Parrinello, N. and Arizza, V. 1992. *Boll. Zool.* **59**, 183-189.

Parry, D. L. 1984. *Mar. Ecol. Prog. Ser.* **17**, 279-282.

Parry, D. L. 1984. *Phycologia* **23**, 503-505.

Parry, D. L. 1985. *Mar. Biol.* **87**, 219-222.

Parry, D. L. 1988a. *Symbiosis* **5**, 1-22.

Parry, D. L. 1988b. *Symbiosis* **5**, 23-33.

Parry, D., Brand, S. G., and Kustin, K. 1992.*Bull. Mar. Sci.* **50**, 302-306.

Pathirana, C. and Anderson, R. 1986. *J. Am. Chem. Soc.* **108**, 8288.

Pau, R. N., Brunet, P. C., and Williams, M. J. 1971. *Proc. R. Soc. (B)* **177**, 565-579.

Paul, V. J., Lindquist, N. and Fenical, W. 1990. *Mar. Ecol. Prog. Ser.* **59**, 109-118.

Pavao, M. S. G., Albano, R. M., and Mouroa, P. A. 1989a. *Carbohydr. Res.* **189**, 374-379.

Pavao, M. S. G., Albano, R. M., Lawson, A. M., and Mouroa, P. A. S. 1989b. *J. Biol. Chem.* **264**, 9972-9979.

Pavao, M. S. G., Mouroa, P. A. S., and Mulloy, B. 1990. *Carbohydr. Res.* **208**, 153-161.

Pawlik, J. R. 1993. *Chem. Rev.* **93**, 1911-1922.

Pearl, H. W. 1984. *Mar. Biol.* **81**, 251-254.

Pearse, A. G. E. 1968. Histochemistry: Theoretical and applied, Churchil, London.

Perry, N. B., Blunt, J. W., and Munro, M. H. G. 1991. *Aust. J. Chem.* **44**, 627-633.

Pestarino, M. 1992. *Boll. Zool.* **59**, 191-194.

Peter, M. G., 1989, *Angew. Chem., Int. Ed. Engl.* **28**, 555.

Pettit, G. R., Kantoci, D., Doubek, D. L., Tucker, B. E., Pettit, W. E., and Schroll, R. M. 1993. *J. Nat. Prod.* **56**, 1981-1984.

Pizarro, J., Andrade, C., and Crivelli, I., 1989. *Comp. Biochem. Physiol.* **94A**, 777-781.

Plate, R., van Hout, R. H. M., Behm, H., and Otenheijm, H. C. J. 1987. *J. Org. Chem.* **52**, 55-560.

Plough, H. H. 1978. Sea squirts of the Atlantic continental shelf from Maine to Texas, The Johns Hopkins University Press, Baltimore, 118 pp.

Plumbo, A., Misuraca, G., D'Ishia, M., Doughdy, F., and Prota, G. 1984. *Comp. Biochem. Physiol.* **78B**, 81.

Pordesimo, E. O. and Schmitz, F. J. 1990. *J. Org. Chem.* **55**, 4704.

Porter, Q. N. 1985. Mass spectrometry of heterocyclic compounds, John-Wiley and Sons, Inc., New York, 928-935.

Potts, B. C. M., Faulkner, D. J., Chan, J. A., Simolike, G. C., Offen, P. Hemling, M. E., and Francis, T. A. 1991, *J. Am. Chem. Soc.* **113**, 6321-6322.

Pourbaix, M. 1966. Atlas of electrochemical qeuilibria in aqueous solutions, Pergamon Press, New York, 92.

Prinsep, M. R., Moore, R. E., Levine, I. A., and Patterson, G. M. L. 1992. *J. Nat. Prod.* **55**, 140-142.

Raftos, D. A., Briscoe, D. A., and Tait, N. N. 1988. *Transplantation* **45**, 1123-1126.

Raftos, D. A., Tait, N. N., and Briscoe, D. A. 1987. *Dev. Comp. Immunol.* **11**, 713-725.

Ratcliiffe, N. A., Rowley, A. F., Fitzgerald, S. W., and Rhodes, C. P. 1985. *Int. Rev. Cytol.* **97**, 183-350.

Raub, M. F., Cardellina, J. H., and Spande, T. F. *Tetrahedron Lett.* **33**, 2257-2260.

Raub, M. F., Cardellina, J. H., Choudhary, M. I., Ni, C.-Z., Clardy, J., and Alley, M. C. 1991. *J. Am. Chem. Soc.* **113**, 3178-3180.

Richards-Gross, S. E. E. 1993. M.S. dissertation. UCSD, San Diego.

Rinehart, Jr. K. L., Kabayashi, J., Harbour, G. C., Hughes, Jr. R. G., Mizsak, S. A., and Scahill, T. A. 1984, *J. Am. Chem. Soc.* **106**, 1524-1526.

Rinehart, Jr. K. L., Kobayashi, J., Harbour, G. C., Gilmore, J., Mascal, M., Holt, T. G., Shield, L. S., and Lafargue, F. 1987. *J. Am. Chem. Soc.* **109**, 3378-3387.

Rinehart, K. L. Jr., Gloer, J. B., Cook, J. C. Jr., Misak, S. A., and Scahill, T. A. 1981a. *J. Am Chem. Soc.* **103**, 1857-1859.

Rinehart, K. L. Jr., Gloer, J. B., Hughes, R. G., Renis, H. E., McGovern, J. P., Swyneneberg, E. B., Stringfellow, D. A., Kuentzel, S. L., and Li, L. H. 1981b. *Science* **212**, 933-935.

Rinehart, K. L. Jr., Harbour, G. C., Graves, M. D., and Cheng, M. T. 1983. *Tetrahedron Lett.* **24**, 1593-1596.

Rinehart, K. L. Jr., Holt, T. G., Fregeau, N. L., Keifer, P. A., Wilson, G. R., Perun, T. J. Jr., Sakai, R., Thompson, A. G., Stroh, J. G., Shield, L. S., Seigler, D. S., Li, L. H., Martin, D. G., Grimmelikhuijzen, C. J. P. and Gade, G. 1990. *J. Nat. Prod.* **53**, 771-792.

Rinehart, K. L. Jr., Holt, T. G., Fregeau, N. L., Stroh, J. G., Keifer, P. A., Sun, F., Li, L. H., and Martin, D. G. 1990a. *J. Org. Chem.* **55**, 4512-4515.

Rinehart, K. L. Jr., Holt, T. G., Fregeau, N. L., Stroh, J. G., Keifer, P. A., Sun, F., Li, L. H., and Martin, D. G. 1990b. *J. Org. Chem.* **56**, 1676.

Rinehart, K. L. Jr., Kishore, V., Bible, K., Sakai, R., Sullins, D., and Li, K.-M. 1988. *J. Nat. Prod.* **51**, 1-21.

Rinehart, K. L. Jr., Kishore, V., Nagarajan, S., Lake, R. J., Gloer, J. B., Bozich, F. A., Li, K.-M., Maleczka, R. E., Todson, W. L., Munro, M. H. G., Sullins, D. W., and Sakai, R. 1987. *J. Am. Chem. Soc.* **109**, 6846-6848.

Rinehart, K. L. Jr., Sakai, R., Holt, T. G., Fregeau, N. L., Keifer, P. A., Sun, F., Li, L. H., and Martin, D. G. 1990c. *Pure Appl. Chem.* **62**, 1277-1280.

Robinson, W. E., Agudelo, M. I., and Kustin, K. 1984. *Comp. Biochem. Physiol.* **78A**, 667-673.

Robinson, W. E., Kustin, K., and Cloney, R. A. 1986. *J. Exp. Zool.* **237**, 63-72.

Roche, J., Andre, S., and Covelli, I. 1960. *C. R. Seanc. Soc. Biol.* **154**, 2201-2206.

Roche, J., Rametta, G, and Varrone, S. 1964. *Gen. Comp. Endocr.* **4**, 277-284.

Roden, L. 1981. In: Biochemistry of glycoproteins and proteoglycans Lenarz, W. L. ed., Plenum Publishing Co., New York, 267-371.

Roll, D. M. and Ireland, C. M. 1985. *Tetrahedron Lett.* **26**, 4303-4306.

Rowley, A. F. 1981. *J. Invert. Pathol.* **37**, 91-100.

Rowley, A. F. 1983. *J. Exp. Zool.* **227**, 319-322.

Rudi, A. and Kashman, Y. 1989. *J. Org. Chem.* **54**, 5331-5337.

Rudi, A., Benayhu, Y., Goldberg, I, and Kashman, Y. 1988a. *Tetrahedron Lett.* **29**, 3861-3862.

Rudi, A., Benayau, Y., Goldberg, I., and Kashman, Y. 1988b. *Tetrahedron Lett.* **29**, 6655-6656.

Rudi, A., Goldberg, I., Stein, Z., Frolow, F., Benayahu, Y., Schleyer, M., and Kashman, Y. 1994. *J. Org. Chem.* **59**, 999-1003.

Ryan, D. E., Ghatlia, N. D., McDermott, A. E., Turro, N. J., Nakanishi, K., and Kustin, K. 1992.*J. Am. Chem. Soc.* **114**, 9659-9660.

Sakamoto, T., KOndo, Y., Sato, S., and Yamanaka, H. 1994. *Tetrahedron Lett.* **35**, 2919-2920.

Saki, R., Rinehart, K. L. Jr., GUan, Y., and Wang, A. H.-J. 1992. *Proc. Natl. Acad. Sci. USA* **89**, 11456-11460.

Santos, T. A., Mulloy, B., and Mouroa, P. A. S. 1992. *Eur. J. Biochem.* **204**, 669-677.

Sato, A., Shindo, T., Kasanuki, N., and Hasegawa, K. 1989. *J. Nat. Prod.* **52**, 975-981.

Satoh, N., 1994, Developmental biology of ascidians, Cambridge University Press, New York.

Saul, S. J. and Sugumaran, M. 1989a. *FEBS lett.* **251**, 69-73.

Saul, S. J. and Sugumaran, M. 1989b. *FEBS lett.* **251**, 340-344.

Schmidt, U. and Griesser, H. 1986. *Tetrahedron Lett.* **27**, 163-166.

Schmidt, U. and Weller, D. 1986. *Tetrahedron Lett.* **27**, 3495-3496.

Schmidt, U., Kroner, M., and Griesser, H. 1988a. *Tetrahedron Lett.* **29**, 3057-3060.

Schmidt, U., Kroner, M., and Griesser, H. 1988b. *Tetrahedron Lett.* **29**, 4407-4408.

Schmidt, U., Utz, R., and Gleich, P. 1985. *Tetrahedron Lett.* **26**, 4367-4370.

Schmitz, F. J., DeGuzman, F. S., Hossain, M. B., and van Helm, D. 1991. *J. Org. Chem.* **56**, 804-808.

Schmitz, F. J., Ksebati, M. B., Chang, J. S., Wang, J. L., Hossain, M. B., van der Helm, D., Engel, M. H., Serban, A., and Slifer, J. A. 1989. *J. Org. Chem.* **54**, 3466-3472.

Schmitz, F., DeGuzman, F. S., Hossain, M. B., and van der Helm, D. 1991. *J. Org. Chem.* **56**, 804-808.

Schor, L. and Seldes, A. M. 1989. *Comp. Biochem. Physiol.* **92B**, 195-196.

Schwenker, G. 1962. *Arch. Pharm. (Weinheim, Ger.)* **295**, 753-758.

Scippa, S., Iazzetti, G., De Vincentiis, M. 1987. *Acta Embryol. Morphol.* **8**, 341-346.

Scippa, S., De Vincentilis, M., and Zierold, K. 1990. *Invert. Reprod. Develop.* **17**, 141-146.

Searlie, P. A. and Molinski, T. F. 1993. *J. Org. Chem.* **58**, 7578-7580.

Seino, A., Kobayashi, M., Kobayashi, J., Fang, Y.-I., Ishibashi, M., Nakamura, H., Momose, K., and Ohizumi, Y. 1991. *J. Pharmacol. Exp. Therap.* **256**, 861-867.

Sesin, D. F. and Ireland, C. M. 1984, *Tetrahedron Lett.* **25**, 403-404.

Sesin, D. F., Gaskell, S. J., and Ireland, C. M. 1986. *Bull. Soc. Chim. Belg.* **95**, 853-869.

Seto, H., Sato, T., Urano, S., Uzawa, J., and Yonehara, H. 1976. *Tetrahedron Lett.* 4367-4370.

Shochet, N. R., Rudi, A., Kashman, Y., Hod, Y., El-Maghrabi, M. R., and Spector, I. 1993. *J. Cellular Physiol.* **157**, 481-492.

Slaytor, M. and McFarlane, I. J. 1968. *Phytochemistry* **7**, 605-611.

Smith, M. J. 1970a. *Biol. Bull. (Woods)* **138**, 354-378.

Smith, M. J. 1970b. *Biol. Bull. (Woods)* **138**, 379-388.

Smith, M. J. 1989. *Experientia* **45**, 452-457.

Smith, M. J. and Dehnel, P. A. 1970. *Comp. Biochem. Physiol.* **35**, 17-30.

Stam, W. T., Boele-Bos, S. A., and Stulp, B. K. 1985. *Arch. Microbiol.* **142**, 340-341.

Stanwell, C., Gescher, A., and Watters, D. 1993. *Biochem. Pharmacol.* **45**, 1753-1761.

Steffan, B. 1991. *Tetrahedron Lett.* **47**, 8729-8732.

Steffan, B., Brix, K., and Putz, W. 1993. *Tetrahedron Lett.* **49**, 6223-6228.

Stevens, D. W., Jensen, R. M., and STevens, L. E. 1989. *Transplantation Proceedings* **21**, 1139-1140.

Stievenart, J. 1971. *C. r. hebd. Seanc Acad. Sci. Paris.* **272**, 1873-1875.

Still, I. W. J. and McNulty, J. W. 1989. *Heterocycles* **29**, 2057-2059.

Stoecker, D. 1978. *Biol. Bull.* **146**, 615-626.

Stoecker, D. 1980a. *Mar. Ecol. Prog. Ser.* **3**, 257-265.

Stoecker, D. 1980b. *Ecology* **61**, 1327-1334.

Strum, J. M., Wicken, J., Stanbury, J. R., and Karnovsky, M. J. 1971. *J. Cell. Biol.* **51**, 162-175.

Sugahara, T., Ohike, T., Soejima, M., and Takano, S. 1990. *J. Chem. Soc. Perkin Trans. I* 1824-1826.

Sugiura, T., Hamada, Y., and Shioiri, T. 1987. *Tetrahedron Lett.* **28**, 2251-2254.

Sugumaran, M. Semensi, V., Kalyanaraman, B., Bruce, J. M., and Land, E. J. 1992. *J. Biol. Chem.* **267**, 10355-10361.

Sugumaran, M., Kundzicz, H., Bedell-Hodgan, D., and Schinkmann, K. 1989. *Arch. Insect. Biochem. Physiol.* **11**, 109-125.

Sugumaran, M., Semensi, V., Kalyanaraman, B., Bruce, J. M., and Land, E. J. 1992. *J. Biol. Chem.* **267**, 10355-10361.

Suzuki, S. and Kondo, Y. 1971. *Gen. Comp. Endocrinol.* **17**, 402-406.

Sybesma, J., van Duyl, F. C., and Bak, R. P. M. 1981. *Mar Ecol. Prog. Ser.* **6**, 53-59.

Tam Ha, T. B., Kokke, W. C. M.C., and Djerassi, C. 1982. *Steroids* **40**, 431-453.

Targett, N. M. and Keeran, W. S. 1984. *J. Nat. Prod.* **47**, 556.

Taurog, A. 1974. Biosynthesis of iodoamino acids. in: Handbook of Physiology. R. O. Greep and E. B. Astwood eds. Vol. 3, 101-133. American Physiological Society, Washington, DC.

Taylor, S. W., Molinski, T. F., Rzepecki, L. M., and Waite, J. H. 1991. *J. Nat. Prod.* **54**, 918-922.

Thorndyke, M. C. 1973. *J. Endocr.* **58**, 679-680.

Thorpe, A., Thorndyke, M. C., and Barrington, E. J. W. 1972. *Gen. Comp. Endocrinol.* **19**, 559-571.

Toda, N., Horikawa, T., Anno, K., and Seno, N. 1978. *Carbohydr. Res.* **62**, 389-392.

Tokuma, Y., Miyairi,N., and Morimoto, Y. 1976. *J. Antibiotics* **29**, 1114-1116.

Tong, W. and Chaikoff, I. C. 1961. *Biochem. Biophys. Acta* **46**, 259-270.

Trischman, J. A. 1993. Ph.D. dissertation, UCSD, San Diego.

Tsubotani, S., Tanida, S., and Harada, S. 1991. *Tetrahedron* **47**, 3565-3574.

Tsukamoto, S., Hirota, H., Kato, H., and Fusetani, N. 1993. *Comp. Biochem. Physiol.* **106C**, 151-153.

Tsukamoto, S., Hirota, H., Kato, H., and Fusetani, N. 1993b. *Tetrahedron Lett.* **34**, 4819-4822.

Tullius, T. D., Gillum, W. O.. Carlson, R. M. K., Hodgson, K. O. 1980. *J. Am Chem. Soc.* **102**, 5670-5676.

Uriz, M. J., Martin, D., Turon, X., Ballesteros, E., Hughes, R., and Acebal, C. 1991. *Mar. Ecol. Prog. Ser.* **70**, 175-188.

Uyama, T., Nishikata, T., Satoh, N., and Michibata, H. 1991. *J. Exp. Zool.* **259,** 196-201.

Uyama, T., Uchiyama, J., Nishikata, T., Satoh, N, and Michbata, H. 1993.*J. Exp. Zool.* **265**, 29-34.

Wahl, M. 1989. *Mar. Ecol. Prog. Ser.* **58**, 175-189.

Wahl, M. and Banaigs, B. 1991. *J. Exp. Mar. Biol. Ecol.* **145**, 49-63.

Wanatnabe, K., Mastunga, S., and Konosu, S. 1984. *Tetrahedron Lett.* **25**, 2003-2004.

Wanty, R. B. and Goldhaber, M. B. 1992*Geochim. Cosmochim. Acta* **56**, 1471-1483.

Wasylyk, J. M. and Alam, M. 1989. *J. Nat. Prod.* **52**, 1360-1362.

Wasylyk, J. M., Biskupiak, J. E., Costello, C. E., and Ireland, C. M. 1983. *J. Org. Chem.* **48**, 4445-4449.

Watters, D., Marshall, K., Hamilton, S., MIcheal, J., MaArthur, M., Seymour, G., Hawkins, C., Gardiner, R., and Lavin, M. 1990. *Biochem. Pharmacol.* **39**, 1609-1614.

Watters, D., Micheal, J., Hemphil, J. E., Hamilton, S. E., Lavin, M. F., and Pettit, G. R. 1992. *J. Cellular Biochem.* **49**, 417-424.

Watts, D. C. 1975. *Symp. Zool. Soc. Lond.* **36**, 105.

Welsh, J. H. and Loveland, R. E. 1968. *Comp. Biochem. Physiol.* **27**, 719-722.

Wever, R. and Kustin, K. 1990. *Adv. Inorg. Chem.* **35**, 81- 115.

Whittaker, J. R. 1973. *Develop. Biol.* **30**, 441-454.

Williams, A. B. and Jacobs, R. S. 1993. *Cancer Lett.* **71**, 97-102.

Williams, D. E., Moore, R. E., and Paul, V. J. *J. Nat. Prod.* **52**, 732-739.

Wright, A. E., Forleo, D. A., Gunawardana, G. P., Gunasekera, S. P., Koehn, F. E., and McConnell, O. J. 1990. *J. Org. Chem.* **55**, 4508-4512.

Wright, R. K. 1981 Urochordates. In: Invertebrates blood cells Vol.2 N. A. Ractcliffe and A. F. Rowley, eds. Academic Press, London, 565-626.

Wright, R. K. and Ermak, T. H. 1982. Cellular defense systems of the Protochordata. In: The Reticuloendothelial system. A conprehensive treatise Cohen, N. and Sigel, M. M. eds. Plenum Press, New York, Vol. 3, 283-320.

Yagimura, S., Asahi, T., Muto, N., and Hayashi, M. 1987. *Jpn. Kodai Tokkyo Koho*, 8 pp.

Yoshida, W. Y., Lee, K. K., Carroll, A. R., and Scheuer, P. J. 1992. *Helv. Chim. Acta* **75**, 1721-1725.

Young, C. M. and Bingham, B. L. 1987. *Mar. Biol.* **96**, 539-544.

Yuh, D. D., Zurcher, R. P., Carmichael, P. G., and Morris, R. E. 1989. *Transplantation Proceedings* **21**, 1141-1143.

Zabriskie, T. M. 1989. Doctoral Dissertation, University of Utah.

Zabriskie, T. M., Foster, M. P., Stout, T. J., Clardy, J., and Ireland, C. M. 1990. *J. Am. chem. Soc.* **112**, 8080-8084.

Zabriskie, T. M., Mayne, C. L., and Ireland, C. M. 1988. *J. Am. Chem. Soc.* **110**, 7919-7920.

Zielinski, J., Kokke, W. C. M. C., Tam Ha, T. B., Shu, A. Y. L., Duax, W. L., and Djerassi, C. 1983. *J. Org. Chem.* **48**, 3471-3477.

Zollo, F., Finamore, E., Gargiulo, D., Riccio, R., and Minale, L. 1986. *Comp. Biochem. Physiol.* **85B**, 559-560.